UNIVERSIDAD COMPLUTENSE DE MADRID

FACULTAD DE FARMACIA

Departamento de Farmacia y Tecnología Farmacéutica

TESIS DOCTORAL

Nuevas formulaciones para la liberación de Anfotericina B

(Noval formulations for Amphotericina B delivery)

MEMORIA PARA OPTAR AL GRADO DE DOCTOR

PRESENTADA POR

Claudia Luengo Alonso

Directores

Juan José Torrado Durán
Mª Paloma Ballesteros Papantonakis
Paolo Caliceti

Madrid, 2018

UNIVERSIDAD COMPLUTENSE DE MADRID

FACULTAD DE FARMACIA

DEPARTAMENTO DE FARMACIA Y TECNOLOGÍA FARMACÉUTICA

UNIVERSITÀ DEGLI STUDI DE PADOVA

DIPARTIMENTO DI SCIENZE DEL FARMACO

Nuevas formulaciones para la liberación de Anfotericina B

(Novel formulations for Amphotericin B delivery)

MEMORIA PARA OPTAR AL GRADO DE DOCTOR PRESENTADA POR:

Claudia Luengo Alonso

Directores:

Dr. Juan José Torrado Durán (UCM)

Dra. Mª Paloma Ballesteros Papantonakis (UCM)

Dr. Paolo Caliceti (UniPd)

Madrid, 2017

PhD Research Title

NOVEL FORMULATIONS FOR AMPHOTERICIN B DELIVERY

Presented by

Claudia Luengo Alonso

Codirected by the University Complutense of Madrid and the University of Padova

*UCM Directors***:**

Dr. Juan José Torrado Durán

Dra. Mª Paloma Ballesteros Papantonakis

UniPd Director:

Dr. Paolo Caliceti

Defense University

UNIVERSIDAD COMPLUTENSE DE MADRID

DEPARTAMENTO DE FARMACIA Y TECNOLOGÍA FARMACÉUTICA

Madrid, 2017

Esta Tesis Doctoral ha sido realizada gracias a una Beca Predoctoral

FPU concedida por el Ministerio de Educación, Cultura y Deporte del Gobierno de

España (Ref. AP2010-0748)

Table of contents

Abbreviations

A.	Aspergillus
AAG	α_1-acid glycoprotein
ABCD	Amphotericin B Colloidal Dispersion
ABLC	Amphotericin B lipid complex
ACN	Acetonitrile
AH	Enthalpy
AIDS	Acquired immune deficiency syndrome
ALA	5-aminolevulanic acid
AS	Entropy
AmA	Amphotericin A
AmB	Amphotericin B
ATCC	American Type Culture Collection
AUC	Area Under the Curve
BCS	Biopharmaceutical Classification System
C.	Candida
C_0	Initial Concentration
C_{24}	Concentration at 24h.
CAC	Critical Aggregation Concentration
CAP	Cellulose Acetate phtalate
CAQYM	Chemical and Microbiology Analysis Centre
CD	Circular Dichroism
CECT	Spanish Type Culture Collection
CFU	Colony Forming Units
CLSI	Clinical and Laboratory Standards Institute
Cmax	Maximum Concentration

CMC	Critical Micelar Concentration
CO	Candidal onychomycosis
Cp	Centipoise
CPF	Chitosan-g-pluronic F-127 copolymer
γ-CD	Gamma cyclodextrin
Da	Dalton
D-AmB	Dimeric Amphotericin B
DBS	Dibutyl sebacate
DDS	Drug delivery system
DEP	Diethyl phthalate
DLC	Double-lenght channel
DLS	Dynamic Light Scattering
DLSO	Distal lateral suungual onychomycosis
DMSA	Dimercaptosuccinid acid
DMPC	Dimyristoylglycerophosphatidylcholine
DMSO	Dimethylsulfoxide
DocNa	Sodium deoxycholate
DSC	Differential Scanning Calorimetry
DSPE	1,2-Distearoyl-sn-glycero-3-phosphoethanolamine
EF	Enhancement Factor
EO	Endonyx onychomycosis
F	Absolute bioavailability
F.	Fusarium
FDA	Food and Drug Administration
FT-IR	Fourier Transform Infrared
GCPQ	Quaternary mmonium palmitoyl glycol chitosan
GMF	Gastric Mimicking Fluid

GT	Glycerol triacetate
HIV	Human Immunodeficiency Virus
H-NMR	Proton Nuclear Magnetic Resonance
HSA	Human Serum Albumin
HSM	Hot Stage Microscopy
ICH	International Conference on Harmonisation
IL	Interleukin
ILA	Intralipid Amphotericin B
iNOS	Inducible Nitric Oxide Synthase
IR	Infrared
ITC	Isothermal Titration Calorimetry
IV	Intravenous
K	Binding constant
Kd	Dissociation constant
Ke	Elimination constant
LNP	Lipid Nanoparticles
MAL	Methyl-aminolevulinate
M-AmB	Monomeric Amphotericin B
MIC	Minimum Inhibitory Concentration
MM	Mixed Micelles
Mw	Molecular weight
NADPH	Nicotinamide adenine dinucleotide phosphate
NMP	N-methyl-2-pyrrolidone
NO	Nitric Oxide
P-AmB	Polyaggregate Amphotericin B
PBS	Phosphate Buffer Saline
PDI	Polydispersity Index

PDT	Photodynamic therapy
PEG	Polyethylene glycol
PLGA	Poly(lactic-co-glycolic acid)
PPG	Propylene glycol
Ppm	Parts per million
PSO	Poximal subungual onychomycosis
Pk	Pharmacokinetics
RBC	Red Blood Cells
RES	Reticulo-Endothelial System
rF	Reconstituted Formulation
RH	Relative Humidity
ROS	Reactive oxygen species
RP-HPLC	Reverse-phase High Performance Liquid Chromatography
S.	Streptomyces
SC	Stratum corneum
SEM	Scanning Electron Microscopy
SLC	Single-lenght channel
$SOCl_2$	Thionyl chloride
Sp.	Specie
TDO	Dystrophic onychomycosis
TEA	Triethylamine
TFA	Trifluoroacetic acid
$T_{1/2}$	Half-life
TLR	Toll-like receptor
TNBS	2,4,6-trinitrobenzene sulfonic acid
UV	Ultraviolet
Var.	Variant

Vd	Volume of distribution
WCH	Women's and Children's Hospital
WFI	Water for injection
WSO	White Superficial Onychomycosis
XRD	X-Ray diffractometry

DRUG UNIPD AMPHOTERICIN B PEG_{5KDA}-CHOLANE FTIR HSM HEMOLYSIS ORAL UCM MONOMER POLYAGGREGATES ITC *IN VITRO* INTRAVENOUS Ke SYNTHESIS mV TNBS RESISTANCE $T_{1/2}$ NMR XRD FORMULATION ACTIVATION IR CANDIDA HPLC 1959 EFFICACY SYNCHROTRON CHOLESTEROL pH CMAX DIMER ORAL NAIL CHARACTERIZATION ΔH 924Da CRITICAL AGGREGATION CONCENTRATION MIC CMC CIRCULAR DICHROISM ONYCHOMYCOSIS STABILITY RELEASE UV TOXICITY TEA HSA C24 TOPICAL ADMINISTRATION AMORPHOUS CONJUGATION AUC MIXED INFECTIONS MEMBRANE ΔS PENETRATION EXCIPIENTS BETA-SHEET $C_{47}H_{73}NO_{17}$ KD2 CM^{-1} ALPHA-HELIX EF ERGOSTEROL FILM-FORMING DERMATHOPHYTE MOLDS AMPHOTERIC PKA DISSOCIATION CRYSTALLINE INTERACTION BALB/C

SUMMARY

RESUMEN

SOMMARIO

SUMMARY

NOVEL FORMULATIONS FOR AMPHOTERICIN B DELIVERY

INTRODUCTION

Amphotericin B (AmB), a macrolide antibiotic with broad spectra of action, has been widely used in the treatment of systemic fungal infections since more than 40 years. Even though several new antifungal drugs have been developed, AmB remains the drug of choice in the treatment of severe systemic fungal diseases and in the treatment of visceral leishmaniasis when the parasite develops resistance to antimonial compounds.

The poor AmB solubility is the main drawback for the development of pharmaceutical formulations. So far, many attempts have been made to develop AmB formulations with enhanced therapeutic profiles, including solid-lipid nanoparticles, polymeric nanoparticles, liposomes, micelles and polymer bioconjugates.

Even though the amphotericin B associated nephrotoxicity is the main drawback for the use of this molecule in clinic, the fact that this antibiotic is only available for intravenous administration also limits its prescription. The development of AmB oral, intravenous and/or topical formulations with decreased toxicity will allow not only for the treatment of systemic fungal infections but also for the treatment of topical mixed-infections resistant to conventional treatments. These formulations will improve patient compliance and reduce the sanitary cost of the treatment.

OBJECTIVE

Taking into account the rising importance and clinical repercussion of the mold infections in humans and animals, the development of new formulations that reinforce the current therapeutic arsenal is needed.

The wide spectra of action of amphotericin B together with its low appearance of resistance, makes this drug a suitable candidate for the treatment of different types of mycosis. Thus, the main objective of the present thesis will be focused on the development of new amphotericin B (AmB) formulations for the treatment of systemic and topical mycosis with reduced side effects.

Two AmB formulations will be developed. The first part of this project will be focused on the development of a new AmB topical formulation; a nail lacquer formulation for the treatment of mixed onychomycosis resistant to conventional treatments.

The second part of the thesis will be performed in collaboration with the University Degli Studi di Padova and it will be focused on the development and optimization of an AmB pegylated formulation for the treatment of systemic fungal infections by oral and intravenous administration. The AmB interactions with cholesterol-type molecules are known to favor the drug solubility. Thus, the conjugation of cholesterol-type molecules with different PEGs will allow for the encapsulation and solubilization of AmB. To achieve this general purpose some specific objectives are proposed which included the synthesis of different AmB pegylated complexes; the solubility studies in different conditions; the complexes characterization by DLS, HPLC, DSC, RX, FTIR, CD, ITC and synchrotron analysis; the *ex vivo* characterization of these complexes (toxicity by hemolysis and antifungal efficacy against *Candida albicans*) and finally, the *in vivo* pharmacokinetic studies after oral and intravenous administration. The pharmacokinetic properties of the new AmB formulation will be determined and compared to the commercialized formulations Ambisome® and Fungizone®.

RESULTS

With regards to the AmB topical formulation, different water permeable and impermeable nail lacquer formulations were prepared. The drying time, viscosity, aspect of the film, extensibility, brightness, AmB incorporation and pH were studied. From all the formulations developed, three of them were selected for further characterization and *in vitro* studies (F11, F13 and F19). Even though formulations 11, 13 and 19 overcame the AmB low solubility problems, the short-term stability of these formulations (1 month) was still a problem. The strategy used to overcome the short AmB stability was focused on obtaining powders for reconstitution. The freeze drying (for F11 and F13) and spray drying (for F19) generated stable lyophilized and spray dried products easily redispersable. *In vitro* nail penetration studies on female human nails, demonstrated the higher nail penetration reached with F19 (EF=1.95) compared to F11, F13 and to the control. The *in vitro* efficacy studies against *Candida albicans* showed that the most active formulation was F19 (103%). The AmB nail lacquer was active against the dermatophyte and non-dermatophyte infections located on keratinized

structures. Treatment (30 days) with F19, administered in alternate days, once daily, cleared up the infections caused by *T. mentagrophytes*, *T. rubrum*, *A. niger*, *F.oxysporum* and *F.solani*. After 30 days of treatment no microorganisms were found nor in the culture media neither in the direct examination.

As far as the AmB pegylated formulation is concerned, the solubility studies showed that PEG_{5kDa}-cholane can increase more than 10^5 times the AmB solubility according to a linear [dissolved drug]/ [polymer concentration] correlation. The different capability of PEG_{5kDa}-cholane to solubilize AmB observed was explained by the effect of the dissolution conditions in the formation of monomeric and multimeric soluble species. The high affinity of AmB for PEG_{5kDa}-cholane was observed by isothermal calorimetry (ITC). This technique highlighted the complexity of the PEG_{5kDa}-cholane interaction with AmB, which takes place with different AmB soluble species, namely monomers, dimers, tetramers, and other multimeric nanoaggregates, of which abundance depends on the pH. The three different binding sites calculated by ITC analyses reasonably result from the PEG_{5kDa}-cholane interaction with different AmB species through hydrophobic interactions between the cholane moiety and the heptaene side of the drug molecule to form different supramolecular structures. The lyophilization process produced a fluffy powder with low moisture content and without cake formation which was stable throughout the time. The CD studies showed that, similarly to Fungizone® and heated Fungizone®, AmB/PEG_{5kDa}-cholane micelles did not induce structural alterations of human serum albumin (HSA). The hemolysis studies confirmed that the AmB/PEG_{5kDa}-cholane micelles were less hemolytic than Fungizone®. Even at concentrations in which the Fungizone® caused 100% hemolysis, the new formulation produced not more than 30% hemolysis. The biological *in vitro* studies showed that the AmB formulated with PEG_{5kDa}-cholane maintains high antimicrobial activity, which is very close to AmB in solution. The oral administration of 5 mg/kg AmB demonstrated that the new formulation developed had the highest half-life of all assayed formulations.

Finally, The IV administration of 1 mg/kg AmB in Ambisome®, Fungizone® and AmB/PEG_{5kDa}-cholane showed that the new formulation developed had a significantly ($P<0.01$) lower apparent elimination constant and consequently, a higher half-life compared to the marketed formulations Ambisome® and Fungizone®.

CONCLUSIONS

This thesis includes the development of two different types of amphotericin B formulations: one topical formulation for the treatment of nail infections (conclusions 1-3) and one intravenous/oral formulation for the treatment systemic fungal infections. (Conclusions 4-12).

Conclusions:

1.- A new water-impermeable stable nail lacquer formulation containing amphotericin B has been designed for the treatment of onychomycosis. The polymer (Eudragit L100®) and the amphotericin B solvent used (N-methyl-2-pyrrolidone) showed no compatibility problems. Once applied over a surface, the nail lacquer formed a continuous, homogenous and smooth film resistant to water.

2.- *In vitro* nail penetration studies showed that the lacquer was able to penetrate the nail (enhancement factor almost twice than the control). *In vitro* activity studies demonstrated the efficacy of the nail lacquer against dermatophyte and non-dermatophyte molds as well as yeasts (gender Candida).

3.- *In vivo* efficacy studies on keratinized structures of animal origin supported the efficacy of amphotericin B. After 30 days treatment on alternate days, the nail lacquer was able to clear up the infections caused by *Trichophyton mentagrophytes, Trichophyton rubrum, Aspergillus niger, Fusarium. oxysporum* and *Fusarium solani*.

4.- A novel formulation for amphotericin B delivery has been developed by using a micelle forming 5 kDa monomethoxy-polyethylene glycol end functionalized with cholanic acid (PEG_{5kDa}-cholane). This polymer was found to increase 10^5 times the amphotericin B solubility with a 12:1 AmB/PEG_{5kDa}-cholane molar ratio (2:1 w/w ratio).

5.- The system AmB/PEG_{5kDa}-cholane forms 30 nm micelles with the hydrophobic cholane moieties localized inside the micelles. Zeta potential analysis showed that at neutral pHs (5.5-7.2) the overall micelle surface is nearly neutral. The PEG_{5kDa}-cholane interacts with amphotericin B according to three binding sites depending on the pH, suggesting that the polymer interaction depends on the amphotericin B ionization and aggregation.

6.- Once lyophilized, the freeze-dried product could be promptly redispersed to form an homogeneous colloidal dispersion. The dispersion was physicochemically stable. Fourier Transform infrared spectrometry, differential scanning calorimetry and X-ray diffractometry showed that in the lyophilized product, amphotericin B and PEG_{5kDa}-cholane interacts intimately.

7.- The amphotericin B release from the PEG_{5kDa}-cholane micelles showed a biphasic profile. The best fittings were obtained with the Higuchi and Korsmeyer-Peppas models.

8.- The toxicity of the new formulation was tested as hemolysis. The new AmB/PEG_{5kDa}-cholane nanoformulation was always less hemolytic than the reference marketed formulation Fungizone®.

9.- The amphotericin B antifungal activity assayed against *Candida albicans* showed that AmB/PEG_{5kDa}-cholane was 15% more active than the free amphotericin B in buffer.

10.- The IV pharmacokinetics profiles of the different formulations studied (Ambisome®, Fungizone® and AmB/PEG_{5kDa}-cholane) were significantly different. The apparent elimination constant (Ke) of the new formulation is significantly ($P<0.01$) lower than both Ambisome® and Fungizone®. Accordingly, the half-life value of this new formulation was found to be higher. The IV administration of 1 mg/kg AmB/PEG_{5kDa}-cholane caused less pain effect in the mice than the administration of the same dose of Fungizone® or Ambisome®.

11.- Oral pharmacokinetic studies confirmed that this new formulation has a higher half-life than Ambisome® and Fungizone® marketed formulations. The AUC_{0-24} values were similar for all tested formulations.

12.- It can be concluded that the new AmB/PEG_{5kDa}-cholane formulation is a promising soluble controlled delivery system for amphotericin B with lower toxicity than the reference marketed formulation Fungizone®.

RESUMEN
NUEVAS FORMULACIONES PARA LA LIBERACIÓN DE ANFOTERICINA B

INTRODUCCIÓN

La anfotericina B (AmB), un antibiótico macrólico con una amplio espectro de acción, se utiliza desde hace más de 40 años para el tratamiento de infecciones micóticas sistémicas. A pesar de que se han desarrollado nuevos fármacos antifúngicos, la AmB sigue siendo el fármaco de elección tanto en el tratamiento de infecciones fúngicas sistémicas graves como en el tratamiento de la leishmaniasis visceral, cuando el parásito desarrolla resistencia a los derivados antimoniales.

La baja solubilidad de la AmB es el principal inconveniente para el desarrollo de nuevas formulaciones. Hasta el momento se han llevado a cabo diversos intentos para desarrollar formulaciones de AmB con mejoras en el perfil terapéutico; se han desarrollado nanopartículas con lípidos sólidos, nanopartículas poliméricas, liposomas, micelas y bioconjugados poliméricos.

Un inconveniente importante para el uso de esta molécula en clínica es su elevada nefrotoxicidad, así como el hecho de que se formule y comercialice solo para administración intravenosa. El desarrollo de nuevas formulaciones orales, intravenosas y/o tópicas de AmB con toxicidad reducida, permitirá no sólo el tratamiento de infecciones fúngicas sistémicas sino también el tratamiento de infecciones tópicas mixtas resistentes a tratamientos convencionales.

El amplio espectro de acción de la anfotericina B junto con su baja apariencia de resistencias hacen de este fármaco un candidato adecuado para el tratamiento de diferentes tipos de micosis.

OBJETIVO

El objetivo principal de la presente tesis es el desarrollo de nuevas formulaciones de anfotericina B (AmB) para el tratamiento de micosis sistémicas y tópicas.

En esta tesis doctoral se desarrollarán dos tipos de formulaciones de AmB. La primera parte de la tesis se centrará en el desarrollo de una nueva formulación tópica, una laca de uñas para el tratamiento de la onicomicosis resistente a tratamientos convencionales.

La segunda parte de la tesis se realizará en colaboración con la Universidad Degli Studi di Padova y se centrará en el desarrollo y la optimización de una formulación pegilada de AmB para el tratamiento de infecciones fúngicas sistémicas por vía oral e intravenosa. Dado que las interacciones de la AmB con moléculas de tipo colesterol favorecen la solubilidad del fármaco, la conjugación de moléculas de este tipo con diferentes PEGs permitirá la encapsulación y solubilización de la AmB. Para lograr ésto se proponen algunos objetivos específicos que incluyen la síntesis de diferentes complejos pegilados de AmB, los estudios de solubilidad en diferentes condiciones, la caracterización de los complejos por DLS, HPLC, DSC, RX, FTIR, CD, ITC y sincrotrón, la caracterización *ex vivo* de estos complejos (toxicidad por hemólisis y eficacia antifúngica contra *Candida albicans*) y finalmente, los estudios farmacocinéticos *in vivo* después de la administración oral e intravenosa. Finalmente se compararán las propiedades farmacocinéticas de la nueva formulación con las de dos formulaciones comercializadas: AmBisome® y Fungizone®.

RESULTADOS

Con respecto a la formulación tópica de AmB, se prepararon diferentes formulaciones de lacas de uñas permeables e impermeables al agua. Se estudió el tiempo de secado, la viscosidad, el aspecto de la película, la extensibilidad, el brillo, la incorporación de AmB y el pH. De todas las formulaciones desarrolladas, tres de ellas fueron seleccionadas para su posterior caracterización y estudio *in vitro* (F11, F13 y F19). Aunque las formulaciones 11, 13 y 19 solventaron los problemas de baja solubilidad de la AmB, la estabilidad a corto plazo de estas formulaciones (1 mes) seguía siendo un problema. La estrategia utilizada para mejorar la corta estabilidad de los preparados de AmB se centró en la obtención de polvos para reconstitución. La liofilización (para F11 y F13) y el secado por pulverización (para F19) generaron productos estables fácilmente redispersables. Los estudios de penetración *in vitro* en uñas de voluntarios sanos demostraron que la penetración obtenida con F19 (EF=1.95) fue mayor en comparación con F11, F13 y con el control. Los estudios de eficacia *in vitro* contra *Candida albicans* mostraron que la formulación más activa fue F19 (103%). La laca de uñas de AmB fue activa contra las infecciones provocadas por dermatofitos y no dermatofitos localizadas en las estructuras queratinizadas. El tratamiento (30 días) con F19, administrado en días alternos y una vez al día, eliminó las infecciones causadas por *T. mentagrophytes*, *T*

rubrum, *A. niger*, *F. oxysporum* y *F. solani*. Tras 30 días de tratamiento no se encontraron microorganismos ni en el medio de cultivo ni en el examen directo.

Respecto a la formulación pegilada de AmB, los estudios de solubilidad mostraron que el PEG_{5kDa}-colánico puede aumentar más de 10^5 veces la solubilidad de la AmB. La diferente capacidad de PEG_{5kDa}-colánico para solubilizar la AmB observada se explica por el efecto que las condiciones de disolución tienen en la formación de especies solubles monoméricas y multiméricas. La alta afinidad de la AmB por el PEG_{5kDa}-colánico se observó mediante calorimetría isotérmica (ITC). Esta técnica resaltó la complejidad de la interacción entre el PEG_{5kDa}-colánico y la AmB que tiene lugar a través de diferentes especies solubles de AmB, principalmente monómeros, dímeros, tetrámeros y otros nanoagregados multiméricos cuya abundancia depende del pH. Los tres sitios de unión diferentes calculados mediante análisis por ITC resultan de la interacción del PEG_{5kDa}-colánico con diferentes especies de AmB mediante las interacciones hidrofóbicas entre el resto colánico y el lado del heptaeno de la molécula de AmB para formar diferentes estructuras supramoleculares. El proceso de liofilización produjo un polvo esponjoso con bajo contenido en humedad y sin formación de torta que se mostró estable a lo largo del tiempo. Los estudios de CD mostraron que de formar similar a la Fungizona® y a la Fungizona® calentada, las micelas de AmB/PEG_{5kDa}-colánico no indujeron alteraciones estructurales de la albúmina sérica humana (HSA). Los estudios de hemólisis confirmaron que las micelas de AmB/PEG_{5kDa}-colánico eran menos hemolíticas que Fungizona®. Incluso a concentraciones en las que la Fungizona® causó 100% de hemólisis, la nueva formulación produjo no más del 30%. Los estudios biológicos *in vitro* demostraron que la AmB formulada con PEG_{5kDa}-colánico mantiene una alta actividad microbiana que está muy cerca de la AmB en solución. La administración oral de 5 mg/kg de AmB demostró que la nueva formulación desarrollada tenía la semivida más alta de todas las formulaciones ensayadas. Por último, la administración intravenosa de 1 mg/kg de AmB en AmBisome®, Fungizone® y AmB/PEG_{5kDa}-colánico mostró que la nueva formulación desarrollada tenía una constante de eliminación aparente significativamente menor ($P<0,01$) y consecuentemente una semivida más alta en comparación con las formulaciones comercializadas Ambisome® and Fungizona®.

CONCLUSIONES

Esta tesis incluye el desarrollo de dos tipos diferentes de formulaciones de anfotericina B; una formulación tópica para el tratamiento de las infecciones de las uñas (conclusiones 1-3) y una formulación intravenosa/oral para el tratamiento de las infecciones fúngicas sistémicas (conclusiones 4-12).

Conclusiones:

1.- Se ha diseñado una laca de uñas de AmB estable e impermeable al agua para el tratamiento de la onicomicosis. El polímero (Eudragit L100®) y el disolvente usado para la anfotericina B (N-metil-2-pirrolidona) no mostraron problemas de compatibilidad. Una vez aplicadas sobre la superficie, la laca de uñas forma una película continua, homogénea, lisa y resistente al agua.

2.- Los estudios de penetración *in vitro* demostraron que la laca era capaz de penetrar la uña (factor de penetración casi dos veces el del control). Los estudios de actividad *in vitro* demostraron la eficacia de la laca de uñas contra hongos dermatofitos y no dermatofitos así como contra levaduras (género Cándida)

3.- Los estudios de eficacia *in vitro* sobre estructuras queratinizadas de origen animal apoyaron la eficacia de la anfotericina B. Después de 30 días de tratamiento en días alternos, la laca de uñas fue capaz de eliminar las infecciones causadas por *Trichophyton mentagrophytes*, *Trichophyton rubrum*, *Aspergillus niger*, *Fusarium oxysporum* y *Fusarium solani*.

4.- Se ha desarrollado una nueva formulación para la liberación de AmB empleando un polímero capaz de formar micelas (5 kDa monometoxi-polietilenglicol funcionalizado con ácido colánico - PEG_{5kDa}-colánico). Se observó que este polímero aumentaba 10^5 veces la solubilidad de la anfotericina B con una relación molar AmB/PEG_{5kDa}-colánico de 12:1 (relación p/p 2:1).

5.- El sistema AmB/PEG_{5kDa}-colánico forma micelas de 30 nm con las cavidades hidrofóbicas del colánico localizadas dentro de las micelas. El análisis del potencial zeta mostró que a pH neutro (pH 5.5 -7.2) la superficie global de la micela es casi neutra. El PEG_{5kDa}-colánico interactúa con la anfotericina B a través de tres sitios de unión dependiendo del pH, lo que sugiere que la interacción polimérica depende del grado de ionización y de la agregación de la anfotericina B.

6.- Una vez liofilizado, el producto obtenido puede ser rápidamente redispersado para formar una dispersión coloidal homogénea. La dispersión es físico-químicamente estable. La espectrometría infrarroja por transformada de Fourier, la calorimetría diferencial de barrido y la difractometría de rayos X mostraron que en el producto liofilizado la anfotericina B y el PEG_{5kDa}-colánico interactúan íntimamente.

7.- La liberación de la anfotericina B de las micelas de PEG_{5kDa}-colánico mostró un perfil bifásico. Los mejores ajustes fueron obtenidos con los modelos de Higuchi y Korsmeyer-Peppas.

8.- La toxicidad de la nueva formulación se ensayó en términos de hemólisis. La nueva nanoformulación de AmB/PEG_{5kDa}-colánico fue en todos los casos menos hemolítica que la formulación comercializada de referencia Fungizona®

9.- La actividad antifúngica de la anfotericina B ensayada contra *Candida albicans* mostró que la formulación de AmB/PEG_{5kDa}-colánico era un 15% más activa que la anfotericina B libre en tampón.

10.- Los perfiles farmacocinéticos IV de las diferentes formulaciones estudiadas (AmBisome®, Fungizona® y AmB/PEG_{5kDa}-colánico) fueron significativamente diferentes. La constante de eliminación aparente (Ke) de la nueva formulación fue significativamente menor ($P<0.01$) que la de AmBisome® y Fungizona®. Consecuentemente, el valor de la semivida de esta formulación fue mayor. La administración intravenosa de 1 mg/kg de AmB/PEG_{5kDa}-colánico causó menos efecto de dolor en las ratones que la administración de la misma dosis de Fungizona® o AmBisome®

11.- Los estudios de farmacocinética oral confirmaron que esta nueva formulación tiene una semivida más alta que las formulaciones comercializadas Ambisome® y Fungizona®. Los valores de AUC_{0-24} fueron muy similares para todas las formulaciones ensayadas.

12.- Se puede concluir que la nueva formulación AmB/PEG_{5kDa}-colánico es un sistema de liberación controlada soluble muy prometedor y con una menor toxicidad en comparación con la Fungizona®

SOMMARIO

NUOVE FORMULAZIONI PER LA VEICOLAZIONE DI AMFOTERICINA B

INTRODUZIONE

L'amphotericina B (AmB) è un antibiotico macrolide con un ampio spettro d'azione, da oltre 40 anni usato nel trattamento di infezioni micotiche sistemiche.

Sebbene recentemente siano stati sviluppati nuovi farmaci antifungni, AmB rimane il farmaco di prima scelta nel trattamento di gravi infezioni fungine e nel trattamento di leismaniasi viscerale nel caso in cui i parassiti sviluppino una resistenza ai composti antimoniali.

La bassa solubilità di AmB è il principale problema al suo sviluppo farmaceutico e ad oggi si sono fatti numerosi tentativi per sviluppare formulazioni di AmB con migliorate caratterisitiche biofarmaceutiche e profilo terapeutico. Tra le principali formulazioni vi sono nanoparticlelle lipidiche solide, nanoparticelle polimeriche, micelle e bioconiugati polimerici

La nefrotossicità è uno dei maggiori problemi all'uso clinico di questo farmaco che si unisce alla difficoltà della somministrazione intravenosa.

Lo sviluppo di formualzioni per uso orale, intravenoso e topico con ridotta tossicità consente l'impiego di AmB nel trattamento di infezioni fungine sistemiche e topiche nel caso di infezioni miste resistenti oltre che nei tratatmenti tradizionali. Pertanto formulazioni innovative consentono un uso più razionale, sicuro e ampio di questo farmaco con una migliore performance terapeutica e compliance del paziente.

OBIETTIVI

La crescente importanza delle ripercussioni cliniche delle infezioni nell'uomo e nell'animale ha portato alla necessità di sviluppare formulazioni che possano essere sempre più efficacy nel trattamento di quetse patologie e in grado di coprire in modo ampio lo sviluppo di infesioni.

L'ampio spettro di azione di amfotericina B (AmB) unitamente alla bassa resitenza sviluppata, rendono questo farmaco un eccellente candidato per il trattamento di vari

tipi di micosi. Pertanto, il principale obiettivo di questo lavoro di tesi è stato lo sviluppo di nuove formulazioni di AmB per il tratatmento topico e sistemico di micosi con ridotta tossicità. Sono state sviluppate due tipi di formulazioni.

Nella prima parte del lavoro di tesi lo studio si è focalizzato su formulazioni per uso topico. In particolare, si è sviluppato uno smalto per unghie contenente AmB per il tratatmento di onicomicosi miste resistenti ai tarttamenti tradizionali.

Nella seconda parte del lavoro di tesi sono stati condotti studi formulativi di AmB in collaborazione con l'Università degli Studi di Padova. In quetso caso si è sviluppata una formualzione di AmB fisicamente PEGilata per il trattamento sistemico di infezioni fungine dopo somministarzione orale o intravenosa. In questo caso si è considerato che AmB è nota interagire con molecole di colesterolo e in generale stereoidee che ne favorisono la sua solubilità. Pertanto, si sono prodotti bioconiugati di moelcole steroidee con PEG in grado di aumentare la solubilità e stabilità di AmB. Si sono quindi preparati bioconiugati PEG-cholane e si sono ottenuti diversi tipi di assemblati AmB/PEG-cholane che sono stati caratterizzati attarverso varie tecniche tra cui: DLS, HPLC, DSC, RX, FTIR, CD, ITC e analisi con sicrotrone. Negli studi *ex vivo* di questi complessi si è studiata la tossicità mediante test di emolisi e l'efficacia antifungina contro *Candida albicans*. Infine, sono stati condotti alcuni studi *in vivo* dopo somministrazione orale e intarvenosa a topi. Le proprietà farmacocinetiche delle formualzioni di AmB sono state esaminate comapartvamente rispetto al farmaco in soluzione libera e a prodotti commerciali quali Ambisome® and Fungizone®.

RESULTATI

Per quanto riguarda le formulazioni di AmB per uso topico, sono state preparate diverse formulazioni di smalto per le unghie sia permeabili che impermabili. Per queste preparazioni sono stati studiati il tempo sdi essiccamento, la visocsità, l'spetto del film, la stesura in film, la brillantezza, il pH e la capacià di incorporamento di AmB. Tra i vari prototipi formulativi preprati, ne sono stati slezionati tre che sono stati oggetto di ulteriori studi *in vitro* (F11, F13 and F19). Sebbene le formulazioni 11, 13 e 19 consentissero di superare i problemi di bassa solubilità di AmB, la stabilità nel breve periodo (1 mese) ha rappresentato ancora un grande limite al loro impiego. La strategia impiegata per superare i problemi d stabilità di AmB ha portato a considerare in particolare lo sviluppo di polveri da ricostituire estemporaneamente. Le tecniche di

freeze drying (nel caso di F11 e F13) e spray drying (nel caso di F19) hanno generato prodotti essiccati e liofilizzati stabili e facilmente risispersibili. Studi di penettrazione unghieale i*n vitro* condotti su unghie femminili umane, hanno dimostrato una maggiore penetrazione nel caso di F19 (EF=1.95) rispetto a F11, F13 e al controllo. Gli studi *in vitro* condotti con *Candida albicans* ha dimostrato che la formualzione più efficace era F19 (103%). Lo smalto per unghie contenente AmB è risultato efficace nel tratatmento di infzsione dermatofitiche e non-dermatofitiche non localizzate nelle strutture cheratinizzate. Il trattamento per 30 giorni con F19, somministarto una volta al giorno a giorni alternati, ha portato all'eliminazione dell'infezione di *T. mentagrophytes, T. rubrum, A. niger, F.oxysporum* and *F.solani*. Dopo 30 giorni di trattamento non si è rilevato alcun microorganizmo né per esame diretto né con studi con culture cellulari.

Per quanto riguarda le formulazioni PEGilate di AmB, gli studi di solubilità hanno dimostrato che il PEG_{5kDa}-cholane può aumentare fino a 10^5 volte la solubilità di AmB con una correlazione lineare [farmaco sciolto]/[polimero]. La diversa capacità del PEG_{5kDa}-cholane di solubilizzare AmB è stata ascritta alle diverse forme fisiche, monmeriche, multimeriche e aggregate del farmaco. Mediante calorimetria isotermica (ITC) è stata osservata una elevata affinità di AmB per PEG_{5kDa}-cholane. Questa tecnica ha evidenziato la complessità delle inetrazioni tra il farmaco e il polimero che avvengono con diverse forme di AmB, monomeri e multimeri, inclusi nanoaggergati solubili la cui composizione e abbndanza dipende dal pH. I tre diversi siti di binding calcolati mediante ITC risultano ragionevolemente dalle interazioni di varie zone idrofobiche eptaeniche di AmB con la frazione dell'acido colanico. Il processo di liofilizzazione ha prodotto una polvere soffice con basso contenuto di umidità senza formazione di un cake. Questo prodotto è risultato stabile nel lungo periodo. L'analisi spettoemtrica CD ha mostrato che come nel caso di Fungizone® e Fungizone® riscaldato, le micelle di AmB/PEG_{5kDa}-cholane non inuucono alterazioni struttirali di albumina (HSA). Gli studi di emolisi hanno confermato che le micelle di AmB/PEG_{5kDa}-cholane sono meno emolitiche di Fungizone®. Anche nel caso in cui Fungizone® induce il 100% di emolisi, la formulazione AmB/PEG-cholane non provoca più del 30% di emolisi. Gli studi di attività biologica hanno mostrato che AmB formulate con PEG_{5kDa}-cholane mantiene una elevata attività antifungina, che è risultata essere molto simile a quella di AmB in soluzione libera. La somministarzione orale di 5 mg/kg di AmB ha mostrato una maggiore emivita plasmatica del farmaco rispetto ad

alter formulazioni. Infine, la somministarzione intravenosa di 1 mg/kg di AmB in Ambisome®, Fungizone® e AmB/PEG_{5kDa}-cholane ha mostrato che la nuova formulazione ha una significativamente ($P<0.01$) minore costante di eliminazione apparente e una maggiore emivita plasmatica rispetto alle formualzioni commerciali Ambisome® and Fungizone®.

CONCLUSIONI

In questo lavoro di tesi vengono riportate le preparazioni di due tipi di formulazioni di AmB, una per uso topico per il trattamento di infezioni fungine unghieali (conclusione 1-3) e una formulazione per la somministrazione intarvenosa o orale per il trattamento di infesioni sistemiche (conclusione 4-12).

Conclusioni:

1.- Un nuovo smalto per unghie impermeabile conetenente AmB è stato prodotto per il trattamento di onicomicosi. Il polimero (Eudragit L100®) e AmB non hanno dimostarto incompatibilità con il solvente (N-methyl-2-pyrrolidone). Una volta applicato sulla superficie lo smalto forma uno strato omogeneo, continuo, liscio e resistente all'acqua.

2.- Studi i*n vitro* hanno dimostrato che lo smalto può penetrare le unghie con un incremento di quasi 2 volte rispetto al controllo. Studi di attività i*n vitro* hanno dimostarto l'efficacia dello smalto per unghie nel trattamento di dermatofiti e non dermatofiti quali muffe (tipo *Candida*).

3.- Gli studi di efficacia i*n vivo* condotti su cheratina di origine animale hanno dimostrato l'efficacia di AmB. Dopo un tratatmento di 30 giorni a giorni alternati, lo smalto per unghie ha eliminato le infezioni da *Trichophyton mentagrophytes*, *Trichophyton rubrum*, *Aspergillus niger*, *Fusarium. oxysporum* e *Fusarium solani*.

4.- E' stata sviluppata una nuova formualzione di AmB usando micelle costituite da un bioconiugato di 5 kDa monometossi polietilene glicole funzioanlizzato ad un terminale con acido colanico (PEG_{5kDa}-cholane). Il polimero aumenta la solubilità di AmB di 10^5 volte con un rapporto molare 12:1 AmB/PEG_{5kDa}-cholane (2:1 rapporto ponderale).

5.- Il sistema AmB/PEG_{5kDa}-cholane forma micelle di 30 nm con le frazioni iderofobiche localizzate nella parte interna delle vescicole. L'anali del potenziale zeta a vari pH (5.5-7.2) ha dimostrato che in superficie le micelle sono quasi neutre. Il

PEG_{5kDa}-cholane interagisce con AmB attarverso tre siti di binding a seconda del pH suggerendo che l'interazione con il polimero dipende dallo stato di ionizzazione e aggergazione di AmB.

6.- Dopo liofilizzaizone, il prodotto può essere estempraneamnete risdisperso per formare una dispersione omogenea colloidale. La dispersione è risultata stabile da un punto di vista fisicochimico. Studi condotti con FTIR, DSC and XRD hanno dimostrato che nel prodotto liofilizzato, AmB e PEG_{5kDa}-cholane interagiscono intimamente.

7.- Il rilascio di AmB dale micelle di PEG_{5kDa}-cholane è riusltato avvenire con un profilo bifasico. Il best fitting dei profili di rilascio è stato ottenuto con il modello di Higuchi e Korsmeyer-Peppas.

8.- La tossicità della nuova formualzione è stata testata in termini di emolisi. La nuova formulazione AmB/PEG_{5kDa}-cholane è sempre risultata meno emolitica rispetto al riferimento Fungizone®.

9.- L'attività antifungina di AmB testate contro *Candida albicans* ha mostrato che AmB/PEG_{5kDa}-cholane è 15% più attiva del farmaco in tampone.

10.- I profili farmacocinetici ottenuti per somministarzione intarvenosa condotti con Ambisome®, Fungizone® e AmB/PEG_{5kDa}-cholane sono risultati significativamente diversi. La costante di eliminazione apparente (Ke) della nuova formulazione è signficativamente ($P<0.01$) più bassa di quella ottenuta con Ambisome® e Fungizone®. Pertanto, il valore di emivita della nuova formulazione è risultata maggiore. Nei topi la somministarzione intravenosa di 1 mg/kg AmB/PEG_{5kDa}-cholane ha causto una minore sofferenza rispetto alla stessa dose di Fungizone® e Ambisome®.

11.- Gli studi farmacocinetici condotti per somministarzione orale hanno dimostrato che questa formualzione consente di ottenere una maggiore emivita rispetto ad Ambisome® e Fungizone®. L' AUC_{0-24} era simile in tutte le formualzioni testate.

12.- Si può quindi concludere che òa nuova formulazione AmB/PEG_{5kDa}-cholane è un sistema di veicolazione promettente in quanto stabile, con minore tossicità rispetto a AmB libera e rispetto al prodotto commericale Fungizone®.

1. INTRODUCTION

1. INTRODUCTION

1.1. Polyene antibiotics

Polyene antibiotics, produced by different species of *Streptomyces*, are considered as a chemical and biological subdivision of the macrolide class. They are characterized by the presence of a macrocyclic lactone ring (carbon atoms closed by lactonization) and a series of conjugated double bonds in their structure. Being the latter, the responsible for the differences observed in between the polyene and erythromicin groups. The main differences accounted for these groups (polyene and erythromicin) are related to the antimicrobial spectrum of action, the site of action and the mode of action [1]. While the erythromicin group is active against gram-positive bacteria, *Haemophilus, Brucella* and *Neisseria*, the polyene antibiotics are inactive against bacteria. With regards to the site of action, the polyene antibiotics act on sterol or ergosterol-containing membranes and the erythromycin group on the 70S ribosome. Finally, the mode of action of the polyene group is based on the alteration of the cell permeability, while the erythromycin antibiotics mechanism of action is based on the peptidyl synthetase inhibition and translocation.

Some of the already described polyene antimycotics, approximately 200 to date, are not unique or even pure [1, 2]. These polyenes differ ones to the others in the number of conjugated carbon-to-carbon double bonds, the size of the conjugated ring and the presence or absence of a hexosamine sugar or aromatic moeity in the molecule [3].

The antibiotics belonging to the polyene group are classified firstly, by the number of conjugated double bonds and secondly, by the presence or lack of a glycosidically linked carbohydrate in their structure [1]. The carbohydrate moiety, if present, is in all cases except for the perimycin, the hexosamine mycosamine. The perimycin has an isomer of the mycosamine (the perosamine) in its structure. Considering the number of double bonds, the polyene antibiotics can be classified as trienes, tetraenes, pentaenes, hexaenes and heptaenes. Tables 1-8 (adapted from [1] summarize the properties of each of the above mentioned groups.

Table 1. Properties of the trienes

Name	Producing organism	Chemical composition and molecular weight	References	
			Discovery	Chemistry
MM-8	*Streptomyces* sp.	4% N, no carbohydrates (Mw 726)	[4]	
Mycotrienin	*Strepromyces* sp.	C_{36} H_{50} N_2 O_8 (Mw 638)	[5]	
Proticin	*Bacillus licheniformis* var. *mesentericus*	C_{31} H_{45} O_7 P (Mw 560)	[6]	[7]
Resistaphylin	*S. antibioticus*	C_{24} H_{34} N_2 O_7 (Mw 463)	[8]	
Trienine	*Streptomyces* sp.	C, 54.7; H, 8; N 1.3 to 1 (Mw 1,300)	[9]	

Table 2. Properties of the mycosamine-containing tetraenes

Name	Producing organism	Chemical composition and molecular weight	References	
			Discovery	Chemistry
Amphotericin A	*Streptomyces nodosus*	C, 60.3; H 8.4; N 1.7 (Mw 915)	[10]	[11]
Lucensomycin	*S. lucensis*	$C_{36}H_{53}NO_{13}$ (Mw 708)	[12]	[13-15]
Nystatin	*S. albulus* *S. noursei*	$C_{47}H_{75}NO_{17}$ (Mw 926)	[16]	[17]
PA 166	*Streptomyces* sp.	$C_{35}H_{53}NO_{14}$ (Mw 712)	[18]	[19]
Pimaricin (Tennecetin)	*S. natalensis* *S. chattanoogensis* *S. gilveosporus*	$C_{33}H_{47}NO_{14}$ (Mw 666)	[20]	[21]
Rimocidin	*S. rimosus*	$C_{38}H_{63}NO_{13}$ (Mw 742)	[22]	[23]
Tetramycin	*S. noursei* var. *jenensis*	$C_{34}H_{53}NO_{14}$ (Mw 699)	[24]	
Tetrin A	*Streptomyces* sp.	$C_{34}H_{51}NO_{13}$ (Mw 681)	[25]	[19]
Tetrin B	*Streptomyces* sp.	$C_{34}H_{51}NO_{14}$ (Mw 697)	[25]	[26]
Unamycin A	*S. fungicidicus*	C, 52.2; H, 7.8; N, 1.7; O, 38.3	[27]	

Table 3. Properties of other tetraenes

Name	Producing organism	Chemical composition and molecular weight	References	
			Discovery	Chemistry
Akitamycin	*Streptomyces akitaensis*	C 53.7; H, 7.7; N, 1.65	[28]	[29]
Antimycoin A	*S. aureus*		[30]	
Chromin	*S. chromogenes*	C, 58.2; H, 7.8; N, 2.3	[31]	[32]
Endomycin A	*S. endus* *S. hygroscopicus* var.	- (Mw ≈845)	[33]	[34]

	enhygrus			
Polifungin	*S. noursei* var. *polifungini*		[35]	[36]
Protocidin	*Streptomyces* sp.	$C_{29}H_{45}NO_{13}$ (Mw 615)	[37, 38]	[39]
7071-RP	*Streptomyces* sp.	C, 58.3; H, 8; N, 1.65; O, 31.5 (Mw 859)	[40]	
Sistomycosin	*S. viridosporus*	Contains N	[41]	

Table 4. Properties of methylpentaenes and lactone-conjugated pentanes

Name	Producing organism	Chemical composition and molecular weight	References	
			Discovery	Chemistry
Methylpentaenes				
No carbohydrate:				
Aurenin	*Streptomyces aureorectus*	$C_{33}H_{54}O_{11}$ (Mw 626)	[42]	
Cabicidin	*S. gougeroti*	$C_{35}H_{60}O_{13}$ (Mw 688)	[43]	
Chainin	*Chainia* sp.	$C_{33}H_{54}O_{10}$ (Mw 610)	[44]	[45]
Durhamycin	*S. durhamensis*	C, 63.8; H, 10.2; O, 25.5	[46]	[47]
Filipin complex (I-IV)	*S. filipensis*	$C_{35}H_{58}O_{11}$ (Mw 655) (Filipin III)	[48]	
Fungichromin (lagostin)	*S. cinnamomeus* var. *cinnamomeus* *S. roseoluteus* *S. cellulosae*	$C_{35}H_{58}O_{12}$ (Mw 671)	[49]	
Neopentaene	*Streptomyces* sp.	C, 61.3; H, 8.8	[50]	
Pentaene	*S. sanguineus*	C, 62.1; H, 9.2; O, 28.9		
Pentamycin (moldcidin B)	*S. pentaticus*	$C_{35}H_{60}O_{13}$ (Mw 688)	[51]	[52, 53]
Xantholycin	*S. xantholyticus*	C, 70.6; H, 9.8; O, 19.7		
Contains carbohydrate:				
Moldcidin A	*Streptomyces* sp.	$C_{42}H_{81}NO_{19}$ (Mw 903)		
Lactone-conjugated pentaenes				
Flavomycoin	*S. roseoflavus* var. *jenensis*	$C_{41}H_{68}O_{10}$ (Mw 721)	[38]	[54]
Mycoticin A (Flavofungin)	*S. ruber*	$C_{37}H_{60}O_{10}$ (Mw 664)	[55]	[56]

Mycoticin B	*S. flavofungini*	$C_{36}H_{58}O_{10}$ (Mw 651)	[57]	[58]

Table 5. Properties of "classical" pentaenes

Name	**Producing organism**	**Chemical composition and molecular weight**	**References**	
			Discovery	**Chemistry**
Contain mycosamine				
Eurocidin A	*Streptomyces albireticuli* *S. reticuli*	$C_{40}H_{65}NO_{15}$ (Mw 800)	[59]	[60]
Eurocidin B	*S. eurocidicus*	$C_{39}H_{63}NO_{15}$ (Mw 787)		
Contain N in unspecified form:				
Aliomycin	*S. acidomyceticus*	Contains S	[61]	
Capacidin	*Streptomyces* sp.	$C_{54}H_{85}N_2O_{18}$ (Mw 1,049)	[62]	
HA106	*Streptoverticillum cinnamoneum* var. *sparsum*	-	[63]	
HA 135	*Streptoverticillum sporiferum*	-	[63]	
HA145	*Streptoverticillum cinnamoneum* var. *albosporum*	-	[63]	
HA 176	*Streptoverticillum cinnamoneum* var. *lanosum*	-	[63]	
PA 153	*Streptomyces* sp.	$C_{37}H_{61}NO_{14}$ (Mw 744)	[18]	
Pentaene	*S. effluvius*	C, 58.4; H, 8.2; N, 2; O, 21.3		
Compound 616	*S. parvisporogenes*	C, 62; H, 7.8; N, 2.7; O, 27.5		
Insufficient data for further classification:				
Distamycin B	*S. distallicus*	$C_{22}H_{27}N_9O_4$ (Mw 481.5)		
Fungichromatin	*Streptomyces* sp.	No N	[48]	

Table 6. Properties of hexanes

Name	Producing organism	Chemical composition and molecular weight	References	
			Discovery	Chemistry
Contains no carbohydrate:				
Demostatin	*S. viridogriseus*	C, 64.9; H, 9; O, 26.1 (Mw 572)	[64]	[65]
Insufficient data for further classification:				
Cryptocidin	Streptomyces sp.	$C_{52}H_{83\text{-}86}NO_{17}$ (Mw 983-986)	[66]	
Endomycin B	*S. hygroscopicus* var. *enhygrus* *S. endus*		[33]	[67]
Flavacid	*S. flavus*	C, 61.6; H, 7.8; N, 1.1; O, 36.3	[68]	
Fradicin	*S. fradiae*		[69]	
Mediocidin	*S. mediocidicus*		[70]	
Mycelin	*S. roseoflavus* *S. diastatochromogenes* *S. fradiae*	N no N	[71]	
Mycelin IMO	*S. diastatochromogenes*		[72]	
Tetrahexin (also contains a tetraene chromphore)	*Streptomyces* sp. ATCC 14972	C, 65; H, 8.5; N, 1.3; O, 24.7	[73]	[74]

Table 7. Properties of heptaenes without aromatic moiety and heptaenes with N-methyl-p-aminoacetophenone

Name	Producing organism	Chemical composition and molecular weight	References	
			Discovery	Chemistry
Contain no aromatic moiety:				
Amphotericin B	*Streptomyces nodosus*	$C_{47}H_{73}NO_{17}$ (Mw 924)	[75]	[76]
Candidin	*S. viridoflavus*	$C_{47}H_{71}NO_{17}$ (Mw 922)	[77]	[78]
Mycoheptin	*S. netropsis*	$C_{48}H_{77}NO_{17}$ (Mw 939)	[79]	
X-63	*Streptomyces* sp.		[80]	
Contain N-methyl-p-aminocetophenone:				

Candimycin	*S. echimensis*	C, 57.2; N, 1.7; H, 8.2	[81]	[82]
DJ400B	*S. surinam*	$C_{66}H_{96}N_2O_{22}$ (Mw 1,269)	[83]	[84]
Perimycin	*S. coelicolor* var. *aminophilus*	$C_{47}H_{75}N_2O_{14}$ (Mw 892)	[85]	[86]
Insufficient data for further classification:				
Antifungin 4915	*S. paucisporogenes*	C, 63.6; H, 7.8; N, 2.8; O, 24.5	[87]	
Eurotin A	*S. griseus*		[88]	
Heptane 757	*Streptomyces* sp.		[89]	
Monicamycin	*Streptoverticillium cinnamomeus* var. *monicae*	C, 58.3; H, 7.85; N, 2.2	[90]	
Neoheptane	*Streptomyces* sp.		[91]	
PA 150	*Streptomyces* sp.	$C_{54}H_{82}N_2O_{18}$ (Mw 1,047)	[92]	

Table 8. Properties of the heptaenes which contains p-aminoacetophenone

Name	**Producing organism**	**Chemical composition and molecular weight**	**References**	
			Discovery	**Chemistry**
Ascosin	*S. canescus*		[93]	
Aureofungin	*S. cinnamomeus* var. *terricola*	C, 60.4; H, 7.9; N, 2.2	[94]	[49]
Ayfactin A	*S. viridofaciens*	C, 62.6; H, 7.8; N, 2.7	[95]	
Ayfactin B	*S. aureofaciens*	C, 62.5; H, 7.6; N, 2.8	[95]	
Azacolutin (F-17-C)	*S. cinnamomeus* var. *azacoluta*		[96]	[97]
Candicidin	*S. griseus*	Ca. $C_{63}H_{85}N_2O_{19}$ (Mw 1,200)	[98]	[99]
DJ 400 B_2	*S. surinam*	$C_{58}H_{86}N_2O_{21}$ (Mw 1,147)	[84]	[84]
Hamycin	*S. primprina*	C, 59.9; H, 7.8; N, 2.2; O, 20.1	[100]	[101]
Heptamycin	*Streptomyces* sp.	$C_{59}H_{93}N_2O_{22}$ (Mw 1,181)	[102]	
Levorin A	*S. levoris*	$C_{62}H_{114}N_2O_{22}$ (Mw 1,238)	[103]	
Levorin B	*S. hachijoensis*	$C_{61}H_{186}N_2O_{21} * 2H_2O$	[103]	

Trichomycin A	*S. abikoensis*	(Mw 1,230) $C_{58}H_{84}N_2O_{18}$ (Mw 1,097.29)	[104]	[105]

The polyene antibiotics are characterized by a really low solubility. The solubility values for these molecules are less than 1 mg/L at physiological pH (6-7) in water or water-free alcohols [106].

All the polyenes interact with sterols, change the membrane permeability of eucaryotic cells and lead to cell lysis [107]. Even though they have the same mechanism of action, their effects on artificial membranes and cells are different. The anion or cation selectivity of the membrane pores produced [108, 109], their relative preference for cholesterol or egosterol-containing membranes [110-113] and their progressive or "all-or-none" modes of action differ [114-117]. A lot of interest has been focused on these antimycotics during the last decades as they have demonstrated to have synergistic antifungal action with other agents [118], to have antitumoral effects [119] and some of them have been shown to have immunoadjuvant properties [120, 121].

Between all these polyene antibiotics, the heptaene non-aromatic polyene amphotericin B has been the most studied molecule of all the above described antibiotics. Its wide antifungal spectrum of action together with its antiparasitic and immunoadjuvant properties made researchers considered this molecule as a lead candidate for the treatment of systemic antifungal resistant infections and leishmaniasis.

1.2. Amphotericin B

1.2.1. Historical background

Amphotericin B (AmB), a polyene antibiotic with a characteristic yellow color, was first isolated in 1959 from cultures of *Sreptomyces nodosus* [122]. *Streptomyces nodosus*, a soil actinomycete, is an aerial mycelium that forms opened and closed spirals [123]. It produces gray spherical to oval spores and the tonality of the spores changes according to the composition of the culture media. It is a nonchromogenic SH_2-negative and strongly proteolitic microorganism. It grows in glucose, mannitol, inositol, xylose, rhamnose, fructose, trehalose and melibiose but no growth is detected in adonitol,

sorbitol, arabinose, cellulose, sucrose, lactose and raffinose. The optimal temperature for the growth of this microorganism is in the range 25-37°C [124].

In 1955, the *S. nodosus* strain was collected along the Orinoco delta in Tembladora, Venezuela by W. Gold, and the extracts obtained from this strain were first tested for its antifungal activity [125].

In 1987 Nicolaou *et al*. described for the first time the complete synthesis of the amphotericin B [126]. Even though this was the first published complete AmB synthesis, the high costs and low yields that this synthesis implied could not compete with the biotechnological production processes already set up and optimized. This is the reason why currently the AmB is only produced from strains of *Streptomyces nodosus* at a large industrial scale.

1.2.2. Physicochemical properties

1.2.2.1. Chemical structure

Amphotericin B is a mycosamine-containing, macrocyclic polyene antibiotic. Chemically it is a (1S, 3R, 4E, 6E, 8E, 10E, 12E, 14E, 16E, 18S, 19R, 20R, 21S, 25R, 27R, 30R, 31R, 33S, 35R, 37S, 38R)-3-[(2R, 3S, 4S,5S ,6R)-4-amino-3,5-dihydroxy-6-methyloxan-2-yl]oxy 19, 25, 27, 30, 31, 33, 35, 37-octahydroxy-18, 20, 21-trimethyl-23-oxo-22,39-dioxabicyclo[33.3.1] nonatriaconta-4, 6, 8, 10, 12, 14, 16-heptaene-38-carboxylic acid. Its molecular formula is $C_{47}H_{73}NO_{17}$ and its molecular weight 924.08 g/mol.

It is characterized by the presence of both hydrophobic (polyenehydrocarbon chain) and hydrophilic (polyhydroxyl chain) domains which confers the molecule its amphoteric nature. As detailed in figure 1, the hydrophilic domain is composed by seven hydroxyl groups and an ester, while the hydrophobic domain is constituted by seven double bounds. The heptaene chain is responsible for the rigidity of the molecule. Apart from the hydrophobic and hydrophilic parts, an internal hemiketal ring is contained. When the AmB is in solution the hemiketal is in equilibrium with the ketone opened ring [127]. The amphotericin B can behave as base or acid as a function of the pH. The carboxyl group (pKa of 5.5) and the amino group located in the mycosamine (pKa of

10) are both ionized at physiological pH [128]. The amphoteric character of this drug is responsible for its poor solubility in both aqueous and organic solvents.

Several chemical modifications on the C-16 carboxyl and/or in the 3' amino groups located in the mycosamine of the AmB have been extensively studied in order to improve the drug solubility. Nevertheless, these new semisynthetic derivates have been never marketed [129]. The hydroxyl groups located in the C-7 to C-10 region are key for the AmB antifungal activity. Therefore, the new approaches for obtaining amphotericin B derivates with higher efficacy and lower side effects are focused on changes on the C-7-C-10 region apart from the carboxyl group located in C-16 [130].

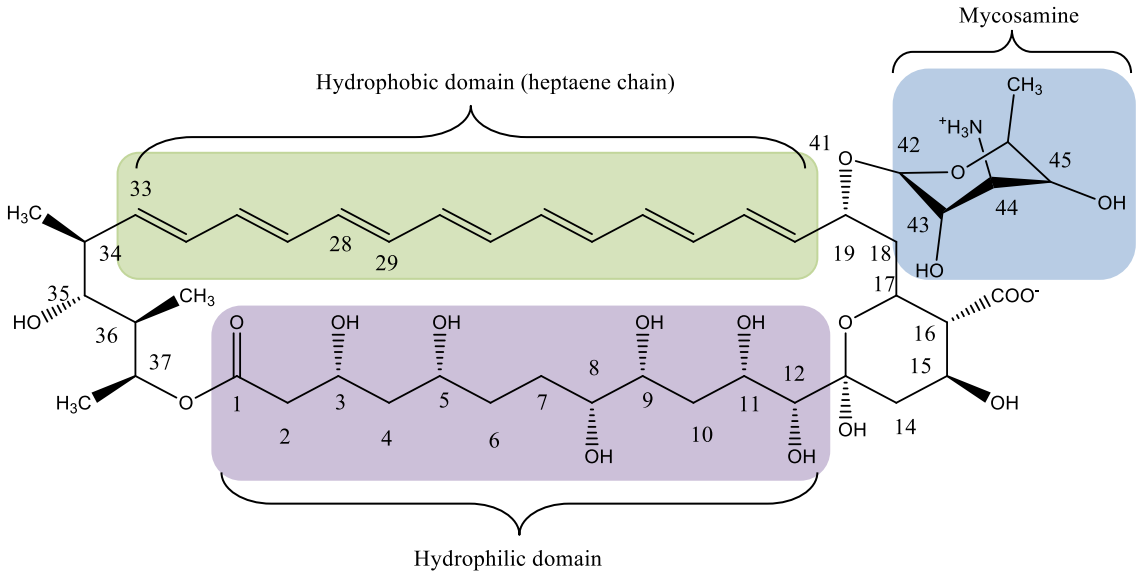

Figure 1. Chemical structure of amphotericin B

As detailed before, the AmB is produced by *Streptomyces nodosus*. This microorganism does not usually produce pure AmB. It generates a mixture of AmB and, in much lower amount, its reduced derivative amphotericin A (AmA). The C28-29 double bond in AmA is reduced, which implies a decrease in potency [131]. For this reason the production of amphotericin B at a large industrial scale should be closely controlled as the pharmacopoeias only accept as amphoterin B those products that contains a mixture of AmB and AmA in which AmB is at least in a 75% [132].

1.2.2.2. Solubility

As previously detailed for the polyene antimycotics, amphotericin B has limited solubility in water (table 9). At pH 6-7 its solubility is lower than 1 mg/L, reason why this drug is almost not orally absorbed (there is almost no gastrointestinal resorption) and it has to be parentally administered [106]. Even though at pHs below 2 (pH<2) and above 11 (pH>11) AmB is water-soluble, at this extreme pHs the molecule is not stable [133]. The AmB higher solubility at those acidic and alkaline pHs is explained by the formation of salts. However this increase in solubility is not only accompanied by a decrease in stability but also by a reduction in the antimycotic activity.

The AmB solubility in organic solvents is slightly higher than in water. Only dimethylsulfoxide (DMSO) solubilizes the AmB at more than 3 mg/mL.

Table 9. AmB solubility in different solvents [132].

Solvent	AmB solubility (mg/mL)
Dimethylsulfoxide	30-40
Ethylenglycol	2.6
Dimethylformamide	2-4
Methanol	2
Acetic acid	1-2
Propylenglycol	1-2
Ethanol	0.5
Acetone	0.35
Isopropyl alcohol	0.11
Alkalin or acidic water	0.1
Chloroform	0.08
Cyclohexane	0.02
Petroleum ether	0.01
Water at physiological pH	<0.001

Many attempts have been performed during the last decades to increase the amphotericin B solubility. First attempts were focused on the use of surfactants as sodium lauryl sulfate or sodium deoxycholate [132]. These solubilizers increased the not only the AmB solubility but also its toxicity [134]. Following attempts considered

the AmB solubilization with phospholipids and /or cholesterol [135] and recent attempts included the AmB covalently binding to polymers, its loading in particles or nanosuspensions, its solubilization in polymeric micelles, etc.

1.2.2.3. Aggregation State

Amphotericin B can be found in different aggregation states; monomeric, dimeric and polyaggregated. Not only the aspect of the AmB changes with the different aggregation states but also the activity, pharmacokinetics and drug toxicity are influenced.

In water suspensions three different AmB forms coexist: monomers, water soluble oligomers and non-water soluble aggregates [136-138]. The molecular weight (Mw) of these species consequently differs. A polyene antibiotic solution can contain species with molecular weights of approximately one thousand dalton (Da) (monomers) to few millions Da (colloid-type micelles) [139].

AmB molecules in the monomeric state are found at concentrations below 10^{-7} M. The critical aggregation concentration for amphotericin B (CAC) is very low, less than 1 µg/ml, which means that above those concentrations the molecules, will associate [134, 140]. These molecules are amphiphatic and thus, in aqueous media and with increasing drug concentrations, they have a high tendency to interact ones to each others (head-to-tail arrangement). The AmB monomeric molecules interaction is lead by hydrophobic forces. The interaction of one monomeric molecule with another (dimerization) forms dimers (figure 2A). The dimerization is considered as the first step of aggregation [141]. The consecutive steps in the aggregation process involves first, the interaction of two dimers which generates a tetramer (figure 2B) and secondly, the interaction of dimers with tetramers constituting larger aggregates. The AmB monomers and self-associated species (oligomers) are water-soluble while the association of oligomers are non-water soluble [136].

Chemically, the interaction between two monomers (dimer) is stabilized by the hydrophobic interactions of the chromophores and the hydrogen bonds formed between the hydroxyl group on C35 and the oxygen located in between the C42 and the C19. On the other hand, the dimers association into tetramers results from the hydrogen bonds formed between the hydroxyl groups in C8 and C3 [142,143]. The external surface of

the tetramer is constituted by the polyene hydrophobic chains which allows for the interaction with other AmB molecules through van der Waals forces [132].

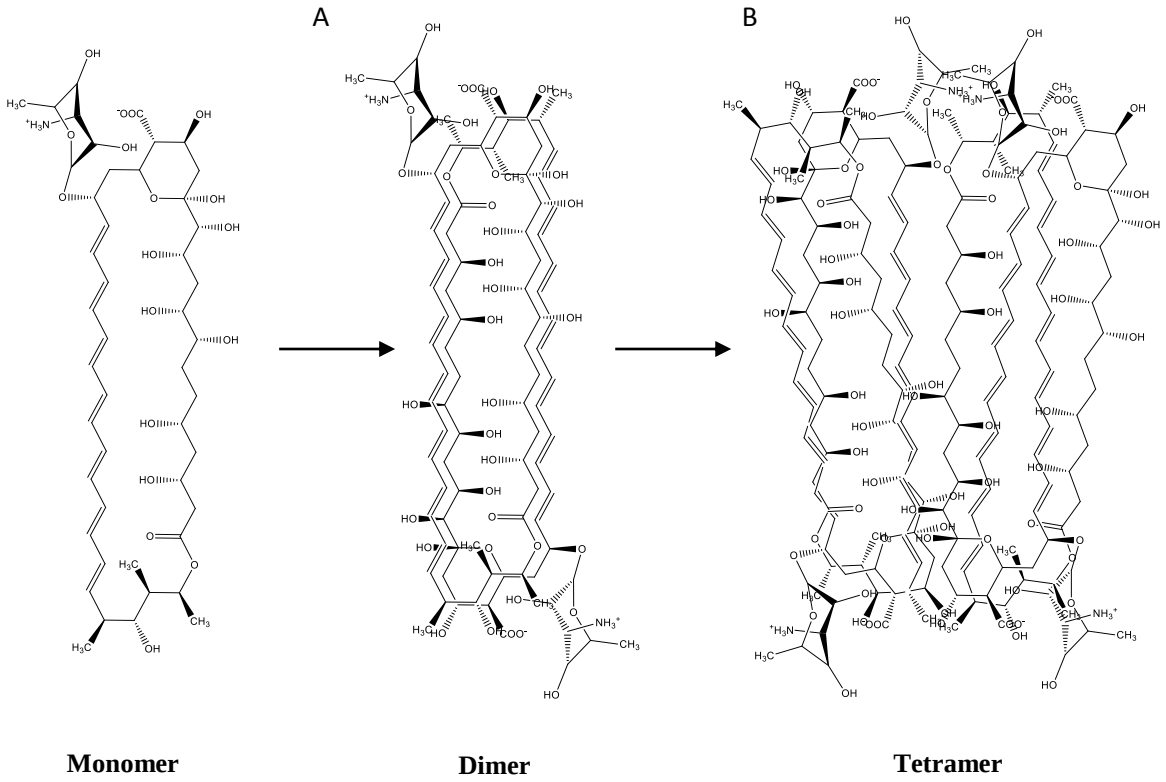

Figure 2. Amphotericin B aggregation process

When the AmB is dissolved as monomers it produces yellow transparent solutions. The dimeric aggregation state generates yellow-orangish translucid colloidal dispersions and finally, the AmB polyaggregates are found as yellow opaque suspensions.

The aggregation properties of the AmB are influenced by pH changes [144]. At pH 7.4 the polyene antibiotic molecules are zwitterions. The dimerization and association constants at this pH suggest that the most soluble species are the dimers. On the contrary, in acidic and alkaline media, (below pH 2 or above pH 10) the AmB molecules have net charge. In this case, the dimerization and association constants decrease due to the repulsive forces between molecules with the same sign of net charge and therefore the AmB is found mainly as monomers [145].

Permeation studies performed by Bolard *et al* in 1991 demonstrated that only self-associated AmB induces damage in cholesterol-containing cells [146]. Two self-association forms of AmB are found in water; one water soluble and another one non-

water soluble. In 1992 Legrand *et al* reported that only the water soluble self-associated species were responsible for the AmB toxicity [136]. Both studies were in fair agreement with the hyphotesis of Gruda and Dussault [147] based on the lower toxicity of the AmB when administered as monomers compared to dimers. Therefore, the AmB monomers are non-toxic towards mammalian cells, permeating only fungal cells, while the water soluble self-associated species are non selective. They are toxic to both mammalian and fungal cells.

The proportion of these chemical species, as well as the aggreation state, depends not only on the AmB concentration but also on the dilution, the AmB solubilizer (organic solvent, surfactant or polymer), the mixing method, the mixing temperature, etc. [148]. The rate of AmB aggregation, for example, is strongly increased with dilution [149].

In order to decrease the AmB associated toxicity in water at physiological pH many strategies have been developed during the last decades (the dimers are the main species found in water at pH 7.4). The use of surfactants that maintain the AmB in the monomeric state [150]; the heat of AmB to produce a new self-associated state ("superaggregates") [151] as well as the inclusion of the polyene antibiotic into carriers, are some of the techniques that have acquired a high relevance in the design of new AmB formulations. As shown in figure 3, the AmB loading into carriers must assure a controlled drug release. Independently of the initial AmB aggregation state, the drug delivery system (DDS) should release the AmB as monomers below the critical aggregation concentration. If the AmB is slowly released in monomers, the rearrangement of AmB molecules into soluble aggregates, once in blood, will not take place and the nephrotoxicity and neurotoxicity will be avoided. Any method that decreases free AmB concentration in plasma is expected to reduce its direct toxicity [151]. Moreover the carriers' integrity upon dilution is a key factor in the design of non-toxic formulations. The carriers should maintain their integrity once injected in plasma in order to avoid the fast AmB release and molecules re-aggregation [152].

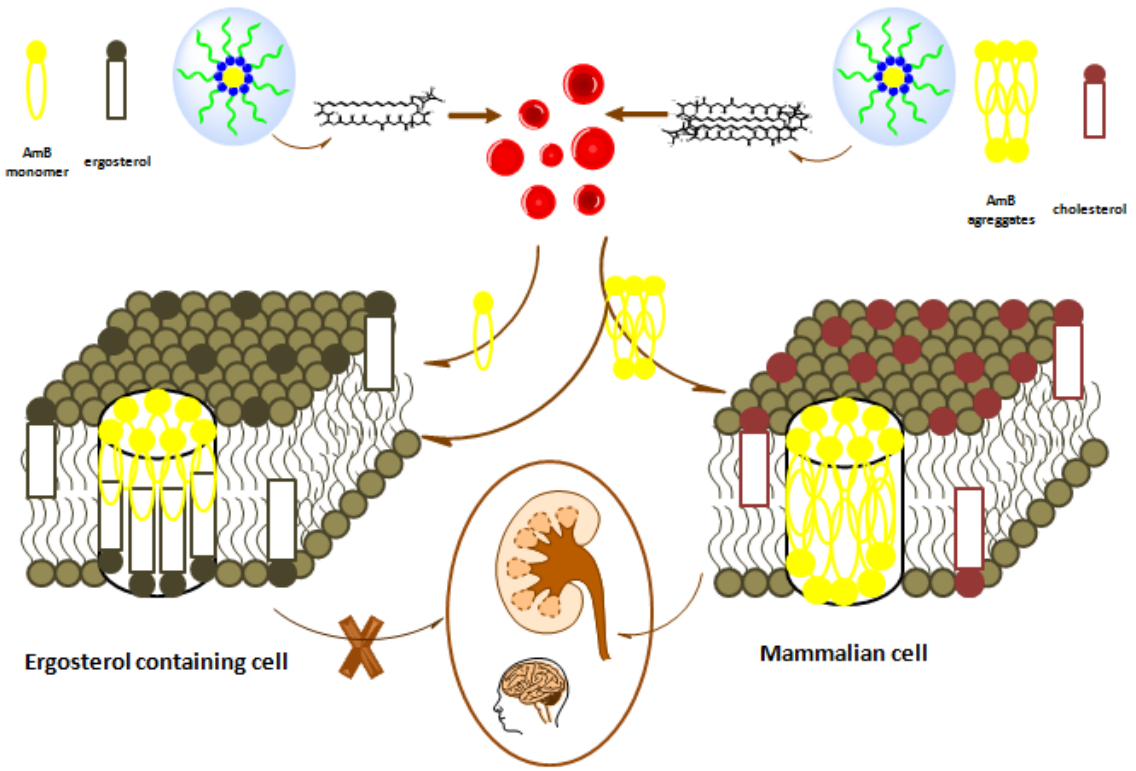

Figure 3. AmB selectivity and toxicity against ergosterol/cholesterol cells depending on the aggregation state. On the left side, AmB being release as monomers and damaging ergosterol cells. On the right side, AmB being released as aggregates and damaging both cholesterol and ergosterol cells.

1.2.2.4. Ultraviolet-Visible spectroscopy

As detailed in point 1.2.2.1, the AmB has a heptaene chain on its structure. These seven conjugated double bonds have a key role on AmB spectroscopic properties. They behave as cromophore.

The ultraviolet (UV) spectra of the AmB differs with increasing drug concentrations (Figure 4) and therefore, the UV spectroscopic analysis are very helpful for the study of the different AmB aggregation states (the aggregation state of the AmB varies with increasing drug concentrations).

At very low concentrations ($< 10^{-7}$ M) the AmB is found as monomer and it spectrum is similar to that obtained for the polar organic solvents [139]. The heptaene chromophore characteristic absorption spectrum is obtained at these low concentrations. As observed in figure 4 (M-AmB), four well-separated bands at 344-350 nm, 363-368, 393-388 and 406-412 nm are detected [153-155].

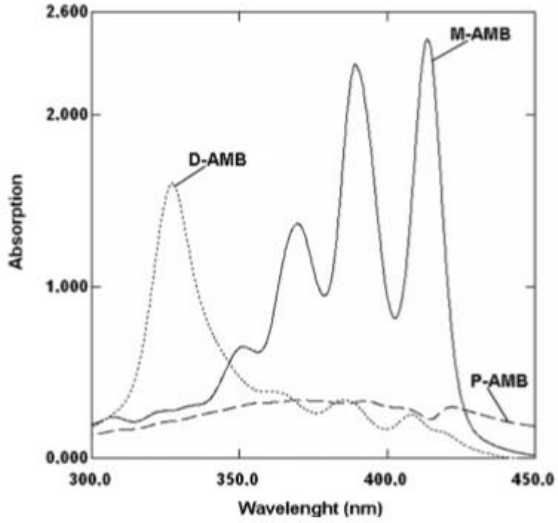

Figure 4. Amphotericin B UV-Visible absorption spectra of its different aggregation states: monomer or M-AmB (___), dimer or D-AmB (.....) an polyaggregate or P-AmB (_ _ _) [156].

With increasing AmB concentrations the spectrum changes, and at concentrations above 10^{-4} M, a completely new spectrum is defined. This is due to the formation of small oligomers, mainly dimers [138].

The dimeric profile of amphotericin B is characterized by a intense band at 328-340 nm due to an hyperchromic shift [157] and less intensive bands at 363-368 nm, 383-388 nm and 406-412 nm due to an hypochromic effect. Moreover in this dimeric profile there appears a new band located at 415-425 nm (bathochromic shift) (figure 4, D-AmB).

At higher AmB concentrations, the chomophore groups from the AmB molecules interact through hydrophobic forces and form bigger aggregates (polyaggreagates). This interaction results in a decrease in bands absorption (hypochromic effect). As shown in figure 4 (P-AmB) the bands located at 360-363 nm, 383-385 nm and 406-420 nm have almost no absorption. This is in accordance to Rinner *et al* publication which stated that the larger AmB aggregates are almost not detected through the spectroscopic techniques [158].

1.2.2.5. Infrared spectroscopy

The first information regarding the infrared spectrum (IR) of amphotericin B was published in 1977. Schwartzman *et al* described two types of forms possibly found in

AmB powders. They demonstrated that the IR spectrum of AmB presented at room temperature, a mixture of two different forms called Types I and II [159]. The first type predominated in hand-ground samples while the second type was mostly found in vibrator ground samples. Both types differed in the size of the fragments which were smaller for Type II compared to Type I. Type I spectrum (figure 5A) was characterized by a sharp C=O stretching band at 1692 cm^{-1}, a C=C stretching band at 1556 cm^{-1} and C-H bands and stretching bands at 850, 1380 and 2680 cm^{-1}. On the contrary, Type II spectrum (figure 5B) showed, in general, broader an less resolved bands which included a broad C=O stretching band at 1712 cm^{-1} and a C=C stretching band at 1566 cm^{-1}. The bands located near 900, 1233, 2930 and 2970 cm^{-1} also differed between types I and II. The differences found in between samples seemed not to be related to the particle size.

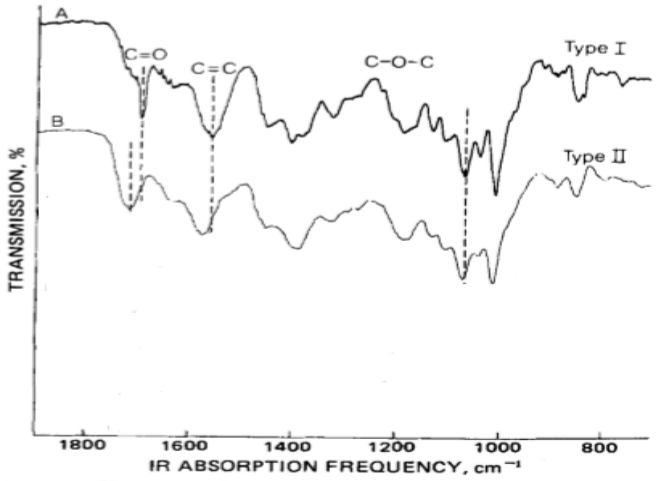

Figure 5. IR spectra of amphotericin B. Hand-ground (A) and vibrator-ground AmB powders (B) [159].

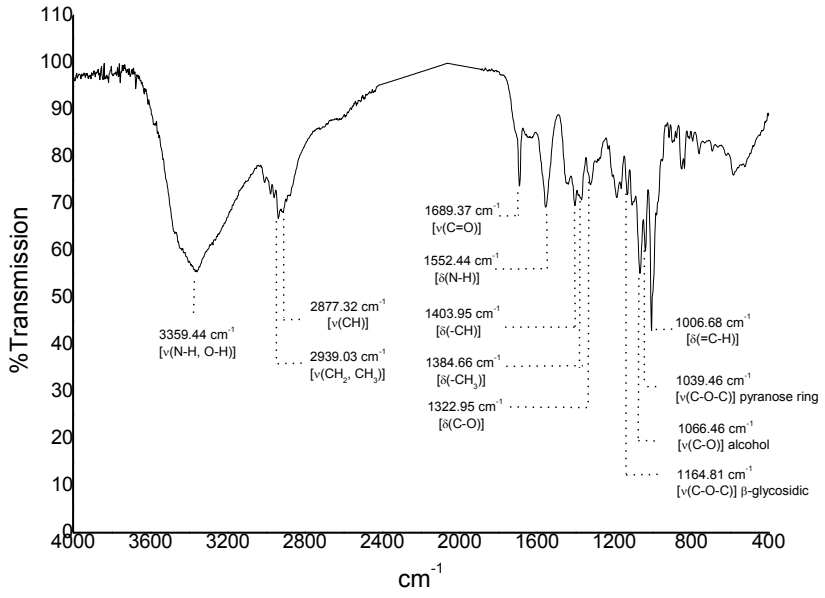

Figure 6. FT-IR Spectra of AmB. ν (stretching vibrations), δ (bending vibrations).

These summarized descriptions of the bands have been completed over the last years. The recent AmB analyses through Fourier-Transform infrared (FT-IR) spectroscopy have been able to detect and identify the main AmB functional groups. From all the peaks observed in figure 6, the ones located at 1689 cm^{-1} and 1552 cm^{-1}, corresponding to stretching vibrations on C=O and bending vibrations on NH_2 respectively, are the most important. This is supported by the fact that those functional groups are directly related to the physicochemical and pharmacological properties of the AmB [108].

1.2.2.6. X-ray diffraction analysis

Amphotericin B is known to have a crystalline structure. The degree of crystallinity in AmB at different conditions have been deeply studied so far [159], concluding that not only the crystalline structure varies with the preparation process (ground) but also with the temperature.

The X-ray diffraction spectrum of the amphotericin B (unheated or unground) demonstrates the crystal structure of the molecule (figure 6A). When the amphotericin B is heated or grounded by vibration, the diffraction pattern changes (figure 6B). On one hand, the heating at 158ºC (figure 6A) reveals a pattern with less intense peaks,

increased background and slight changes in *d*-spacings (the amorphous fraction is increased). On the other hand, the vibrator-ground powder shows very low intense and broad peaks (figure 6B). This pattern is typical of amorphous powders.

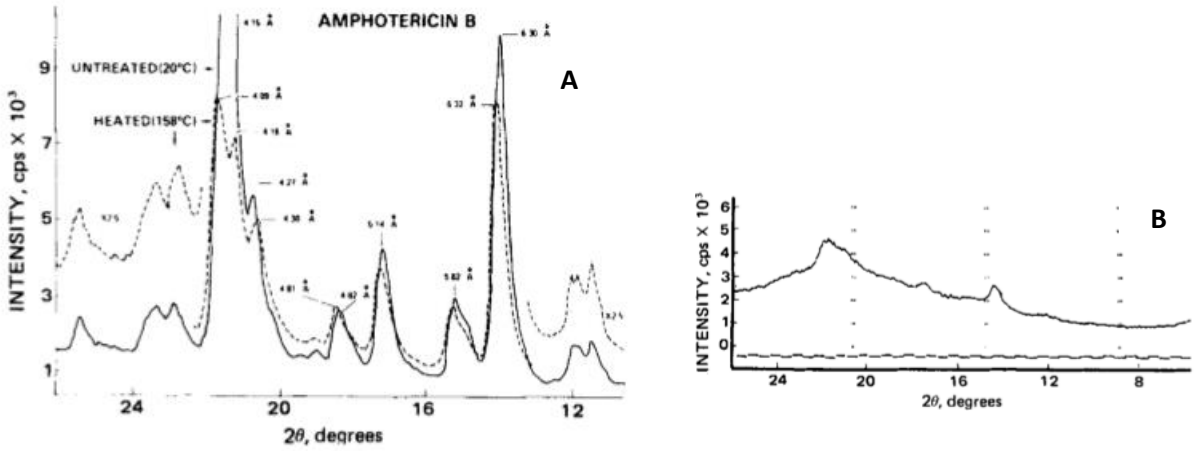

Figure 6. X-Ray spectrum of amphotericin B. (A) Unheated versus heated AmB at 158ºC. (B) Vibrator-ground AmB powder [159].

1.2.3. Mechanism of action

Amphotericin B mechanism of action is still not well determined. It seems that the AmB affects cells at two levels [160]:

- Binding to the ergosterol contained in the membranes and
- Inducting oxidative damage.

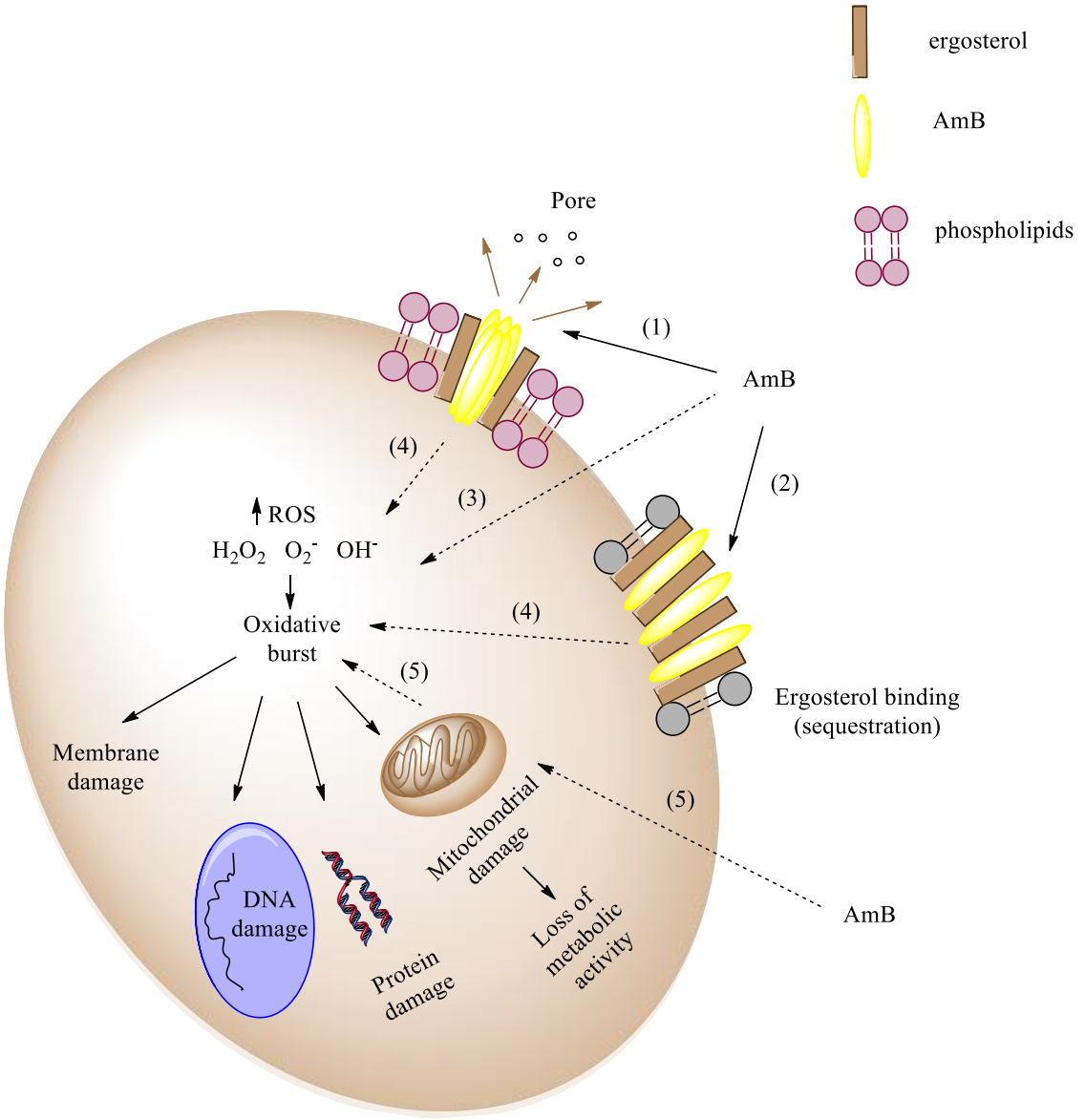

Figure 7. Amphotericin B mechanism of action on fungal cells. At the membrane, pores formation (1) or ergosterol sequestrion (2). Inside the cell the AmB can induce oxidative burst through different pathways: acting directly as prooxidant (3), first binding to ergosterol and then oxidizing (4) or influencing the mitochondrial activity (5).

The amphotericin B effect on the cell membrane can lead to pore formation or ergosterol sequestration while, its intracellular effect falls on the induction of oxidative stress (figure 7).

1.2.3.1. AmB effects on cell membrane

AmB has the ability to insert into the fungal and parasitic lipid membrane bilayer. This insertion takes place through its hydrophobic domains. As a result of this interaction multimeric pores are formed in which the hydrophobic domains (polyene chains) of the drug are in contact with the membrane lipids. The pores increase the cell permeability to small cations such as K^+, Ca^+ and Mg^+, leading to a loss of intracellular ions and therefore, cell death.

AmB does not only bind to ergosterol containing cells but also to others sterols cell membranes, such as cholesterol (mammalian cells). However, the affinity of AmB for other sterols is lower than for ergosterol. It has to be considered, as detailed in point 1.2.2.3 that the affinity, and therefore the toxicity of AmB for the different sterols depends on its aggregation state.

AmB binding to ergosterol or cholesterol-containing membranes can take place in two different ways (figures 8 and 9).

Figure 8 (adapted from [161]) shows the hydrogen bonds formed between the sterols and the drug. These constitute the first type of interaction. This interaction forms a "cage" like structure in which the hydrogen bonds are mainly formed in between the hydroxyl groups of the sterol and the carboxyl group in C-18 of the AmB. The presence of water is responsible for this type of interaction. The AmB mycosamine amine group also participates in this binding; it strengthens the AmB-sterol interaction. As both, ergosterol and cholesterol molecules are 3-β-hydroxy sterols, their hydrogen bond reaction with AmB is assumed to be similar [161].

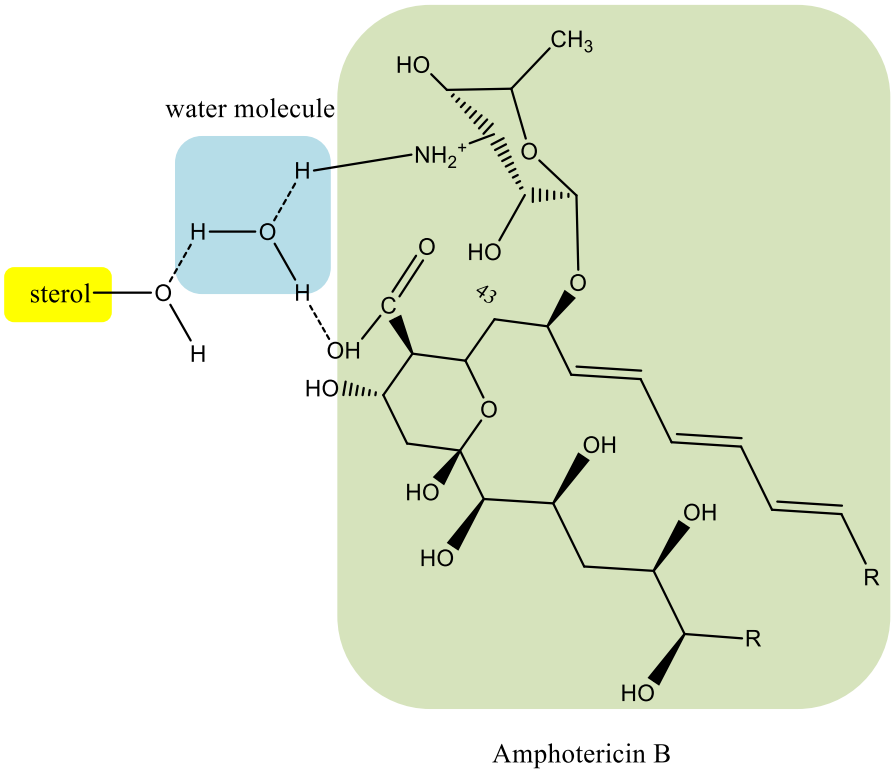

Figure 8. Interaction between AmB and sterols through hydrogen bonds.

The second type of interaction (figure 9) is based on the Van der Waals forces that might appear between the polyene rigid chain (7 double bonds) of AmB and the whole sterol molecule. A study performed in 1989 by Hervé *et al*., concluded that the greater affinity of AmB to ergosterol compared to cholesterol was explained by the double bond located in C-22 of ergosterol [162, 163]. The conformational studies of both molecules showed that the overall shape of ergosterol conformers was flat while the cholesterol flat shape was just one of its possible conformations. The absence of a double bond in the side chain of cholesterol (C-22) confers more flexibility to this molecule [161,164] .

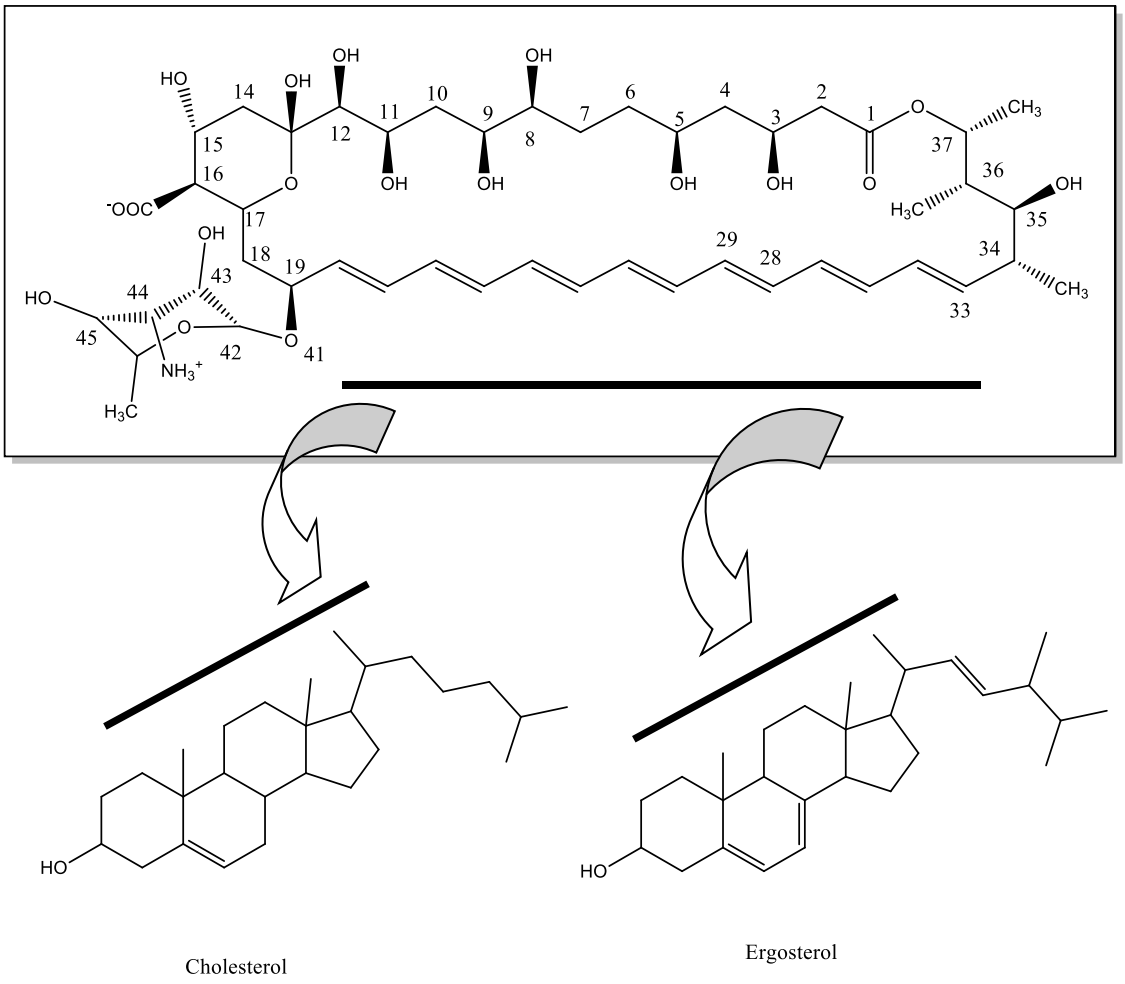

Figure 9. Interaction between AmB and cholesterol or ergosterol through Van der Waals forces.

In 2011, Palacios *et al*., described two different mechanisms for AmB cell membrane damage: sterol sequestration (membrane destabilization) and membrane permeabilization (ions depletion) [165]. The sterol, and concretely, the cholesterol sequestration by AmB, avoids the interaction of parasite-macrophage in the *Leishmania* infections. This mechanism, even though, will cause damage on the host cells as the cholesterol is sequestrated, is considered as a novel and useful AmB mechanism for the treatment of visceral Leishmaniasis [166]. Ergosterol is needed in a large number of cellular processes: endocytosis, vacuole fusion, stabilization of proteins, etc. [167]. AmB binding and sequestration of ergosterol is enough to damage cells due to the multiple cell processes in which ergosterol is implied. The pore formation enhances to the antifungal efficacy but it is not essential for the fungal cells death [168].

As for the pore formation is concerned, several studies have revealed that AmB forms two different kind of pores. The mechanism of AmB pore formation as well the mechanism of AmB membrane entrance are still very unclear. Some hypothesize that the AmB monomers enter in some way the membrane and form binary complexes with the lipids located at this level, generating the channels. This is called "sequential" mechanism. Others hypothesize that AmB supramolecular complexes are firstly formed in the membrane surface and then enter the membrane producing a membrane reorganization towards functional channels. This is considered as the "one step" mechanism [169].

The two types of AmB pores are formed in different moments and their substrate specificity and killing effects are different [160,170]. After cells contact with AmB the non-aqueous pores are firstly formed. These pores are permeable to monovalent cations but show low affinity for monovalent anions [171]. Later on, the aqueous pores are formed. In this case, the pores are permeable to monovalent anions and cations, and large electrolytes (eg. glucose). The pore formation is a fast process that usually takes place in milliseconds [160]. Depending on the membrane composition (content of ergosterol or cholesterol) and the AmB delivery system, the speed of the process and the AmB concentration needed to form the pores differs [172].

Figure 10, taken from [173] simulates the AmB-cholesterol/ergosterol channels. The yellow balls simulate the sterols molecules; the red balls represent the AmB carboxyl groups and, the N-P and O-N refer to the interactions that take place between the amine group of the AmB and the phosphate of the dimyristoylglycerophosphatidylcholine (DMPC), and between the oxygen of the AmB carboxyl group and the amine of the DMPC when the distance in between them is lower than 4Å. This model is in fair agreement with other previously described simulations in which the AmB-sterol channel is composed by eight AmB and sterol molecules non-covanlently associated [174,175]. These channels are surrounded by 34 DMPC molecules, have cylindrical shape and are solvated in both sides and in the interior by 1666 water molecules [173].

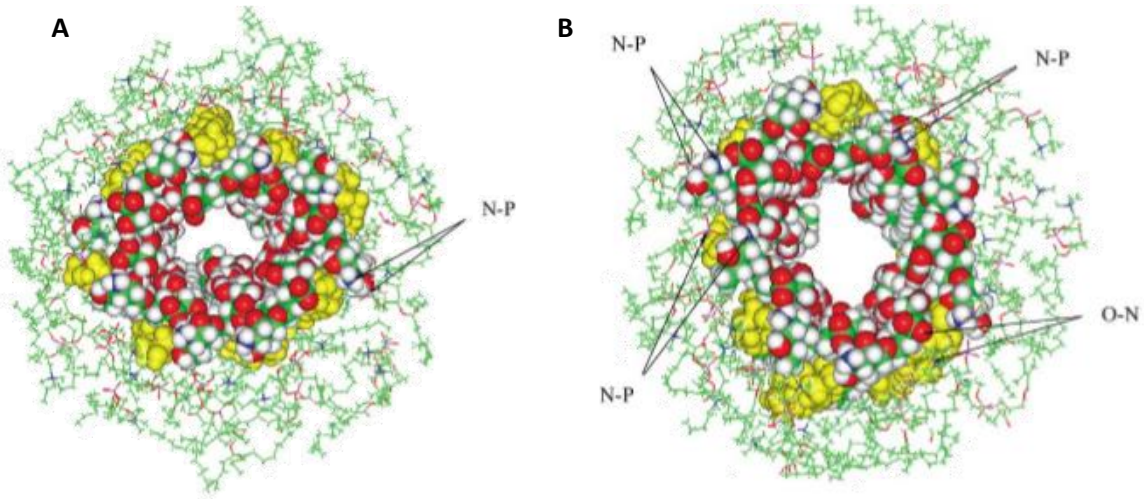

Figure 10. Simulation of AmB channels formed with cholesterol (A) and with ergosterol (B). Figure adapted from [173].

Even though it has been widely accepted that sterol presence in the membrane is necessary for the AmB pore formation so **B** studies have revealed that the antibiotic is able to conduct channels even in the absence of sterols. Nevertheless, the drug concentration required to form pores in these conditions, is much higher than in the presence of sterols [176,177].

As previously detailed, the small structural differences found for cholesterol and ergosterol are enough to produce great disimilarities in AmB affinity. These disimilarities can be explained by the fact that many AmB molecules are involved in the formation of single membrane channels. The cumulative effect of such slight differences can significantly influence the stability of the pore [173]. Apart from the non-aqueous and aqueous pores, AmB can form two types of channels; single-length channel (SLC) and double-length channel (DLC). The DLCs are formed when two SLCs are arranged into a tail-to-tail configuration [178]. The DLCs are only form when the antibiotic is added from both sides of the membrane, reason why the SLCs are considered as the only possible channels during *in vivo* administration.

1.2.3.2. Induction of oxidative damage

Apart from the study performed by Gray *et al* [168], several other studies have demonstrated that pore formation is not enough to produce cell death [160] and that the chemical modifications on the AmB domains responsible for the pore formation, do not affect its antifungal activity [179]. Therefore, AmB may generate other killing mechanisms. Mowat *et al* [180] and Sokol-Anderson [181] described the AmB mechanism of action as complex. It depends not only on the growth phase of fungi but also on the presence of oxygen in between other factors. In this sense, as demonstrated by Sokol-Anderson, the addition of antioxidants (eg. superoxide dismutase) protects *C. albicans* from the lytic effect of AmB. In 2005, Liu *et al* [182] published a paper in which they described the AmB induction in stress genes expression.

Many studies have been performed during the last years but the oxidative damage role of AmB on its antifungal activity is still unknown.

1.2.3.3. Immunomodulatory properties

Apart from its antifungal and antiparasitic effect, AmB has also immunostimulatory properties [183]. The AmB enhancement of the host immune response offers another alternative mechanism of action for this antifungal drug. However, it has an important drawback. The immunomodulatory effect has been related to the AmB associated toxicity [160].

The AmB interaction with endothelial cells, finally leads to an increase in nitric oxide (NO). The AmB increases the expression of the inducible isoform of the nitric oxide synthase (iNOS) which produces the rise of NO production. NO is implied in the vasodilatation and protection processes against pathogens [184]. The proinflammatory effect of AmB has been associated with protective effects during infection [160]. Opposite to this protective effect some studies have revealed that the increase in proinflammatory cytokines is related to the drug toxicity in the host [185]. The AmB renal toxicity has been somehow related to modifications in the expression of NO synthase and the induction of apoptosis [186].

Even though, the drug immunomodulatory mechanism is not well known, the AmB seems to interact to the toll-like receptors (TLR), mainly TLR2 and TLR4, and to CD14

receptors (figure 11) [160]. When AmB binds TLR2, there is a release of proinflammatory cytokines (IL-6, IL-8, TNFα, MCP-1, MCP-1) while the interaction with TLR4 produces a release of anti-inflammatory cytokines (IL-10) [132,160,187]. The AmB interaction with CD14, activates the TLR signaling pathway [188].

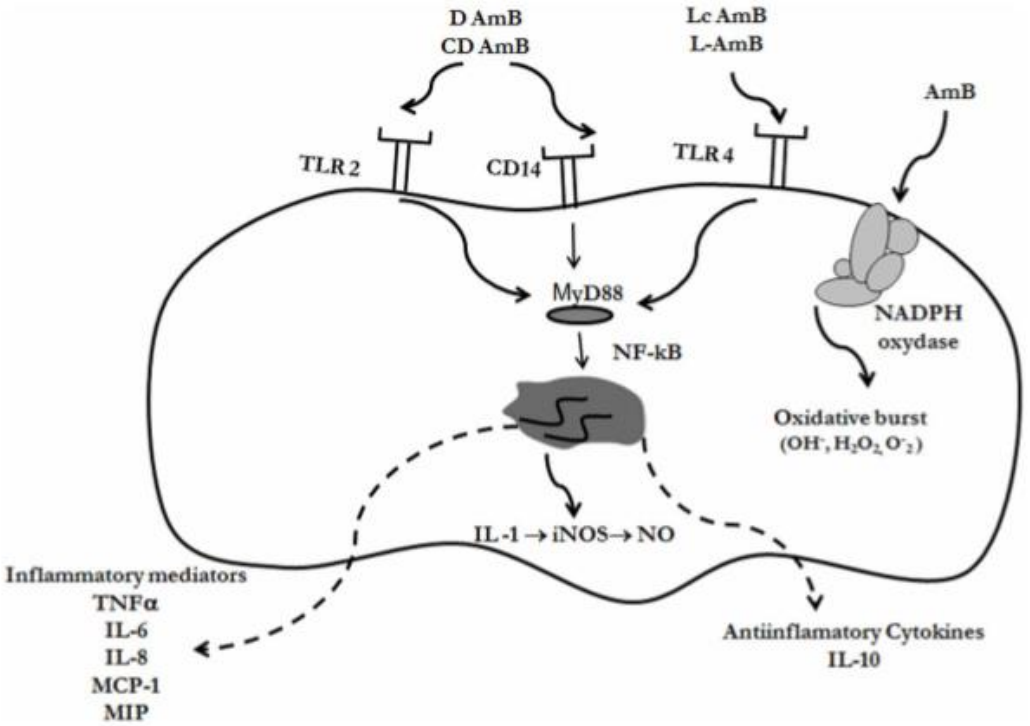

Figure 11. Immunomodulatory effects of AmB [160].

Moreover, the AmB binding to sterols can lead to conformational changes that could activate some membrane enzymes as NADPH oxidase, involved in the oxidative stress. The enzymes activation will finally generate the accumulation of free radicals with antimicrobial properties (reactive oxygen species, ROS) [132].

1.2.4. Pharmacokinetics

Amphotericin B is considered as a class IV drug according to the Biopharmaceutical Classification System (BCS). Class IV drugs are characterized by low solubility and

low permeability properties. The amphoteric nature of the drug, which is responsible for the low solubility values, together with its high molecular weight (924.09 Da) difficult its absorption. AmB is poorly absorbed after oral administration. Several oral pharmacokinetic (PK) studies have reported serum concentrations of approximately 0.04-0.5 µg/mL AmB after oral administration of 1.6-5 g of drug per day during two days [189,190].

1.2.4.1. Plasma levels

The serum levels detected after intravenous administration of AmB are dose-related. These levels are not only influenced by the dose but also by other parameters such as the frequency of administration and the rate of infusion [123]. Independently on the dose (one dose daily or twice the daily dose on alternate days), the AmB minimum serum concentrations are not modified. Nevertheless, there exist a relationship between the dose and the serum levels [191]. AmB fast infusion (45 minutes infusion) increases the mean serum concentration values after 1 h of the end of infusion but the concentrations do not differ at 18 h and 42 hours post-infusion [192].

1.2.4.2. Biodistribution

The drug distribution was considered initially to follow a three-compartment model [193-195]. This model provided the best fit for the observed distribution and elimination phases of AmB [196]. However, the model that best fits may differ in between formulations. For instance, the liposomal amphotericin B formulation (AmBisome®) or the colloidal AmB dispersion (Amphocil®) best fits to a two-compartment model [197-198].

The apparent volume of distribution (V_d), as well as the distribution model, varies depending on the formulation. While Akitson *et al* reported in 1978 a V_d value of 4 L/kg [193], the AmB formulated with sodium deoxycholate, first marketed formulation, has been reported to have a different V_d depending on the initial dose administered. For instance, the administration of 0.6 and 1 mg/kg AmB led to V_d values of 5.1 and 2.4 L/kg, respectively [197,199]

As already mentioned, the apparent volume of distribution, as well as the other pharmacokinetic parameters, may differ from one formulation to another. Table 10 summarizes the pharmacokinetics parameters analyzed in humans after intravenous

administration of different amphotericin B commercialized formulations. C_{max}, AUC, V_d and $t_{1/2}$ corresponds to maximum concentration, area under the curve, volume of distribution and terminal half-life elimination, respectively.

Table 10. Pharmacokinetic properties of the commercialized AmB formulations. Adapted (132).

Formulation	**Structure**	**Particle size (µm)**	**Dose (mg/kg)**	**Cmax (µg/mL)**	**AUC (µg*h/mL)**	**V_d (L/kg)**	**$t_{1/2}$ (h)**	**Ref.**
Fungizone®	Deoxycholate micelles	0.035	0.6	1.1	17.1	5.1	-	[199]
			1	1.7	18.7	2.4	26.8	[197]
			0.8	1.46	17.2	-	-	[209]
Abelcet®	Lipid complex (ribbon-like)	1.6-11	5	1.7	9.5	131	173.4	[199,210]
			5	2.39	19.17	132.8	393	[211]
			2.5	1.09	8.9	-	-	[212]
Amphocil®	Cholesterol dispersion (discs)	0.11-0.14	5	3.1	43	4.3	-	[199]
			0.25	0.8	9.4	3.4	86	[196]
			0.5	0.84	21.0	5.5	157	[196]
			1	2.2	46.3	7.6	244	[196]
			1.5	2.5	57.3	8.9	235	[196]
AmBisome®	Unilamilar liposomes	0.06-0.08	5	83	555	0.11	-	[199]
			1	8	27	0.58	10.7	[213]
			2.5	19	65	0.69	8.1	[213]
			5	58	269	0.22	6.4	[213]
			7.5	90	476	0.26	8.5	[213]
Fungisome™	Multilamilar liposomes	2.7-3.5	1	1.012	11.43	2.28	17.2	[214]

AmB is characterized by a high degree of plasma protein binding (91-95%) [200-202]. Due to this binding, the AmB unbound fraction in plasma is very low, approximately a 5-9% (some studies have reported unbound values even lower than 4% [201]. It binds

principally to lipoproteins, albumin, cholesterol or cholesterol-containing membranes (erythrocytes) [136, 203-205]. The major AmB binding in plasma takes place with β-lipoprotein [133,206]. However, there is also evidence of AmB binding with high affinity to human serum albumin (HSA) and α_1-acid glycoprotein (AAG) [151, 207].

AmB low permeability explains the fact that this polyene antibiotic is not usually found in tissues with the exception of liver, spleen and lung [208]. The amount of drug detected in the pleural, synovial and peritoneal fluids is low (approximately half of its serum concentration) [123]. Amphotericin B crosses the placental barrier, and low concentrations are attained in the amniotic fluid. The drug distribution into breast milk has not been yet study in humans.

1.2.4.3. Metabolism

Amphotericin B metabolism has not been already well-elucidated [197]. Characterization studies performed in urine and feces samples containing AmB, showed the absence of metabolites and concluded that AmB was eliminated unchanged [215].

1.2.4.4. Elimination

AmB follows a biphasic elimination profile [193]. The drug is characterized by a fast initial serum half-life of 24-48 h followed by a slower elimination phase (terminal half-life) of up to 15 days [216,217]. The metabolism seems to play a minor role on AmB elimination [216] as the AmB is mainly eliminated unaltered. Regarding the AmB elimination there is some controversy. In 1980 and 1990, some studies reported that the amount of AmB detected in urine after 24 h administration was very low (approximately 3%) and that less than half of the dose was biliary or renal excreted [123,218]. The unchanged AmB renal excretion was considered a minor elimination pathway and therefore, it should not be altered in patients with impaired renal function. However, as reported by Bury *et al*, the AmB plasma clearance increased with increasing severity of renal dysfunction. Renal excretion of unchanged AmB was found to be lower in the uremic patients with respect to healthy volunteers and also the hepatic clearance raised in renal dysfunction [201]. AmB levels in bile and urine were detected up to 12 and 27-35 days after administration, respectively [219]. In 2002, Bekersky *et al* reported a 20% unchanged AmB excretion in urine and 40% excretion in feces [207]. Urinary and fecal clearance amounted a 75% of the total drug clearance.

All the above information refers to AmB in general but, as previously detailed, the pharmacokinetic profile differs between formulations. For more detailed information each formulation should be discussed separately.

1.2.5. Spectrum of action and resistance

1.2.5.1. Spectrum of action

Amphotericin B is a macrolide antibiotic with a broad spectrum of action. It is the only polyene agent from approximately 200 known, whose toxicity allows for its intravenous administration [220]. As previously detailed, its mechanisms of action is basically based on its binding to sterols. This binding causes either disruption of the osmotic membrane integrity, disturbance of the oxidative enzymes or leakage of intracellular magnesium and potassium. Depending on the microorganism susceptibility and the drug concentration in the infection site, the AmB can behave as fungicide or fungistatic [221]. Amphotericin B is generally used in the treatment of fungal invasive and systemic infections. Particularly, the AmB is useful in treating candidosis, cryptococcosis, histoplasmosis, blastomycosis, parococcidiodomycosis, coccidiodomycosis, aspergillosis, extracutaneous sporotrichosis and mucormycosis. But it is also used in the treatment of some cases of hyalohyphomycosis and phaeohyphomycosis [220]. It is worth pointing out that most of the strains are inhibited at AmB concentrations in between 0.03 and 1 μg/mL [222].

Tables 11 and 12 describe the AmB spectrum of action against the most clinically important yeasts and molds.

The MIC_{90} (mg/mL) refers to the minimum inhibitory concentration (MIC) at which the 90% of the isolates are inhibited. The data contained in the tables has been compiled from the literature and the WCH Mycology Unit.

AmB is not active against bacteria, rickettsias or virus [222]. However, it has activity against some protozoos as *Leishmania*, *Trypanosoma*, *Acanthamoeba, Naegleria* or *Plasmodium* [106, 229-232].

Table 11. AmB spectrum of activity against the most clinically relevant yeasts. Adapted from [220].

Species	**MIC_{90} (mg/mL)**	**References**
C. albicans	0.25-1	[223, 224]
C. parapsilosis	1	[223, 224]
C. glabrata	0.25-2	[223, 225]
C. tropicalis	0.5-1	[223, 225]
C. krusei	2	[223, 224, 226]
C. kefyr	1	[226]
C. famata	1	[227]
C. guilliermondi	0.5-1	[224, 228]
C. lusitaniae	0.5-2	[226]
C. neoformans	0.25-1	[223, 226]
M. furfur	S	
S. cerevisiae	0.25-1	[225]
T. beigelii	2	[227]

Table 12. AmB spectrum of action against the most clinically important moulds. Adapted from [220].

Species	**MIC_{90} (mg/mL)**	**References**
Histoplasma capsulatum	0.5	[233]
Coccidioides immitis	0.5-1	[233]
Blastomyces dermatitidis	0.5	[233,234]
Paracoccidiodes brasiliensis	0.5	[235]
A. fumigatus	1-2	[236, 237]
A flavus	1-1-42	[236, 237]
A. terreus	1-2	[238]
A. nidulans	1	[238]
A. niger	1->16	[238]
S. apiospermum	4->16	[239, 240]
S. prolificans	0.5-4	[239, 240]
S. schenckii	0.26->116	[226]
Paecilomyces sp.	1->4	[241, 242]
Penicillium sp.	0.5-1	[242]
Fusarium sp.	0.5-1	[236, 237]
Bipolaris sp.	1-4	[227]
Exophiala sp.	0.5-2	[226]
Cladophialophora sp.	0.5-2	[240, 241]
Absidia sp.	0.5-2	[240]
Apophysomyces sp.	0.5-2	[242]
Cunninghamella sp.	0.5-2	[242]
Mucor sp.	0.5-2	[242]
Rhizomucor sp.	0.5-2	[242]
Rhizopus sp.	0.5-2	[237, 243]
Saksenaea sp.	0.5-2	[244]

1.2.5.2. Resistance

Resistance to AmB (MIC > 2 mg/mL) is a slow process that usually emerges from patients treated for a long period of time with this antibiotic. It is quite rare and it is usually caused by either a change in the sterol structure which leads to decreases in AmB binding or a decrease in the amount of ergosterol in the plasmalemma [220]. Some fungal cells present a mutation in their ergosterol biosynthesis pathway that leads to the production of ergosterol-like compounds which have less binding affinity for AmB.

Despite the wide use of amphotericin B over more than 40 years, almost no resistances have been developed [245,246]. AmB resistance tends to be specie-dependent. After long patient treatments with this polyene antibiotic, some strains of *Candida albicans, Candida tropicalis, Candida parapsilosis* and *Candida lusitaniae* have developed resistance to AmB. Some isolates of *Fusarium spp, Sporothrix schenckil* and *Scedosporium apiospermum* have shown primary resistance whereas all strains of *Scedosporium prolificans have* demonstrated to be completely resistant to this drug [220].

The microorganism resistance to amphotericin B can take place through three different pathways summarized below [132].

1. **Decrease in the membrane ergosterol content**. The appearance of resistance is related to either a mutation in the ergosterol biosynthesis pathway or to changes in the components of the cellular membrane wall [247]. It has to be pointed out that the co-administration of azoles together with the amphotericin B may cause resistance, as the azoles inhibits the ergosterol synthesis [248].
2. **Modifications in the mitochondrial respiratory chain**. Even though there is not confirmed evidence, it is assumed that the mitochondrial respiratory chain has a key role on the AmB development of resistance. The respiratory chain does not only participates in the biosynthesis of ergosterol but also can be implied in the accumulation of free radicals inside the cells [249].
3. **Tolerance to oxidative stress**. The yeasts exposure to inhibitory concentrations of fluconazole can induce a mechanism that make the yeasts turned more resistant to the oxidative and nitrosative stress (caused by ROS or NO). The

higher yeast resistant to the stress made then more tolerant to the oxidative stress caused by AmB [250,251].

1.2.6. Amphotericin B formulations

1.2.6.1. Fungizone®

In 1958, the first AmB formulation was marketed under the brand Fungizone®. Fungizone®, developed and commercialized by Bristol-Myers Squibb, Co. is a micellar dispersion of AmB with a bile salt, sodium deoxycholate, in a molar ration 1:2, in a phosphate buffer (figure 12) [148]. The lyophilized formulation contains 41 mg sodium deoxycholate and 50 mg AmB. The particle size of the micelles is approximately 1 µm [252]. Contrary to what it was thought at the beginning, Fungizone® consists of large aggregates rather than small mixed micelles (MM) [253].

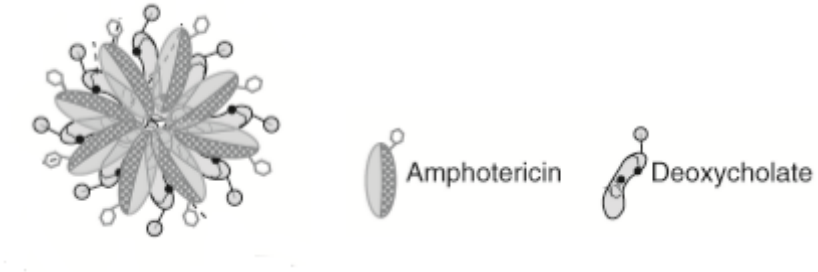

Figure 12. Fungizone® structure. Adapted from [214].

When it was first commercialized, Fungizone® had the broadest spectrum of action of all available antifungal agents. Even though it had a great efficacy, therapeutic doses caused severe sides effects, including pain at the site of injection, fever, chills, nausea, vomiting, electrolyte abnormalities, lysis of red blood cells (RBCs) and nephrotoxicity [254,255]. These side effects were directly related to the dose. The side effects increased with increasing dosage. The infusion-related side effects (fever, rigors, chills) are very common but medical management of these symptoms suffices to allow continuation of the treatment. However, renal insufficiency in association with azotemia, renal tubular acidosis and impaired urinary concentrating ability resulting in electrolyte imbalance might be severe enough to reduce the dose or to change to an alternate days dosing [256]. The dose-related toxicity is a limiting factor for all patients

but most importantly for immunocompromised patients (AIDS and cancer) that are undergoing intensive cytoreductive therapy [257].

Regarding its nephrotoxicity, Fungizone® has a concentration-dependent profile of toxicity and its selectivity depends on its aggregation state [258]. The critical micelle concentration (CMC) of Fungizone® ($2\text{-}6.10^{-3}$ M) is responsible for its associated toxicity. Once in blood, the formulation suffers a dilution process in which the micelles loss their integrity releasing the amphotericin B molecules. The amphotericin B rapidly rearrange into soluble aggregates which are not selective against ergosterol, damaging either ergosterol or cholesterol cells. Moreover, the high concentration of sodium deoxycholate, which is a toxic bile salt, plays an important role in the hemolysis caused by this formulation. The sodium deoxycholate is also assumed to be responsible for the diarrhea observed in patients after Fungizone® administration [259].

This associated toxicity has limited the daily dose of Fungizone® to approximately 1 mg per kg [260].

1.2.6.2. Strategies to reduce amphotericin B associated toxicity

In order to reduce the AmB associated toxicity different tactics have been investigated during the last years. Regarding the Fungizone®, first attempts where focused on saline loading, dose reduction and alternative day dosing but none of them worked [135]. The design and development of novel amphotericin B formulations should be mainly focused on the reduction of nephrotoxicity. As previously mentioned, the amphotericin B selectively and therefore, toxicity, is related to its aggregation state, reason why the target of the new formulations was centered on the maintenance of low free AmB serum concentrations. If the AmB concentration in serum remains low, the drug molecules will not rearrange into soluble aggregates and the selectivity against ergosterol containing cells will be maintained [151]. To achieve this aim, the AmB was included in carrier systems that exhibited controlled drug release.

In the early 1990s a new generation of AmB formulations were developed. The sodium deoxycholate contained in the Fungizone® was replaced by either phospholipids (Abelcet®), cholesterol (Amphocil®) or both (Ambisome®). Even though all these formulations improved the therapeutic indexes of the AmB included in Fungizone® the

cost of these new treatments was 12 to 40 times higher than the latest. Moreover, these new formulations did not avoid the need of hospitalization or the side effects associated to the treatment (they reduced the side effects but did not remove them).

Apart from these liposomes (Ambisome®) and emulsions (Abelcet® and Amphocil®), other particulate carrier systems were developed during the 90s.

Besides the above detailed drawbacks, it has to be considered that most particulate formulations are rapidly removed from the circulations by the reticulate endothelial phagocyte system (RES) cells, leading to a very low serum half-life of AmB combined with low bioavailability and irregular distribution in the body. Even though for most the pathologies this phenomenon is considered as a disadvantage, in the treatment of visceral leishmaniasis, where the parasite reside in this cells, is a great advantage [106].

Table 13 summarizes the strategies followed in the design of new amphotericin B formulations as well as the microorganisms aim of treatment.

Table 13. Strategies for the design of new AmB formulations

Carrier	**Composition**	**Microorganism**	**Reference**
Liposomes	AmB, hydrogenated soy bean lecithin, phosphocholine, cholesterol, sucrose, α-tocopherol, sodium succinate hydrate (AmBisome®)	*Leishmania* spp	[261- 266]
	AmBisome®	*Candida albicans*	[267, 268]
	Nanosomes (AmB, soy phosphatidylcholine sodium cholesteryl sulfate)	*Aspergillus* spp	[269]
Colloidal dispersions and emulsions	AmB cholesterol dispersion = ABCD (Amphocil®)	*Leishmania* spp	[266,270,271]
	Amphocil®	*Candida* spp, *Aspergillus* spp, *Mucor* spp	[272, 273]
	AmB lipid complex containing dimyristoylphosphatidylcholine, dimyristoylphosphatidylglycerol (Abelcet®)	*Candida* spp	[274, 275]
	AmB, stearic acid, Tween 80, chitosan	*Leishmania* spp.	[276]
Nanosuspensions	AmB, Tween 80, Pluronic F68, sodium cholate	*Leishmania* spp	[277]
		Ballamuthia mandrillaris	[278]
	AmB, Eudragit RS 100	*Fusarium* spp	[279]
Albumin nanoparticles	AmB, human serum albumin, dimethylsulfoxide	*Leishmania* spp	[280]
		Candida spp	[260]

Carrier	**Composition**	**Microorganism**	**Reference**
Emulsions	AmB, fat and phospholipids (EAmB - US Patents 5,576,016)	*Candida* spp.	[281]
	AmB, deoxycholate, soya bean oil	*Leishmania* spp	[282, 283]
	AmB Intralipid (ILA) emulsions	*Candida* spp.	[284, 285]
Micellar systems	AmB, sodium deoxycholate	*L. donovani*	[264, 286, 287]
	AmB, poly(ethylene oxide)-block-poly-(L-amino acid=aspartamide)	*Candida* spp, *Aspergillus* spp, *Cryptococcus* spp.	[152, 288]
	AmB, chitosan-g-pluronic F-127 copolymer (CPF)	*Candida* spp, *Aspergillus* spp	[289]
Cyclodexrins	AmB, methyl-beta-cyclodextrin (MβCD)	*Leishmania* spp.	[166]
	AmB, gamma-cyclodextrin (γ-CD)	*Leishmania* spp, *Candida* spp.	[290, 291]
	AmB, hydroxypropyl-γ-CD (vaginal gel)	*Candida* spp	[292]
Cochleates	AmB, phospholipid calcium precipitates	*Leishmania* spp *Leishmania* spp	[293, 294]
		Candida spp.	[293, 295]
		Aspergillus spp.	[296]
Polymer particles	AmB, polylactide-co-glycolide (PLGA)	*Leishmania* spp.	[297, 298]
		Aspergillus spp.	[299]

Carrier	**Composition**	**Microorganism**	**Reference**
Polymer particles	AmB, PLGA, dimercaptosuccinic acid (DMSA)	*Paracoccidioides brasiliensis*	[300]
	AmB, Poly(α-glutamic acid)	*Leishmania* spp	[301]
	AmB, ethylcyanoacrylate	*Leishmania* spp	[302]
	AmB, polybutylcyanoacrylate	*Cryptococcus* spp	[303]
	AmB, sodium alginate	*Candida* spp	[304]
	AmB, sodium alginate, chitosan stearate	*Leishmania* spp	[305]
	AmB, polyethylenimine-dextran-sulfate	(pendant *in vivo* results)	[306,307]
	AmB, chitosan-dextran-sulfate	(pendant *in vivo* results)	[306]
	AmB, gelatin	*Leishmania* spp	[308]
	AmB, GCPQ (quaternary ammonium palmitoyl glycol chitosan)	*Leishmania* spp	[309]
	AmB, Polyethylene glycol (PEG), lipid nanoparticles (LNP)	*Aspergillus* spp	[310]
Inclusion complexes + liposomes	AmB, hydroxypropyl/sulfo butyl ether β-CD and cholesterol/L-PC	*Aspergillus* spp, *Cryptococcus* spp	[311]

Some of these carriers has not been only used in the treatment of candidiasis and leishmaniasis but also in the prophylaxis of invasive fungal infections in inmunocompromised patients [312,313].

1.2.6.3. Commercialized amphotericin B formulations

Here in, there is a brief description of the main commercialized amphotericin B formulations used in therapeutics.

1.2.6.3.1. AmBisome®

AmBisome® was the first lipidic AmB marketed formulation. The AmB (50 mg) was included into small sonicated unilamellar liposomes (figure 13) composed by hydrogenated soy bean lecitine (213 mg), cholesterol (52 mg) and distearoyl phosphaidylglycerol (84 mg) [314]. AmBisome® developed by Vestar, Inc., was first marketed in Europe in 1989 by NeXstar Pharmaceuticals [148]. Since then and so far over 500,000 patients have been treated with AmBisome® [315].

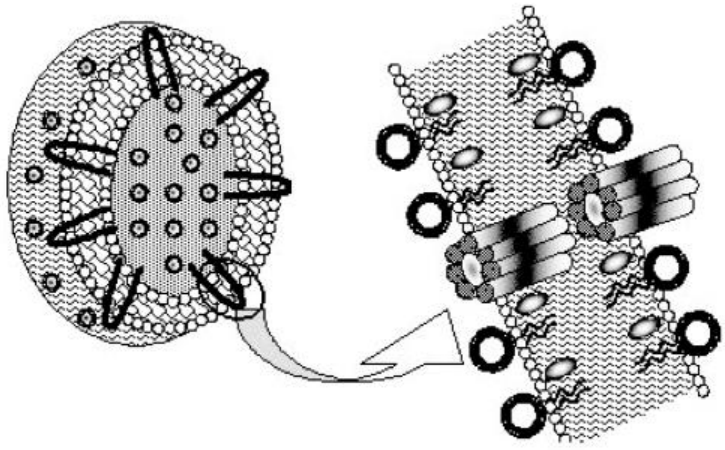

Figure 13. Ambisome® structure. Proposed arrangement of the AmB molecules (black) into the lipid bilayer [316].

It is commercially available as a lyophilized powder for reconstitution. It has to be reconstituted in water (water for injection - WFI) prior to administration. The reconstitution generates liposomes with a mean diameter of 60-80 nm [106,317,318]. Apart from the lipidic content, the formulation also includes sucrose for obtaining an isotonic solution, and α-tocopherol and disodium succinate hydrate.

The pharmacokinetic profile of Ambisome® has been reported to be significantly superior to that of Fungizone®. The serum elimination half-life is improved, the effective plasma concentrations are enhanced and the plasma clearance is therefore, reduced [106,278, 319]. After parenteral administration of this formulation most of the AmB is retained in liver and spleen but the molecule can also be found in lungs and kidneys (the retention in these two organs is much lower). Ambisome® higher concentrations in spleen and brain compared to Fungizone® makes this formulation suitable for the treatment of Leishmaniasis [320,321,322].

It has a less toxic profile than Fungizone® and it is well tolerated by patients at risk, including transplant patients [323] and children with cancer [324].

1.2.6.3.2. Abelcet®

Abelcet® is the first non-liposomal AmB-lipid complex (ABLC) marketed in Europe. This non-liposomal formulation contains AmB (100 mg) in a lipidic suspension of dimyristoylphosphatidylcholine (68 mg) and dimyristoylphosphatidylglycerol (30 mg) [325]. The lipid complexes have a ribbon-like structure (figure 14) with a mean particle size of 1-6 μm [326].

Compared to Fungizone®, Abelcet® has reduced toxicity but maintains its therapeutic efficacy. Abelcet® shows a lower risk of renal disorders than Fungizone® at a dose of 1-5 mg kg^{-1} day^{-1} [326].

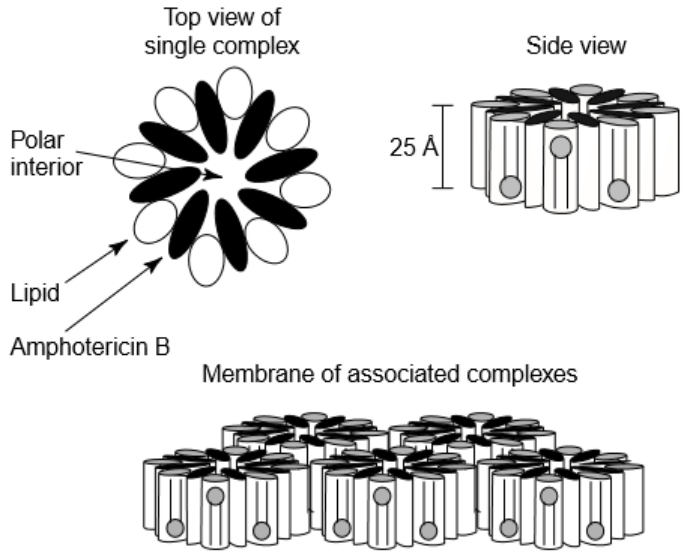

Figure 14. Abelcet structure. AmB and lipids are arranged in a 1:1 interdigitated complex [326].

The main drawback of this formulation, the fast clearance, is related to its colloidal properties. It is quickly removed from the circulation by the cells of the mononuclear phagocyte system (eg. Kupfer cells) enhancing the risk of possible hepatic disorders [106].

1.2.6.3.3. Amphocil®

Amphocil® was the second non-liposomal AmB marketed formulation. It is an AmB colloidal dispersion (ABCD) developed by Liposome Technology, Inc and first commercialized in 1994 in the United Kingdom. It consists of AmB (50 mg) and sodium cholesteryl sulfate (26.4 mg) in equimolar concentrations [325]. The particle structure resembles discs (figure 15) of 4 nm thick and a 100 nm mean diameter [327].

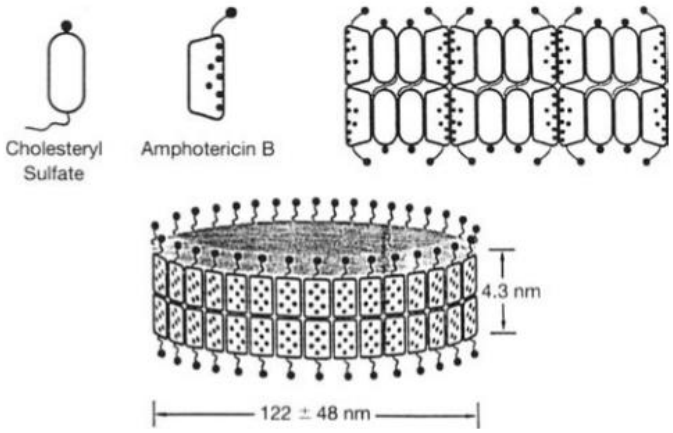

Figure 15. Amphocil® structure. The interaction of AmB with the cholesterol sulfate forms rigid and tightly packed lipid bilayers [326].

As for the other lipid-based formulations, it has also a similar antifungal efficacy than Fungizone® but it has reduced cytotoxicity and hemolysis [106].

1.2.6.3.4. Fungisome™

Fungisome™ is the most recent AmB marketed formulation. It is a multilamellar liposome AmB formulation first commercialized in India in 2003. It is composed by phosphatidylcholesterol and cholesterol in a molar ratio of 7:3. It forms multilamellar vesicles with a particle size ranging between 2.74 - 3.45 μm (figure 16). It is commercialized as a liquid formulation [214].

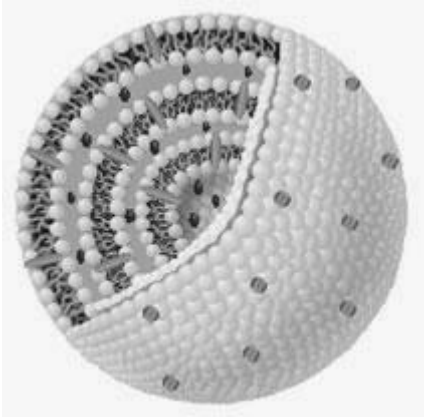

Figure 16. Fungisome™ structure

As well as for AmBisome®, this new liposomal formulation accumulates in liver, spleen and, in less degree, in lungs. Nevertheless, the pharmacokinetic profile of this

new formulation is completely different to that of AmBisome®. This can be explained by their difference in particle size. The Fungisome™ larger particle size, makes it easily recognizable by the RES.

1.2.6.4. New approaches in the design of amphotericin B delivery systems

1.2.6.4.1. Polymeric micelles

Even though the lipidic systems described above, do not display the high toxicity of Fungizone®, their high cost and biopharmaceutical instability are important limiting factors to their use [279,311]. Abelcet®, the AmB/lipid complex, is formed by large size particles that are rapidly taken up by macrophages thus cumulating in liver and spleen, which in one side shortens the circulating period and on the other increases the volume of distribution and clearance. Ambisome®, the lyophilized liposomal AmB formulation, substantially escapes recognition and uptake by the mononuclear phagocyte system but tends to accumulate in high amount in the liver and spleen. Finally, Amphotec®, an AmB colloidal dispersion, exhibits dose-limiting infusion-related toxicities. Interestingly, clinical trials showed that despite the lipid-associated formulations were significantly less nephrotoxic than AmB/deoxycholate, they were not significantly better than the latter for treatment of several diseases, including AIDS-associated acute cryptococcal meningitis [328].

Polymeric micelles have some advantages over lipid-based systems such as easy preparation process, higher thermodynamic and kinetic stability (which confers higher stability toward dilution *in vivo*), long shelf-life at room temperature, ability to withstand autoclaving for sterilization, prolonged blood circulation due to a lower uptake from the reticulo-endothelial system (RES) and low cost of production [288] [106]. A few PEG containing polymers have been used to produce AmB pharmaceutical products. PEG is indeed a soluble non-toxic, low immunogenic and low antigenic polymer widely applied for prolonging the circulation of colloidal drug delivery systems as it prevents the massive accumulation in RES organs, namely liver and spleen [310] [253], reduces the kidney filtration and avoids the capillary penetration [134,329,330,331]. Therefore, these long circulating carriers may be able to increase the therapeutic index of AmB at low dose, low risk of toxicity and low cost [332]. Micelle formulations obtained using poly(ethylene glycol)-block-poly(-caprolactone-co-

trimethylenecarbonate) and PEG-DSPE showed that the solubility could increase of 2 order of magnitude [155]. Interestingly, the physical combination of PEG-DSPE with sterol molecules was found to determine both the solubility and the aggregation state of AmB.

Monomeric AmB is known to selectively interact with ergosterol in fungal cell membranes, forming channels by the classic barrel stave motif, while aggregated AmB preferentially associates with cholesterol, which causes toxicity in mammalian cells. Therefore, polymers containing sterol molecules have been hypothesized to be suitable materials for preparation of stable AmB colloidal formulations. Typically, PEG-cholesterol type polymers have been found to produce micelles with about 10^{-6} M CMC [329,331,333,334], which are much more stable compared to sodium deoxycholate (CMC 2-6.10^{-3} M) [334]. Recently, self-assembling polymers obtained by end conjugation of cholanic acid to monomethoxypoly(ethylene glycol) chains have been investigated for the delivery of proteins and low mol wt drugs [335,336]. These PEG-cholane polymers were found to associate with proteins by cholanic moiety docking into the hydrophobic clefts and interaction with hydrophobic surfaces of proteins yielding novel supramolecular systems for protein delivery. Furthermore, preliminary unpublished studies showed that PEG-cholane can enhance the solubility of poorly soluble drugs, namely tamoxifen and paclitaxel.

Due to the strong affinity of sterol moieties for AmB and the ability of PEG-cholane to dissolve hydrophobic drugs by forming micelles, these polymers seem to possess the requisites for obtaining new efficient colloidal systems for delivery of this antifungal drug.

Even though the amphotericin B associated nephrotoxicity is the main drawback for the use of this molecule in clinic, the fact that this antibiotic is only available for intravenous administration also limits its prescription. The development of AmB oral or topic formulations with decreased toxicity will allow not only for the treatment of systemic fungal infections but also for the treatment of topical mixed-infections resistant to conventional treatments. These formulations will improve patient compliance and reduce the sanitary cost of the treatment.

2. OBJECTIVE AND JUSTIFICATION OF THE NEED OF COLLABORATION

2. OBJECTIVE AND JUSTIFICATION OF THE NEED OF COLLABORATION

Justification of the need of collaboration

Taking into account the rising importance and clinical repercussion of the mold infections in humans and animals, the development of new formulations that reinforce the current therapeutic arsenal is needed.

As detailed in the introduction the wide spectra of action of amphotericin B together with its low appearance of resistance, makes this drug a suitable candidate for the treatment of mycosis. Thus, the main objective of the present thesis will be focused on the development of new amphotericin B (AmB) formulations, with reduced side effects, for the treatment of topical and systemic mycosis.

To achieve this purpose, the experience of the UCM research group in the development and characterization of new amphotericin B formulations was complemented with the long experience of the University Javeriana of Bogotá on microbiology and clinical practice and the wide expertise of the University Degli Studi di Padova on chemical conjugation.

Therefore, two collaborations were established alongside this PhD project. The first collaboration, set with the University Javeriana of Bogotá, aimed in studying the efficay of an AmB nail lacquer. While the second and main collaboration, which was established with the University Degli Studi di Padova (Italy) aimed in developing a new AmB formulation for the treatment of systemic mycosis. This last collaboration lead to the codirection in between Spain-Italy of the present PhD project.

The PhD project is therefore structured in two main chapters. The first experimental part approaches the development of an amphotericin B nail lacquer useful in the treatment of onychomycosis while the second experimental part focuses on the solubilization and inclusion of amphotericin B in the colloid system formed by the polymer PEG_{5kDa}-cholane.

Objective

As previosly mentioned, the main objetive of the current thesis is the development of two amphotericin B formulations. One topical formulation for the treatment of onychomycosis and one formulation for the treatment of systemic mycosis.

The specific objectives are differenciated with regards to the formulation to be developed.

EXPERIMENTAL PART 1 - AmB nail lacquer

The increasing incidence of concomitant nail infections caused by dermatophytes or non-dermatophytes and *Candida* spp, or by different species of *Candida* at the same time, has raised during the last years. These concomitant infections are an important healthy issue as most of the commercialized treatments are not effective against mixed infections. Therefore, the development of a formulation able to penetrate the nail and effective against dermatophyte, non-dermatophyte molds and *Candida* spp. is needed.

Taking into account that amphotericin B is a polyene antibtioc and antifungal drug with a broad spectrum of action and low incidence of resistances, we have considered this molecule as an alternative for the treatment of nail mixed infections. Thus, the main objective of this first chapter is focused on the development and characterization of an amphotericin B nail laquer for the treatment of onychomycosis. The efficacy of the nail lacquer will be assayed in collaboration with the research group of Dra. Parras from the University Javeriana of Bogotá (Colombia).

To reach this general objective, some specific targets are proposed:

1. AmB solubility studies on different solvents.
2. Development of AmB nail lacquers using different film-forming agents.
3. Characterization of the nail lacquers.
4. *In vitro* nail penetration studies
5. *In vitro* and *in vivo* efficacy studies. Determination of the minimum inhibitory concentrations and efficacy studies on infected keratinized structures of animal origin.

EXPERIMENTAL PART 2 - AmB/PEG$_{5kDa}$cholane formulation

During the last years, the research group from the UCM has designed and developed new formulations for amphotericin B (AmB) delivery which are characterized by a great therapeutic efficacy. Furthermore, these preparations have lower side effects compared to other commercialized formulations. The experience of this group on this research topic (amphotericin B) is supported by 8 PhD thesis (Moreno, 2000), (Brime, 2002), (Sánchez-Brunete, 2003), (Valdespina, 2007), (Espada, 2008), (Ruiz, 2010), (Serrano, 2013) and (López, 2015) and by the publication of different articles in specialized journals.

On the other hand, the research group from the University of Padova (lead by Professor Caliceti), is a worldwide known reference group on the design of pegylated drug carriers. The conjugation with different polyethylene glycols (pegylation), which is one of the most important lines of research in the drug delivery field, allows for a higher drug bioavailability. Professor Caliceti is a world expert in the synthesis and conjugation of different molecules with polyethylene glycols and his group has done important scientific contributions related to this topic.

Based on the promising results obtained on both research groups and taking into account the rising importance and clinical repercussion of the mold infections, the main objective of this thesis focuses on the development and optimization of an amphotericin B pegylated formulation for the treatment of fungal infections. The AmB interactions with cholesterol-type molecules are known to favor the drug solubility. In this sense, the conjugation of cholesterol-type molecules with different PEGs will allow for the encapsulation and solubilization of AmB.

To achieve this general purpose, some specific objectives conforming the working plan are proposed:

1. Synthesis of different AmB pegylated complexes
2. Characterization of these complexes by studying their solubility in different conditions. The complexes characterization will include DLS, HPLC, DSC, RX, FTIR, CD, ITC and synchrotron analysis.

3. *Ex vivo* characterization of these complexes. Study of the toxicity by hemolysis and study of the antifungal efficacy against *Candida albicans*
4. *In vivo* pharmacokinetic studies after oral and intravenous administration. The pharmocokinetic properties of the new AmB formulation will be determined and compared to the commercialized formulations Ambisome® and Fungizone®.

3. EXPERIMENTAL PART

3.1. EXPERIMENTAL PART 1

EXP.1-1. MATERIALS & METHODS

EXP1-1. MATERIALS & METHODS

EXP1-1.1. Nail lacquers

Nail lacquer, also known as nail varnish or nail polish, is a lacquer that can be applied to human finger and toenails in order to decorate, protect and/or treat the nails.

An ideal nail polish should have the properties detailed below;

- Be dermatologically innocuous to the nail,
- Avoid compound precipitation with time,
- Ease of application, covering homogenously all the targeted surface,
- Adhesive - the film formed has to be resistant and flexible,
- When colored, the nail lacquer must have the same color in the container than over the nail,
- Relatively fast drying, allowing the application if necessary of three layers of lacquer and,
- Easy removal using appropriate solvents. Once removed, the nail should not be colored or stained.

Not all commercially available lacquers reach all these properties but at least they should be innocuous, adhesive, fast-drying and be easily removed.

EXP1-1.2. Excipients

Nail polishes usually present in their composition the following groups of compounds.

- Film-forming agents
- Resins
- Plasticizers
- Solvents and cosolvents
- Colorants and pigments
- Viscosity modifying agents

The excipients used in the development of an AmB nail polish are the film-forming agents, the plasticizers, the solvents and the cosolvents. A brief description of each of the groups included in the nail polish composition is described below.

EXP1-1.2.1. Film-forming agents

Film formers are chemical compounds that generate flexible, cohesive and continuous layers when applied to a surface. Depending on their solubility properties they can generate permeable or impermeable films.

The film forming agents studied in the development of an AmB nail polish were Plasdone K90®, Eudragit L100®, cellulose acetate phthalate and Pluronic F127®. They were included in a 10 to 20 weight (%). Each of the film forming agents used, as well as their properties, are detailed in appendix 1 (AP1.2).

EXP1-1.1.2.2. Plasticizers

Plasticizers are compounds that improve the flexibility, brightness and durability of the film formed. They are present in an amount of 2 to 10% (weight) as higher percentages can generate weak layers that are easy breakable. The plasticizer assayed for the new AmB-based nail lacquer were polyethyelen glycol (PEG), propylene glycol (PPG), glycerin triacetate (GT), diethyl phthalate (DEP), castor oil (CO) and dibutyl sebacate (DBS).

The properties and the chemical structure of the above mentioned plasticizers is detailed in appendix 1 section AP1.2.

EXP1-1.1.2.3. Solvents

The solvents constitute the volatile part of the nail polish. They are a key factor in the polish composition as they directly influence the dryness and ease of application. Highly volatile mixtures can cause difficult and non homogenous applications while low volatile mixtures produce thin and slow drying layers.

The solvents used in the AmB nail polish composition were ethanol or a mixture of ethanol and water in an amount of 38 to 70 wt. %.

EXP1-1.1.2.4. AmB solubilizers

From a chemically point of view, amphotericin B is an amphiphilic molecule with low water solubility. Its low solubility (less than 1 mg/L) in water or water-free alcohols at phisiological pH, constitutes the main drawback when developing any kind of pharmaceutical formulation (topical, oral or intravenous). To overcome the AmB solubility problems, many strategies have been followed during the last years. These include the use of sodium deoxycholate (DocNa), gamma cyclodextrin (γ-CD), polymers, etc. Here in, it is reported for the first time the use of N-methyl-2-pyrrolidone (NMP) and Plasdone® K90 as AmB solubilizer agents.

For the development of the new AmB lacquer, DocNa, γ-CD, NMP and Plasdone® K90 were used. Each of them, was able to solubilize the AmB in a different way.

The composition, properties and chemical structures of the AmB solubilizers is detailed in section AP1.2 of the appendix 1.

EXP1-1.2.5. Cosolvents

The use of water-soluble polymers, such as Plasdone® K90, in the development of a water soluble film forming lacquer, would imply the addition of a co-solvent with short evaporation rates in order to achieve dryings time within the range 3-5 minutes (once applied over the nail). Due to its properties and compatibility, the ethanol would be the selected co-solvent in the water permeable nail lacquers.

EXP1-1.3. Amphotericin B solubility studies

In order to know in which solvents AmB had the highest solubility, the following study was performed. The aim of this study was to find the most suitable solvents for the development of an AmB topical formulation.

Method

AmB solubility in acetic acid, acetone, acetonitrile (ACN), cyclohexane, dimethylformamide (DMF), dimehtylsulfoxide (DMSO), ethanol, isopropyl alcohol, glycol ethylenglycol dimethylether, N-methyl-2-pirrolidone (NMP), and petroleum ether was studied.

As a low AmB solubility was expected for all the solvents, apart from DMSO and NMP, samples were prepared at 5 mg/mL. When DMSO and NMP where assayed the samples contained 50 mg/mL of AmB.

Briefly, 1 mL of solvent was added to the eppendorfs containing 5 or 50 mg AmB and vortex for 1 min. Once shaked, they were left stirring in a mechanic oscillator at 25 °C for three hours. Afterwards, the samples were centrifuged at 12,000 rpm for 10 min and 20 µL supernatant were taken. The supernatant was then diluted to 1 mL with methanol (MeOH) and centrifuged again at 12,000 rpm for another 10 min. Finally, 50 µL supernatant were analyzed by RP-HPLC. The AmB concentration was referred to a curve linear in the range 12 ng/mL – 40 µg/mL (r^2=0.999). The samples were prepared in triplicate.

EXP1-1.4. Developement of an AmB nail lacquer for the treatment of onychomyosis.

EXP1-1.4.1. Study design

The study design used in the development of an AmB nail lacquer for the treatment of onychomycosis is detailed in figure 17.

The first step implied the bibliographic research. The excipients that were used, as well as the amphotericin B solubility method, were selected in basis of the possible patentability. The second and third steps consisted of the formulations development and their short-term stability studies. The fourth step supposed the selection of three lead candidate formulations. These formulations were physicochemical characterized and studied during step 5 in terms of *in vitro* nail penetration and efficacy. The data generated on step 5 allowed for the selection of the final lead candidate. This lead candidate was sent to Colombia for further *in vitro* and *in vivo* studies.

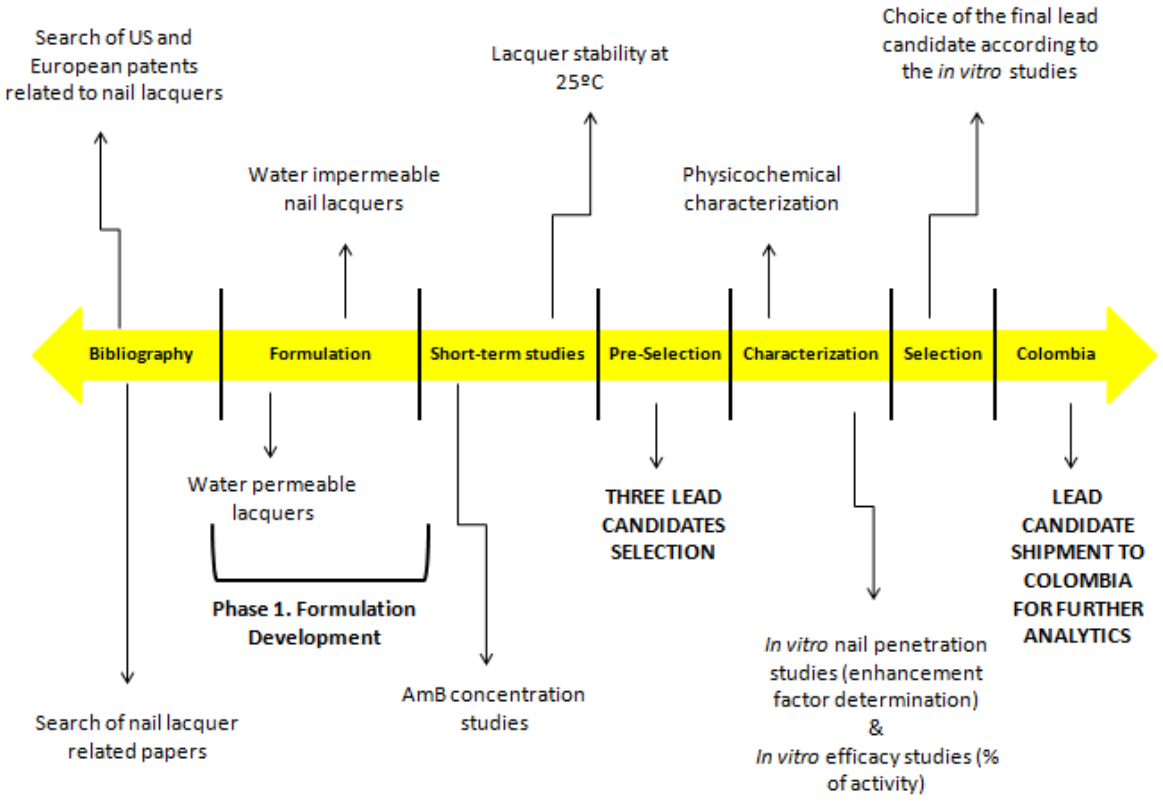

Figure 17. Study design for the development of an amphotericin B nail lacquer.

EXP1-1.4.2. Formulation development (second step of the study design)

20 different nail lacquer compositions were prepared following the information compiled from a deep bibliographic research (articles and patents). The formulations were studied in terms of physical and chemical stability and the below parameters were evaluated using a 1-5 scale, where 1 was the minimum score and 10 the maximum.

- Water permeability of the film formed,
- viscosity of the formulation,
- brightness of the formulation and film formed,
- film drying time over the nail,
- stickiness of the film once dried,
- extensibility of the formulation,
- homogeneity of the film formed and
- pH of the formulation

The formulations prepared were classified in two main groups according to the type of polymer used as film forming agent: water soluble and non-water soluble lacquers.

EXP1-1.4.3. Short-term stability studies (third step in the study design)

The formulations stability, as well as the AmB concentration, were studied in all the formulations during 1 month at room temperature and exposed to light.

EXP1-1.4.4. Pre-selection of three lead candidates (fourth step in the study design)

Based on the results obtained in the short term stability studies, three formulations were selected for the complete characterization.

EXP1-1.4.5. Characterization of the three lead candidates (fifth step in the study design)

The selected formulations were physicochemically characterized and studied in terms on *in vitro* penetration and efficacy.

EXP1-1.4.5.1. Physicochemical characterization

EXP1-1.4.5.1.1. Dynamic light scattering

Nail polish (3 mg/g AmB) was prepared as described above and diluted 1:5 with purified water in order to have a sample with suitable properties that allow for the particle size analyses. Fresh and reconstituted samples were analyzed at different times (0, 7 and 15 days) by dynamic light scattering (DLS) using a Malvern Zetasizer Nano-ZS (Malvern, Worcestershire, UK). The analyses were performed in triplicate at 25 ºC, 633 nm wavelength and 173º detection angle to assess the mean particle size and size distribution.

EXP1-1.4.5.1.2. Freeze drying

The freeze drying technique was used to obtain a dehydrated nail polish powder easily redispersible with a mixture of ethanol and water.

5 g of 3 mg/g AmB water-permeable nail lacquers (F11 and F13) were prepared as described above. However, due to the low freezing temperature of the ethanol, the lyophilization process was performed in the absence of this solvent. The samples were frozen at -20°C and lyophilized using a Lio-labor® instrument (Telstar, Barcelona, Spain) for 48 h. The freezing and sublimation temperatures in the lyophilization chamber were -45ºC and from -45 to 25ºC, respectively. The sublimation pressure was $4.54\ 10^{-4}$ atm. The moisture content in the lyophilized product was determined as weight loss after heating at 105ºC using a Mettler PM100 balance equipped with a Mettler LP16 infrared drying unit (Mettler Toledo, Greifensee, Switzerland). The end point was estimated after 120 s without weight variation. Reconstitution of the freeze dried samples was performed by the addition of a mixture of water and ethanol in different proportions depending on the composition of the freeze dried formulation.

Particle size and AmB concentration analyses of reconstituted solutions were carried out at times 0, 7 and 15 days by DLS and RP-HPLC, according to the analytical protocols reported above.

EXP1-1.4.5.1.3. Spray drying

The spray drying technique was used to transform a liquid (the AmB impermeable nail lacquer [F19]), into a powder. The aim of this assay was to obtain a powder with suitable properties (low humidity and stability) for reconstitution.

As reported above, the freeze drying is not an appropriate technique for those formulations containing organic solvents. This is due to the extremely low freezing temperature that should be reached in the chamber when these compounds are included. For this reason, the spray drying technique was considered as a good choice for obtaining a powder with the Eudragit® based formulations.

5 g of 3 mg/g AmB water-impermeable nail lacquer were prepared as previously reported with modifications. The NMP was substituted for DMSO and the ethanol for methanol. The NMP has a high evaporation temperature (202 ºC) that difficult its drying with this technique. The DMSO although presents a slightly lower evaporation temperature (189 ºC) than NMP; in combination with methanol it evaporates at lower

temperatures. Preliminary studies performed by the research group showed that the mixture DMSO-methanol evaporates at 75 ºC (data not shown).

The study was performed at 2 bars pressure, with an aspiration of 100% and with a flow rate of 3 mL/min. The inlet and outlet temperatures were 75 ºC and 60 ºC, respectively. Once the formulation was spray dried, the product was removed from the collector and weighted in order to calculate the yield. Then, the moisture content in the sample was determined as reported in the freeze-drying method. Reconstitution of the spray dried formulation was performed by the addition of a mixture of ethanol and NMP in a ratio 7:1.

EXP1-1.4.5.1.4. Scanning electron microscopy (SEM)

The superficial characteristics of the film formed by the water permeable and impermeable AmB nail lacquers were studied by SEM using a JEOL JSM 6335F microscope. One drop of 3 mg/g AmB nail polish was placed on a Formvar® carbon coated grid (F196/100 3.05 mm, Mesh 300) and left drying at room temperature for 5 min. The grids were then covered with a thin gold layer and the samples were analyzed. The assay was performed at an accelerating voltage of 15 kV.

EXP1-1.4.5.1.5. Rheological properties

General considerations

The nail lacquers must have a viscosity that allows for an easy administration and avoid, if included, the precipitation of the pigments or other substances included as suspension. Generally, the nail lacquers are known to be Newtonian liquids with viscosity values ranging from 200 to 400 cPs. The rheological behavior and the viscosity of the nail lacquers vary a lot depending of the nature of the polymer used as film-forming agent. Thus, polymers such as Eudragit® generate low viscous liquids (<100 cPs) that are suitable for nail application.

Therefore, the formulations developed were studied in terms of viscosity and rheological behavior to check whether or not they were appropriate for nail administration.

Method

2 g of 3 mg/g AmB nail lacquer were placed on a thermostated cell and measured in a Brookfield DV-III viscometer (MAB industrial, Barcelona).The experiment was performed at 5 to 62.5 rpm using a CP41 needle. The interval of shear rate was set from at 0 to 125 s^{-1} and the temperature at 25 ºC. The temperature (25 ± 2 °C) was controlled using water bath connected to a Tempette® Junior TE-8J resistance. Prior to sample analysis the instrument was calibrated using a Brookfield viscosity standard of 975 cPs at 25 ºC.

The rheological behavior of the samples was studied by plotting the viscosity (mPa.s) versus the shear rate (1/s), and the shear stress (Pa) versus shear rate (1/s).

EXP1-1.4.5.2. Stability studies

Short-term stability studies (15 days) were performed on freshly, freeze dried and spray dried AmB nail lacquers. Particle size, moisture content, viscosity and AmB concentration were determined at 0, 7 and 15 days.

Long-term stabilities studies following ICH normative are being carried out at this moment (data not shown).

EXP1-1.4.6. *In vitro* penetration and efficacy studies

EXP1-1.4.6.1. *In vitro* nail penetration studies

General considerations

The nail penetration studies aimed in determining the *in vitro* penetration efficacy of the lead candidates. The enhanced penetration of the formulations will be compared to a control. The formulation with the higher penetration and activity will be selected as the final lead candidate.

Method

The penetration study was performed on nails donated by both female and male healthy volunteers aged ranging between 25-35 years. The experiments were performed in triplicate and in each experiment 5 samples of each formulation were prepared. The formulations tested were those that showed the best physicochemical properties for

AmB nail delivery. The control used for this study was an AmB suspension at pH 5.5 that was prepared by the addition of 15 mg AmB to 5 mL purified water at pH 12 (NaOH 0.1 M) followed by pH decrease to 5.5 with ortophosphoric acid 0.1 M.

The nails were collected and weighted prior to administration. Nail thickness was also measured using a caliper Mitutoyo (Illinois, USA).

One nail was added to each glass tube containing 0.5 g of formulation and left under stirring for 15 min at 25°C. Then, with the help of the tweezers, the nails were removed and left drying over a watch glass for 20 min. The nails were again weighted to check the increase in weight after treatment and introduced into glass tubes. The racks containing the tubes were placed in a thermostatized bath set at 32 ºC, 60 rpm for 24 h. Later, the nails were taken out from the tubes, washed three times with water and three times with ethanol for the water permeable lacquers, and viceversa for the water impermeable lacquers. The AmB from the nails was then extracted using DMSO. Briefly, each nail was added to a glass tube containing 1 mL DMSO and left under stirring at 25°C for 1 h. 10 µL DMSO containing the AmB were diluted to 1 mL with MeOH and analyzed by RP-HPLC.

The AmB concentration was expressed as µg of AmB per mg of nail (µg AmB/mg nail) and the enhancement factor (EF) was calculated. It was calculated, as shown in equation 1, as the ratio between the µg of AmB that penetrated per mg of nail when applied the formulation, and the µg of AmB that penetrate per mg of nail when applied the control.

$$EF = \frac{(\mu g\ AmB/mg\ nail)F}{(\mu g\ AmB/mg\ nail)C}$$

Equation 1. Calculation of the enhancement factor (EF).

EXP1-1.4.6.2. *In vitro* efficacy study

The *in vitro* antifungal activity of AmB as suspension (control) and AmB included in water permeable and impermeable nail polishes (samples), were assessed against the yeast *Candida albicans* CECT1394. The control was prepared by solubilizing 5 mg of AmB in 5 mL aqueous solution at pH 12 (NaOH 0.1 M) and then decreasing the pH to 5.5 using orthophosphoric acid 0.1 M. This 1 mg/mL AmB suspension was then diluted to 96 µg/mL using phosphate buffer at pH 10.5. The buffer was prepared by the addition

of 3.5 g of potassium phosphate dibasic (0.2 M) to 100 mL deionized water at pH 10.5 (NaOH 0.1 M).

Yeast cells were cultured in Petri dishes containing agar Sabouraud (72 h at 30 ºC) and then 3 mL of a 0.5 McFarland standard suspension (1-5.10^6 CFU/mL) were seeded in plates of Agar Mueller Hinton supplemented with glucose [337]. Methylene blue was used as contrast agent.

Paper disks, impregnated with the AmB dissolved in DMSO were used as reference (S_1 600 μg/mL; S_2 200 μg/mL; S_3 96 μg/mL; S_4 38.4 μg/mL; S_5 18.4 μg/mL). One disk impregnated with 20 μL of S_3 (reference at the same concentration as the control and samples) and one disk with 20 μL of 96 μg/mL control were placed on each petri dish.

3 mg/g AmB water permeable or impermeable lacquers were diluted to 96 μg/mL using 0.2 M phosphate buffer (pH 10.5) and DMSO, respectively. The impermeable lacquers were diluted with DMSO as they form a precipitate in contact with aqueous solutions.

Then, papers disks impregnated with 20 μL of 96 μg/mL AmB nail lacquers were placed on the plates and incubated at 30 ºC for 48 h. After 48 h of incubation, the inhibition zones were accurately measured using a caliper and referred to the standard (96 μg/mL AmB, S_3).

EXP1-1.4.7. Selection (sixth step on the study design)

The results generated in the physicochemical characterization together with the *in vitro* penetration and efficacy data, allowed for the selection of the final lead candidate.

EXP1-1.4.8. Collaboration with the University Javeriana of Colombia (seventh and last step on the study design)

The lead candidate formulation was sent to Colombia for further analytics.

The translated instructions sent to Colombia together with the labels to identify the content of the different vials included in the shipment is attached at the end of Materials and Methods.

EXP1-1.4.8.1. Evaluation of the antimycotic effect of an AmB nail lacquer against the etiological agents responsible for the onychomycosis

In collaboration with the research group of Dra. Claudia Parras from the University Javeriana of Bogotá (Colombia), the *in vitro* and *in vivo* efficacy of formulation 19 (water impermeable nail lacquer) was assayed. This collaboration aimed in determining the *in vitro* minimum inhibitory concentration (MIC) of amphotericin B against dermatophytes and non-dermatophytes molds; as well as, evaluating the nail lacquer activity on keratinized structures (animal origin) infected *in vitro*.

EXP1-1.4.8.1.1. Determination of the minimal inhibitory concentration (MIC)

The minimal inhibitory concentration (MIC) of AmB included in formulation 19 was studied against the main etiological agents responsible for the nail infections. *Trichophyton rubrum, Trichophyton mentagrophytes, Aspergillus niger, Fusarium oxysporum* and *Fusarium solani* were the microorganisms assayed. These molds belonged to the Microorganisms Collection of the University Javeriana of Colombia.

For the *in vitro* MIC studies, seven disks containing AmB at different concentrations (table 14) were prepared from a stock solution of 5 mg/mL AmB. DMSO was used as control.

Table 14. AmB nail lacquer concentrations prepared for the MIC study.

Standard	Dilution
S1 (2400 µg/mL)	480 µL of stock solution + 520 µL of DMSO
S2 (960 µg/mL)	400 µL of S1 + 600 µL of DMSO
S3 (384 µg/mL)	400 µL of S2 + 600 µL of DMSO
S4 (154 µg/mL)	400 µL of S3 + 600 µL of DMSO
S5 (61 µg/mL)	400 µL of S4 + 600 µL of DMSO
S6 (25 µg/mL)	400 µL of S5 + 600 µL of DMSO
S7 (9.8 µg/mL)	400 µL of S6 + 600 µL of DMSO
Control	DMSO

The *in vitro* evaluation was performed according to the parameters detailed on the CLSI M38 A2 guideline. Briefly, each microorganism was replicated in PDA tubes (16 x 150) and incubated at 28ºC during the times established in the guideline. The inocula were prepared using a 0.85% sterile saline solution added of tween 20. The microorganisms

loading was adjusted by UV spectroscopy and counted in a Newbauer chamber. The conidia concentration used in the experiment was in the range 0.4-5 10^4 CFU/mL and 1-3 10^4 CFU/mL for dermatophytes and non-dermatophytes molds, respectively.

Once the inoculums were prepared, they were seeded in non-supplemented agar Müller-Hinton. The seeding was performed following the three-directions seeding method in order to cover the maximum surface. Once the plates had been seeded, the disks were impregnated with 20µL of the different AmB nail lacquer concentrations detailed on table 14. The disks were left dry at room temperature for 15 min and then place over the agar. Prior to incubation, the agar plates were refrigerated for 2 hours at 5ºC. After that, the dishes were incubated at 30ºC for 48h.

To note that as quality control, the reference strains *Candida parasilopsis* ATCC 22019 and *Candida krusei* ATCC 6258 were used in the assay.

EXP1-1.4.8.1.2. Evaluation of amphotericin B nail lacquer efficacy in the mycotic infections of keratinized structures of animal origin.

Figure 18 shows the timelines and the steps included in the efficacy study designed to probe the AmB nail lacquer efficacy against the main pathogens responsible for the onychomycosis.

In order to evaluate the efficacy of the topical AmB nail lacquer formulation, keratinized structures of animal origin (chicken nails) were infected with dermatophyte and non-dermatophyte molds. Conidia concentrations of 5 10^8 CFU/mL were prepared for each microorganism. 10 µL of each were inoculated in the surface of the keratinized structures. The nails were washed and disinfected prior the applications, and the absence of microorganisms was established. After the inoculation, the nails were daily monitored during 15 days. At day 15, the nail was sanded down for infection confirmation. The infection was confirmed by the observation of the mycotic structures in the direct examination with KOH and the later isolation in agar Sabouraud + chloramphenicol and Mycosel.

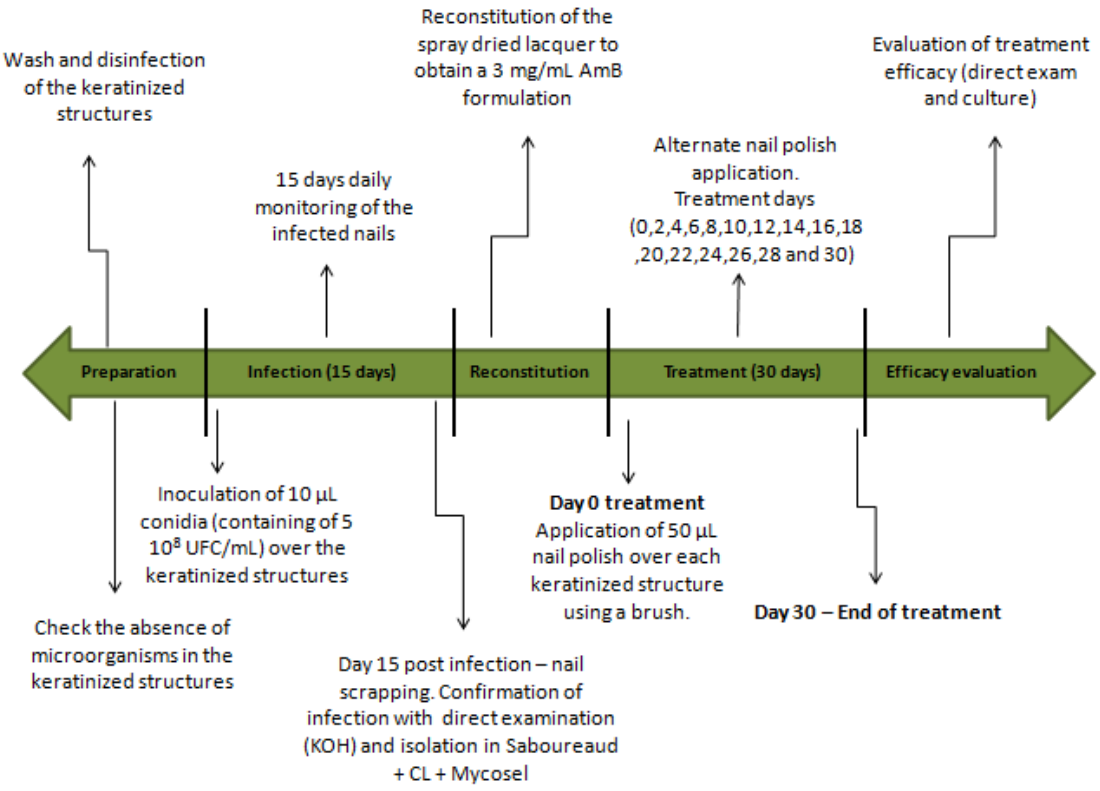

Figure 18 Study design and schedule for the efficacy studies on keratinized structures.

Once the infection was confirmed, the AmB nail lacquer (formulation 19) at 3 mg/mL AmB was applied over the nail using a brush. The formulation was reconstituted prior to administration and shake in order to assure the correct dispersion (see appendix 2). Each brush-stroke contained approximately 50 µL formulation that were directly applied over the infected nails. The formulation was applied on alternate days (1-0-1-0-1-0-1 and 0-1-0-1-0-1-0 from Monday to Sunday). After 30 days treatment the AmB nail lacquer efficacy was assayed by means of direct examination and culture.

In this study design the following groups were included as controls: sterility of the culture media, sterility of the topical formulation, sterility of the keratinized structures, and growth.

EXP1-1.4.8.1.3. Formulation 19 in vivo efficacy studies - A case study

- ✓ Case study of a 20 year-old boy infected by *Candida* spp.

The research group of Dra. Claudia Parras in Colombia works in collaboration with physicians treating immunosupressed patients with severe infections. One of these patients was a 20 year-old boy that presented deep candidiasis infections in mouth and throat that were resistant to usual treatments but not to Amphotericin B. As this patient did not respond to oral therapies, the drugs were being administered using catheters but these catheters were being infected by *Candida*. In order to be able to successfully administer the treatments required by this patient and to avoid more complications, it was decided to cover the catheters with formulation 19. As it dries really fast and leaves an impermeable AmB thin film, the infections might be avoided. In fact, the patient did not have any recurrence due to catheters infections when they were covered by formulation 19 leading to treatment accomplishment. Once the catheter was remove it was observed and analyzed. The catheter maintained the yellowish color due to the lacquer layer applied and there were no signs of candidiasis in the patient.

SPRAY DRIED NAIL LACQUER

SPRAY DRIED AMB NAIL LACQUER INSTRUCTIONS & LABELS

RECONSTITUTION

- Each vial contains 1.015 g of spray dried product that has to be reconstituted with 4 mL of the reconstitution solution (mixture of ethanol: NMP 7:1).

- Once the 4 mL have been incorporated, the vial has to be shake until complete dissolution. The reconstituted product will have the aspect of a translucent yellow-organish lacquer.

- The vials should be securely closed in order to avoid ethanol evaporation.

FINAL ASPECT AND CONTENT AFTER RECONSTITUTION

- After reconstitution, each vial will contain 5 g of lacquer that will last for 1 week treatment. AmB concentration in the final reconstituted product will be 0.3% (3 mg/mL).

HOW TO USE THE LACQUER

- Before each use/administration, the lacquer should be shake.
- With the help of a brush, apply a layer of nail lacquer and leave dry for 5 min.
- The lacquer forms a water impermeable film. If the layer has to be removed, the removal will be done with ethanol.

STORAGE

- Once reconstituted, the lacquer has to be stored at room temperature and protected from light.

Number of vials sent: **4**

Each vial can be used for **1 week treatment**

Treatment duration: **1 month** (30 days)

IMPORTANT:

- The spray dried product has to be **REFRIGERATED** (2-8ºC) and protected from light. If possible, maintain it inside a humid-controlled ambient or in a bag/bottle containing silica.

- The nail lacquer, once reconstituted, can be stored at **ROOM TEMPERATURE** and protected from light.

LABELS USED TO IDENTIFY THE CONTENT OF THE VIALS SENT TO COLOMBIA

- RECONSTITUTION SOLUTION

RECONSTITUTION SOLUTION FOR AMB NAIL LACQUER

Vial content: 10 mL of the mixture ethanol + NMP (7:1)

Shake before use

Add 4 mL of this solution to each spray dried lacquer vial

STORE AT ROOM TEMPERATURE AND PROTECTED FROM LIGHT

- SPRAY DRIED AMB NAIL LACQUER

SPRAY DRIED AMB NAIL LACQUER

Vial content: 1.015 g

Each 1.015 g of spray dried product contains 15 mg AmB

Reconstitute with 4 mL of the mixture Ethanol: NMP. Shake until homogenous reconstitution.

Final concentration: 0.3% AmB (3 mg/mL)

Content and final aspect: 5 g of AmB nail lacquer. Translucent and yellow-orangish lacquer.

Reconstitution valid for 7 days at room temperature.

THIS BAG CONTAINS 4 VIALS (1 PER WEEK) FOR 1 MONTH TREATMENT

STORE AT ROOM TEMPERATURE AND PROTECTED FROM LIGHT. KEEP INSIDE THE SILICA BAG.

STRAINS PEAK AREA STABILTY DMSO-MEOH CALIBRATION CURVES CANDIDA PARAPSILOSIS MG/ML MATRIX AUC/1000 SHELF-LIFE LYOPHILIZED YIELD %HUMIDITY DERMATOPHYTE TREATMENT FUSARIUM OXYSPORUM SHEAR RATE MONOMER HEALTHY FEMALE STUDENTS F13 DLS SEM 30ºC 48H TRYCHOPHYTON MENTAGROPHYTES INHIBITION ZONES C. KRUSEI NAIL MOLECULAR WEIGHT

EXP.1-2. RESULTS

SHEAR STRESS NAIL WEIGHT MYCOSEL FLUFFY F. SOLANI SOLUBILITY RECONSTITUTION P<0.05 MEAN PARTICLE SIZE NON-ELECTROSTATIC YELLOWISH C. KRUSEI LEAD CANDIDATE KERATINIZED STRUCTURES INFECTION STERILITY ASPERGILLUS NIGER mPa.s HALO LACQUER AGAR SHEAR STRESS F11 T. RUBRUM INHIBITION MOLDS POWDER FOR RECONSTITUTION VARIABILITY F19

EXP1-2. RESULTS

EXP1-2. 1. Amphotericin B solubility studies

EXP1-2.1.1. Reverse-phase high pressure liquid chromatography (HPLC)

The AmB concentration in the different samples was determined by RP-HPLC following the protocol reported by Espada *et al*. (2008). Two calibration curves, one for the extrapolation of the AmB solubility and another one for the determination of the AmB concentration on the nail lacquers and on the human nails treated, were performed by analyzing different AmB standards of known concentration. For each calibration curve, 13 AmB standards were prepared in triplicate by serial dilution using MeOH as solvent and starting from a stock solution containing 100 μg/mL AmB in a mixture of DMSO-MeOH (1/10). Tables 15 and 16 show the results obtained for both calibration curves.

The AmB solubility studies were performed in Italy, while the AmB determination on the nail lacquers and on the human nails were made in Spain (different instruments were used which implied the execution of two different calibration curves). This is the reason why there are two different calibration curves.

The AmB concentration for the solubility studies was extrapolated from a curve linear in the range 0.012 – 40 μg/mL [(AmB concentration) =115.1(peak area)-1.665; R^2=0.99], while the AmB concentration in the nail lacquer samples was extrapolated from a curve linear in the range 0.012 – 40 μg/mL [(AmB concentration)=113.2(peak area)-3.5076; R^2=0.99]. As shown in figures 19 and 20, in order to avoid mistakes when extrapolating low AmB concentrations, both curves were divided into two sub-curves; one used in the determination of low AmB concentrations and another one used for calculating high AmB concentrations.

Table 15. Concentration and area under the curve (AUC) of the different AmB standards used for the calibration curve employed in the determination of AmB concentration on nail lacquer and in the human nails.

Concentration [µg/mL]	**AUC/1000**	**AUC/1000**	**AUC/1000**	**Mean AUC**	**SD**
50	Out of range	Out of range	Out of range	NA	NA
40	4,508.5	4,520.8	4,498.1	4,509.13	11.36
25	2,823.1	2,902.6	2,875.6	2,867.1	40.42
12.5	1,375.7	1,396.1	1,386.4	1,386.06	10.20
6.25	690.2	699.7	702.1	697.33	6.29
3.125	342.8	356.2	339.5	346.16	8.84
1.5625	162.4	175.4	170.7	169.5	6.58
0.78125	81.91	80.32	82.1	81.44	0.97
0.3906	41.75	45.71	43.88	43.78	1.98
0.1953	20.73	19.85	21.63	20.73	0.89
0.09765	10.81	11.32	10.36	10.83	0.48
0.04882	5.34	5.61	5.95	5.63	0.30
0.02441	2.67	2.98	2.71	2.78	0.16
0.0122	1.09	1.51	1.36	1.32	0.21

Table 16. Concentration and area under the curve (AUC) of the different AmB standards assayed for the calibration curve used in the AmB solubility studies.

Concentration [µg/mL]	**AUC/1000**	**AUC/1000**	**AUC/1000**	**Mean AUC**	**SD**
50	Out of range	Out of range	Out of range	x	x
40	4,607.61	4,596.99	4,604.38	4,602.99	5.44
25	2,885.17	2,862.01	2,874.42	2,874.42	11.67
12.5	1,452.02	1,437.13	1,450.07	1,446.07	7.75
6.25	708.15	702.03	707.85	706.01	3.45
3.125	357.49	354.18	358.59	356.75	2.29
1.5625	177.69	176.04	178.04	177.25	1.06
0.78125	89.43	86.94	88.42	88.26	1.25
0.3906	45.14	42.14	45.07	44.11	1.71
0.1953	23.27	19.98	21.35	21.53	1.65
0.09765	11.48	9.76	10.17	10.47	0.89
0.04882	5.67	4.61	5.01	5.09	0.53
0.02441	2.74	2.19	2.45	2.46	0.27
0.0122	1.17	1.02	1.08	1.09	0.07

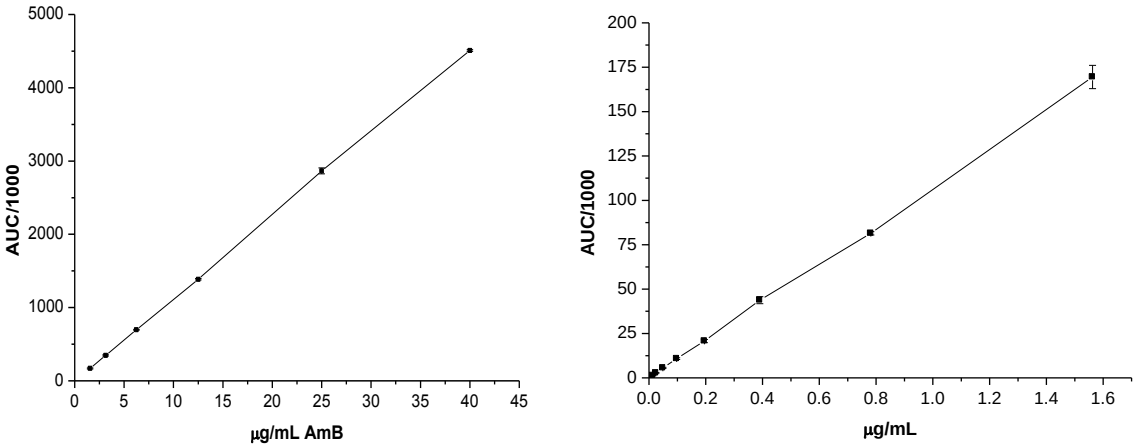

Figure 19. Calibration curves used to calculate: (left) high concentrations (y=113.41x-9.11, r^2=0.99) and (right) low concentrations of AmB (y=107.78x+0.0694, r^2=0.99) included in the nail lacquers.

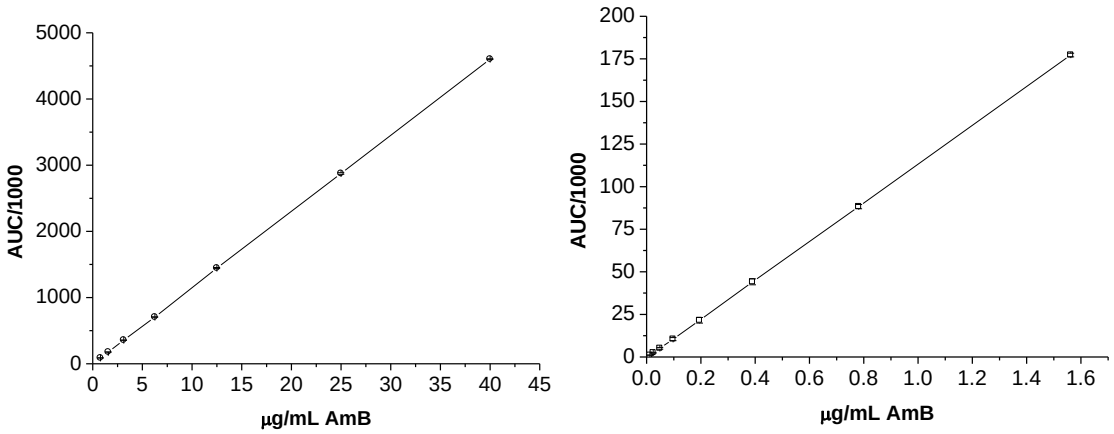

Figure 20. Calibration curves used to calculate: (left) high (y=115.22x-3.6765, r^2=0.99) and (right) low AmB concentrations (y=113.7x-0.454, r^2=0.99) on the solubility studies.

EXP1-2.1.2. Solubility studies

The AmB showed extremely low solubility values in almost all the solvents assayed with the exception of acetic acid, dimethyl formamide, DMSO and NMP. Table 17 shows the RP-HPLC results from the AmB solubility studies. As detailed in section EXP.1-1.2. from Materials and Methods, the samples were diluted with methanol prior

to injection (20 µL of sample + 980 µL of methanol). In the case of DMSO and NMP, as the solubility was expected to be much higher, those samples were diluted twice; first 20 µL sample were diluted with 4980 µL methanol and then, the resulting solution was diluted again as detailed for the other samples.

The higher AmB solubility in acetic acid compared to the other solvents is due to the charges generated on this molecule in the presence of an acidic environment due to its amphoteric character.

Table 17. RP-HPLC results obtained in the AmB solubility studies

Solvent	**Mean AUC (/1000)**	**Retention time (min)**
Acetic acid	3.028.45	8.567
Acetone	13.54	8.633
Acetonitrile	21.80	8.600
Cyclohexane	5.07	8.592
Dimehtylformamide	2.368.44	8.717
Dimethylsulfoxide (DMSO)	358.05*	8.575
Ethanol	95.85	8.608
Ethylenglycol dimethylether	24.04	8.658
Isopropyl alcohol	17.58	8.542
N-methyl-2-pyrrolidone (NMP)	433.66*	8.542
Petroleum ether	2.19	8.692

***** These samples were diluted twice prior to injection.

The highest solubility values were found with NMP and DMSO (see table 18). It is well known that AmB is highly soluble in DMSO and it can be found as monomer when dissolved on it. However, this solvent is not usually used as AmB solubilizer due to its high toxicity.

On the other hand, the solubility of AmB in NMP had never been studied. This is the first data published on AmB solubility in NMP. The NMP has demonstrated to be the best solvent for AmB. It solubilizes the drug in its monomeric state (figure 21).

Table 18. AmB solubility studies in different organic solvents.

Solvent	AmB (mg/mL)
Acetic acid	4.48 ± 0.16
Acetone	0.006 ± 0.0003
Acetonitrile	0.0098 ± 0.00002
Cyclohexane	0.0024 ± 0.00002
Dimethylformamide	4.12 ± 0.0708
Dimethylsulfoxide	39.41 ± 0.0032
Ethanol	0.0423 ±0.0001
Ethylenglicol dimethylether	0.0072 ± 0.0001
Isopropyl alcohol	0.0079 ± 0.0003
N-metil-2-pirrolydone	47.73 ± 0.022
Petroleum ether	0.0011 ± 0.00008

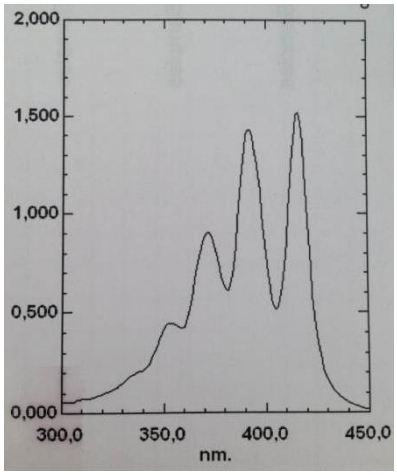

Figure 21. UV scan (450 -300 nm) of AmB dissolved in NMP.

EXP1-2.2. Formulation development

Our aim in the development of an amphotericin B nail lacquer was first focused on obtaining an appropriate matrix that served as nail polish, and then, on the incorporation of amphotericin B on that matrix. Thus, we aimed in obtaining a nail lacquer able to form an homogenous film and dry within 5 minutes when applied to the nail.

Tables 19 and 20 summarize the aim of the formulations as well as the problems found during preparation and/or characterization. Table 19 refers to the water soluble while table 20 to the non-water soluble nail lacquers.

Table 19. Summary of the water soluble nail lacquers prepared

A. Water soluble nail lacquers		
A.1. Water soluble matrix		
Formulation	**Aim of the formulation**	**Comments**
Formulation 1	Design a water soluble matrix	High viscosity
Formulation 2	Decrease the viscosity of F1	Decreased viscosity
A.2. Incorporation of AmB in the water soluble matrix using Plasdone K90 as film former		
Formulation	**Aim of the formulation**	**Comments**
Formulation 3	AmB solubility with NMP	NA
Formulation 4	AmB solubility with γ-CD	Stability problems
Formulation 5	Modifications to increase the stability of F4	Increased stability
Formulation 6	AmB solubility with Plasdone	Long drying times
Formulation 7	Overcome the drying problems of F6	Long drying times (shorter than F6)
Formulation 8	Overcome the drying problems of F7	Shorter drying times
Formulation 9	AmB solubility with Fungizone® simile	Drying problems
Formulation 10	Incorporation of urea to F9	Drying problems
Formulation 11	Shorten drying times of F9	Reduced drying times
Formulation 12	Incorporation of urea to F11	Increased drying times
Formulation 13	Reduce the drying time of F12	Reduced drying times
A.3. Incorporation of AmB in the water soluble matrix using PluronicF127 as film former		
Formulation 14	AmB solubility with Fungizone® simile	NA
Formulation 15	Incorporation of urea to F14	Stability problems
Formulation 16	Ethanol removal to improve stability of F14 and F15	NA
Formulation 17	AmB solubility with γ-CD	

Table 20. Summary of the water insoluble nail lacquers prepared

B. Water insoluble nail lacquers		
B.1. Incorporation of AmB in water insoluble matrix using Eudragit®L100		
Formulation 18	AmB and Eudragit dissolution in NMP	Drying problems
Formulation 19	Addition of ethanol to overcome drying problems	Short drying times
Formulation 20	Incorporation of urea to F19	No soluble

More detailed information on the nail lacquer matrix and the problems found during preparation and/or stability can be found in sections AP1.3. and AP1.4. appendix 1.

EXP1-2.3. Pre-selection of the lead candidate formulations

Between all the water permeable and impermeable lacquers developed, the three lead candidates considered as possible carriers for AmB delivery were Formulation 11, Formulation 13 (water permeable lacquers) and Formulation 19 (water impermeable polish). These formulations were chosen according to their stability, characteristics of the film formed and the drying times.
In the following experiments, these 3 formulations were used.

EXP1-2.4. Characterization of the three lead candidate formulations

EXP1-2.4.1. Physicochemical charaterization

EXP1-2.4.1.1. Lyophilization/spray drying

As detailed in Materials and Methods (EXP1-1.3.5.1.2 and EXP1-1.3.5.1.3) the water soluble nail lacquers were lyophilized in order to obtain a powder for reconstitution. This method aimed in generating a product with a longer shelf life compared to the freshly prepared formulations. Formulations 11 and 13 were prepared following the protocol previously detailed, frozen with liquid nitrogen and lyophilized during 48 h. The freeze dried powders obtained were yellowish and slightly electroscopic (figure 22A). Its water content, measured by IR, was 6.91% and 4.96% for F11 and F13, respectively.

Regarding the water impermeable formulation, F19, a lyophilization process could not be performed. The freeze-dried method does not allow for the use of organic solvents.

Therefore, another method had to be used for obtaining a F19 stable powder for reconstitution. The spray drying technique was used as an alternative to the freeze drying. As the solvents included in F19 had high evaporation temperatures, some changes were made on the initial F19 composition. The ethanol was substituted by methanol and the NMP by DMSO. Even though DMSO had lower evaporation temperature compared to NMP, this value was still too high. Experiments performed by our research group (data not shown) demonstrated that the mixture DMSO-methanol, at low DMSO contents, evaporated at 75ºC. To note that the substitution of ethanol by methanol was based not only on the studies performed in terms of evaporation, but also to the fact that the mixture DMSO-methanol assures AmB in-process stability. The mixture DMSO-methanol has been widely used in our research group for the AmB concentration determination, as the AmB is completed solubilized in this mixture (monomeric aggregation state). Once the spray drying method was set up, the F19 powder for reconstitution was obtained with yields ranging between 89-94%. The aspect of the recovered product was that of a fluffy, yellowish, non-electrostatic powder (figure 22B). As well as for the lyophilized products, the humidity value was measured in this powder. The % of humidity was 7.03%.

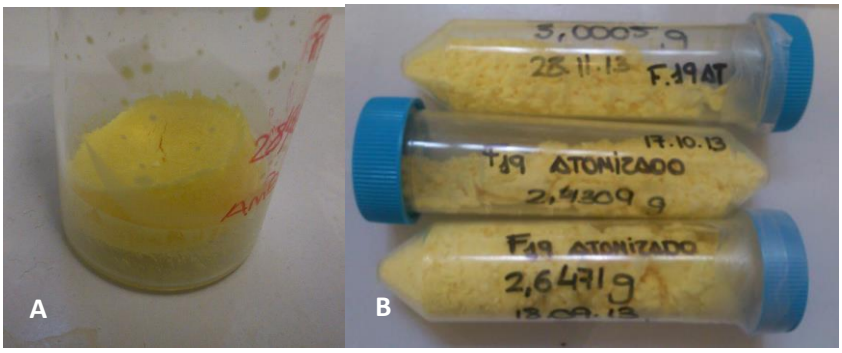

Figure 22. A. Lyophilized F11 and B. Spray dried F19

Both methods, freeze drying and spray drying, provided stable powders for reconstitution. The addition of water or mixture NMP-Ethanol to F11, F13 and F19, generated nail lacquers with the same properties of the freshly prepared formulations. The reconstitution lasted less than 5 min and it was favored by agitation.

EXP1-2.4.1.2. Stability studies

The AmB concentration in freshly prepared and reconstituted formulations was studied over the time. As shown in table 21 and figure 23, the AmB content in freshly prepared

formulations remained stable during at least 3 weeks at 25ºC. At week 4 a small decrease in AmB content was detected.

Table 21. Concentration values of F11, F13 and F19 during 28 days storage at 25ºC.

Formulation	% AmB (g of amB/100 g formulation)				
	0 days	7 days	15 days	21 days	28 days
F11	0.3001	0.2998	0.2962	0.2959	0.2792
F13	0.2999	0.2995	0.2951	0.2943	0.2819
F19	0.3010	0.3005	0.2978	0.2965	0.2854

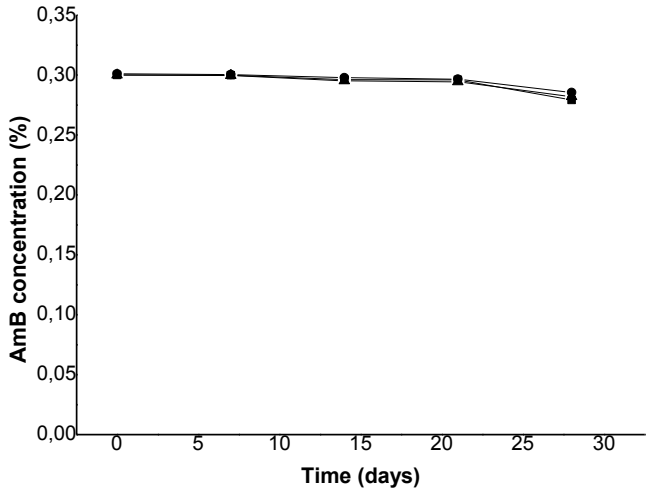

Figure 23. AmB concentration on F11, F13 and F19 after 28 days storage at 25ºC.

Table 22 shows the concentration values obtained for the reconstituted powders (rF11, rF13, rF19) during 15 days storage at room temperature. These reconstituted solutions were designed to be used only for 1 week treatment and therefore, a stability of 15 days is accepted.

Table 22. Concentration values of rF11, rF13 and rF19 during 28 days storage at 25ºC.

Formulation	% AmB (g of amB/100 g formulation)		
	0 days	7 days	15 days
rF11	0.2998	0.2981	0.2977
rF13	0.2989	0.2978	0.2972
rF19	0.3008	0.2993	0.2989

A complete stability study on the powders for reconstitution has been designed. The powders will be exposed to 4ºC, 25ºC and 40ºC and its physicochemical properties as well as the AmB concentration will be analyzed over time.

EXP1-2.4.1.3. Dynamic light scattering (DLS)

Tables 23 and 24 show the particle size in number of the two water permeable lead candidates analyzed by DLS. The mean particle size was higher for formulation 13 compared to 11 for all the assayed period. Both formulations had a mean particle size ranging between 20-30 nm which remained stable during at least 15 days after reconstitution. The mean particle size was increased after 3 weeks reconstitution (38.03 ± 2.86 nm and 40.15 ± 2.21 nm for F11 and F13, respectively) and some of the formulations showed signs of desestabilization at day 35 (four populations with a particle size of 1824, 853, 234.4 and 27.41 nm were detected).

Formulation 19 could not be analyzed by DLS because, in contact with water, the polymer precipitates forming a film.

Table 23. Mean particle size of AmB fresh lacquer over 15 days.

Formulation	**Time (days)**		
(fresh formulation)	**0**	**7**	**15**
Formulation 11	20.01 ± 2.56 nm	22.86 ± 1.43 nm	21.57 ± 1.21nm
Formulation 13	25.80 ± 4.28 nm	30.56 ± 0.89 nm	29.46 ± 2.33 nm
Formulation 19*	-	-	-

Table 24. Mean particle size of AmB reconstituted lacquer over 15 days.

Formulation	**Time (days)**		
(after reconstitution)	**0**	**7**	**15**
Formulation 11	21.98 ± 1.37 nm	23.19 ± 2.75 nm	24.85 ± 1.98 nm
Formulation 13	26.05 ± 2.24 nm	29.93 ± 3.16 nm	30.17 ± 3.05 nm
Formulation 19*	-	-	-

EXP1-2.4.1.4. Scanning electron microscopy

The films formed by the different formulations are shown on figure 24.

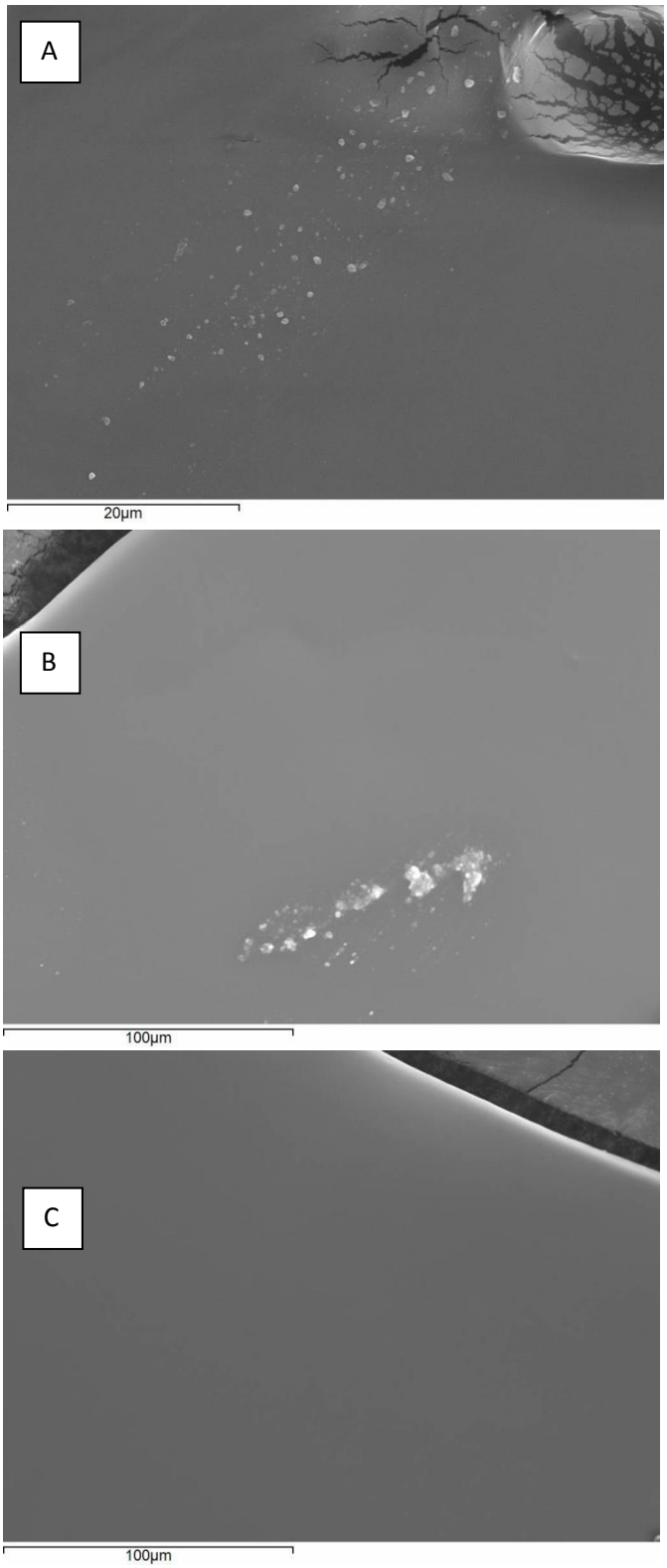

Figure 24. SEM microphotographies of the film formed by F11 (A), F13 (B) and F19 (C).

Formulation 19 formed a homogenous film while F11 and F13 generated a film in which some deposits could be detected. Those deposits were chemically analyzed by SEM, concluding that they are not composed by AmB crystals. They might appear as a consequence of incomplete dissolution of any of the formulation components.

Figure 25 shows the amplified zoom of the deposits found on the film formed by formulations 11 and 13.

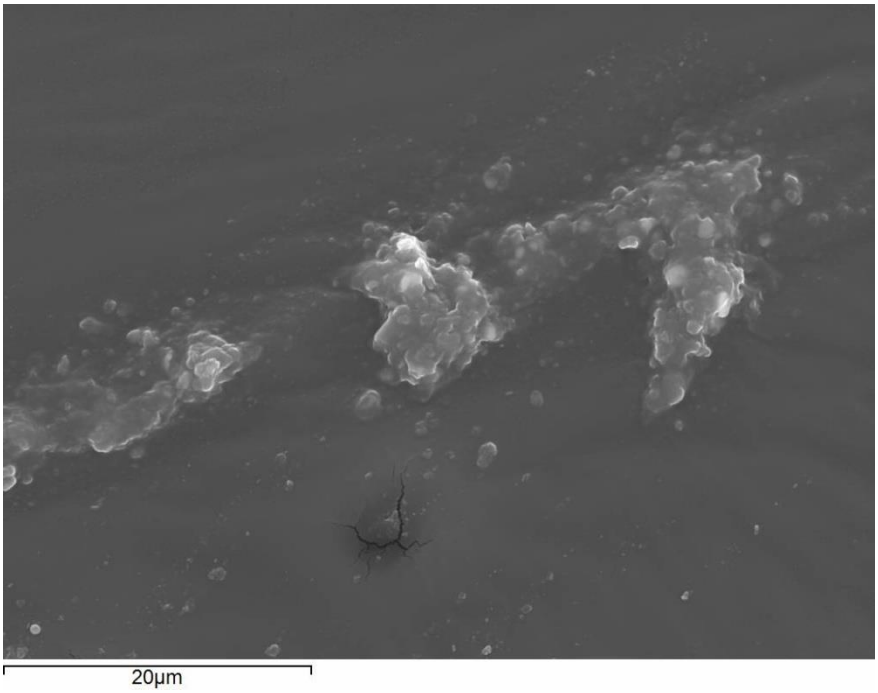

Figure 25. Amplified picture of the filmed formed by F13.

EXP1-2.4.1.5. Rheological characterization

Tables 25 and 26 show the viscosity results from F11, F13 and F19 in the fresh and reconstituted formulations at 0, 1 and 2 weeks. The viscosity values were recorded in cPs.

Table 25. Viscosity data (cPs) from F11, F13 and F19 fresh formulations.

Fresh formulation			
Formulation	**Time 0**	**Time 7 days**	**Time 15 days**
Formulation 11	265.85±2.48	245.26±4.21	255.49±1.28
Formulation 13	326.55±3.60	313.75±3.60	319.88±1.85
Formulation 19	80.45±1.26	79.38±1.85	89.05±0.95

Table 26. Viscosity data from F11, F13 and F19 reconstituted formulations.

Reconstituted formulation			
Formulation	**Time 0**	**Time 7 days**	**Time 15 days**
Formulation 11	259.85±2.45	251.38±4.27	261.49±1.28
Formulation 13	323.98±1.95	327.02±1.21	328.58±1.18
Formulation 19	88.78±0.57	88.82±0.90	89.93±0.57

The viscosity values measured for F11 and F13 where higher than those of F19. The higher values obtained for the water permeable lacquers are related to the higher molecular weight of the Plasdone® K90 compared to the Eudragit® L100.

On the other hand, the differences found in between F11 and F13 can be explained by the incorporation of urea in the formulation. The addition of 10% urea on F13, entailed a 10% decrease on solvents content (5% water and 5% ethanol). This decrease generated, as expected, a higher viscous lacquer.

As shown in table 26, the viscosity values in the reconstituted samples did not differed to those of the freshly prepared formulations. Moreover, as for the freshly prepared lacquers, the values remained stable during the whole assayed period.

Figures 26 and 27 show the rheological behavior of freshly prepared and reconstituted F11.

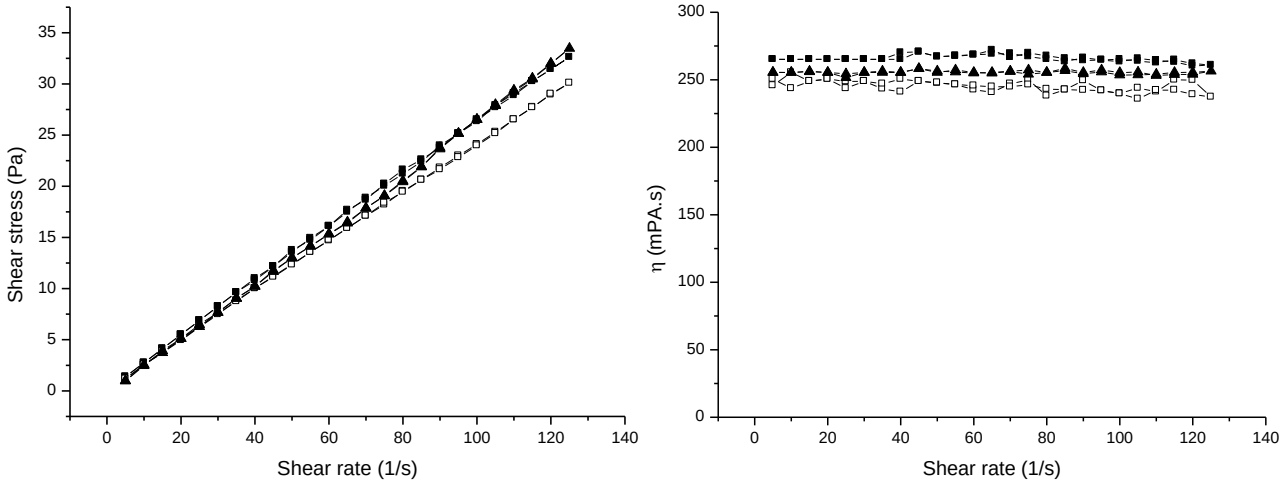

Figure 26. Viscosity profile of fresh F11 at time 0 (-■-), after 1 week (-□-) and after 2 weeks storage at 20±2 ºC (-▲-).

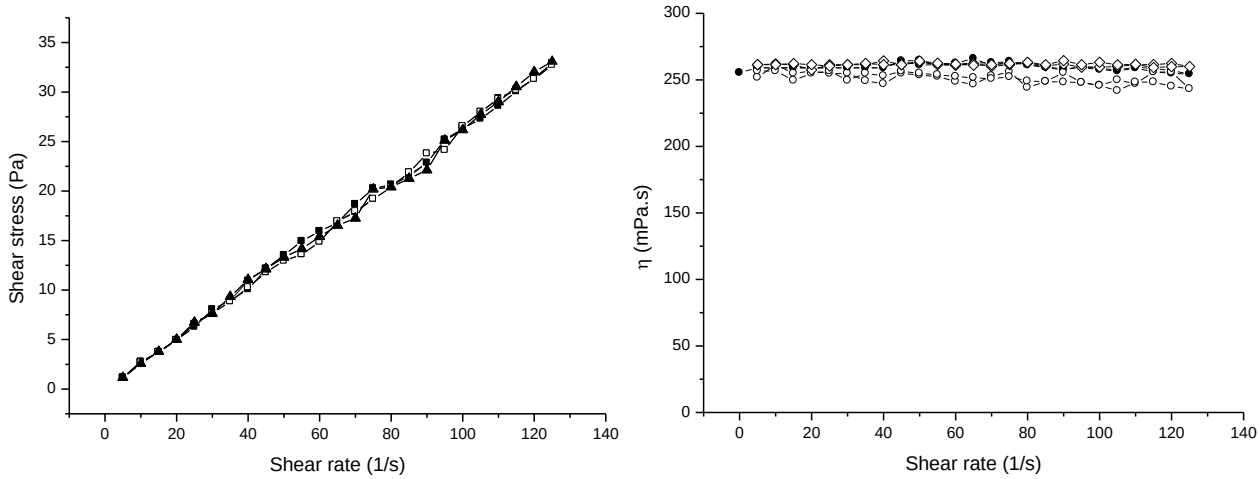

Figure 27. Viscosity profile of reconstituted F11 at time 0 (-●-), after 1 week (-○-) and after 2 weeks 20±2 ºC (-◊-).

Figures 28 and 29 show the rheological behavior of freshly prepared and reconstituted F13.

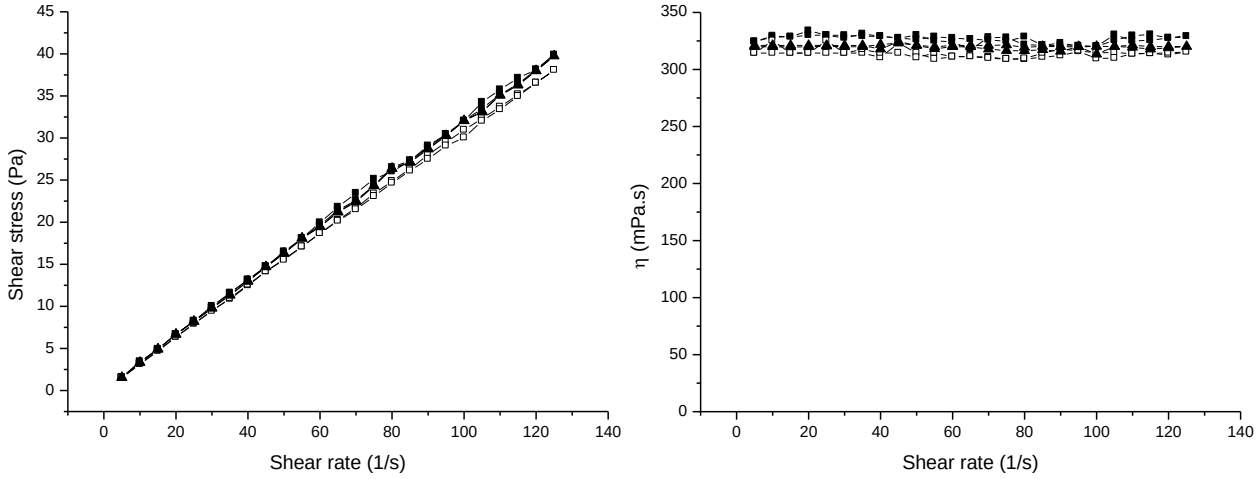

Figure 28. Viscosity profile of fresh F13 at time 0 (-■-), after 1 week (-□-) and after 2 weeks storage at 20±2 ºC (-▲-).

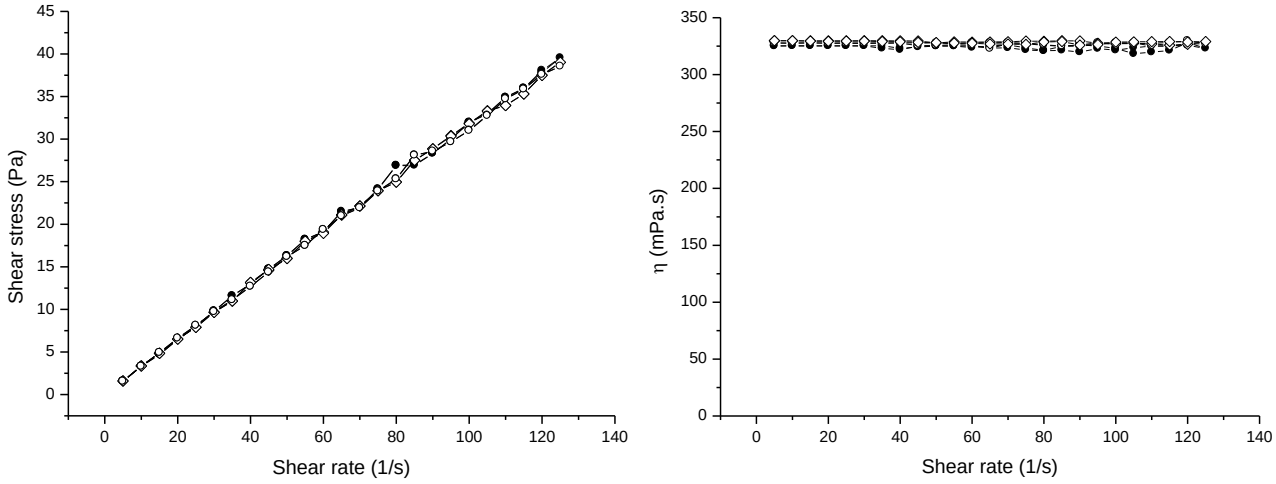

Figure 29. Viscosity profile of reconstituted F13 at time 0 (-●-), after 1 week (-○-) and after 2 weeks 20±2 ºC (-◊-).

And finally, figures 30 and 31 show the rheological behavior of freshly prepared and reconstituted F19.

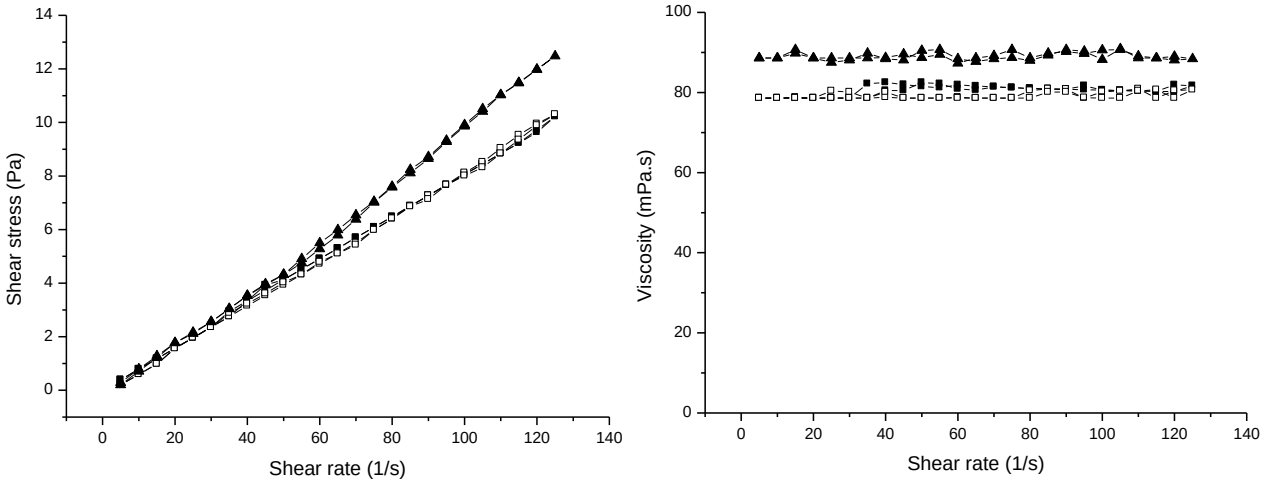

Figure 30. Viscosity profile of fresh F19 at time 0 (-■-), after 1 week (-□-) and after 2 weeks storage at 20±2 ºC (-▲-).

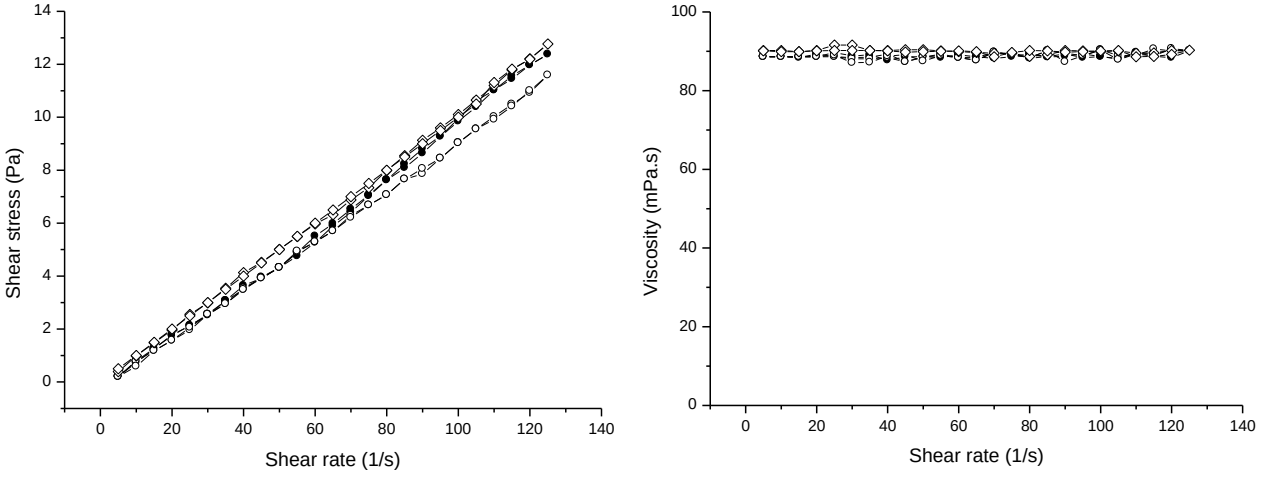

Figure 31. Viscosity profile of reconstituted F19 at time 0 (-●-), after 1 week (-○-) and after 2 weeks 20±2 ºC (-◊-).

All three lead candidates (F11, F13 and F19) showed Newtonian flow properties regardless the formulation preparation (freshly or reconstituted). This was in accordance to other nail antifungal formulations used in the treatment of onychomycosis [338].

EXP1-2.5. *In vitro* nail penetration and efficacy studies

EXP1-2.5.1. *In vitro* nail penetration studies

The *in vitro* efficacy studies on the three lead candidates were performed on female human nails. The nails were donated by healthy female students whose age ranged between 25-35 years old.

Formulations 11, 13 and 19 were those that showed the best physicochemical properties and therefore, these were the ones assayed *in vitro* in terms of penetration, activity and efficacy.

As indicated in Materials and Methods (EXP1-1.3.6.1), 5 nails were used for each formulation on each of the experiments. The nails, whose weight differed between donors and in between the same donor, were weighted prior and after incubation with 0.5 g of the different formulations. The nails weight was found to be in the range 2.8-8 mg. As the µg of AmB that penetrated into the nail were expressed as function of the nail weight, this variability did not affect the final results. Not only the weight of the nails was checked, but also the amount of formulation added (0.5001- 0.05104 g).

Once the nails containing the lacquer, were incubated at 32ºC for 24 hours, their superficial lacquer film was removed in order to assure that the AmB concentration detected by HPLC was extracted only from inside the nail. The washing was performed following the protocol described in Materials and Methods (EXP1-1.3.6.1).

The AmB extraction was first assayed with NaOH. The literature describes the addition of high molarities NaOH solutions as the best mechanism to dissolve the nails. Nevertheless, this method generated some problems. First of all, the AmB at high pH not only get dissolves but also gets degraded. This degradation produced low, almost no detectable, peaks in the HPLC (false negatives). Secondly, the nail dissolution generated many compounds which did not allow for a proper AmB UV determination. The spectra (300-450 nm) showed new peaks which absorbed at the same AmB

wavelengths. Finally, the HPLC did not work either. When neutralizing the samples for injection, some molecules precipitated and even though the samples were filtered, new peaks were found to overlay the AmB monomer peak at 406 nm. Several changes were performed on this method (different NaOH solutions, filtrations, addition of AmB solvents in the dissolved nails followed by centrifugation, modifications on the mobile phase composition, insertion of gradients, etc.) but none of them worked.

As an alternative to nail dissolution with sodium hydroxide and, as a result of some observations made by our research group during this project, the addition of DMSO was considered as an acceptable method for AmB nail extraction. A study performed on nails exposed to DMSO during 48 hours showed that this solvent attacks the nail and generates similar degradation products to those detected with NaOH treatment. As this method worked slower and was not so aggressive as NaOH (the nail is not dissolved), the AmB that penetrated the nail was successfully recovered and analyzed.

Once the extraction method was set up, the *in vitro* penetration studies were design. Figures 32 shows a scheme of the planned studies.

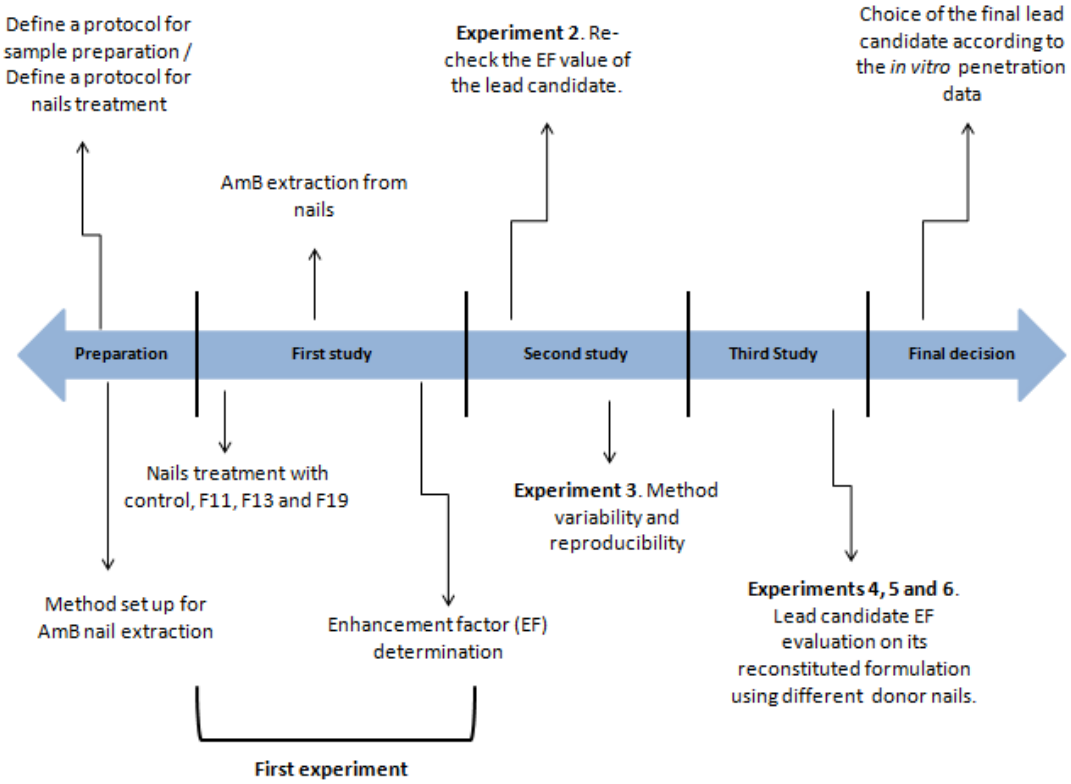

Figure 32. *In vitro* nail penetration study design.

The first *in vitro* study aimed to establish the different penetration efficacies of a control (an AmB suspension) and F11, F13 and F19 formulations. The experiments were performed in triplicate and 5 nails were used for each formulation on each experiment. The *in vitro* penetration nail studies are known to have a wide variability and therefore, the higher the number of nails used and the higher the number of experiments performed, the better.

Table 27 shows the µg of AmB extracted from mg of nail (µg that theoretically penetrated the nail) as well as the enhancement factor (EF). The EF measures the higher or lower penetration of a formulation with respect to a control. Usually the control is a commercialized formulation, but in this case it was an AmB suspension (no excipients added).

Table 27. First *in vitro* penetration study. µg of AmB per mg of nail and enhancement factor.

Formulation	**µg AmB/mg nail (mean)**	**SD**	**EF**
Control	0.2928	0.005	NA
F11	0.221	0.065	0.75
F13	0.192	0.079	0.66
F19	0.571	0.055	**1.95**

SD, standard deviation; EF, enhancement factor

The results of this first experiment demonstrated that F19 was the formulation with highest enhanced penetration. Surprisingly, F11 and F13 showed lower nail penetration (EF<1) values. Not only F19 penetrated more but also the NMP efficacy as penetrating enhancer was demonstrated to be higher than that of urea (F13).

The second study (second and third experiments) was conducted in order to check the reproducibility and variability of the EF value obtained for F19, and therefore, of the method. In these experiments, the control and the F19 were the only samples analyzed. Tables 28 and 29 show the results for the second and third experiments. Both experiments, as previously stated, were performed in triplicate.

Table 28. Second *in vitro* penetration study. µg of AmB per mg of nail and enhancement factor for F19. Experiment 2.

Formulation	µg AmB/mg nail (mean)	SD	EF
Control	0.0853	0.05	NA
F19	0.151	0.04	**1.77**

Table 29. Second *in vitro* penetration study. µg of AmB per mg of nail and enhancement factor for F19. Experiment 3.

Formulation	µg AmB/mg nail (mean)	SD	EF
Control	0.2571	0.14	NA
F19	0.4341	0.064	**1.69**

The three experiments performed on different nails, gave an EF value of 1.69-1.95 for F19. In the three cases the values were similar and always higher than those of the control.

Once the method reproducibility was tested another three experiments (experiment 4, 5 and 6) were designed to confirm the *in vitro* penetration of the reconstituted F19 (rF19) compared to the freshly prepared formulation. Tables 30, 31 and 32 show the EF values obtained for both F19 and rF19.

Table 30. Third *in vitro* penetration study. µg of AmB per mg of nail and enhancement factor for F19 and rF19. Experiment 4.

Formulation	µg AmB/mg nail (mean)	SD	EF
Control	0.2232	0.03	NA
F19	0.4181	0.14	**1.87**
rF19	0.4648	0.12	**2.02**

Table 31. Third *in vitro* penetration study. µg of AmB per mg of nail and enhancement factor for F19 and rF19. Experiment 5.

Formulation	µg AmB/mg nail (mean)	SD	EF
Control	0.1659	0.05	NA
F19	0.3120	0.05	**1.88**
rF19	0.3282	0.07	**1.98**

Table 32. Third *in vitro* penetration study. µg of AmB per mg of nail and enhancement factor for F19 and rF19. Experiment 6.

Formulation	µg AmB/mg nail (mean)	SD	EF
Control	0.1722	0.03	NA
F19	0.3139	0.05	**1.83**
rF19	0.3137	0.05	**1.82**

The EF values obtained for F19 and rF19 were really similar. Regardless the small differences due to method accuracy, both formulations behaved identically. The spray drying process did not alter the physicochemical properties of F19 nor its nail penetration.

The EF values calculated along all the studies, were in the range [1.73-1.92] and [1.82 - 2.09] for F19 and rF19, respectively.

At this point and pending on the *in vitro* efficacy studies, the F19 was considered as possible lead candidate for the following experiments planned with the scientists of Colombia.

It is worth noting that the best method to study the *in vitro* nail penetration is based on the use of Franz cells. The research group is currently setting up the conditions for this experiment (data not generated yet).

EXP1-2.5.2. *In vitro* efficacy against *Candida albicans* CECT1394

The efficacy of the three lead candidates (F11, F13 and F19) was studied against *Candida albicans* CECT1394. As described in materials and methods, the 3 formulations were diluted to 96 µg/mL using phosphate buffer or DMSO. The water permeable lacquers (F11 and F13) were diluted with phosphate buffer, while the water

impermeable lacquer (F19) was diluted with DMSO. As previously mentioned, the film forming agent included in F19 (Eudragit® L100) forms a solid film in contact with water, reason why it cannot be diluted with phosphate buffer.

Once the dilutions were prepared, the paper disks where loaded with 20 µL sample, placed over the agar containing the *Candida* and incubated at 30ºC for 48 h. The inhibition halos generated for F11, F13 and F19, as well as the formulations efficacy compared to the standard (S3, standard with the same concentration), are detailed in table 33. An AmB suspension was used as control.

The experiment was performed in triplicate and what is detailed on table 33 is the mean of the three experiments. Each experimental value was generated from the measurement of 5 inhibition zones.

Table 33. Inhibition halos (mm) and % of activity obtained with F11, F13 and F19.

Formulation	Mean inhibition halo (mm)	SD	% Activity compared to S3
Control	14.25	0.52	64.6
S3	22.06	0.13	100
F11	20.90	0.71	103.1
F13	18.01	0.18	94.7
F19	22.75	0.73	81.65

As shown in table 33, F19 was the formulation that generated the higher inhibition zones (22.75 mm) in all three experiments. The slightly higher activity of F19 compared to S3 can be related to the presence of NMP on the formulation. The antifungal activity of the AmB included in this formulation might be increased by the penetrating effect conferred by NMP. These assumptions would be accepted or rejected when more experimental data would be generated (following experiments).

The results obtained in the efficacy study, provided the information necessary to select the final lead candidate formulation. All the data allow us to conclude that F19, was the selected formulation.

In order to check that the spray dried F19 nail lacquer had the same activity than the freshly prepared formulation, the efficacy study was performed again in triplicate. In this case, the control, the fresh F19, the reconstituted formulation (rF19) and the S3 standard were assayed. Table 34 shows the results obtained from this study.

Table 34. Inhibition halos (mm) and % of activity obtained with freshly prepared and reconstituted F19 (rF19)

Formulation	Mean inhibition halo (mm)	SD	% Activity compared to S3
Control	14.19	0.48	64.5
S3	21.98	0.04	100
F19	22.26	0.03	101.3
rF19	22.31	0.12	101.5

This *in vitro* efficacy study showed that both, fresh and reconstituted F19, had the same activity. The spray drying did no modify the formulation efficacy.

Moreover, the differences previously found in activity for F19 compared to S3, decreased in this experiment. These small differences were related to the method accuracy and not to a real higher F19 efficacy.

In order to compare the activity of F19 and rF19 to commercially available AmB disks (Neo-sensitabs®), a third experiment was performed. In this case, the control, the S3, the Neo-sensitabs®, F19 and rF19 were assayed against *Candida albicans* CECT1394. The results obtained are indicated in table 35.

To note that the F19 and rF19 disks were impregnated with 20 µL of 96 µg/mL AmB (load=1.92 µg AmB) while the AmB content of the Neo-sensitabs® disks was 10 µg. The experiment was performed with a higher initial AmB concentration on Neo-sensitabs® disks.

Table 35. Inhibition zones (mm) and % of activity obtained with freshly prepared and reconstituted F19 (rF19) compared to Neo-sensitabs®

Formulation	Mean inhibition halo (mm)	SD	% Activity compared to S3
Control	14.51	0.67	66.0
S3	21.98	0.06	100
Neo-sensitabs®	21.68	0.23	98.6
F19	22.44	0.07	102.1
rF19	22.48	0.17	102.3

Even though the initial AmB concentration on the Neo-sensitabs® disks was 5 times higher than in the other formulations, its inhibition zone, as well as its percentage (%) of activity, was lower than for F19, rF19 and S3.

In all three *in vitro* activity studies performed, the highest inhibition zone and the highest percentage of activity was found for both fresh and reconstituted F19.

EXP1-2.6. Lead candidate selection

The better performance of F19 compared to F11 and F13 (higher *in vitro* nail penetration and efficacy against *Candida albicans*) together with its high stability and novelty, are some of the reasons why it was selected as lead candidate. Formulation 19 was sent to the Colombia scientists for establishing the minimum inhibitory concentrations (MICs) against the etiological agents responsible for the onychomycosis as well as for the *in vitro* efficacy studies against infected keratinized structures.

EXP1-2.7. Evaluation of the antimycotic effect of an AmB nail lacquer against the etiological agents responsible for the onychomycosis - *In vitro* studies performed in Colombia.

AmB efficacy studies against the dermatophyte and non-dermatophyte molds responsible for the onychomycosis, as well as the *in vitro* efficacy against an infected model, were performed in collaboration with University Javeriana of Bogotá (Colombia). A summary of the results generated is indicated below.

EXP1-2.7.1. Determination of the minimal inhibitory concentration (MIC). AmB efficacy

For the determination of the amphotericin B activity, several concentrations ranging between 9.8 to 2,400 µg/mL were prepared. Two of those concentrations being higher that the ones described in the guideline CLSI. The samples prepared correspond to those concentrations in which there is the appearance of an inhibition halo.

Method validation

In order to evaluate the validity of the test, two strains of *Candida* were used as reference; *Candida parapsilosis* ATC22019 and *Candida krusei* ATCC6258. Both strains were evaluated against all the concentrations prepared for the study. As the commercially available disks contain 25 µg/mL AmB, the concentration used for the

method validation was also 25 µg/mL. Figures 33 and 34 show the results obtained from the reference strains.

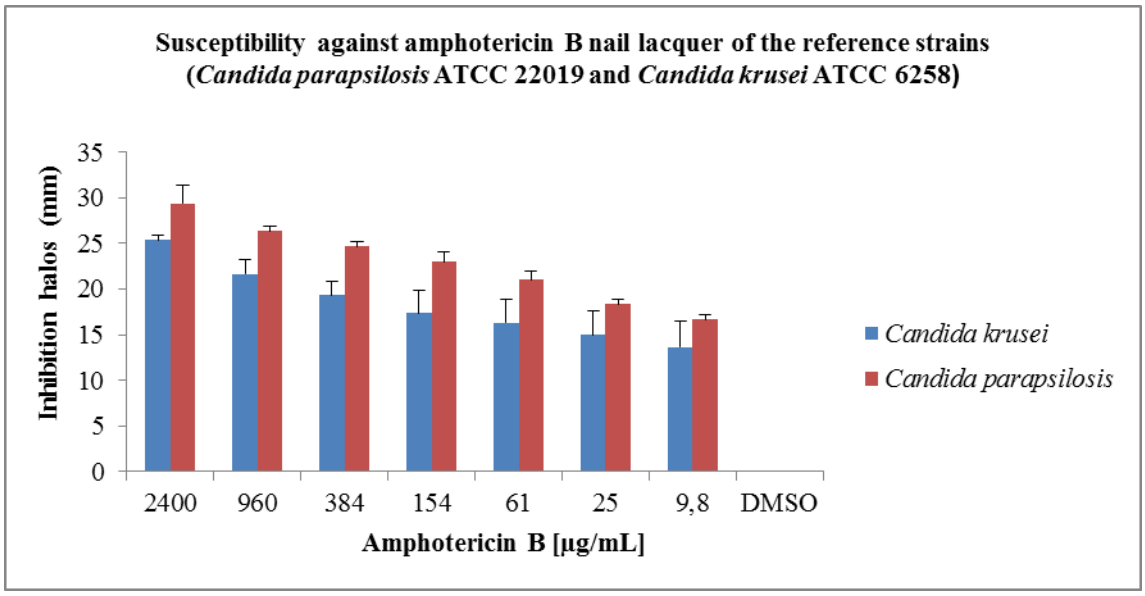

Figure 33. MIC test validation using two reference strains of *Candida*.

At an AmB concentration of 25 µg/ml the inhibition zones obtained for *Candida krusei* and *Candida parapsilosis* were 14-25 mm and 17-29 mm, respectively. These values were in accordance with the cut points detailed on CLSI guideline (M44 A2). Therefore, the test demonstrated its validity for MIC determination.

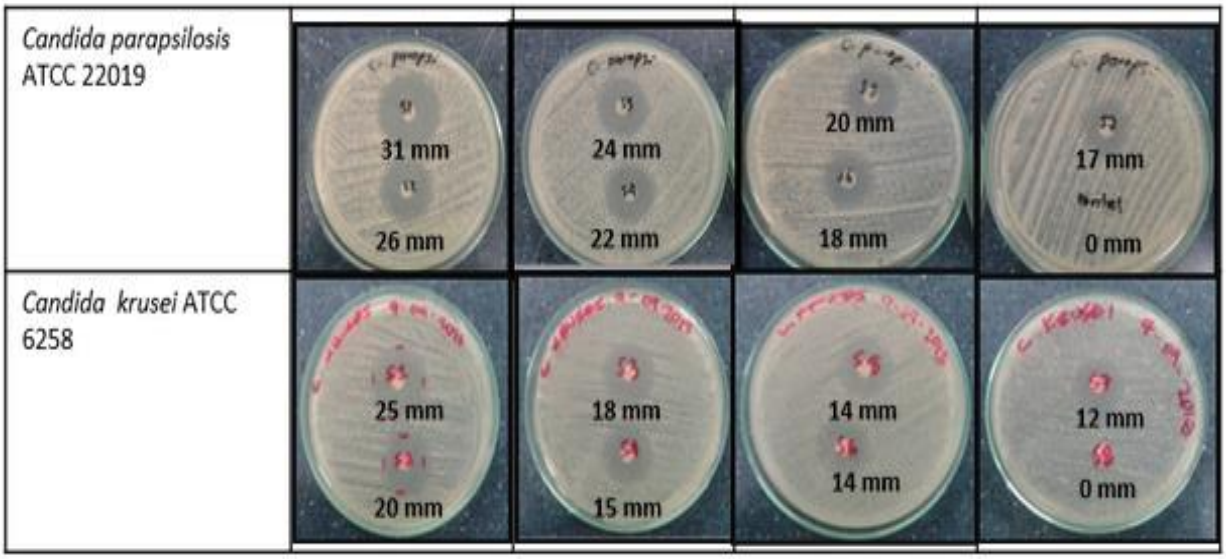

Figure 34. Method validation using C. parapsilosis and C. Krusei. Inhibition zones (mm) generated by both strains

To note that the zones of inhibition obtained for the rest of the concentrations are in fair agreement with the expected results, as the inhibition zones diameter might be directly related to the drug concentration.

EXP1-2.7.1.1. AmB activity against dermatophyte and non-dermatophyte molds

EXP1-2.7.1.1.1. Activity against dermatophyte molds

The evaluation of the amphotericin B activity against *Trichophyton mentagrophytes* and *Trichophyton rubrum* was determined by means of the inhibition halo generated (measured in mm) against each microorganism. The AmB inhibition halos for both spp are detailed in figure 35.

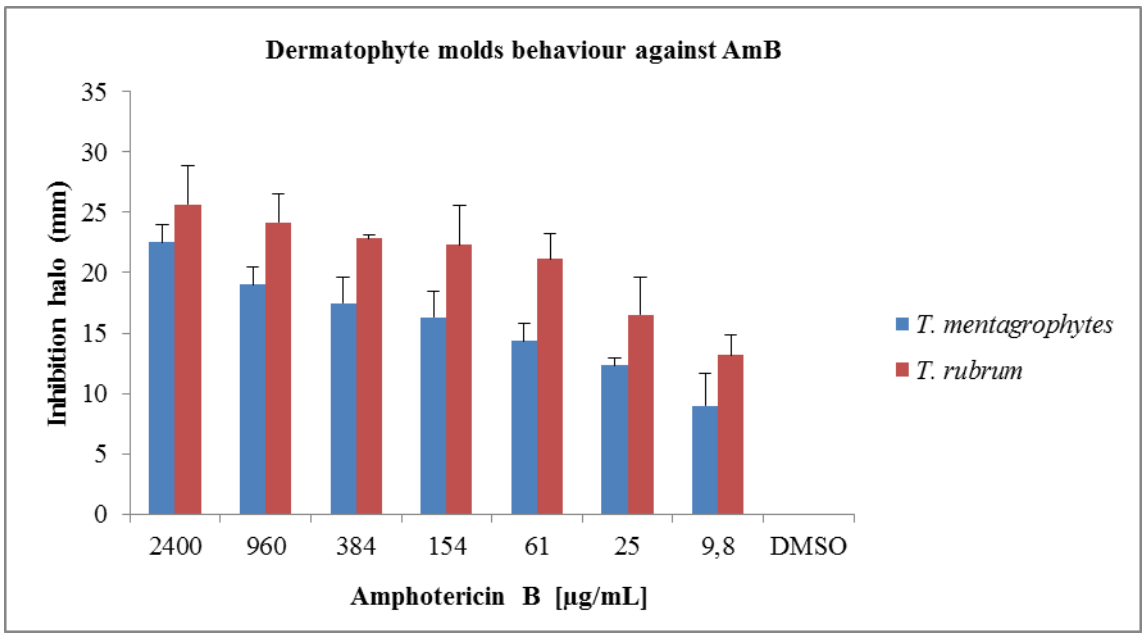

Figure 35. Inhibition halos generated by AmB on *T.mentagrophytes* and *T rubrum* cultures.

As detailed in the C*andida* assays, it can be observed how the AmB efficacy against dermatophyte molds is directly related to the concentration administered. Nevertheless, AmB efficacy against *T. rubrum* was found to be higher than for *T. mentagrophytes* (p=0,0). As for *T. rubrum* is concerned, all the inhibitions zones generated with AmB concentrations ranging between 61-2,400 µg/mL were higher than 20 mm, while in *T. mentagrophytes*, an inhibition halo of 22 mm was only found at 2,400 µg/mL.

EXP1-2.1.1.2. Activity against non-dermatophyte molds

AmB activity against non-dermatophyte molds (*Aspergillus niger*, *Fusarium solani and Fusarium oxysporum*) is detailed on figure 36.

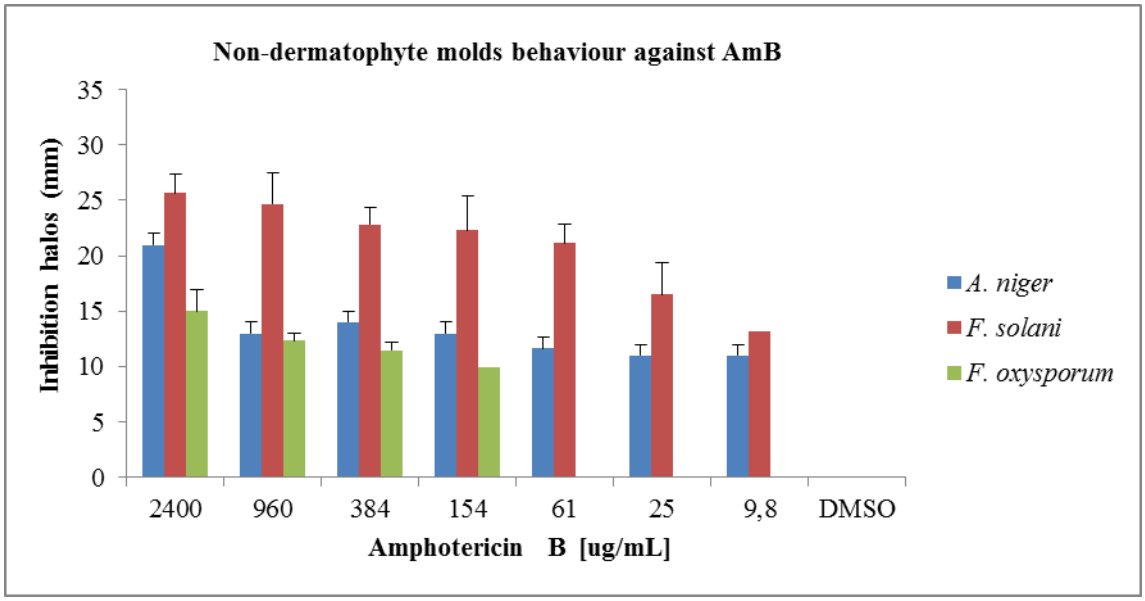

Figure 36. Inhibition halos generated by AmB on *A. niger*, *F. solani* and *F. oxysporum*

The study of the AmB activity against non-dermatophyte molds showed a greater AmB efficacy against *F. solani* compared to *F. oxysporum*, being these differences statistically significant ($p<0.05$). The inhibition halos obtained for *F. solani* were found to be higher than 15 mm for 25 µg/mL and all the above concentrations.

The results obtained for *F. oxysporum* showed that at concentrations below 154 µg/mL (61, 25 and 9.8 µg/mL) the microorganism is resistant to AmB. The inhibition halos obtained for concentrations higher than 61 µg/mL were directly related to the concentrations. The more AmB concentration, the higher the inhibition halo. However, none of the inhibition halos measured were above 15 mm.

The inhibition zones obtained for *A. niger*, showed an homogenous behavior for all the concentrations included in the range 9.8-960 µg/mL. These concentrations showed inhibition halos below 15 mm. Only when the discs were loaded with 2,400 µg/mL AmB, the inhibition halos obtained had 20 mm.

Figure 37 shows the inhibition halos obtained with different AmB concentrations.

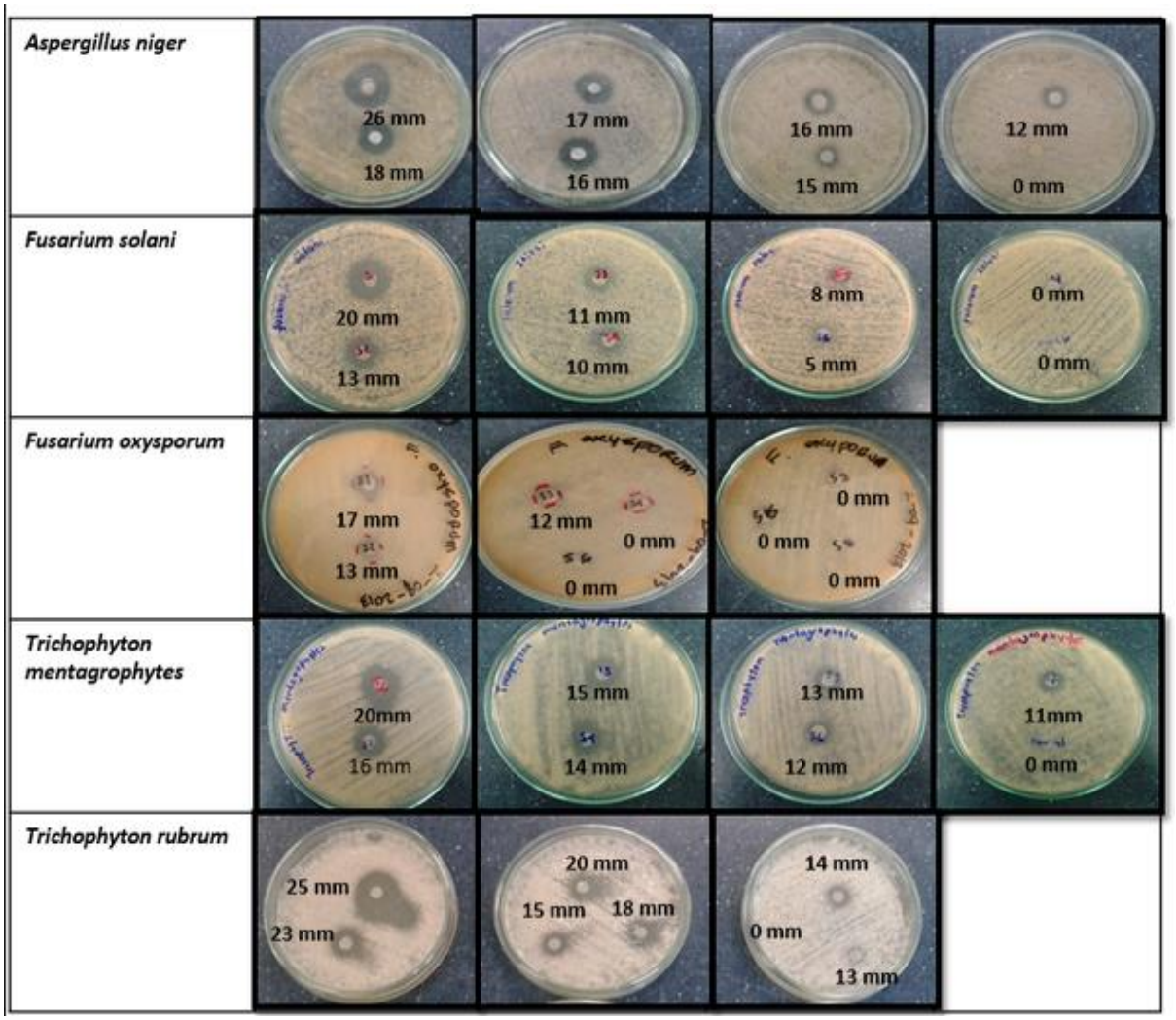

Figure 37. Inhibition zones (mm) caused against different dermatophyte and non-dermatophyte molds when several concentrations of AmB were tested.

EXP1-2.7.2. AmB efficacy against mycotic infections on keratinized structures

The evaluation of the therapeutic effect of AmB in the treatment of the onychomycosis located in keratinized structures of animal origin (chicken nails) was studied as described in Materials and Methods (EXP1-1.3.8.1.2). Briefly, the nails were drilled and inoculated with different conidia suspensions (depending on the type of microorganism to be infected with). Total nail infection was confirmed at 15 days post-inoculation. The infection was verified by direct examination using 30% KOH as well as by means of the etiological agent isolation in agar Sabouraud + Cloranfenicol + Mycosel (figure 38).

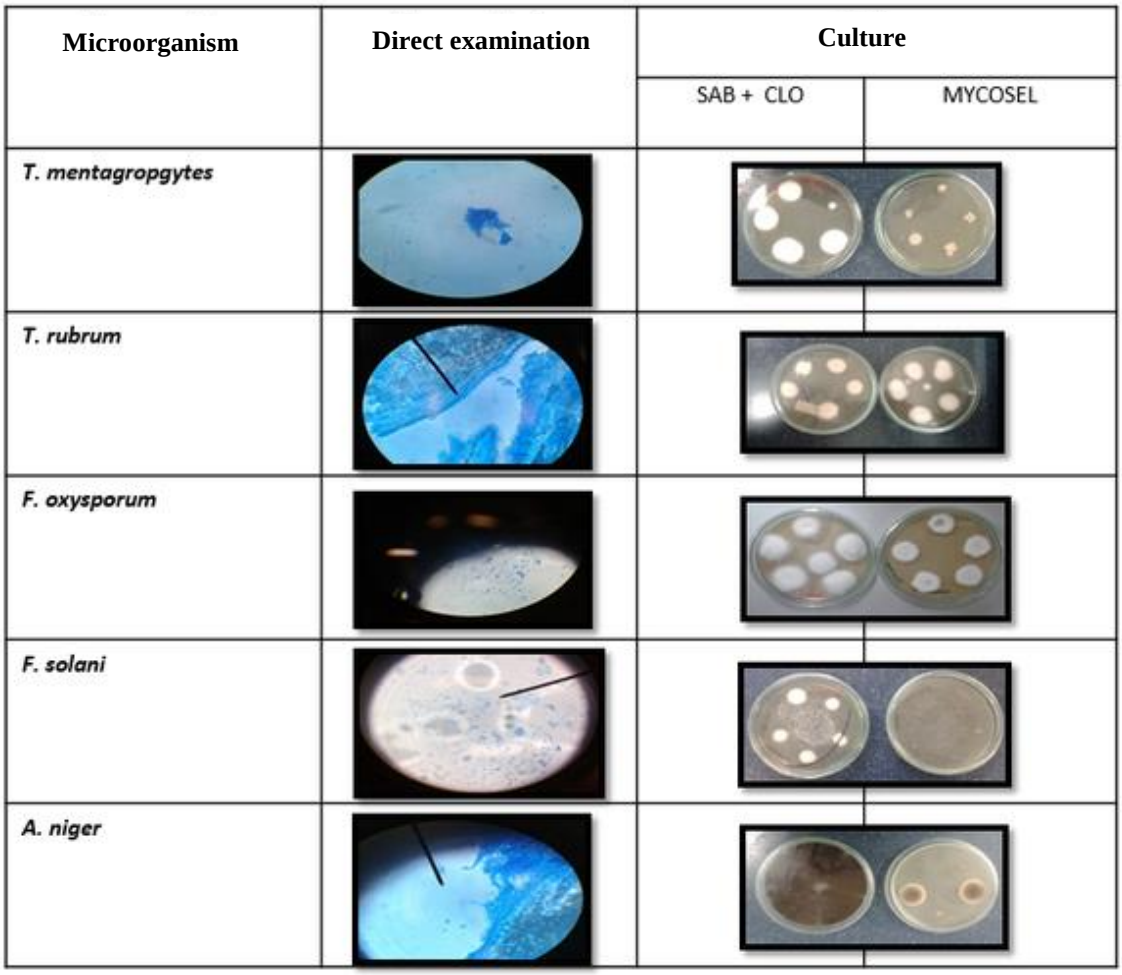

Figure 38. Fungal infection on keratinized structures (direct examination and culture).

The nail lacquer was applied in alternate days during 30 days. At day 30, the efficacy was evaluated by direct examination and culture, as previously described. Figures 39 and 40 show the infection of the keratinized structures and its resolution after 30 days treatment with formulation 19.

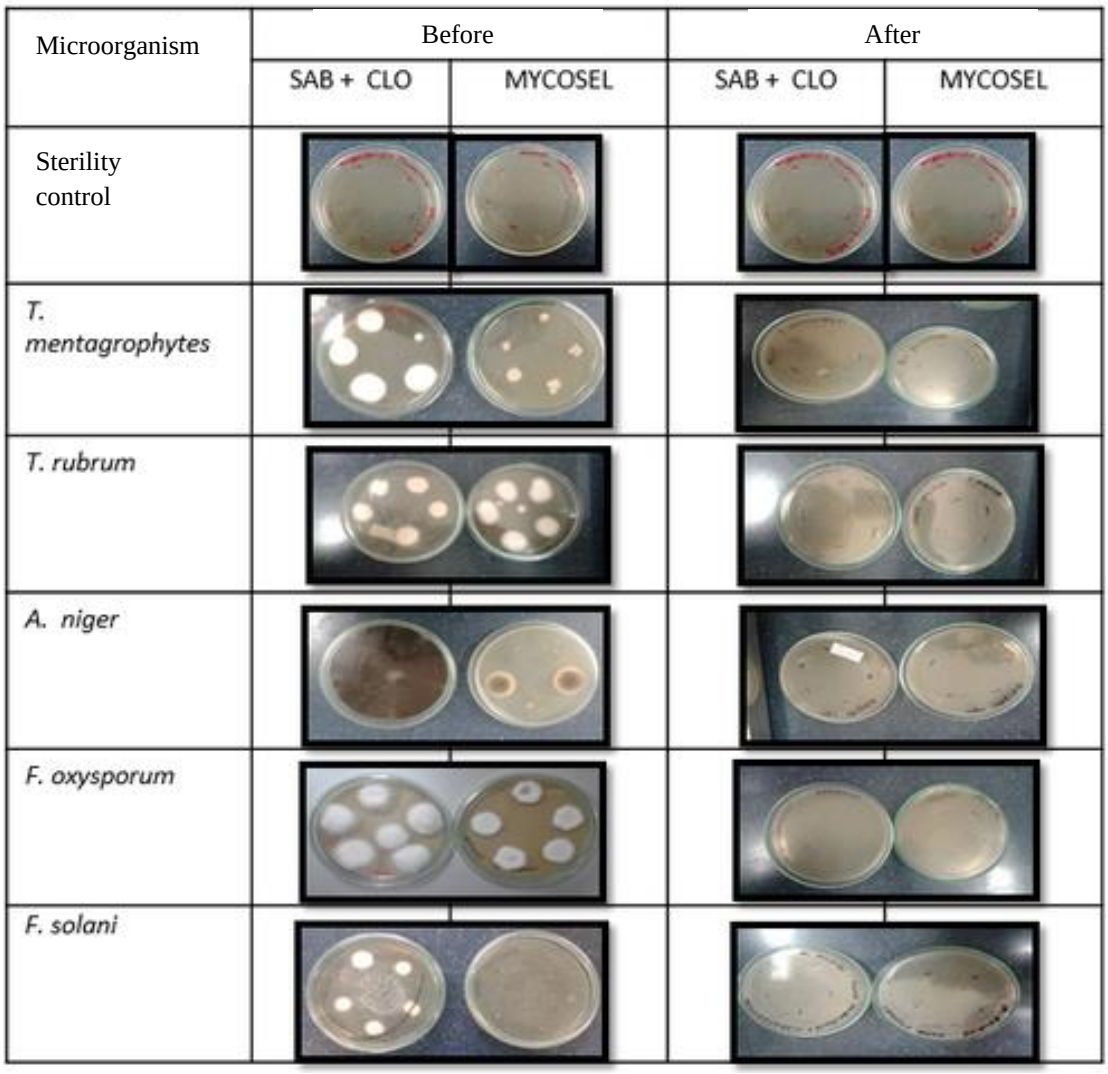

Figure 39. Culture of infected nails prior and after 30 days administration of F19.

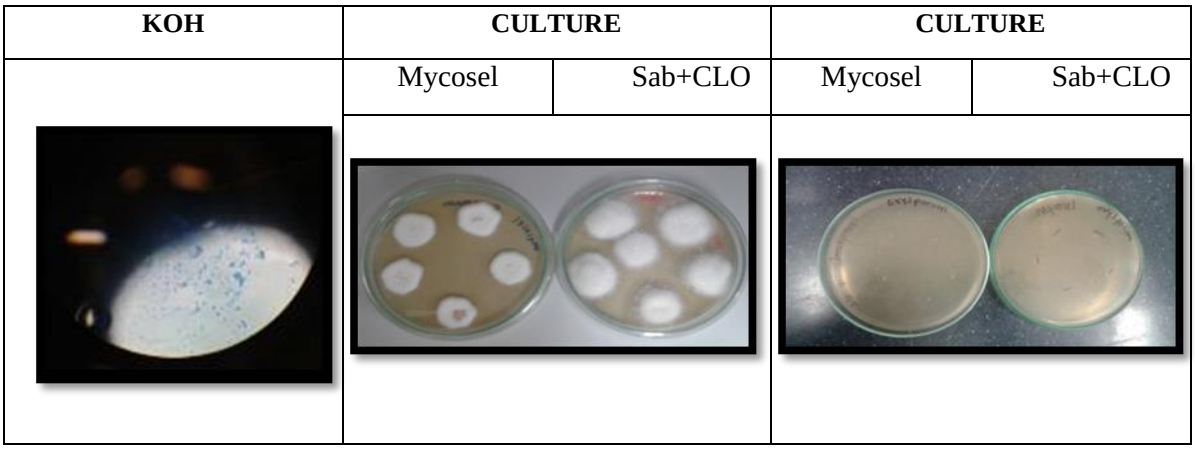

Figure 40. Direct examination (KOH) and culture of infected nails prior and after F19 administration for 30 days.

As shown in figure 39, the formulation assayed (3 mg/mL AmB nail lacquer) was active against both dermatophyte and non-dermatophyte molds after 30 days treatment. The use of NMP did not only increase the amphotericin B solubility, but also enhanced its penetration through the nail.

The results of the *in vitro* efficacy study conducted with F19 on keratinized structures, supported the *in vitro* inhibition results. The inhibition zones caused on fungal cultures were found to be in agreement with the sensitivity data, regardless the differences found on some of the microorganisms.

IN VIVO EFFICACY CANDIDA SP. COSOLVENTS DRYNESS SODIUM DEOXYCHOLATE PENETRATION SPRAY DRYING H_2O N-METHYL-2-PYRROLIDONE AGE NAIL PLASTICIZER PEG ENHANCEMENT FACTOR AMPHOTERICIN B ONYCHOMYCOSIS LACQUER ETHANOL FILM-FORMING SEM POLOXAMER DLS F19 MIXED INFECTIONS STABILITY F13 *EX VIVO* UNIVERSITY JAVERIANA ANIMAL ORIGIN PPG

EXP.1-3. DISCUSSION

TRYCHOPHYTON MENTAGROPHYTES ACTIVITY DERMATOPHYTE BRIGHTNESS TOE-NAIL MIC PATHOGENS ADHESIVE LEAD CANDIDATE MOISTURE YIELD KERATINE MYCOTIC GLYCERIN EUDRAGIT® L100 FREEZE DRYING PLASDONE K90 CELLULOSE γ-CYCLODEXTRINS HPLC SCANNING ELECTRON MICROSCOPY RHEOLOGY MIXED INFECTIONS PENETRATION CLSI EFFICACY PARTICLE SIZE 1/S F11

EXP1-3. DISCUSSION

Amphotericin B solubility studies using different organic solvents (acetic acid, acetone, acetonitrile, cyclohexane, dimethylformamide, ethanol, ethylenglycol dimethylether, isopropyl alcohol, dimethylsulfoxide (DMSO), N-methyl-2-pyrrolidone (NMP) and petroleum ether) provided information on the maximum amount of drug that could be dissolved on them. The highest AmB solubility values were obtained for DMSO and NMP (39 mg/mL and 47.73 mg/mL, respectively). While DMSO solubilizing effect on AmB had been widely studied, this is the first time that the AmB solubility in NMP is reported. NMP not only solubilizes higher amounts of AmB but also avoids the toxicity associated to DMSO administration. Furthermore, the studies of AmB aggregation on both solvents demonstrated that the AmB is found in its monomeric state when dissolved with either DMSO or NMP.

Different water permeable and impermeable nail lacquer formulations were prepared. The drying time, viscosity, aspect of the film, extensibility, brightness, AmB incorporation and pH were studied. From all the formulations developed (20), three of them were selected for further characterization and *in vitro* studies. F11, F13 and F19 were the formulations that showed the best physicochemical properties. These three formulations were selected as lead candidates.

Even though formulations 11, 13 and 19 overcame the AmB low solubility problems, the short-term stability of these formulations was still an issue. Preliminary stability studies showed that the formulations were stable up to 1 month at room temperature. The strategy used to overcome the short AmB stability was focused on obtaining powders for reconstitution. These powders would be stored at 2-8ºC and protected from light and humidity.

The freeze drying (for F11 and F13) and spray drying (for F19) methods generated stable lyophilized and spray dried products easily redispersable. Immediately after solvent addition, formulations with the same physicochemical properties than the freshly prepared F11, F13 and F19 were obtained and the water content detected by IR was lower than 8% regardless the method and the formulation prepared. The spray drying technique provided an alternative method for obtaining an F19 powder for

reconstitution. The method was successfully set up and the yields obtained were in the range 89-94% for all the experiments performed. The AmB concentration detected by HPLC was 0.3% in the freshly prepared F11, F13 and F19. After 1 month storage at 25ºC the concentration decreased up to 0.28%. The reconstituted formulations demonstrated its stability during 15 days storage in the same conditions. Further stability studies are currently on going.

The particle size of the freshly prepared and reconstituted F11 and F13 was in the range 20-30 nm. The dimensions of the freshly prepared formulations remained stable during 15 days at 25ºC. On the contrary, the particle size of the reconstituted formulations slightly increased with increasing exposure times. The small increase in size was not considered as an indicative of instability as in none of the formulations the size was greater than 30 nm. F19 could not be analyzed by DLS due to its water impermeable properties.

SEM images of the film formed by F11, F13 and F19 provided information on the differences found in between formulations. While SEM microphotographies of F19 showed a continuous, homogenous and smooth film, the film formed by F11 and F13 presented some deposits. The chemical composition of the deposits was analyzed by SEM and it was concluded that they were no generated by the accumulation of AmB crystals. The deposits might me related to incomplete solubilization of any of the components included in the formulation.

The viscosity values obtained for F11, F13 and F19 were different. The higher viscosity values recorded for the water permeable formulations are explained by the higher molecular weight of the Plasdone® K90 compared to the Eudragit® L100. The differences detected in between F11 and F13 were related to higher solids content on F13. The viscosity values were, in all cases, stable during 15 days at 25ºC and no significant differences were observed in between them. The rheological behavior was identical for all three formulations. Regardless the initial differences in viscosity, F11, F13 and F19 showed Newtonian flow properties. Even though the pseudoplastic flow properties are believed to confer the nail lacquer improved film stability and therefore, are preferred, there are some studies that support that Newtonian flow properties are adequate for nail delivery [338].

In vitro nail penetration studies on female human nails, demonstrated the higher nail penetration reached with F19 compared to F11, F13 and to the control. The EF value for F19 (EF=1.95) was almost twice the value of the control (EF=1) and approximately three times the value of F11 and F13. Despite the assumed experimental variability given by the use of human keratinized structures, the method generated close-related results. The EF value was not influenced by the formulation preparation process (fresh or reconstituted lacquers). Although the protocol used in these *in vitro* penetration studies provided useful information for the selection of a lead candidate, it has to be taken into account that the most reliable penetration data would be obtained in a Franz cells experiment.

The *in vitro* efficacy studies against *Candida albicans* showed that the most active formulation was F19 (103%). The greater % of activity found for F19 compared to the control was considered to be related to the method accuracy. No differences in activity between F19 and its reconstituted product were found. The activity of this formulation compared to Neo-sensitabs® (commercialized AmB loaded disks) demonstrated that F19 was more effective than the latest, even at 5 times less concentration. The study of the *in vitro* efficacy of this formulation was of great importance as the main objective of the present chapter was to develop and AmB nail lacquer effective against dermatophyte, non-dermatophyte, candidal onychomycosis and, most importantly, against mixed infections.

Taking into account all the above summarized results (physicochemical characterization and *in vitro* penetration and efficacy studies), F19 was selected as lead candidate.

F19 powder for reconstitution was sent to the University Javeriana of Bogotá (Colombia) for analysis. The group of Dra. Parras, determined the minimum inhibitory concentration (MIC) and the F19 efficacy on keratinized infected structures of animal origin. The efficacy was assayed on nails infected with *T. mentagrophytes*, *T. rubrum*, *F. solani*, *F. oxysporum* and *A. niger*, main etiological agents responsible for the onychomycosis.

The new AmB formulation was effective against dermatophyte and non-dermatophyte molds. Even though there are some studies that report the absence of AmB activity against dermatophyte molds and, some clinical trials in which the AmB administration has produced treatment failures, the data obtained from the MIC studies, support the

AmB efficacy. This activity was greater against *T. rubrum* compared to the other dermatophyte molds, and in general to all the microorganisms assayed. This is in accordance with the studies performed by Lu Yu, *et al*., [338] and Yenisehirli *et al*., [340].

The AmB was active against *F. solani* at almost all the concentrations assayed, but it had limited activity against *F. oxysporum*. Only at high AmB concentrations, the molecule was effective. These data differed from those included in the studies carried out by Wildfeuer *et al*., [244] and Lalitha *et al*. [341]. These studies supported the highly efficacy of AmB against different *Fusarium* spp. Moreover, the studies performed by Pujol *et al*.; Azor *et al*.; O'Donnell *et al.* and Alastruey *et al.* [342-345] stated that the AmB was the most active drug against *Fusarium* spp. The MIC results should be, therefore, validated against different isolations of the same *Fusarium spp*. in order to determine the MICs (the guidelines does not detail the cut points for the determination of sensitivity or resistant).

The small inhibition zones obtained when AmB formulation was applied to *Aspergillus niger* cultures could be explained by the difficulties found in the treatment of this microorganism. Even though *A. niger* is not the most commonly responsible etiological agent for the non-dermatophyte onychomycosis, when it is the causative agent, its treatment should not be performed with AmB. The A. *niger* reduced sensitivity against AmB has been previously reported by García-Martos et al [346]. On the contrary, other studies conducted by Pfaller [347] and Wildfeuer [348] showed that the AmB was effective against *Aspergillus* spp.

The AmB nail lacquer was active against the dermatophyte and non-dermatophyte infections located on keratinized structures. 30 days treatment with F19, administered in alternate days, once daily, cleared up the infections caused by *T. mentagrophytes*, *T. rubrum*, *A. niger*, *F.oxysporum* and *F.solani*. After 30 days of treatment no microorganisms were found nor in the culture media neither in the direct examination. These results were in fair agreement with the *in vitro* penetration studies performed on human nails supporting the enhanced AmB nail penetration due to the presence of NMP in the formulation.

The *in vivo* application of F19 was described as a case study. The water impermeable AmB layer generated on the surfaces of the catheters avoided their contamination. After

patient treatment success and removal of the catheters, it could be observed how the yellowish AmB film remained intact.

The selection of a lead candidate formulation for AmB nail delivery was conducted through a screen study of more than 20 formulations. Short-term stability and AmB concentration studies were performed on 20 of those formulations. The results obtained in these studies provided valuable information for the initial selection of three lead candidates. The physicochemical characterization and the *in vitro* penetration and efficacy studies, demonstrated the better performance of the water impermeable lacquer compared to the other two formulations. Based on those results, F19 was chosen as lead candidate and further *in vitro* and *in vivo* efficacy studies were performed. The formulation was effective against the main etiological agents responsible for the onychomycosis, resolving the *in vitro* infections within 30 days treatment.

In sum, an AmB nail lacquer effective in the treatment of onychomycosis has been developed for the first time. This new nail lacquer constitutes a promising alternative for AmB nail delivery. However, further *in vivo* efficacy studies as well as futher studies related to its application over catheters should be performed.

AMB/PEG$_{5KDA}$-CHOLANE RECOVERY NMR REFLUX SYNCHROTON KINETICS HSM FREE ENERGY CONJUGATION TEM FTIR DSC DISSOCIATION CONSTANT HSA PLASMA ISOTHERMAL TITRATION CALORIMETRY ENTROPY CIRCULAR DICHROISM SYNTHESIS HEMOLYSIS GASTRIC MIMICKING FLUID ΔH CM^{-1} Kd AMORPHOUS MG/KG EXTRACTION TAIL MICELLES TREATMENT ANTIBIOTIC PARTICLE SIZE

3.2. EXPERIMENTAL PART 2

ENTHALPY POLARIZATION AGGREGATION KD2 ANALYSIS NEUTRAL SURFACE CHARGE MOLAR RATIO NEGATIVE-STAINING AMBISOME® STOICHIOMETRY ABSORBANCE DIMER COLLOIDAL DISPERSION TEA SIZE UNFORMULATED DRUG/POLYMER INTERACTION ΔS NANOAGGREGATES FUNGIZONE® HEAT PPM ORAL/IV PHARMACOKINETICS STOMACH TMAX BENDING/STRETCHING VIBRATIONS β-SHEET C24

EXP.2-1. MATERIALS & METHODS

EXP2-1. MATERIALS & METHODS

EXP2-1.1. Materials

Amphotericin B (AmB) was purchased from Azelis (Barcelona, Spain), Fungizone® from Bristol-Myers Squibb (Madrid, Spain) and Ambisome® by Gilead Sciences (Madrid, Spain). Globulin free human serum albumin, naproxen and 5β-cholanic acid were supplied by Sigma-Aldrich (Milan, Italy). 5 kDa amino-terminating monomethoxy-terminating poly(ethylene glycol) (PEG_{5kDa}-NH_2) and hydroxyl-terminating monomethoxy-terminating poly(ethylene glycol) (PEG_{5kDa}-OH) were supplied by Iris Biotech GmbH (Marktredwitz, Gemany). Heparinized capillaries (75 mm) were purchased from Heinz Herenz (Hamburg, Germany) and heparine 5000 UI from Rovi. Dialysis membranes (Spectra/Por®Float-A-lyzer®G2 MWCO: 3.5-5kDa) were supplied by Spectrum®Labs (Wurzburgo, Germany). Certified *Candida albicans* strain (CECT1394) was a gift of Dr. Pérez Carrasco from Centro de Análisis Químico y Microbiológico (CAQYM), Universidad Alcalá de Henares (Madrid, Spain). Culture media were purchased from Pronadisa-Conda Lab (Madrid, Spain). Technical grade and HPLC grade solvents and salts were purchased from Merck (Milan, Italy). In this thesis the purified water was always obtained from MilliQ, Millipore (USA).

EXP2-1. 2. Methods

EXP2-1.2.1. Synthesis and characterization of the poly(ethylene glycol)-cholane bioconjugate

Monomethoxy-poly(ethylene glycol)-cholane (PEG_{5kDa}-cholane) was synthesized according to the protocol reported in the literature with modifications [335]. The synthesis was based on a two step reaction where the first step consisted on the activation of the carboxyl group from the cholanic acid while the second step included the conjugation of the activated group with a monomethoxy-poly(ethylene glycol)amine of 5 kDa molecular weight (MeO-PEG_{5kDa}-NH_2) (figure 41). The two steps of the reaction are summarized in figure 41.

1. Activation of the cholanic acid

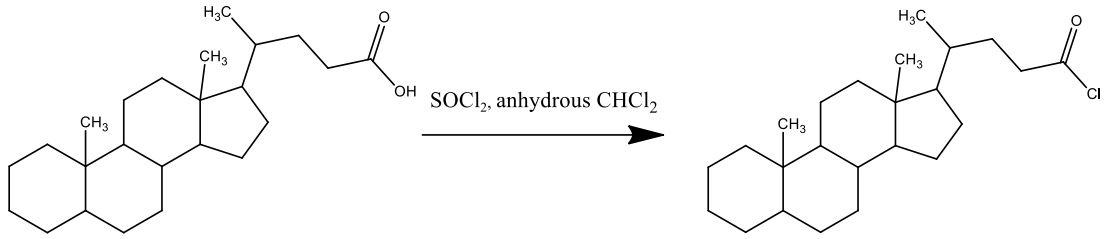

2. Conjugation with MeO-PEG_{5kDa}-NH_2

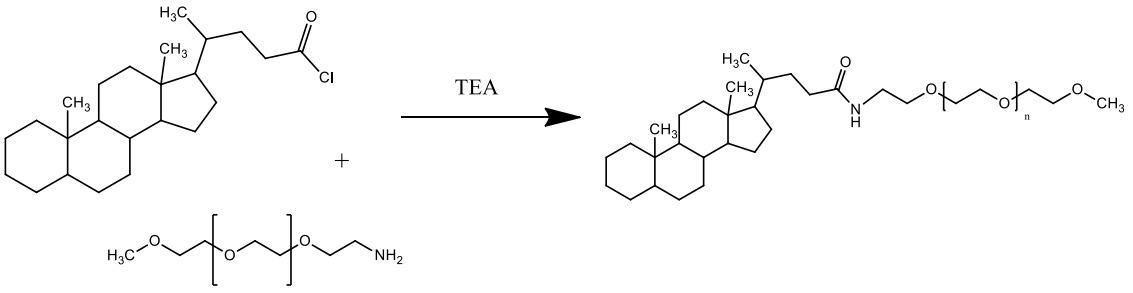

Figure 41. Chemical synthesis of PEG_{5kDa}-cholane.

EXP2-1.2.1.1. Activation of the carboxyl group

It is important to point out that for this step the maintenance of the anhydrous conditions not only in the cabinet but also in the products and the material needed for the reaction is a key factor. A high degree of activation will be expected if these conditions are maintained.

The activation (figure 42) was performed by the addition of thionyl chloride (524 µL, 7.2 mmol) in a ratio 1:10 (cholanic acid: thionyl chloride) to a flask containing the 5β-cholanic acid (260 mg, 0.72 mmol) dissolved in 6 mL CH_2Cl_2. The bottom of the flask was slightly submerged into a glycerin bath set at 50 ºC. The temperature was manually adjusted in order to control the boiling and therefore the reflux. The mixture was refluxed under nitrogen atmosphere for three hours. During the process the reaction was controlled in order to assure that the micelle was not getting dried. When necessary, some drops of CH_2Cl_2 were added. After the three hours, the distillation column was

assembled and the unreacted thionyl chloride was removed by distillation. Finally, to assure the complete solvent removal, the product was left in a rotavapor for 1 h.

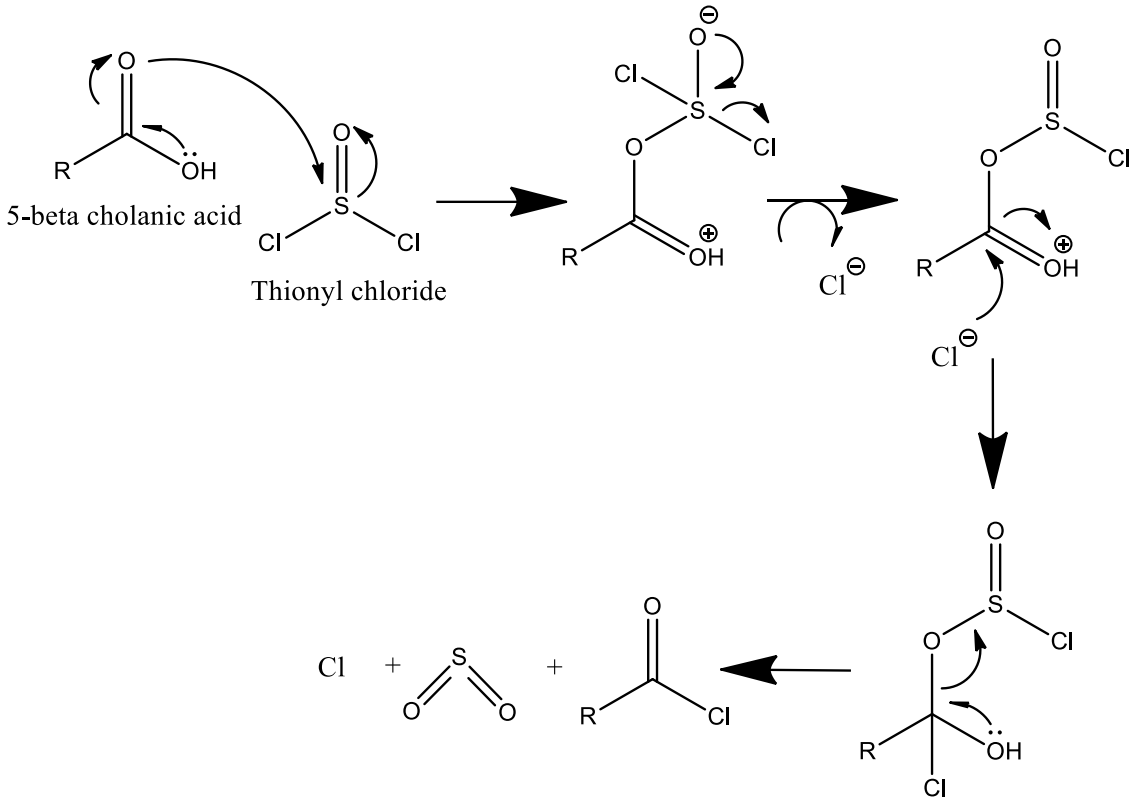

Figure 42. Chemical activation of the carboxyl group from the cholanic acid.

Once activated, the product generated was analyzed by nuclear magnetic resonance in order to check the degree of activation.

- **Degree of activation by nuclear magnetic resonance (NMR)**

After solvent evaporation an aliquot of the activated cholane was reacted with 200 µL CH_3OH (figure 19). The methyl ester of the cholanic acid was first vortex for 5 min and then centrifuged at 10000 rpm for another 5 min using a Sigma centrifuge D-37520 (Osterode am Harz, Germany). 150 µL of the micelle were added to an eppendorf and placed under vacuum using a Heto Vacuum Centrifuge VR-mini St. a.-1 (Allerod, Denmark) during one and a half hours in order to eliminate the excess of CH_3OH. Finally, 700 µL deuterated chloroform were added (figure 43) and the product was analyzed by ^{1}H-NMR spectrometry using a Bruker Spectrospin 300 spectrometer (Bruker, Fallanden, Switzerland) to estimate the activation degree. By the integration of the peaks corresponding to the 3H from the CH_3 of the methanol that sterifies the

cholanic and the 3H from the CH_3 placed in position 19 of the cyclopentane perhydro phenanthrene ring and by using the following equation (equation 1) the degree of activation can be estimated.

$$Degree\ of\ activation\ (\%) = \left(\frac{peak\ integration\ from\ the\ 3H\ of\ MeOH}{peak\ integration\ from\ the\ 3H\ of\ the\ C19}\right) \times 100$$

Equation 1. Calcule of the carboxyl group degree of activation

The knowledge of the degree of activation was necessary to proceed with the next step of the reaction.

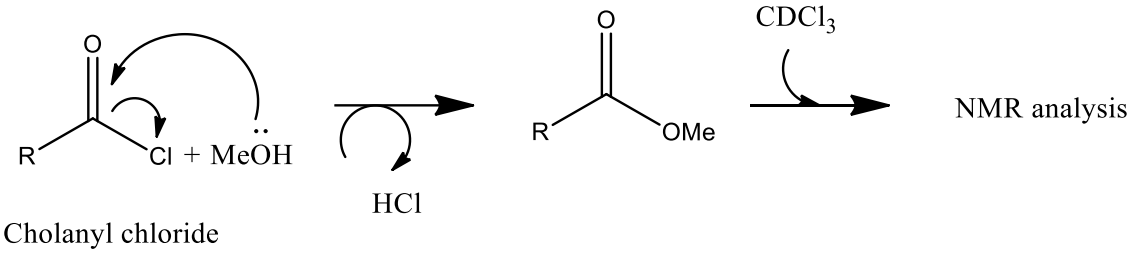

Figure 43. Sample preparation for NMR analysis

EXP2-1.2.1.2. Conjugation with MeO-PEG$_{5kDa}$-NH$_2$

The conjugation was performed taking into account that the stoichiometry of the reaction was 1:3:2 (MeO-PEG$_{5kDa}$-NH$_2$: cholanyl chloride : triethylamine (TEA)) and considering a certain degree of cholanyl activation (previously calculated).

Cholanyl chloride (218 mg, 0.576 mmol) in 1 mL CH_2Cl_2 was added of 53.5 µL TEA (0.384 mmol) and 4 mL CH_2Cl_2 of 242.7 mg/mL PEG$_{5kDa}$-NH$_2$ (970.8 mg, 0.192 mmol) (figure 44). The reaction solution was maintained overnight under stirring at room temperature and then dropwise added to 35 mL of diethyl ether. The precipitate, immediately generated, was refrigerated at 4 ºC (left in the fridge for 10 min) to enhance the polymer precipitation and then, recovered by centrifugation at 4000 rpm for

15 min and re-dissolved in 5 mL CH_2Cl_2. The precipitation was repeated three times. The precipitate was desicated under vacuum and finally lyophilized in a Hetossic equipment (HETO Lab, Birkerod, Denmark).

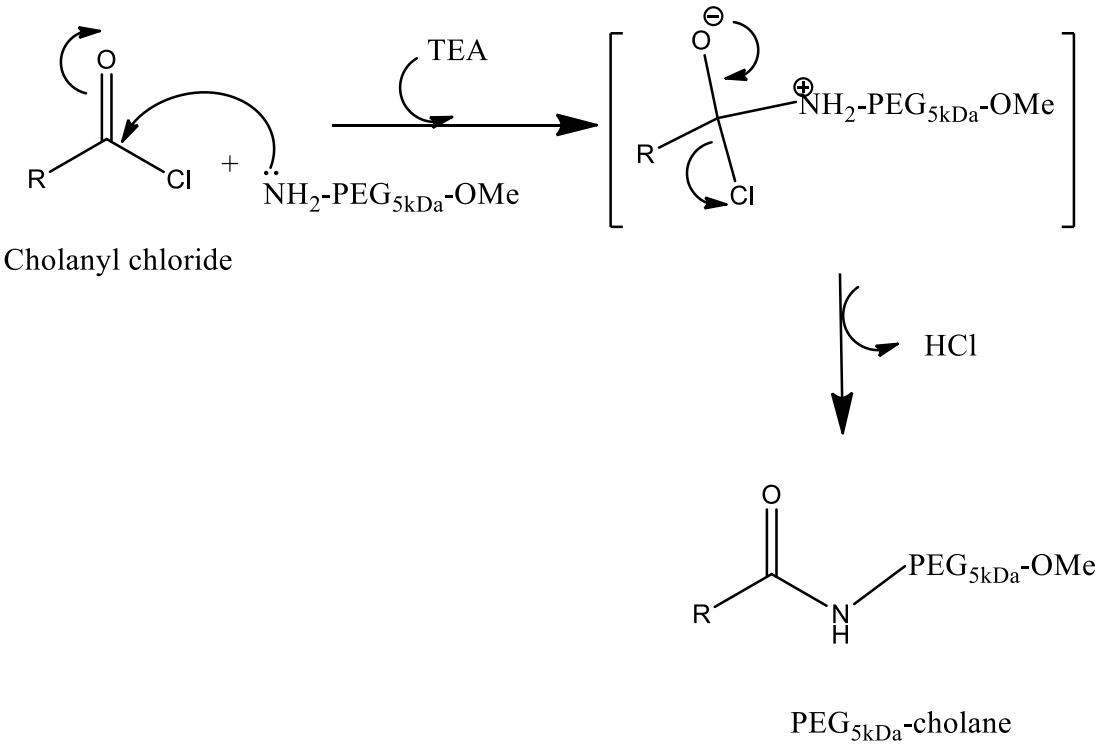

Figure 44. Cholanyl chloride conjugation with 5 kDa amino-terminating monomethoxy-terminating poly(ethylene glycol).

The degree of PEG-NH_2 derivatization with cholanyl chloride was evaluated by the TNBS colorimetric assay, which allows for determination of unreacted amino groups [349] and by ^{1}H NMR spectrometry.

- **TNBS colorimetric assay**

The 2,4,6-trinitrobenzene sulfonic acid, known as TNBS, is a highly sensitive and fast chemical used in the quantification of free amino groups. The reaction of TNBS with

primary amines generates highly chromogenic products that can be measured by UV [350].

For this assay, also known as Snyder test, 30 mL of a 0.1 M borate buffer were prepared by the addition of 185.5 mg of boric acid (61.3 g/mol) in purified water at pH 9.3 (NaOH 0.5 M). Then, a stock solution of MeO-PEG_{5kDa}-NH_2 (reference) and PEG_{5kDa}-cholane (synthesized product) were prepared at 2.157 mM. 5 mg of both MeO-PEG_{5kDa}-NH_2 ($9.89\ 10^{-4}$ mmol, mol wt 5056 Da) and PEG_{5kDa}-cholane ($9.232\ 10^{-4}$ mmol, mol wt 5416 Da) were added of 456.2 µL and 428 µL of borate buffer, respectively. For the sample preparation, 30 µL of TNBS diluted in borate buffer (1:30) and 940 µL of borate buffer were added to both 30 µL of MeO-PEG_{5kDa}-NH_2 stock solution and 30 µL of PEG_{5kDa}-cholane stock solution. After 30 min reaction, the samples were measured by UV spectroscopy in a Perkin Elmer Spectrophotometer Lambda 25 (Massachusetts, USA) set at 420 nm (wavelength of maximum absorption for the compound generated as a consequence of the reaction with TNBS). The blank used for the experiment was borate buffer (940 µL) added of 30 µL TNBS. The samples were prepared in triplicate.

The degree of derivatization was calculated from the equation 2.

$$Degree\ of\ derivatization\ (\%) = 1 - \left({}^{Abs\ synthesized\ product}/_{Abs\ reference}\right) \times 100$$

Equation 2. Calcule of the degree of derivatization by TNBS

- **Degree of conjugation by NMR**

The degree of conjugation was also confirmed by ^1H NMR spectrometry. The samples were prepared following the same protocol reported above. The yield was calculated by dividing the integration of the peak corresponding to the 3H from the CH_3 placed in position 19 of the cyclopentane perhydro phenanthrene ring by the 3H from the CH_3 of the last methoxy group located in the PEG chain.

$$Degree\ of\ conjugation\ (\%) = \left(\frac{peak\ integration\ from\ the\ 3H\ of\ C19}{peak\ integration\ from\ the\ 3H\ of\ the\ methoxy}\right) \times 100$$

Equation 3. Calcule of the degree of conjugation by NMR

The polymer synthesized was stored in a freezer at -20ºC until use.

EXP2-1.2.2. Amphotericin B dissolution studies with PEG_{5kDa}-cholane

AmB dissolution studies with PEG_{5kDa}-cholane were carried out according to three different methods: Direct dissolution; Co-solvent dissolution and Dissolution/pH change. The aim of this assay was to find the method that produces the maximum AmB dissolution with the polymer.

EXP2-1.2.2.1. Direct dissolution

Samples of 4 mg AmB in 500 µL CH_3OH where desiccated using a speed-vac system. The dried samples were added of 500 µL of 0.5, 1, 1.5, 2, 3 and 6 mg/mL PEG_{5kDa}-cholane or PEG_{5kDa}-OH in water, pH 7.2, and maintained overnight under top-down mixing. The samples were centrifuged at 12000 rpm for 10 min. The AmB concentration in the supernatant was determined by the RP-HPLC method previously described.

EXP2-1.2.2.2. Co-solvent dissolution

Samples of 4 mg of AmB in 500 µL CH_3OH were added of 100 µL of 2.5, 5, 7.5, 10, 15 and 30 mg/mL PEG_{5kDa}-cholane or PEG_{5kDa}-OH in water, pH 7.2. The mixtures were dried in speed-vac and the residues were re-dispersed in 500 µL water at pH 7.2 and maintained overnight under top-down mixing. The samples were centrifuged at 12000 rpm for 10 min and the AmB in the supernatant was analyzed by RP-HPLC as reported above.

EXP2-1.2.2.3. Dissolution/pH change

The AmB dissolution was performed according to the method described by Higuchi and Connors [351]. Briefly, 20 mg of AmB were dissolved in 1 mL of 0.5, 1, 1.5, 2, 3 and 6 mg/mL PEG_{5kDa}-cholane or PEG_{5kDa}-OH in 0.05 N NaOH. The pH was then shifted to 7.2 with 0.1 M ortophosphoric acid and the suspensions were centrifuged at 12000 rpm for 10 min. The AmB in the supernatant was analyzed by RP-HPLC as reported above.

EXP2-1.2.3. Physicochemical characterization of the AmB/PEG_{5kDa}-cholane complex

EXP2-1.2.3.1. Reverse-phase high pressure liquid chromatography

The AmB concentration in the different samples was determined by reverse-phase chromatography (RP-HPLC) using a Thermo Hypersil BDS® C18 column (200 x 4.6 mm, 5 µm) operated on a Jasco HPLC system equipped with a Jasco PU-1580 pump and UV-visible detector set at 406 nm (Jasco, Tokyo, Japan). The column was isocratically eluted at a flow rate of 1 mL/min with 52:4.3:43.7 v/v/v acetonitrile/acetic acid/water mobile phase [352]. The AmB concentration in the samples was determined on the basis of the elution peak area (AmB is eluted after 8 min), which was referred to a titration curve obtained by eluting AmB samples at concentrations in the range of 0.012-40 µg/mL [(AmB concentration)=115.1(peak area)-1.665; R^2=1]. When analyzing biological samples, the AmB concentration was referred to a curve linear in the range 0.012-50 µg/mL [(AmB concentration)=113.7(peak area)-12.45; R^2=0.99]. In order to avoid mistakes in the extrapolation of low AmB concentrations, both curves where divided in two sub-curves; one for low AmB concentrations (from 0.012 to 1.5625 µg/mL R^2=0.999) and another for high AmB concentrations (from 0.78125 to 40 or 50 µg/mL R^2=0.999). After sample analysis, the column was isocratically washed with MeOH:H_2O (60:40) at 0.4 mL/min, 406 nm, for 1 hour when analyzing non-biological samples and, with a gradient of ACN(TFA 0.05%) and H_2O(TFA 0.05%) at 1 mL/min, 220 nm, for 1 hour after biological samples analysis. The gradient used was 40% ACN, 60% H_2O from 0 to 3 min; from min 3 to min 12 the amount of ACN was increased from 40 to 90% and the water content decreased from 60 to 10%; from min 12 to min 15 the washing phase consisted of 90% ACN and10% H_2O, from min 15 to min

18 the ACN was decrease to 40% and the H_2O increased to 60% and from min 18 to 20 the phase remained as 40% ACN, 60% H_2O.

When necessary, a 5 M HCl Guanidine solution was injected to remove the plasma proteins attached to the column.

EXP2-1.2.3.2. Dynamic light scattering and zeta potential analyses

AmB/PEG_{5kDa}-cholane aqueous solutions (1 mg/mL AmB, 12:1 AmB/PEG_{5kDa}-cholane molar ratio) prepared by dissolution/pH change were analyzed at different times (0, 7, 14, 21, 28, 35, 42, 49, 56 and 63 days) by dynamic light scattering (DLS) using a Malvern Zetasizer Nano-ZS (Malvern, Worcestershire, UK). The analyses were performed in triplicate at 25ºC, 633 nm wavelength and 173º detection angle to assess the mean particle size, size distribution and zeta potential. Particle size, size distribution and zeta potential of unloaded micelles (0.5 mg/mL PEG_{5kDa}-cholane aqueous solutions) were also studied.

EXP2-1.2.3.3. Freeze drying

AmB/PEG_{5kDa}-cholane samples (10 mL of 1 mg/mL AmB, 12:1 AmB/PEG_{5kDa}-cholane molar ratio) were prepared by dissolution/pH change, frozen with liquid N_2 and lyophilized using a Lio-labor® instrument (Telstar, Barcelona, Spain) for 48 h. The freezing and sublimation temperatures in the lyophilization chamber were -45ºC and from -45 to 25ºC, respectively. The sublimation pressure was 4.54 10^{-4} atm. The moisture content in the lyophilized product was determined as weight loss after heating at 105 ºC using a Mettler PM100 balance equipped with a Mettler LP16 infrared drying unit (Mettler Toledo, Greifensee, Switzerland). The end point was estimated after 120 s without weight variation. Reconstitution of the freeze dried samples was performed by the addition of 10 mL of 10 mM phosphate buffer, 0.15 M NaCl (PBS), pH 7.2. Particle size and AmB concentration analyses of reconstituted solutions were carried out at times 0, 7, 14, 24 and 31 days by DLS and RP-HPLC, respectively, according to the analytical protocols reported above.

EXP2-1.2.3.4. Isothermal titration calorimetry

Description of the technique

Isothermal titration calorimetry (ITC) is a technique used to measure the energetic of molecular interactions or biochemical reactions [353]. It is the most direct method to measure the heat change on formation of a complex at constant temperature. The basics of this technique are simple. The experiment is performed at a constant temperature by titrating one binding partner ("titrant"), placed on the syringe, into a solution containing the other binding partner ('titrand'), located in the sample cell of the calorimeter. Both, titrant and titrand solutions should have the same buffer composition. After each addition of a small aliquot of titrant, the heat released or absorbed in the sample cell is measured with respect to a reference cell filled with the buffer. If the interaction is exothermic, the ITC uses less energy to heat the cell; if the interaction is endothermic, the ITC uses more energy to heat the cell. The heat change is expressed as the electrical power ($J\ s^{-1}$) required to maintain a constant small temperature difference between the sample cell and the reference cell, which are both placed in an adiabatic jacket. The addition of the titrant is automated and occurs from a precision syringe driven by a computer-controlled stepper motor. Precise measurement of the energy required to maintain temperature of the cell during the course of several injections leads to the calculation of free energy, enthalpy (ΔH), entropy (ΔS), dissociation constant (Kd), and stoichiometry of binding from one single experiment. In commercially available instruments volumes of sample cells are in the range 0.2–1.5 ml. The amount of titrand required per experiment depends on the magnitude of the heat change [354].

Method

ITC analyses were carried out using an MSC-ITC instrument (Microcal Inc., Northampton, MA). AmB solutions were prepared by dissolution/pH change and their concentration was determined by RP-HPLC prior to sample analysis. AmB ($1.1\ 10^{-5}$ M) and PEG_{5kDa}cholane ($0.6\ 10^{-3}$ M) solutions in water at pH 3.5, 5.5, 7.2, 8.5 and 11.0, were degassed and thermostated at 25 ºC before the analysis. At 5 min intervals, 5 µL volumes of PEG_{5kDa}-cholane solutions were injected in 10 s into the calorimeter cell containing 1.5 mL AmB solutions at the same pH. Each assay was performed in triplicate and the data was analyzed with the Microcal Origin 3.5 software.

EXP2-1.2.3.5. Structural characterization

Samples of AmB, PEG_{5kDa}-OH, PEG_{5kDa}-cholane, lyophilized AmB/PEG_{5kDa}-cholane (12:1 AmB/PEG_{5kDa}cholane molar ratio) prepared by dissolution/pH change and AmB/PEG_{5kDa}-cholane physical mixtures (12:1 AmB/PEG_{5kDa}-cholane molar ratio) obtained by mixing AmB and PEG_{5kDa}-cholane dry powders were analyzed by differential scanning calorimetry, hot stage microscopy, X-ray diffractometry and Fourier-transformed infrared spectroscopy in order to characterized the new system developed.

EXP2-1.2.3.5.1. Differential scanning calorimetry

Differential scanning calorimetry (DSC) analyses were performed using a Mettler TA3000 differential scanning calorimeter DSC 20 (Mettler Toledo, Greifensee, Switzerland). Samples (10 mg) were placed on a pinhole aluminum lidded pan and heated in atmospheric air at a rate of 10ºC/min from 30 to 250ºC.

EXP2-1.2.3.5.2. Hot stage microscopy

Hote stage microscopy (HSM) analyses were performed by placing the samples on a microscope covered slide and heated at a rate of 2ºC/min from 25 to 250ºC. Microscopy determinations were carried out using a Thermo Galen microscope fitted with the Kofler stage (Leica, Wien, Austria) [355].

EXP2-1.2.3.5.3. X-ray diffractometry

X-Ray diffractometry (XRD) analyses were carried out with an X-ray diffractometer Philips®X' Pert–MPD (PANalytucal, Amelo, Netherlands). The samples were placed on a carrier, irradiated with monochromatized CuK α-radiation and analyzed between 2θ angles of 5º and 50º with 0.04º steps of 1 s. The assay was performed at 30 mV voltage and 30 mA intensity.

EXP2-1.2.3.5.4. Fourier-transformed infrared spectroscopy (FT-IR)

Fourier-transformed infrared spectroscopy (FT-IR) spectra were recorded over the range 4000-400 cm^{-1} using a FT-IR Nicolet Magna 750 spectrometer (0.5 cm^{-1} resolution) equipped with an attenuated total reflectance (ATR) Spectra Tech Performer with diamond crystal (Thermo Fisher Scientific, Waltham, MA USA). The data were analyzed with Thermo software.

EXP2-1.2.3.6. Synchrotron

In order to analyze the superficial characteristics of the AmB/PEG_{5kDa}-cholane micelles and the interactions that take place between the AmB and the polymer, some samples were prepared and analyzed by synchrotron. This analysis was performed in collaboration with the group of Milan University Bicocca that has access to the instrument placed in Geneve.

For the synchrotron analysis, the polymer and each single component of the formulation has to be prepared at a concentration of 10 mg/mL in order to assure the highest resolution.

As previous studies showed that PEG_{5kDa}-cholane in the presence of AmB, NaOH and orthophosphoric acid jellifies at 7.5 mg/mL, a 5 mg/mL PEG_{5kDa}-cholane solution and a 10 mg/mL AmB in AmB/ PEG_{5kDa}-cholane micelles containing 5 mg/mL polymer were prepared.

The medium was obtained by the addition of 40 µL NaOH 0.1 M and 30 µL ortophosphoric acid 0.1 M to 4.930 mL purified water. 1 mL medium was used to solubilize 5 mg of PEG_{5kDa}-cholane. The AmB/PEG_{5kDa}-cholane micelles (10 mg/mL AmB, 5 mg/mL PEG_{5kDa}-cholane) were prepared by the pH/change method. The samples were centrifuged at 4500 rpm for 5 min using a Hermle Z- 306 centrifuge (Wehingen, Germany) to ensure complete solubilization and to eliminate air bubbles.

As the solution containing the AmB/PEG_{5kDa}-cholane micelles was slightly viscous, another formulation with fewer amounts of AmB and PEG_{5kDa}-cholane was prepared. This second formulation contained half AmB half polymer. In order to perform the

experiment not only the formulation but also a sample of the polymer alone at 2.5 mg/mL was prepared.

1 mL of each sample was placed in an eppendorf, frozen with liquid nitrogen and stored in freezer at -20 ºC until expedition.

EXP2-1.2.3.7. Transmission electron microscopy

Samples for negative-stain transmission electron microscopy (TEM) analysis were prepared by depositing one drop of AmB/PEG_{5kDa}-cholane (12:1) micelles, prepared by dissolution/pH change, stained with 1% phosphotungstic acid for 20 seconds into Formvar/carbon-coated TEM copper grids (size 3.05 mm) for 30 s. The grids were left drying at room temperature for 15 min before the analysis. The samples were examined and photographed in a Jeol JEM 1010 transmission electron microscope (Jeol Ltd, Tokyo, Japan) equipped with a *Megaview* II imaging camera and operating at 100 kV (resolution 0.35 nm).

EXP2-1.2.3.8. Human Serum Albumin circular dichroism analyses

Description of the technique

Circular dichroism (CD) spectroscopy is a spectroscopic technique used to study chiral molecules. The basics of this method are referred to the differential absorption of the left and right circularly polarized components of equal magnitude of the plane-polarized radiation. If after passing through the sample that is being examined, the left and right components are not absorbed or equally absorbed, the recombination of both would regenerate polarized radiation in the original plane. However, if both are differently absorbed, the resulted radiation would be said to possess elliptical polarization (figure 45) [356]. A CD signal is generated when a chromophore is chiral (optically active) either intrinsically by reason of its structure; by being covalently linked to a chiral centre or by being placed in an asymmetric environment [357].

CD instruments measure the difference in absorption between the left and right circularly polarized components ($\Delta A = A_L - A_R$) and usually express this measurement as ellipticity in degrees [356].

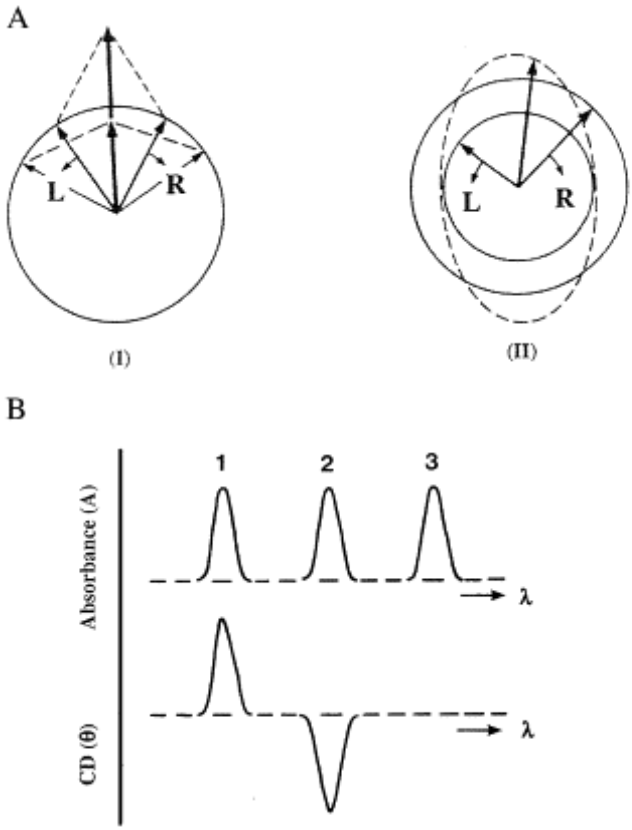

Figure 45. Circular Dichroism bases. Image taken from [356].

In figure 45, the scheme **A** part I show the behavior of the two components when they both have the same amplitude while part II refers to the resultant of the difference between the two components (dashed line) when they are elliptically polarized. In the scheme **B**, as shown in the spectra, the absorption bands can generate different signals on the CD depending on the left and right absorption. The higher left absorption compared to the right, generates a positive band in the CD (band 1); the higher right absorption compared to the left, produces a negative band (band 2) while the achiral chromosphere doesn't generate a signal (band 3).

CD spectroscopy is widely used to study chiral molecules of all types and sizes, but it is in the study of large biological molecules where it finds its most important applications. It is mainly used in the analysis of the secondary structure or conformation of macromolecules, particularly proteins. As protein secondary structure is sensitive to its environment, temperature or pH, CD can be used to observe how secondary structure

changes with environmental conditions or on interaction with other molecules. Structural, kinetic and thermodynamic information about macromolecules, as well as, aggregation and stability information about small molecules, can be derived from circular dichroism spectroscopy.

Method

Circular dichroism analyses were performed either in the far or near UV. The far UV was used to detect possible changes in the human serum albumin (HSA) secondary structure caused by the presence of AmB included in different systems. Changes in the protein structure could possibly lead to side effects when administered this formulation *in vivo*. On the other hand, the CD analyses in the near UV were performed in order to get information about the AmB aggregation state in the presence or in the absence of HSA. It is well known that formulated AmB in the presence of HSA disaggregates and joins the protein in a monomeric state [151]. The speed at which this process takes place is directly related to the toxicity of the formulation.

- **Far UV**

Human serum albumin (HSA) solution ($1.5\ 10^{-7}$ M) in PBS, pH 7.2, in the absence or in the presence of $1.37\ 10^{-7}$ M AmB or equivalent AmB concentration of Fungizone®, heated Fungizone® (obtained by 30 min heating Fungizone® at 70ºC) or AmB/PEG_{5kDa}-cholane micelles (12:1 AmB/PEG_{5kDa}-cholane molar ratio) prepared by dissolution/pH change were analyzed by CD in the far UV (200-300 nm, 50 nm/s with 8 s response and 2 nm band width) using a J-810 Jasco spectrodichrograph (Jasco, Tokyo, Japan). The spectra were processed by Dicroprot software and the protein secondary structure was calculated by KD2 analysis. CD analyses were performed after sample incubation at 37ºC for 15 min [151].

- **Near UV**

HSA solutions ($2.3\ 10^{-4}$ M) in PBS, pH 7.2, in the absence or in the presence of $5\ 10^{-6}$M AmB or AmB equivalent concentration of Fungizone®, heated Fungizone® and AmB/MeO-PEG_{5kDa}cholane (12:1 AmB/PEG_{5kDa}-cholane molar ratio) samples were incubated at 37 ºC for 15 min [151] and then analyzed by circular dichroism (CD) in the near UV (300-450 nm).

EXP2-1.2.3.9. Absorption and kinetics studies

The AmB aggregation in the different formulations, at different temperatures and in the presence and absence of HSA, as well as, the kinetics of the AmB disaggregation process in the presence of HSA, were studied as described below.

AmB (5 10^{-5}M) or AmB equivalent concentration of Fungizone®, heated Fungizone® and AmB/PEG_{5kDa}-cholane micelles (12:1 AmB/PEG_{5kDa}-cholane molar ratio) prepared by dissolution/pH change in PBS, pH 7.2, were 1:10 diluted with a 2.3 10^{-4} M HSA in the same buffer and spectrophotometrically analyzed by UV absorption in the range of 300- 450 nm at 25 and 37ºC using an Evolution 201 UV-Visible spectrophotometer equipped with a single cell peltier system (Thermo Fisher Scientific). Absorption spectra were recorded at 0, 1, 2, 5, 10, 20 and 45 min. Kinetic analysis were performed recording the absorption at 413 nm, at 15 s intervals for the first 5 min and then at 1 min intervals for further 40 min [358].

EXP2-1.2.3.10. Dialysis studies

The AmB release from the core of the PEG_{5kDa}cholane micelles was studied by dialysis.

One milliliter of 30 μg/mL AmB or AmB equivalent AmB/PEG_{5kDa}cholane micelles (12:1 AmB/ PEG_{5kDa}cholane molar ratio) in PBS, pH 7.4, was dialyzed at 25 ºC against PBS buffer, pH 7.4 using a Float-A-Lyzer® G2 system, 3.5-5 kDa cut-off. The AmB concentration inside the dialysis bag was determined at fixed time points by RP-HPLC. The analysis was performed in triplicate and the data was elaborated to find the best fit according to different mathematical models (table 36).

Table 36. Mathematical models used in the study of the AmB kinetic release profile

Model	**Equation**
Zero order	$Q_t = Q_0 + kt$
First order	$\log Q_t = \log Q_0 + kt/2{,}303$
Hixon-Crowel	$Q_t = kt^{1/2}$
Higuchi	$Q_\infty^{1/3} - Q_t^{1/3} = kt$
Baker-Lonsdale	$3/2[1-(-1(Qt/Q_\infty))^{2/3}]-(Q_t/Q_\infty)=kt$
Korsmeyer-Peppas	$Q_t/Q_\infty = kt^n$

EXP2-1.2.4. Stability studies

ICH stability studies

The stability studies were designed following the International Conference of Harmonisation guidelines (ICH) [359]. The stability guideline (ICHQ1A), exposes that the conditions for the accelerated studies for those drugs that should be stored at 4 ºC, are 6 months analysis at 25 ± 2 ºC with a relative humidity (RH) of 60 ± 5%.

Following the ICH, 15 mL of 1 mg/mL AmB, 12:1 AmB/PEG_{5kDa}-cholane solution and FD micelles were prepared for the stability studies. 200 µL AmB/PEG_{5kDa}-cholane solution and re-dispersed product were added to 60 vials and stored in a desiccator at 25 ± 2 ºC and 60% RH. The temperature was controlled three times a week and the RH was obtained by the addition of a saturated solution of NaCl.

At each sampling time, three vials from both formulations were analyzed by RP-HPLC in order to determine the remaining AmB concentration.

Gastric mimicking fluid stability studies

AmB/PEG_{5kDa}-cholane stability studies in gastric mimicking fluid (GMF) were performed in order to get information about the percentage of AmB still available in the formulation after being exposed to these extreme conditions. The aim of the study was to check whether or not the new formulation could be orally administered.

The GMF was prepared according to the European pharmacopeia [360]. Briefly, 0.2 g of NaCl and 0.32 g of pepsin 800/2500 U/mg were added to 100 mL of deionized water at pH 1.2 (7 mL of 0.1 M HCl). The gastric mimicking fluid was kept at 37 ºC and

under stirring during the entire assay (4 hours). At time 0, 5 mL of 1 mg/mL AmB in AmB/PEG_{5kDa}-cholane micelles (12:1 AmB/PEG_{5kDa}-cholane molar ratio) were added to the GMF. At fixed times, 100 µL media were taken and analyzed by RP-HPLC.

The analysis was performed in triplicate and the data was elaborated to find the best fit according to different mathematical models (table 14).

EXP2-1.2.5. *In vitro* toxicity studies

EXP2-1.2.5.1 Hemolysis

The hemolytic effect of AmB included in Fungizone® and PEG_{5kDa}-cholane micelles (12:1 molar ratio) was studied as reported elsewhere [330].

Blood was collected from Sprague Dowley rats. Blood was collected from the tail vein and added of sodium citrate (3.8%) to avoid coagulation.

2 mL of non-coagulated blood were diluted with 8 mL PBS buffer, pH 7.2, and centrifuged at 1500 rpm for 5 min. Then, the pellet was washed 5 times with PBS in order to obtain a clear supernatant and the hematocrit was adjusted to 5% (w/v) in PBS. Two control samples were prepared. As for the negative control 1 mL PBS was added of 30 µL red blood cells (RBC) (0% hemolysis). With regards to the positive control, this was prepared by the addition of 30 µL RBC to 1 mL purified water (100% hemolysis).

To study the AmB hemolytic effect, 30 µL of RBC were added of 1 mL of 0, 2.5, 5, 10, 20, 30, 40, 50 and 60 µg/mL AmB included in the different formulations prepared in PBS. Samples were incubated in a water bath at 37ºC for 5 h. The hemolysis was stopped by decreasing the temperature to 0ºC using ice and the unlyzed RBC were removed by centrifugation at 1500 rpm for 4 min. The supernatant was analyzed by UV/VIS spectroscopy at 541 nm.

The study was performed in triplicate and the percentage of hemolysis was calculated from the following equation:

$$\%\ Hemolysis = (Abs - Abs0)\ /\ (Abs1 - Abs0)$$

Where Abs, Abs_0 and Abs_1 are the sample absorbance, control absorbance with 0% hemolysis and control absorbance with 100% hemolysis, respectively.

EXP2-1.2.6. *In vitro* efficacy studies

In vitro antifungal activity of AmB and AmB/PEG_{5kDa}-cholane micelles (12:1 AmB/ PEG_{5kDa}-cholane molar ratio) in PBS, pH 7.2, prepared by dissolution/pH change, was assessed against *Candida albicans* CECT1394. Yeast cells were cultured in Petri dishes containing agar Sabouraud medium for 72 h at 30 ºC and then 3 mL of a 0.5 McFarland standard suspension (1-5.10^6 CFU/mL) were seeded in plates of Agar Mueller Hinton supplemented with glucose [337]. Methylene blue was used as contrast agent. Paper disks, impregnated with the AmB dissolved in DMSO were used as reference (S_1 600 μg/mL; S_2 200 μg/mL; S_3 96 μg/mL; S_4 38.4 μg/mL; S_5 18.4 μg/mL). Twenty microliters of 96 μg/mL AmB or equivalent AmB concentration of AmB/PEG_{5kDa}cholane in 0.2 M phosphate buffer, pH 10.5, were placed onto the paper disk that was then placed on the plates and incubated at 30ºC. After 48 h of incubation, the inhibition zones were accurately measured using a caliper and referred to the reference (96 μg/mL AmB, S_3).

EXP2-1.2.7. *In vivo* studies

The analysis of biological samples requires the addition of an internal standard to assure the efficiency during sample preparation, or the performance of drug recovery studies to detect the amount of drug that can be recovered in plasma.

Both, the use of an internal standard and the drug recovery studies, were considered and studied before performing the *in vivo* oral and intravenous pharmacokinetic studies in animals.

It is important to point out that all the *in vivo* experiments were conducted following the European guidelines...

EXP2-1.2.7.1. Internal standard

General considerations

The internal standard can be defined as a chemical compound added to a sample at a known concentration in order to provide a basis for comparison in quantification. The addition of known quantities of internal standard to biological samples is used to assure the efficiency of the sample preparation. The ratio obtained between the area of the drug and the area of the internal standard allow for the determination of the drug concentration in the biological samples.

In the choice of the internal standard some factors may be considered [361]:

- The compound must be detected at the same wavelength as the drug,
- It has to be eluted near the peaks of the sample but it has to be well-resolved from the drug,
- It must be available in pure form,
- It should be a stable compound and no react with the sample,
- And ideally, its physicochemical properties should be similar to the drug object of study.

Due to the large experience of the research group in Padua using naproxen, this drug was selected as candidate for the the internal standard studies.

Internal standard calibration curve

A naproxen stock solution of 50 mg/mL was prepared by the addition of 25 mg naproxen to 0.5 mL methanol. From this stock solution, 14 samples were prepared by serial dilution ranging from 0.003 to 50 mg/mL and analyzed by RP-HPLC at 406 nm starting from the more diluted sample. The analysis was performed in triplicate.

EXP2-1.2.7.2. AmB recovery studies in plasma

Drug recovery studies are necessary when working with biological samples. Sample preparation protocols usually include several steps (centrifugation and precipitation) where some of the drug can be lost. Moreover, even the solvent used to precipitate the plasma proteins is selected as function of the drug solubility; part of the drug can precipitate if joined with the proteins. Therefore, the knowledge of the amount of drug

lost during sample preparation allows the extrapolation of the real amount of drug contained in blood.

Samples preparation and analysis

1 mg/mL stock solutions of AmB in DMSO, AmB in dextrose (5% w/v), Fungizone®, Ambisome® and AmB/PEG_{5kDa}-cholane were diluted in order to obtain 6 samples with 1, 2, 4, 6, 8 and 10 μg/mL concentration. Then, 5 μL of each sample were added of 100 μL blood; slightly shake in order to avoid the hemolysis and centrifuged at 3500 rpm for 3 min. After centrifugation, 30 μL of supernatant were withdrawn, added of 100 μL MeOH (to induce faster protein precipitation the samples were stored 10 min at 4 ºC) and centrifuged at 12000 rpm for 5 min. Finally, 100 μL supernatant (plasma without proteins) were withdrawn and 30 μL of those, analyzed by RP-HPLC.

The blood (2 mL) was extracted from Balb/c female mice, age ten weeks, following the protocols established by the animal facilities of the University of Padua.

By plotting the AmB initial concentration versus the AmB concentration detected in plasma, a regression equation (y=a+bx) was obtained. The "b" value which corresponds to the slope of the curve multiplied by 100 was the percentage of recovery. This value was used to extrapolate the real AmB concentration in blood.

EXP2-1.2.7.3. Oral pharmacokinetic studies

Introduction

AmB is a class four drug (low solubility and low permeability) whose log P (0.95) and molecular weight (924.09 g/mol) are responsible for its low oral absorption. In spite of these disadvantages the oral administration of AmB will, not only enhance the therapeutic patient compliance, but also allow for the interruption of the treatment if severe side effects are detected. Moreover, in the undeveloped countries, where the infections caused by of Candida and Leishmania are severe, an oral AmB formulation will solve the problems related to the treatment access (the intravenous therapies requires long-term hospitalization).

The high stability of the AmB included in the PEG_{5kDa}-cholane micelles as well as the integrity of the system at a wide range of pHs (3-5-8.5), make this new formulation suitable for oral administration.

In order to check whether or not the AmB in the PEG_{5kDa}-cholane micelles reaches a comparable C_{max} value to that obtained with other commercialized formulations (eg. Fungizone® and Albelcet®) the following oral *in vivo* study was designed.

Method

The oral pharmacokinetic experiments were performed in healthy female BALB/c mice, age ten weeks and 20 g body weights. 5 mg/kg AmB were administered via gavage using 1 mL syringes fitted with an appropriate needle which allowed the formulation to directly reach the stomach. The different formulations (AmB in 5% dextrose w/v, Ambisome®, Fungizone® and AmB/PEG_{5kDa}cholane) were prepared at a concentration of 1 mg/mL AmB in purified water. Blood samples (100 µL) were extracted at each sampling time (0.5, 1, 2, 4, 8 and 24 h) from the right eye of each mouse (via seno retro-orbital) using heparinized capillary tubes. The blood was added to an eppendorf containing 2 µL heparine and slightly moved to avoid blood coagulation. Blood was centrifuged at 4500 rpm for 5 min and the supernatant (plasma) was removed, frozen in liquid nitrogen and kept at -20°C until sample analysis.

Protocol for sample preparation

Samples were prepared following the 10-steps protocol detailed below.

1. The formulations, 2 per day, were prepared on the day of adminitration at 1mg/mL AmB using water for injection (WFI) as vehicle.

2. The theoretical AmB concentration contained in the formulations was analyzed by RP-HPLC before administration. Briefly, 30 µL of each formulation were diluted with 970 µL methanol and analyzed by RP-HPLC.

3. BALB/c mice were divided into different cages - 4 mice per formulation on each cage. The tail of the animals was marked in blue or red depending on the

formulation, with and indelible marker. In order to avoid mistakes, each mouse had a different number on its tale (“I”, “II”, “III”, IIII”).

4. Prior to administration each mouse was weighted. The AmB dose was adjusted as function of the animal weight in order to achieve the correct dose (5 mg/kg). Assuming an animal weight of approximately 20 g, 100 μL of 1 mg/mL AmB formulations should be administered.

5. The 1 mL syringes (without needle) used for the oral administration were charged with 650 μL formulation. After loading, the needle was fitted into the syringes and 150 μL formulation were displaced (50 μL discarded, and 100 μL charged in the needle).

6. At time 0, 100 μL formulations were orally administered to each mouse as shown in figure 46.

7. Prior to blood extraction, 24 eppendorfs (0.5 mL capacity) containing 2 μL heparine were prepared for each formulation. Heparine was used to avoid later blood coagulation.

8. At each sampling time (scheme 1), using heparinized capillary tubes, approximately 100 μL blood was extracted from the right eye of the mice via seno retro-orbital and deposited into the heparinized eppendorfs. The eye of the mice was then cleaned and the animals were again left in the cage.

9. Blood samples were centrifuged at 4500 rpm for 5 min. Then, 45 μL plasma were added to the empty eppendorfs, frozen with liquid nitrogen and kept at -20°C until RP-HPLC analysis.

10. RP-HPLC analysis - Prior to HPLC analysis, the samples were thawed at room temperature. Once thawed, 45 μL methanol were added in order to precipitate the proteins and the eppendorfs were first vortex for 30 s and then centrifuged at 12000 rpm for 15 min. The supernatant was finally analyzed by HPLC. During

samples analysis, the mobile phase was eluted at 1 mL/min and the elution time was fixed at 30 min*.

*The extended elution time with respect to the non-biological samples was due to the plasma peak detected at 20-21 min (λ=406 nm) during the recovery studies. To avoid possible interferences with the AmB peak, the elution time was increased up to 30 min instead of 12 min.

Scheme 1. Study design of the oral pharmacokinetics experiments performed in female BALB/c mice. Day 1. Oral administration of 5 mg/kg AmB in Dextrose (5% w/v) and 5 mg/kg AmB as Ambisome® to four mice. Day 2. Oral administration of 5 mg/kg AmB as Fungizone® and AmB/PEG_{5kDa}cholane to four mice.

Day 1

AmB in Dextrose (5% w/v)

Ambisome®

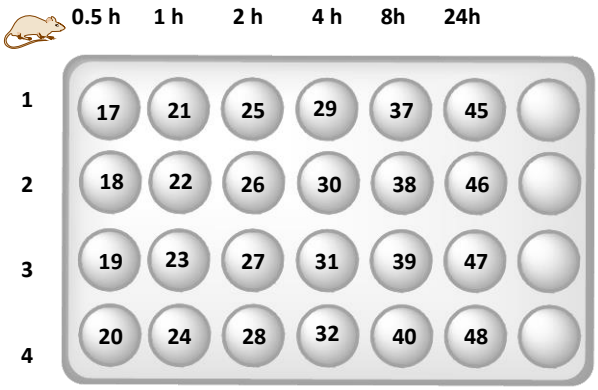

Day 2

Fungizone®

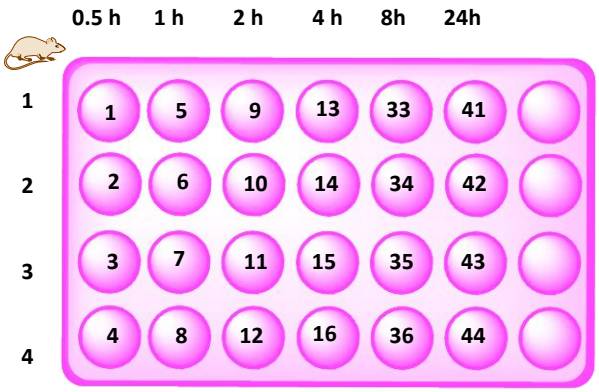

AmB/PEG_{5kDa}-cholane (12:1)

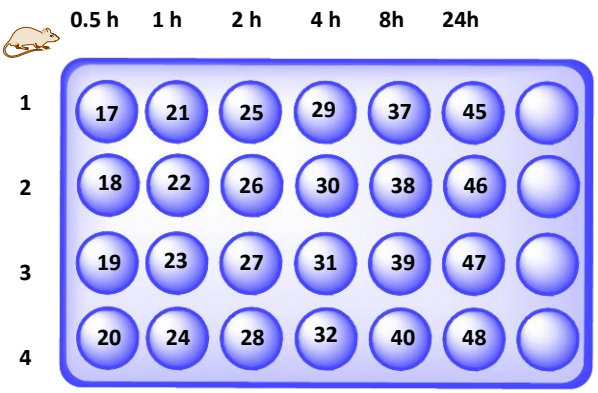

EXP2-1.2.7.4. Intravenous pharmacokinetics studies

Introduction

The intravenous (iv) administration of AmB is still nowadays the main route of administration for this antibiotic. Between all the AmB commercialized formulations (Fungizone®, Ambisome®, Abelcet®), the lipidic formulations are the ones whose use is more spread [269,311,362,363] . This is due to the low sides effects associated to its administration. Nevertheless, these lipidic formulations have a high cost that significantly increases the cost of the treatment with respect to the non-lipidic formulations (Fungizone®) [364-367]. Therefore, the development of an iv AmB formulation whose efficacy is comparable, if not higher, to the lipidic formulations (Ambisome®); its side effects are lower and the price is decreased, could significantly reduce the cost of the treatment.

The efficacy of the AmB/PEG_{5kDa}cholane micelles was assayed intravenously as detailed above. This new formulation will potentially decrease by seven the actual treatment cost.

Method

The intravenous pharmacokinetics experiments were performed in healthy female BALB/c mice, age ten weeks (born on 16.02.15) and 20 g weight. A dose of 1 mg/kg AmB (0.020 mg AmB – 80 μL of 0.25 mg/mL AmB in NaCl 0.9%/Dextrose 5% w/v (1:1)) was administered intravenously in the lower part of the tail. At time 1 min, 5 min, 10 min, 30 min, 1 h, 2 h, 4 h, 8 h and 24 h, 80-100 μL of blood were extracted from the right eye of each mouse via seno retro-orbital using heparinized capillary tubes. For each formulation 6 mice were used (for AmB/PEG_{5kDa}cholane 7). The blood was added into an eppendorf containing 2 μL heparine (5000 UI), centrifuged at 4500 rpm during 15 min and then, 45 μL supernatant for Ambisome® and Fungizone® and 40 μL for AmB/PEG_{5kDa}-cholane were placed in a new eppendorf, frozen with liquid nitrogen and kept in the freezer (-20ºC) until analysis. For the RP-HPLC analysis, the plasma samples were first thawed and then added of 45 μL methanol. After methanol addition the samples were vortex in order to precipitate the proteins and centrifuged at 12000 rpm for 15 min. The supernatant was finally analyzed by RP-HPLC.

Protocol for sample preparation

As for the oral pharmacokinetic experimernts, samples were prepared following a 10-steps protocol.

1. Formulations were prepared on the same day of the experiment (2 one day and the other the next day) at 1 mg/mL AmB using WFI as vehicle. Prior to administration, the samples were diluted to a final concentration of 0.25 mg/mL using a mixture (1:1) of NaCl 0.9% and Dextrose 5% w/v (formulations were prepared 1 h before the experiment started).

2. The theoretical AmB concentration was checked by RP-HPLC before administration. 30 μL f each formulation were diluted with 970 μL methanol and analyzed by HPLC.

3. BALB/c mice were divided into different cages -6 mice per formulation with the exception of AmB/PEG_{5kDa}-cholane. 7 mice were used for the latest. The tail of the animals was marked on its upper part in blue or red, depending on the formulation, with an indelible marker. In order to avoid mistakes, each mouse had a different number on its tale ("I", "II", "III", IIII, IIIII and IIIIII").

4. Prior to administration each mouse was weighted and the AmB dose was adjusted as function of the animal weight in order to achieve the correct dose (1 mg/kg). Assuming an animal weight of approximately 20g, 80 μL of 0.25 mg/mL AmB formulations in a mixture (1:1) of NaCl 0.9% and dextrose 5% w/v were iv administered.

5. 1 mL syringes (insulin-type) were loaded with 150 μL formulation. The needle was then fitted and 70 μL were discarded in order to display the air and have the correct dose in the syringe.

6. At time 0, 80 μL of each formulation were intravenously administered in the lower part of the mouse tail.

7. 33 eppendorfs (0.5 mL capacity) were prepared for each formulation by adding 2 μL heparine. The heparine was added in order to avoid later blood coagulation.

8. At each sampling time (tables 37-39), using heparinized capillary tubes, approximately 80-100 μL blood were extracted from the right eye of each mice via seno retro-orbital and deposited into the heparinized eppendorfs. The eye of the mice was then cleaned and the animals were again left in the cage. The mandibular extraction (via mandibular vein) using a needle was also assayed. This technique is known to be less painful for the mice but the amount of blood recovered was really low and therefore, the extraction was performed through the eye.

9. Blood samples were centrifuged at 4500 rpm for 15 min and then, 45 μL (for Ambisome® and Fungizone®) or 40 μL (AmB/PEG_{5kDa}-cholane) plasma were added to empty eppendorfs, frozen with liquid nitrogen and kept at -20°C until HPLC analysis.

10. RP-HPLC analysis - The samples were thawed at room temperature and once thawing was completed, 50 μL methanol were added in order to precipitate the proteins. After methanol addition, the eppendorfs were first vortex 30 s, stored in the fridge for 5 min in order to induce faster protein precipitation and then centrifuged at 12000 rpm for 15 min. The supernatant (20 or 30 μL depending on the sampling time) was precipitated again with methanol (100, 50 or 60 μL) and vortex for 30 s. After 5 min in the fridge the samples were centrifuged again at 12000 rpm for 15 min. The final supernatant was analyzed by RP-HPLC. During sample analysis the mobile phase was eluted at 1 mL/min and the elution time was fixed at 30 min*

*the extended elution time with respect to the non-biological samples analysis was due to the plasma peak detected at 20-21 min (λ=406 nm) during the recovery studies performed with plasma.

Table 37. Protocol design for blood extraction after iv administration of 1 mg/kg Ambisome®

Time	Mouse 1	Mouse 2	Mouse 3	Mouse 4	Mouse 5	Mouse 6
Injection	09:51	10:02	10:09	10:23	10:32	10:54
1 min	09:52 (1)	10:03 (2)	10:10 (3)	10:24 (4)	10:33 (5)	10:55 (6)
5 min	09:56 (7)	10:07 (8)	10:14 (9)	-	-	-
10 min	-	-	-	10:33 (10)	10:42 (11)	11:04 (12)
30 min	10:21 (13)	10:32 (14)	10:39 (15)	-	-	-
1 h	-	-	-	11:23 (16)	11:32 (17)	11:54 (18)
2 h	11:51 (19)	12:02 (20)	12:09 (21)	-	-	-
4 h	-	-	-	14:23 (22)	14:32 (23)	14:54 (24)
8 h	17:51 (25)	18:02 (26)	18:09 (27)	-	-	-
24 h	09:51 + 1 day (28)	10:02 + 1 day (29)	10:09 + 1 day (30)	10:23 + 1 day (31)	10:32 + 1 day (32)	10:54 + 1 day (33)

Table 38. Protocol design for blood extraction after iv administration of 1 mg/kg Fungizone®

Time	Mouse 1	Mouse 2	Mouse 3	Mouse 4	Mouse 5	Mouse 6
Injection	09:54	10:05	10:14	10:27	10:48	10:58
1 min	09:55 (34)	10:06 (35)	10:15 (36)	10:28 (37)	10:49 (38)	10:59 (39)
5 min	09.59 (40)	10:10 (41)	10:19 (42)	-	-	-
10 min	-	-	-	10:37 (43)	10:58 (44)	11:08 (45)
30 min	10:24 (46)	10:35 (47)	10:44 (48)	-	-	-
1 h	-	-	-	11:27 (49)	11:48 (50)	11:58 (51)
2 h	11:54 (52)	12:05 (53)	12:14 (54)	-	-	-
4 h	-	-	-	14:27 (55)	14:48 (56)	14:58 (57)
8 h	17:54 (58)	18:05 (59)	18:14 (60)	-	-	-
24 h	09:54 + 1 day (61)	10:05 + 1 day (62)	10:14 + 1 day (63)	10:27 + 1 day (64)	10:48 + 1 day (65)	10:58 + 1 day (66)

Table 39. Protocol design for blood extraction after iv administration of 1 mg/kg AmB/PEG_{5kDa}-cholane

Time	Mouse 1	Mouse 2	Mouse 3	Mouse 4	Mouse 5	Mouse 6	Mouse 7
Injection	09:41	09:57	10:01	10:11	10:17	10:24	10:43
1 min	09:42 (67)	09:58 (68)	10:02 (69)	10:12 (70)	10:18 (71)	10:25 (72)	10:44 (100)
5 min	09:46(73)	10:02 (74)	10:06 (75)	-	-	-	-
10 min	-	-	-	10:21 (76)	10:27 (77)	10:34 (78)	10:53 (101)
30 min	10:11 (79)	10:27 (80)	10:31 (81)	-	-	-	-
1 h	-	-	-	11:11 (82)	11:17 (83)	11:24 (84)	11:43 (102)
2 h	11:41 (85)	11:57 (86)	12:01 (87)	-	-	-	-
4 h	-	-	-	14:11 (88)	14:17 (89)	14:24 (90)	14:43 (103)
8 h	17:41 (91)	17:57 (92)	18:01 (93)	-	-	-	-
24 h	09:41 + 1 day (94)	09:57 + 1 day (95)	10:01 + 1 day (96)	10:11 + 1 day (97)	10:17 + 1 day (98)	10:24 + 1 day (99)	10:43 + 1 day (104)

CHOLANYL CHLORIDE AMB-PEG$_{5KDA}$-CHOLANE AUC α-HELIX CIRCULAR SHAPE RAPIDLY REDISSOLVED PLASMA DECOMPOSITION ENDOTHERMIC PEAK CRYSTALLINE GRAY SHADOW CONCENTRATION-DEPENDENT HEMOLYSIS PEPSIN MATHEMATICAL MODELS DISSOCIATION RATES CANDIDA ALBICANS Ke NEUTRAL SURFACE CHARGE MOLAR RATIO NEGATIVE-STAINING AMBISOME® STOICHIOMETRY

EXP.2-2. RESULTS

ABSORBANCE DIMER FUNGIZONE® HEAT PPM COLLOIDAL DISPERSION TEA SIZE UNFORMULATED DRUG/POLYMER INTERACTION ΔH CM^{-1} Kd AMORPHOUS BENDING/STRETCHING VIBRATIONS ΔS NANOAGGREGATES STOMACH TMAX MONOMER β-SHEET C24 ^{128}H-NMR SPECTRUM ANOVA CMAX F T-STUDENT SECONDARY PROTEIN STRUCTURE ABSROPTION C. ALBICANS REFERENCE MATERIAL

EXP2-2. RESULTS

EXP2-2. 1. Synthesis and characterization of the poly(ethylene glycol)-cholane bioconjugate

EXP2-2.1.1. Activation of the cholanic acid

The degree of cholanic acid derivatization with thionyl chloride was measured by ^{128}H-NMR and the spectra were proceeded with MestreNova software. Figure 46 shows the spectrum obtained for the treated cholanyl chloride sample.

By the integration of the peak at 0.64 ppm and the peak at 3.66 ppm the degree of activation was calculated as detailed below.

$$Degree\ of\ activation\ (\%) = \left(\frac{2.37}{3}\right) \times 100 = 79\ \%$$

Knowing that there is an activation of 79% and that the stoichiometry of the reaction is 1:3:2 (MeO-PEG$_{5kDa}$-NH$_2$: cholanyl chloride : triethylamine (TEA)) the amount of reagents needed for the following step (conjugation) was calculated.

EXP2-2.1.2. Conjugation with MeO-PEG$_{5kDa}$-NH$_2$

The degree of cholanyl chloride conjugation with MeO-PEG$_{5kDa}$-NH$_2$ was calculated by two different techniques: ^{128}H-NMR and TNBS colorimetric assay.

Figure 47 shows the spectra obtained for the NMR analysis of the conjugated sample. The two main peaks, 0.64 ppm (CH$_3$ in position 19) and 3.38 ppm (CH$_3$-O in ended position of PEG$_{5kDa}$ chain), were integrated in order to calculate the degree of conjugation.

$$Degree\ of\ conjugation\ (\%) = \left(\frac{2.85}{3.0}\right) \times 100$$

As reported in the above equation, the degree of conjugation calculated by NMR was found to be 95%.

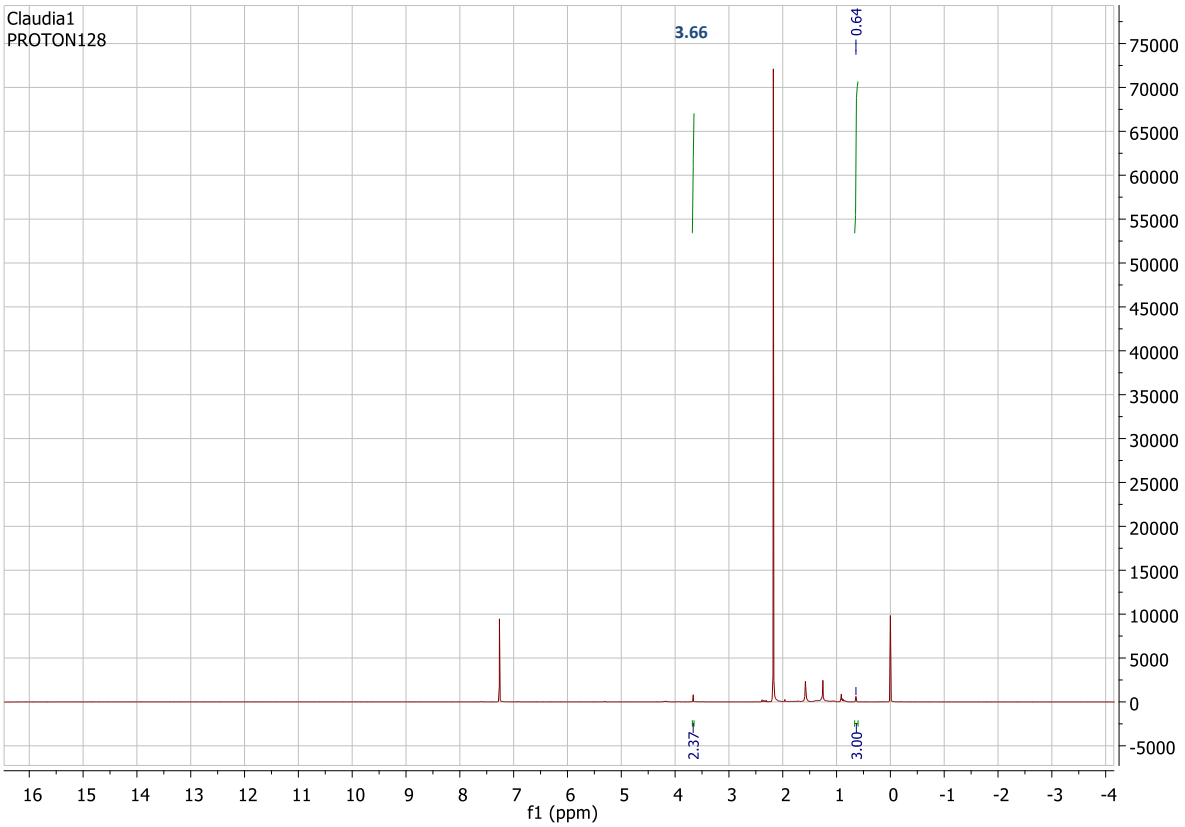

Figure 46. ^{128}H-NMR spectrum of the activated cholanic acid

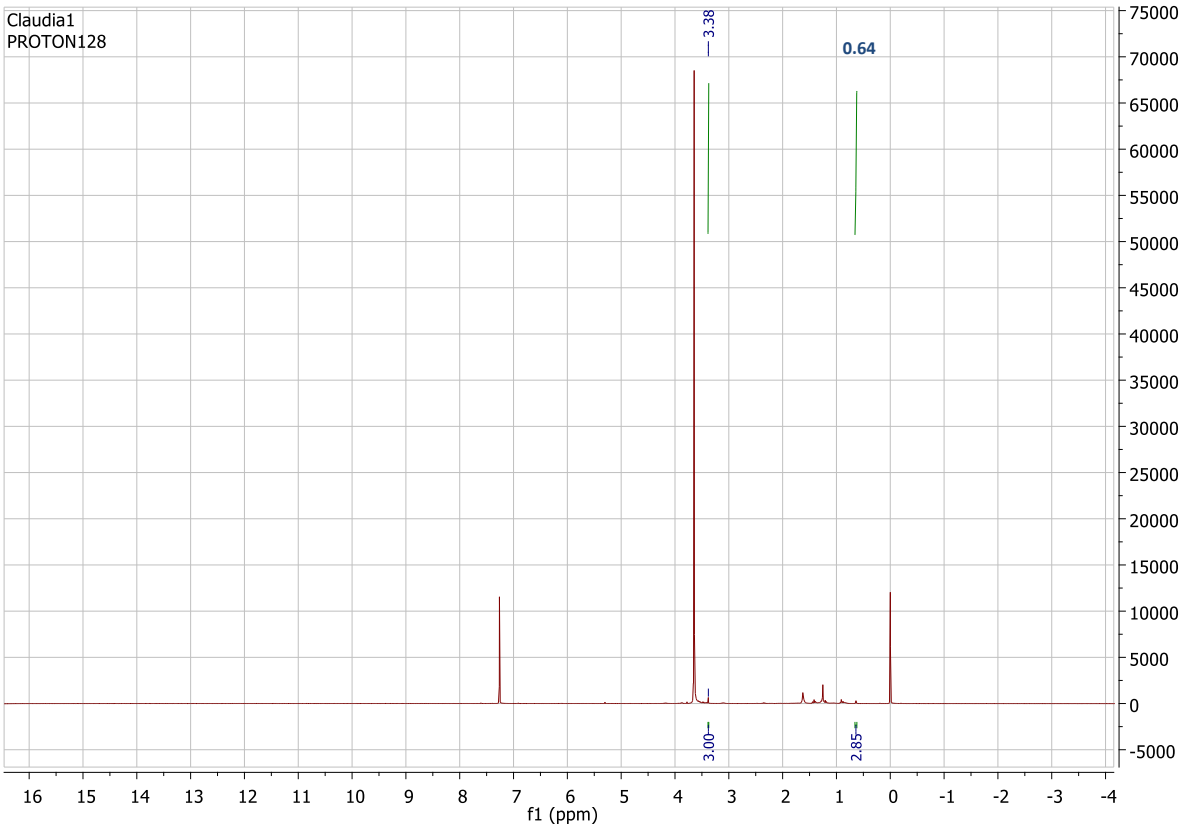

Figure 47. ^{128}H-NMR spectrum of the conjugated cholanyl chloride

The TNBS colorimetric assay was performed as a complementary experiment to corroborate the degree of activation and therefore, the success of the reaction. The NMR itself is reliable but as the integration of the peaks is made manually, some small errors can be generated. To make sure that the data obtained by NMR were totally reliable, the TNBS was carried out.

Table 40 shows the absorbance values obtained for the reference sample (PEG_{5kDa}-NH_2) and the conjugated (PEG_{5kDa}-cholane) when treated with TNBS.

Table 40. Absorbance values for the reference sample and conjugate.

	Reference	**Conjugate**
Absorbance 1	0.9161	0.0398
Absorbance 2	0.9264	0.0469
Absorbance 3	0.9178	0.0375

The degree of activation by TNBS was calculated as detailed in the following equation.

$$Degree\ of\ conjugation\ (\%) = 1 - \left({}^{Abs\ conjugate}/_{Abs\ reference}\right) \times 100$$

The values obtained for the three samples were 95.6%, 94.9% and 95.9%, respectively. The mean of those values gave a percentage of conjugation of 95.4% ± 0.51%.

The values of conjugation calculated by both techniques were found to be similar. 95% versus 95.4% with NMR and TNBS, respectively.

EXP2-2.2. Amphotericin B dissolution studies with PEG_{5kDa}-cholane

Solubility studies were carried out at pH 3.5, 5.5, 7.2, 8.5 and 11.0 by combining fixed amounts of AmB with increasing amounts of PEG_{5kDa}-cholane according to three different experimental protocols: 1. direct dissolution; 2. co-solvent dissolution; 3. dissolution/pH change. For comparison, the solubility of AmB in the presence of increasing amounts of PEG_{5kDa}-OH was also examined.

Preliminary studies showed that in the absence of PEG_{5kDa}-cholane and PEG-OH, the direct AmB dissolution yielded lower drug concentrations than co-solvent dissolution and dissolution/pH change. This behavior was observed at all examined pHs (figure 48

and table 41) and was in fair agreement with studies reported in the literature [145]. The UV spectra of dissolved AmB (figure 49) showed that the three dissolution methods yielded different physical forms of dissolved AmB, namely monomers and soluble aggregates such as dimers and tetramers. According to the literature, the absorption at 322 nm ($A\lambda_{322}$) and 413 nm ($A\lambda_{413}$) were elaborated to estimate the content of monomeric and nanoaggregated AmB in solution [288,358,368]. The lower $A\lambda_{322}/A\lambda_{413}$ ratio obtained by direct dissolution indicated that the monomeric form was the predominant AmB specie in solution. On the contrary, the higher $A\lambda_{322}/A\lambda_{413}$ ratio obtained by co-solvent dissolution and dissolution/pH change indicated that in such a case the main specie in solution was the nanoaggregated AmB. Therefore, AmB dissolved by direct dissolution tends to be in the monomeric form while AmB dissolved by dissolution/pH change and co-solubilization was mainly in aggregated form.

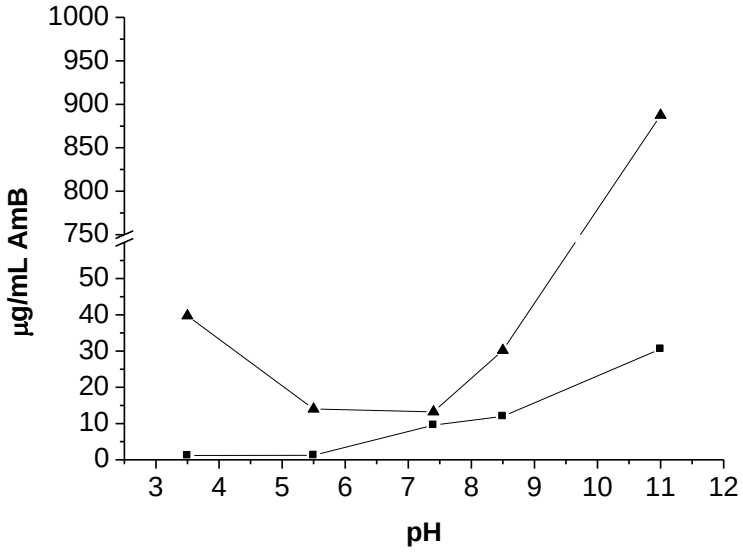

Figure 48. AmB solubility (µg/mL) at different pHs by dissolution/pH change (-▲-) and by direct dissolution (-■-).

Table 41. Concentration of AmB dissolved at different pHs by direct dissolution and dissolution/pH change.

pH	AmB (µg/mL) dissolved by direct dissolution	AmB (µg/mL) dissolved by dissolution/pH change
3.5	1.21±0.03	39.73±0.45
5.5	1.24±0.06	14.02±0.09
7.2	9.54±0.16	13.23±0.08
8.5	11.98±0.19	30.21±0.20
11	30.57±0.09	887.47±7.71

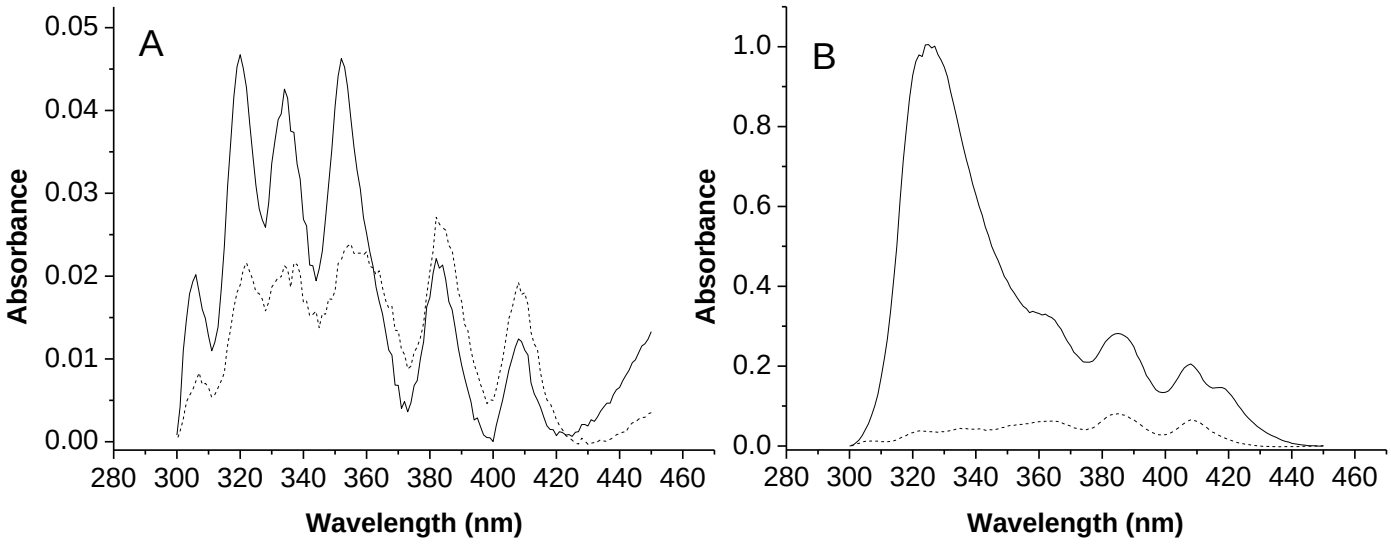

Figure 49. UV-Vis spectra of AmB (A) and AmB/PEG_{5kDa}-cholane (B) solutions prepared by co-solvent dissolution or dissolution/pH change (—) and by direct dissolution (····).

The solubility profiles reported in Figure 50 show that PEG_{5kDa}-OH has not relevant effect on the AmB solubility, which increased from 6 µg/mL to 17 µg/mL as the polymer concentration increased from 0.5 to 6 mg/mL (table 42). Furthermore, similarly to AmB in the absence of polymers, the dissolution method did not affect remarkably the AmB solubility (data not shown). On the contrary, PEG_{5kDa}-cholane dramatically increased the drug solubility and the dissolution method was found to significantly affect the AmB solubility (table 43). The direct dissolution yielded less than 0.5:1 AmB/PEG_{5kDa}-cholane molar ratio while the co-solvent dissolution and the

dissolution/pH change protocols resulted in 12:1 AmB/PEG_{5kDa}-cholane molar ratio, with identical dissolution profiles.

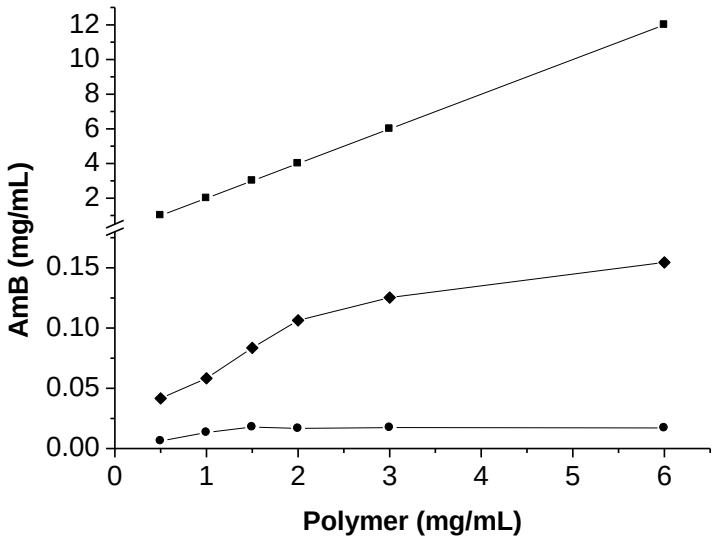

Figure 50. Solubility profile of AmB with: PEG_{5kDa}-cholane by direct dissolution (-♦-); PEG_{5kDa}-cholane by dissolution/pH change and by co-solubilization (-■-); PEG_{5kDa}-OH by dissolution/pH change (-●-).

Table 42. Concentration of AmB (µg/mL) dissolved by the dissolution/pH change method using increased amounts of PEG_{5kDa}-OH.

PEG_{5kDa}-OH (mg/mL)	**AmB dissolved (µg/mL)**
0.5	6.29±0.04
1	13.34±0.12
1.5	16.64±0.09
2	17.80±0.14
3	17.09±0.07
6	17.44±0.25

Table 43. Concentration of AmB (μg/mL) dissolved by direct dissolution and dissolution/pH change using increased amounts of PEG_{5kDa}-cholane.

PEG_{5kDa}-cholane (mg/mL)	**AmB (μg/mL) dissolved by direct dissolution**	**AmB (μg/mL) dissolved by dissolution/pH change**
0.5	41.66±0.77	1010±4.58
1	58.29±0.71	2005±7.09
1.5	83.56±2.38	3001±2.64
2	106.42±2.74	3999±7.63
3	125.35±1.43	6002±3.60
6	154.58±3.88	12001±1.52

The UV analysis of the AmB/PEG_{5kDa}-cholane obtained by direct dissolution (figure 49B) showed that the dissolved AmB was mainly in the monomeric form while the high absorption at 322 nm of samples obtained by co-solvent dissolution and dissolution/pH change demonstrated that in these samples nanoaggregated AmB specie predominated.

The maximal solubility of AmB with PEG_{5kDa}-cholane could not be determined because high polymer concentrations produced viscous dispersions that prevented the accurate analysis of dissolved AmB.

EXP2-2.3. Physicochemical characterization of the AmB/PEG_{5kDa}-cholane complex

EXP2-2.3.1. Reverse-phase high pressure liquid chromatography

The AmB concentration in the different samples was determined by RP-HPLC following the protocol reported by Espada *et al*. Two calibration curves, one for non-biological samples and another one for biological samples, were performed by analyzing different AmB standards of known concentration. 13 AmB standards were prepared in triplicate for each calibration curve by serial dilution using MeOH as solvent starting from a stock solution of 100 μg/mL AmB in a mixture of DMSO-MeOH (1/10). Tables 44 and 45 show the results obtained for both calibration curves.

The AmB concentration in non-biological samples was extrapolated from a curve linear in the range 0.012 – 40 μg/mL [(AmB concentration)=115.1(peak area)-1.665; R^2=1] while the AmB concentration in biological samples was extrapolated from a curve linear in the range 0.012 – 50 μg/mL [(AmB concentration)=113.7(peak area)-12.45;

R^2=0.99]. As shown in figures 51-54 both calibration curves were divided into two sub-curves, one for low AmB concentrations and another one for high AmB concentrations in order to avoid mistakes when extrapolating low AmB concentrations.

Table 44. Concentration and area under the curve (AUC) of the different AmB standards assayed for the calibration curve used in the non-biological samples.

Concentration [µg/mL]	AUC/1000	AUC/1000	AUC/1000	Mean AUC	SD
50	Out of range	Out of range	Out of range	**x**	**x**
40	4607.61	4596.99	4604.38	**4602.99**	**5.44**
25	2885.17	2862.01	2874.42	**2874.42**	**11.67**
12.5	1452.02	1437.13	1450.07	**1446.07**	**7.75**
6.25	708.15	702.03	707.85	**706.01**	**3.45**
3.125	357.49	354.18	358.59	**356.75**	**2.29**
1.5625	177.69	176.04	178.04	**177.25**	**1.06**
0.78125	89.43	86.94	88.42	**88.26**	**1.25**
0.3906	45.14	42.14	45.07	**44.11**	**1.71**
0.1953	23.27	19.98	21.35	**21.53**	**1.65**
0.09765	11.48	9.76	10.17	**10.47**	**0.89**
0.04882	5.67	4.61	5.01	**5.09**	**0.53**
0.02441	2.74	2.19	2.45	**2.46**	**0.27**
0.0122	1.17	1.02	1.08	**1.09**	**0.07**

Table 45. Concentration and area under the curve (AUC) of the different AmB standards assayed for the calibration curve used in the biological samples.

Concentration [µg/mL]	AUC/1000	AUC/1000	AUC/1000	Mean AUC	SD
50	5705.01	5664.78	5693.92	**5687.90**	**20.77**
25	2837.72	2800.49	2829.76	**2822.65**	**19.60**
12.5	1392.24	1380.03	1378.19	**1383.48**	**7.63**
6.25	682.73	655.53	676.81	**671.69**	**14.30**
3.125	330.82	327.94	332.7	**330.48**	**2.39**
1.5625	157.79	161.19	159.63	**159.53**	**1.70**
0.78125	78.92	78.41	78.79	**78.70**	**0.26**
0.3906	38.97	38.15	38.67	**38.59**	**0.41**
0.1953	18.71	18.42	18.54	**18.55**	**0.14**
0.09765	9.01	8.91	8.99	**8.97**	**0.05**
0.04882	4.70	4.57	4.59	**4.62**	**0.07**
0.02441	2.64	2.54	2.56	**2.58**	**0.05**
0.0122	1.21	1.18	1.20	**1.19**	**0.01**

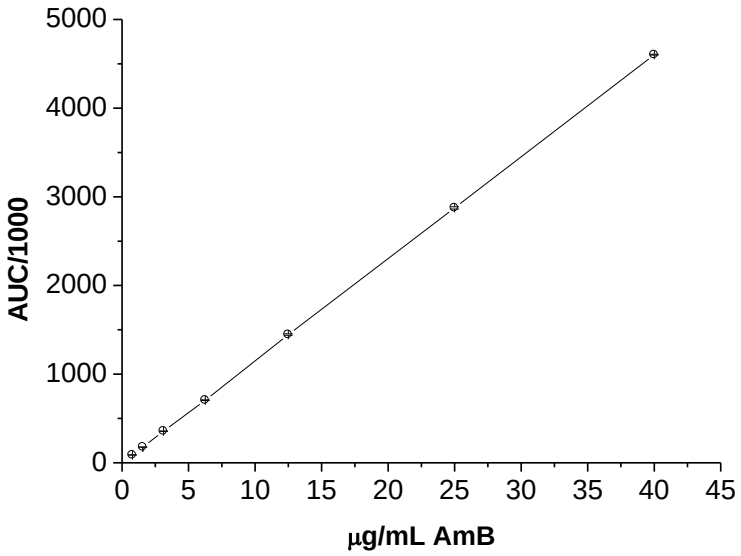

Figure 51. Calibration curve for high AmB concentrations in non-biological samples.

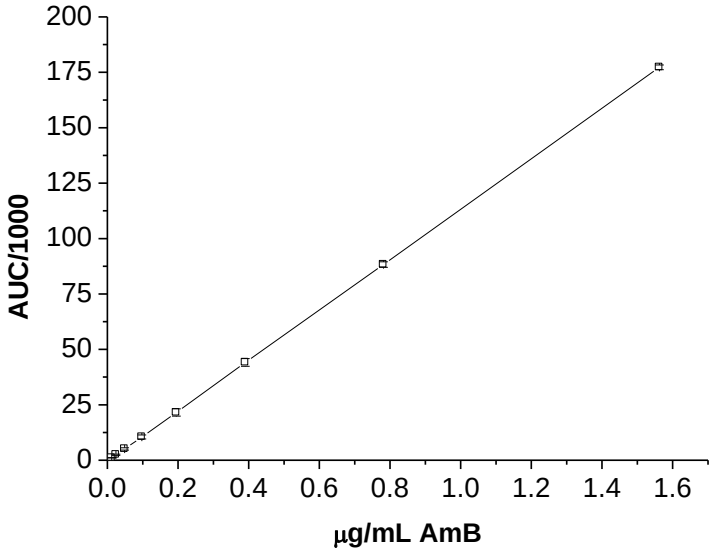

Figure 52. Calibration curve for low AmB concentrations in non-biological samples.

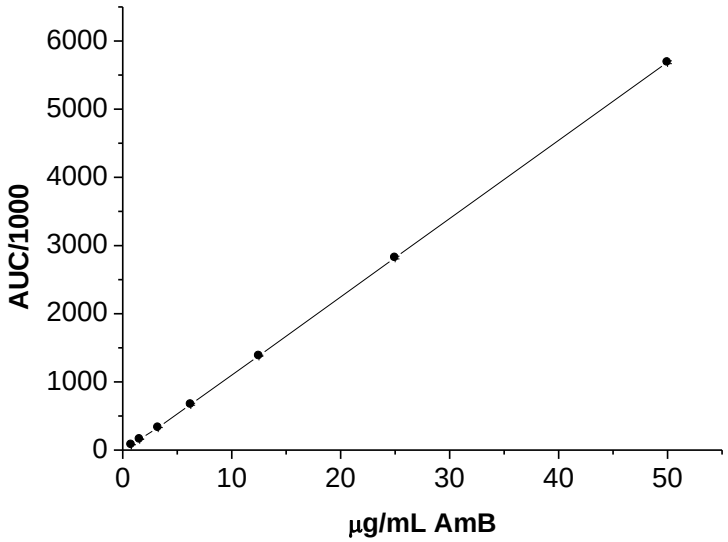

Figure 53. Calibration curve for high AmB concentrations in biological samples.

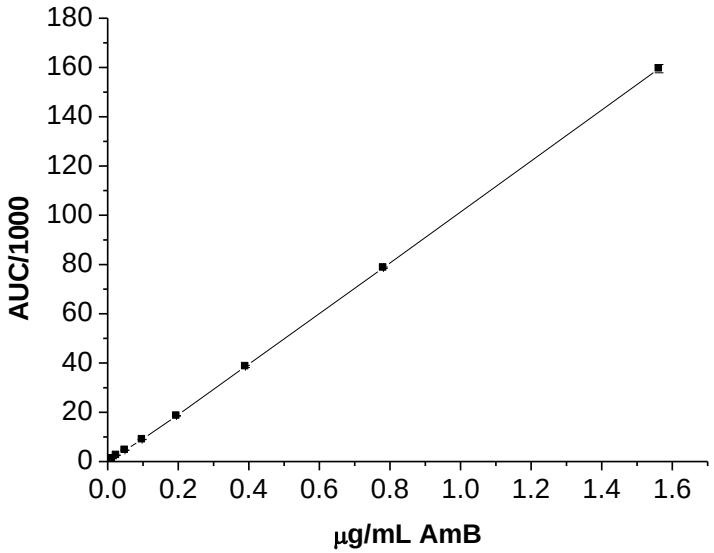

Figure 54. Calibration curve for low AmB concentrations in biological samples.

EXP2-2.3.2. Dimensional, morphological and surface characterization of AmB/PEG$_{5kDa}$-cholane formulations

Dynamic light scattering (DLS) and transmission electron microspcopy (TEM) analyses were performed to evaluate the dimensional, morphological and surface features of the AmB/PEG$_{5kDa}$-cholane formulations obtained by dissolution/pH change. The DLS profile reported in figure 55A showed that the AmB association with PEG$_{5kDa}$-cholane forms monodisperse size distribution micelles with mean diameter of 33.2±1.2 nm (PDI 0.16), which is in good agreement with the dimensional values obtained with AmB free PEG$_{5kDa}$-cholane formulations [369]. DLS analyses of AmB/PEG$_{5kDa}$-cholane formulation performed in the pH range of 3.5-11.0 yielded similar dimensional profiles while AmB/PEG$_{5kDa}$-OH mixtures did not show micelle formation at all pHs. The particle size of AmB loaded and unloaded PEG$_{5kDa}$-cholane micelles remained stable in all the pH range assayed (table 46).

The TEM image reported in figure 55B confirms the dimensional features obtained by DLS. The AmB/PEG$_{5kDa}$-cholane micelles have circular shape and gray shadow around the micelles due to the negative-staining of the PEG chain by phosphotungstic acid.

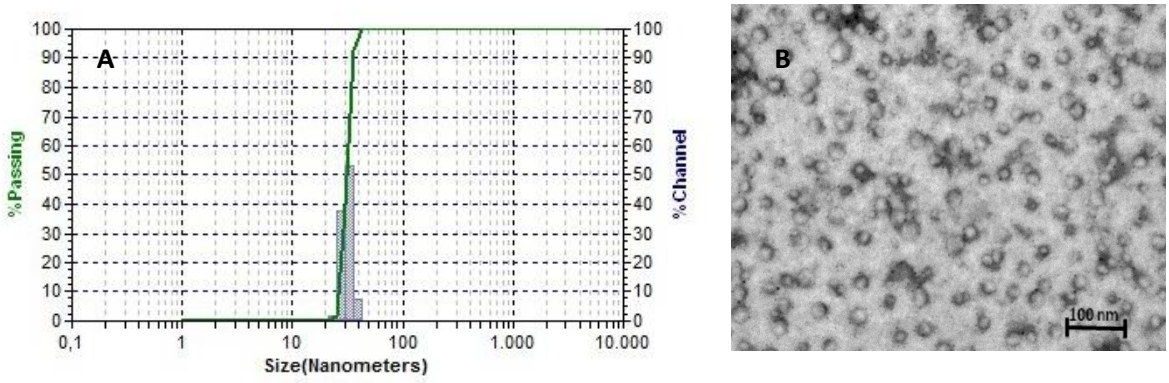

Figure 55. Dynamic light scattering profile (A) and transmission electron microscopy image (B) of AmB/PEG$_{5kDa}$-cholane formulations.

Table 46. Particle size of AmB loaded and unloaded PEG_{5kDa}-cholane micelles at different pHs.

pH	Particle size (nm)	
	AmB loaded PEG_{5kDa}-cholane micelles	**AmB unloaded PEG_{5kDa}-cholane micelles**
3.5	32.93±1.26	16.63±0.44
5.5	33.05±0.95	18.18±1.06
7.2	33.31±1.14	18.42±2.13
8.5	32.86±1.81	18.15±2.22
11	33.58±2.29	19.89±1.95

Figure 56A and table 47 show the zeta potential of the micelles at different pHs. At pH 5.5-7.2 the overall micelle surface was nearly neutral. At pH below 5.5 the zeta potential shifted to slightly positive values and above pH 7.2 to negative values. Similar zeta potential values were obtained with AmB free PEG_{5kDa}-cholane micelles (figure 56B, table 47).

Table 47. Zeta potential values of loaded and unloaded PEG_{5kDa}-cholane micelles at different pHs.

pH	**Loaded PEG_{5kDa}-cholane micelles**		**Unloaded PEG_{5kDa}-cholane micelles**	
	Zeta potential (mV)	**SD**	**Zeta potential (mV)**	**SD**
3.5	2.79	0.45	3.81	0.84
5.5	-0.07	0.09	0.54	0.43
7.4	-0.43	0.18	0.387	0.46
9.5	-7.23	0.29	-8.92	0.11
12	-13.26	1.11	-12.96	2.05

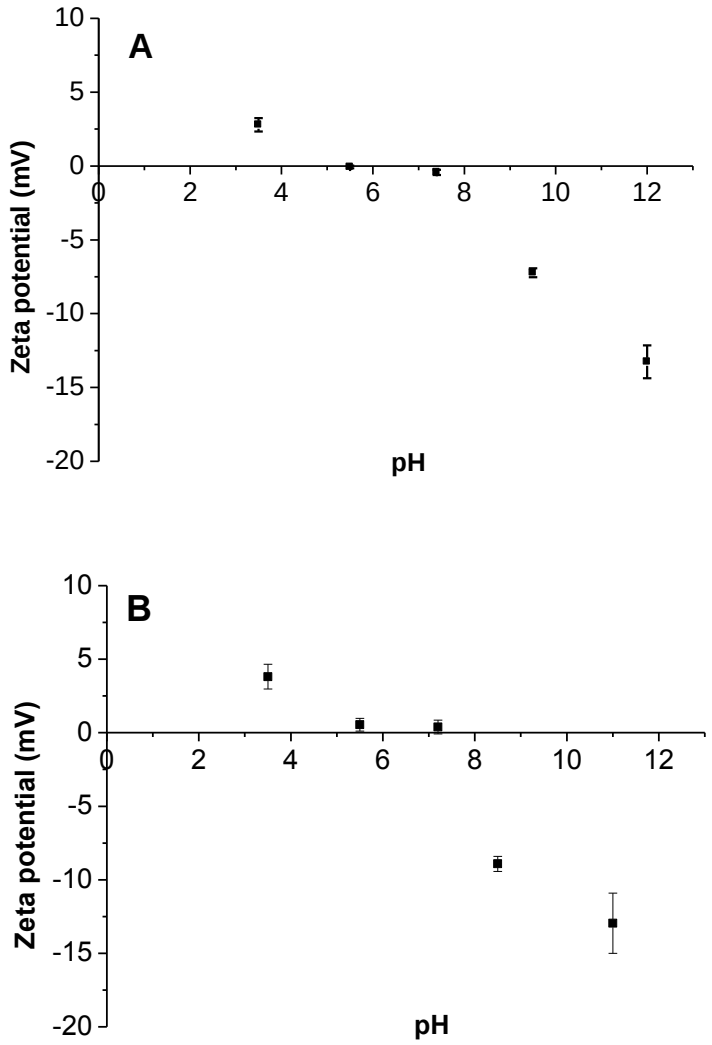

Figure 56. Zeta potential profiles of AmB loaded (A) and unloaded (B) PEG_{5kDa}-cholane micelles at different pHs.

EXP2-2.3.3. AmB/MeO-PEG_{5kDa}-cholane formulation lyophilisation and stability

The lyophilization of AmB/PEG_{5kDa}-cholane formulations obtained by dissolution/pH change produced yellowish, fluffy and slightly electrostatic powders (figure 57, insert A). The moisture content in the lyophilized product was 7%. The lyophilized powder rapidly re-dissolved in buffer at pH 7.2 to regenerate a clear yellow colloidal dispersion (figure 57, insert B).

After re-dispersion, at 25°C, the micelle size of the colloidal system was 32.2±3.4 nm and AmB was completely re-dissolved. Figure 31 shows that both micelle size and AmB concentration remained stable over 1 month. The chemical degradation during the first month was less than 5%. After 2 months storage neither the micelle size nor the size distribution changed while the AmB concentration decreased on an 8±0.3%. Similar results were obtained with freshly prepared micelles.

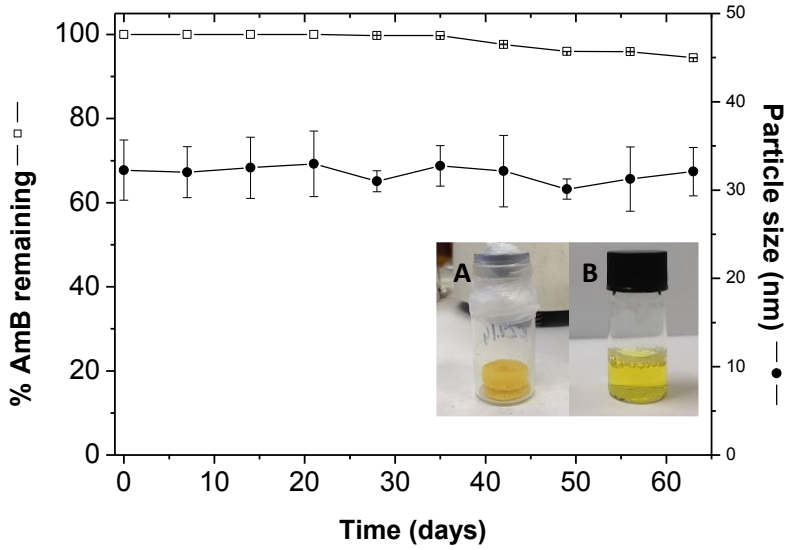

Figure 57. Micelle size (-●-) and residual AmB content (-□-) time course profiles of lyophilized AmB/PEG_{5kDa}-cholane formulation re-dispersed in buffer at pH 7.2. Insert **A** lyophilized formulation; insert **B** re-dispersed formulation.

EXP2-2.3.4. Isothermal titration calorimetry assays

Isothermal titration calorimetric (ITC) analyses were performed to investigate the AmB interaction with PEG_{5kDa}-cholane at different pHs: 3.5, 5.5, 7.2, 8.5 and 11.0. The ITC study was carried out by injecting volumes of polymer solutions into the cell containing the AmB solutions. The operative conditions were selected on the basis of the results obtained by the solubility studies. Blank runs were carried out by injecting polymer solutions into the cell containing AmB free buffer or by injecting buffer into the cell containing AmB solutions.

The buffer injection into AmB solutions did not elicit significant thermal effect. Instead, the injection of aliquots of polymer solutions into the cell containing buffer produced pH independent bimodal exothermic ITC profiles, which was due to the demicellisation and polymer dilution as reported elsewhere [336]. The thermal profiles reported in figure 58 show that the polymer interaction with AmB occurs according to a multimodal pH-dependent behavior. The calorimetric raw data subtracted of the values obtained with the corresponding blanks were found to fit a three sequential binding site fitting model, with good correlation (Chi^2). The association parameters derived from the analysis are summarized in table 48.

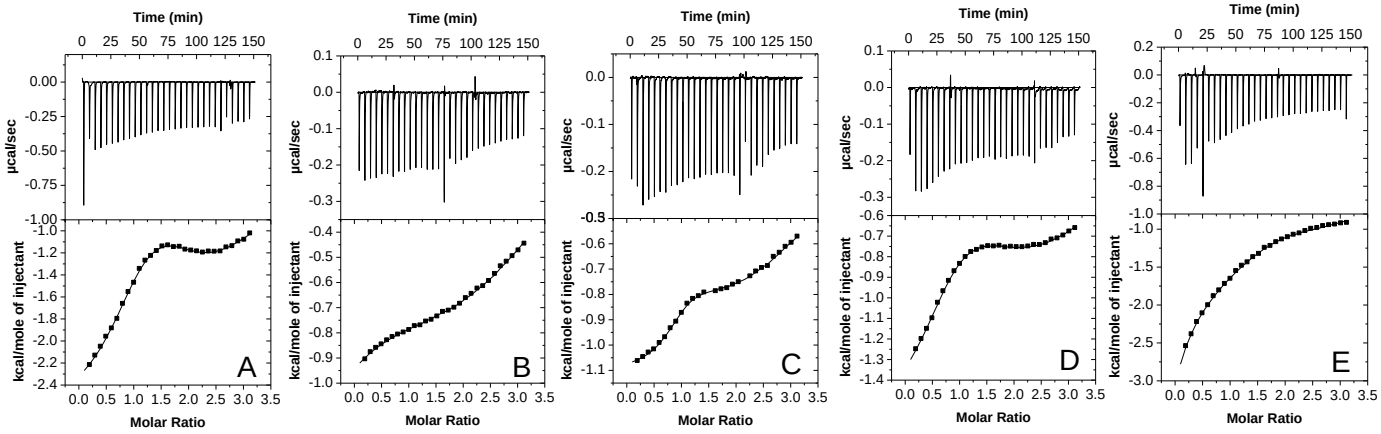

Figure 58. Isothermal calorimetry profiles of AmB titrated with PEG_{5kDa}-cholane at pH 3.5 (A), 5.5 (B), 7.2 (C), 8.5 (D) and 11.0 (E).

In all cases, the binding affinity constants (K) were found to decrease from the first to the third binding site and the drug/polymer interactions occurred according to strong exothermic contributions (ΔH). The first binding was found to occur with high enthalpic and entropic contribution (ΔH1 and ΔS1, respectively). The second binding occurred with the lowest enthalpic contribution (ΔH2) even though it was strongly favored by a positive entropic change (ΔS2). The third binding was characterized by the lowest affinity constant (K3) and entropic contribution (ΔS3) but the highest enthalpic contribution (ΔH3). To note that at pH 11.0, the third binding occurred with negative ΔS.

Table 48. Calorimetric parameters obtained by AmB titration with PEG_{5kDa}-cholane at pH 3.5, 5.5, 7.2, 8.5 and 11.0: affinity constant (K), differential enthalpy (ΔH) differential entropy (ΔS), Chi squared (Chi^2/DoF).

	pH				
	3.5	**5.5**	**7.2**	**8.5**	**11.0**
K1 10^5 M^{-1}	9.83±0.46	1.54±0.069	7.87±0.28	3.31±0.096	2.36±0.12
ΔH1	-2349±14.3	-1071±9.36	-1101±3.64	-1414±7.99	-3206±47.0
ΔS1	19.5	20.1	23.3	20.5	13.8
K2 10^5 M^{-1}	1.22±0.088	0.554±0.023	0.356±0.027	0.435±0.016	1.52±0.12
ΔH2	-485.4±24.5	-769.1±21.4	-964.5±29.3	-104.9±19.3	-125.5±56.4
ΔS2	21.6	19.1	17.6	20.9	23.3
K3 10^5 M^{-1}	0.149±0.009	0.531±0.022	0.234±0.012	0.246±0.008	0.062±0.004
ΔH3	-5251±134	-1061±23.8	-2053±50.8	-3127±27.2	-6924±277
ΔS3	1.49	18.1	13.1	9.60	-5.87
Chi^2/DoF	114.7	17.87	18.29	19.19	142.5

EXP2-2.3.5. Structural characterization

Comparative structural characterizations of AmB, PEG_{5kDa}-cholane, PEG_{5kDa}-OH, lyophilized AmB/PEG_{5kDa}-cholane micelles and physical AmB/PEG_{5kDa}-cholane mixture were performed by differential scanning calorimetry (DSC), X-Ray diffractometry(XRD), Fourier transformed infrared (FTIR), .

The DSC profiles (figure 61) showed the typical water loss, melting and decomposition behaviors of the various samples. Unformulated AmB (figure 59A) exhibited the characteristic endothermic peak of this drug at 104.6ºC corresponding to the water loss process [364] and the characteristic decomposition peak above 160ºC, namely at 188.6ºC [370]. PEG_{5kDa}-cholane (figure 59B) showed a sharp endothermic peak at 58.9ºC, corresponding to the polymer melting as observed by hot stage microscopy (60 °C), followed by an exothermic event at 171.3ºC, which corresponds to the polymer decomposition. Similarly to PEG_{5kDa}-cholane, PEG_{5kDa}-OH (figure 59C) melted at

64.1ºC and decomposed at 155.0°C. The thermal profile of the physical AmB/PEG_{5kDa}-cholane mixture (figure 59D) showed two endothermic peaks at 60.9ºC and 92.9ºC, and an exothermic peak at 178.5ºC, which were in fair agreement with AmB melting and PEG_{5kDa}-cholane melting and decomposition. The DSC profiles of AmB/PEG_{5kDa}-cholane micelles (figure 59E) showed only one endothermic peak at 172.5ºC, corresponding to the PEG_{5kDa}-cholane decomposition.

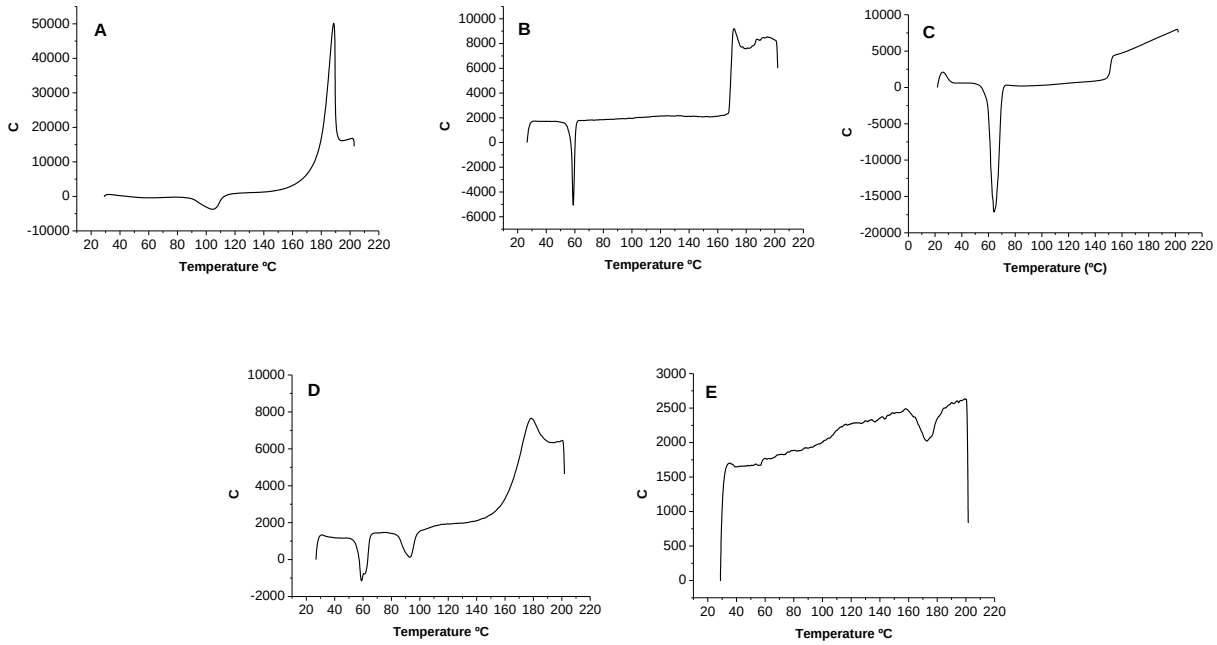

Figure 59. Differential scanning calorimetry profiles of AmB (A), PEG_{5kDa}-cholane (B), PEG_{5kDa}-OH (C), physical AmB/PEG_{5kDa}-cholane mixture (D) and lyophilized AmB/PEG_{5kDa}-cholane vesicles (E).

The X-Ray diffractometric (XRD) spectra (figure 60) showed the characteristic peaks of the crystalline form of unformulated AmB (figure 60A) at diffraction angles of 2θ 14.82º, 17.22º, 18.38º, and 21.66º [292,364,371]. PEG_{5kDa}-cholane (figure 60B) displayed broad peaks at 19.02º and 23.38º while the AmB/PEG_{5kDa}-cholane physical mixture (figure 60C) showed the peaks corresponding to both crystalline AmB and PEG_{5kDa}-cholane. The lyophilized AmB/PEG_{5kDa}-cholane micelle formulation (figure 60D) did not show the characteristic peaks of AmB and PEG_{5kDa}-cholane while exhibited two peaks at 22.11º and 26.14º.

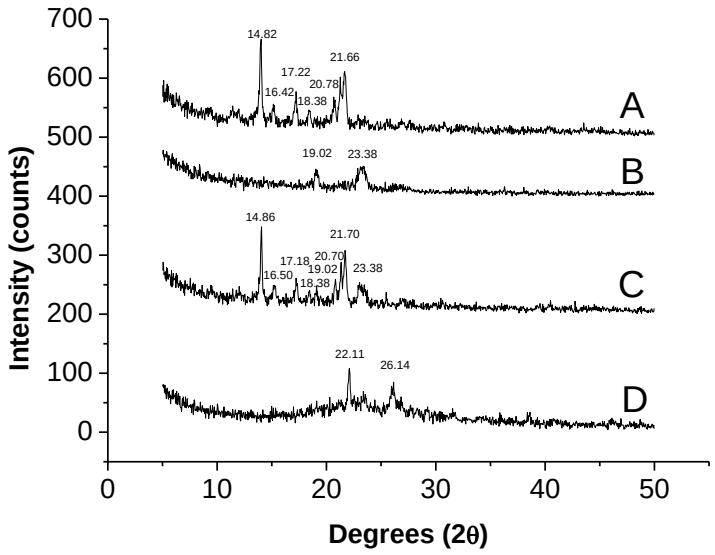

Figure 60**.** X-Ray diffractometric index patterns of AmB (A), PEG_{5kDa}-cholane (B), physical AmB/PEG_{5kDa}-cholane mixture (C) and lyophilized AmB/PEG_{5kDa}cholane micelles (D).

The Fourier transformed infrared (FTIR) spectra (figure 61) provided additional information about the physical AmB/PEG_{5kDa}-cholane interaction in the micelle lyophilized product. The unformulated AmB spectrum showed the typical signals reported in the literature [292,364,371]. The spectrum of the physical AmB/PEG_{5kDa}-cholane mixture showed the signals corresponding to both AmB, i.e. at 1039 cm^{-1},[ν(C-O-C)] pyranose, and PEG_{5kDa}cholane, i.e. at 1465 cm^{-1}[δ(CH2)], 1359 cm^{-1}[δ(CH)], 840.43 cm-1 [δ(C-H)] cyclic. The lyophilized AmB/PEG_{5kDa}-cholane micelles displayed the same signals of the other samples. However, below 1700 cm^{-1} the main peaks characteristic of AmB [i.e. 1689.37 cm^{-1}, ν(C=O); 1552.55 cm^{-1}, δ(N-H); 1006.68 cm^{-1}, δ(=C-H)] [373, 374] and PEG_{5kDa}-cholane [i.e. at 1465cm^{-1}, δ(CH_2); 1342 cm^{-1}, δ(C-O); 1097 cm^{-1}, ν(C-N); 960 cm^{-1}, δ(C-H)] were missing.

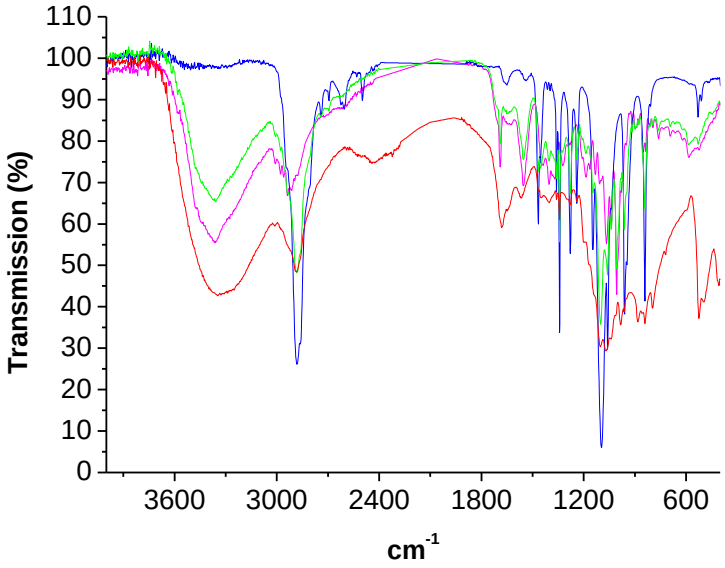

Figure 61. Fourier transformed infrared profiles of: unformulated AmB (---); PEG_{5kDa}-cholane (---); Physical mixture (---) and Freeze dried product (---).

Tables 49-52 summarize the main signals (cm^{-1}) of unformulated AmB, PEG_{5kDa}-cholane, physical AmB/PEG_{5kDa}-cholane mixture and lyophilized AmB/PEG_{5kDa}-cholane micelles, respectively. The "ν" refers to the stretching vibrations and the "δ" to the bending vibrations

Table 49. Main FTIR signals of unformulated AmB.

Signal (cm^{-1})	**% Transmission**	**Functional Group**
3359.44	55.44	[ν(N-H, O-H)]
2939.03	66.82	[ν(CH_2, CH_3)]
2877.32	71.66	[ν(CH_2, CH_3)]
1689.37	73.72	[ν(C=O)]
1552.44	69.30	[δ(N-H)]
1403.95	69.56	[δ(C-H)]
1384.66	71.78	[δ(CH_3)]
1322.95	74.04	[δ(C-O)]
1164.81	73.16	[ν(C-O-C)]
1066.46	55.16	[ν(C-O)alcohol]
1039.46	59.88	[ν(C-O-C)pyranose]
1006.68	42.98	[δ(=C-H)]

Table 50. Main FTIR signals of PEG_{5kDa}-cholane.

Signal (cm^{-1})	**% Transmission**	**Functional Group**
2881.18	26.13	[ν(CH_2, CH_3)] alquil
1650.80	93.52	[ν(C=O)amide]
1540.87	94.56	[δ(N-H)]
1465.66	59.98	[δ(CH_2)]
1359.59	67.69	[δ(CH)]
1342.24	33.76	[δ(C-O)]
1241.95	64.99	[ν(C-N)amide]
1147.46	53.81	[ν(C-O-C)]
1097.32	6.06	[ν(C-N) amine]
1060.67	29.76	[ν(C-O)ether]
840.83	41.40	[δ(C-H)cyclic]

Table 51. Main FTIR signals of AmB/PEG_{5kDa}-cholane physical mixture.

Signal (cm^{-1})	% Transmission	Molecule	Functional Group
3359.44	65.33	AmB	[ν(N-H, O-H)]
2881.18	48.81	PEG_{5kDa}cholane	[ν(CH_2, CH_3)] alquil
1689.37	79.29	AmB	[ν(C=O)]
1650.80	86.56	PEG_{5kDa}cholane	[ν(C=O)amide]
1556.30	75.58	PEG_{5kDa}cholane/AmB	[δ(N-H)]
1465.66	72.73	PEG_{5kDa}cholane	[δ(CH_2)]
1403	75.14	AmB	[δ(C-H)]
1359.59	70.89	PEG_{5kDa}cholane	[δ(CH)]
1342.24	55.65	PEG_{5kDa}cholane	[δ(C-O)]
1241.95	75.57	PEG_{5kDa}cholane	[ν(C-N)amide]
1170.60	78.69	AmB	[ν(C-O-C)]
1147.46	67.43	PEG_{5kDa}cholane	[ν(C-O-C)]
1097.32	37.21	PEG_{5kDa}cholane	[ν(C-N) amine]
1060.67	47.69	PEG_{5kDa}cholane	[ν(C-O)ether]
1039.46	58.70	AmB	[ν(C-O-C)pyranose]
1006.68	49.54	AmB	[δ(=C-H)]
840.43	63.92	PEG_{5kDa}cholane	[δ(C-H)cyclic]

Table 52. Main FTIR signals of the lyophilized AmB/PEG_{5kDa}-cholane micelles.

Signal (cm^{-1})	% Transmission	Molecule	Functional Group
3347.87	42.67	AmB	[ν(N-H, O-H)]
2881.18	48.52	PEG_{5kDa}cholane	[ν(CH_2, CH_3)] alquil
1241.95	65.43	PEG_{5kDa}cholane	[ν(C-N)amide]
1103.10	30.34	PEG_{5kDa}cholane	[ν(C-N) amine]
1070.32	29.31	AmB	[ν(C-O)alcohol]
1039.46	32.16	AmB	[ν(C-O-C)pyranose]
998.96	41.09	AmB	[δ(=C-H)]
865.90	38.97	PEG_{5kDa}cholane	[δ(C-H)cyclic]

EXP2-2.3.6. Synchrotron

Synchrotron analysis are not yet completed. Preliminary results show that the AmB/PEG_{5kDa}-cholane presents an ordered structure.

EXP2-2.3.7. Human Serum Albumin circular dichroism analyses

Circular dichroism studies were carried out to investigate the interaction of AmB with plasma proteins, which can either alter the protein structure or induce drug disaggregation [358,151]. The study was comparatively performed by using AmB, Fungizone®, heated Fungizone® and AmB/PEG_{5kDa}-cholane.

Table 53 reports the secondary protein structure obtained by the KD2 elaboration of the far UV CD spectra shown in figure 62A. The results reported in the table show that the secondary protein structure was not significantly altered by AmB regardless the formulation.

Table 53. Secondary structure (α-helix and β-sheet content) of human serum albumin (HSA) and HSA incubated with AmB, Fungizone®, Heated Fungizone® and AmB/MeO-PEG_{5kDa}-cholane

	α-helix	**β-sheet**
HSA	0.67	0.04
AmB	0.63	0.06
Fungizone®	0.63	0.06
Heated Fungizone®	0.64	0.05
AmB/MeO-PEG_{5kDa}cholane	0.69	0.04

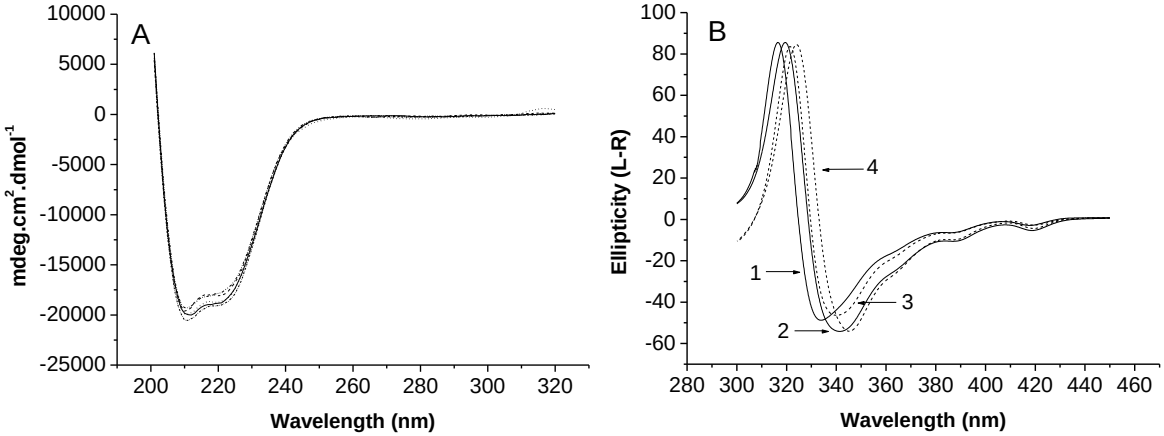

Figure 62. Circular dichroism spectra. **A**. Far UV spectra of HSA incubated with AmB (—), Fungizone® (···); heated Fungizone® (- -) and AmB/PEG_{5kDa}-cholane micelles (·-·) **B**. Near UV spectra of AmB/PEG_{5kDa}-cholane micelles in the absence of HSA (1); AmB/PEG_{5kDa}-cholane micelles in the presence of HSA (3); Fungizone® in the absence of HSA (2); Fungizone® in the presence of HSA (4).

Figure 62B reports the near UV CD spectra of AmB/PEG_{5kDa}-cholane micelles and Fungizone® showing the typical doublet (intense biphasic dichroic signals) of AmB in the absence or in the presence of HSA. The wavelengths of maximum (λ_{max}) and minimum (λ_{min}) ellipticity and the maximum-minimum ellipticity amplitude intensity (Ai) represent the AmB aggregation: the lower λ_{max} and λ_{min}, the higher the AmB aggregation; the higher Ai, the higher AmB aggregation [151].

In the comparative study (figure 63), AmB in solution presented the highest λ_{max} and λ_{min}, and the lowest Ai either in the absence or in the presence of HSA (λ_{max}327nm, λ_{min}353nm and Ai 83.8 θ in the absence of HSA; λ_{max} 326 nm, λ_{min} 351 nm and Ai 44.4 θ in the presence of HSA). In the absence of HSA the λ_{max}, λ_{min} and Ai of AmB/PEG_{5kDa}-cholane were 316.5 nm, 333.8 nm and 134.3 θ respectively, while in the presence of HSA λ_{max}, λ_{min} and Ai were 321.4 nm, 340.2 nm and 129.9 θ, respectively. In the absence of HSA, Fungizone® showed 319.5 nm λ_{max}, 341.3 nm λ_{min} and 139.71 θ Ai while in the presence of HSA λmax, λmin and Ai were 324 nm 345.3 nm 138.66 θ. Heated Fungizone® showed the lowest λ_{max} and λ_{min} and the highest Ai (λ_{max} 313 nm, λ_{min} 330 nm and Ai 175.7 θ in the absence of HSA; λ_{max} 314nm, λ_{min} 332 nm and Ai 184.59 θ in the presence of HSA). Accordingly, the spectra obtained with Fungizone®

and AmB/PEG_{5kDa}-cholane micelles showed a higher presence of aggregated AmB [151] either in the absence or in the presence of HSA compared to unformulated AmB. In both cases, the λ_{max} and λ_{min} of the doublet of Fungizone® was 3-8 nm higher compared to the ones obtained with AmB/PEG_{5kDa}-cholane micelles indicating that AmB in Fungizone® was less aggregated than in the PEG_{5kDa}-cholane micelles. The addition of HSA was found to red-shift of 4-7 nm the doublet of AmB formulated with PEG_{5kDa}-cholane and Fungizone® indicating that in both cases HSA promotes the AmB disaggregation [375-377].

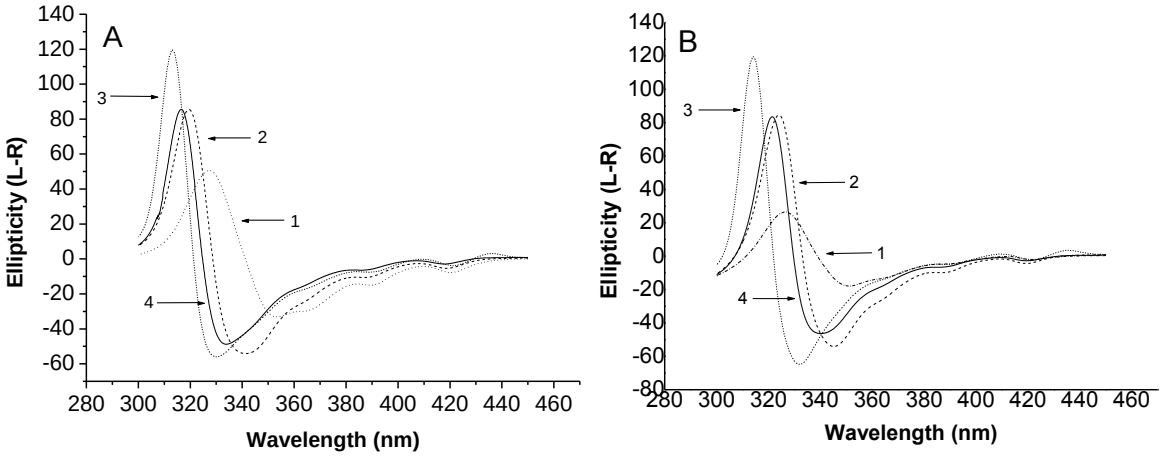

Figure 63. Circular dichroism profiles in the absence (A) and presence (B) of HSA of: AMB (1); Fungizone® (2); Heated Fungizone® (3) and AmB/PEG_{5kDa}-cholane micelles (4) at 37ºC.

EXP2-2.3.8. Absorption and kinetics studies

UV-Vis absorption spectroscopic studies were performed in the range 300-450 nm to determine the time course profile of AmB disaggregation in presence of HSA. The studies were comparatively performed with AmB, Fungizone®, heated Fungizone® and AmB/PEG_{5kDa}-cholane micelles at 25°C and 37°C and the AmB disaggregation was determined by Gaussian fit of peak IV. The increase of the absorption area of peak IV (λ 413 nm), which represents the monomeric state of AmB, indicates the drug disaggregation.

The time course profiles reported in figure 38 show that at 37°C the unformulated AmB undergoes significant disaggregation. Fungizone® disaggregation was found to occur at less extent than free AmB while heated Fungizone® was pretty stable as its disaggregation was very low. The extent of AmB disaggregation from the AmB/PEG_{5kDa}-cholane micelles was found to be in between Fungizone® and heated Fungizone®. After 45 min, the peak IV area was 2.1 and 1.7 for Fungizone® and AmB/PEG_{5kDa}-cholane, respectively.

The curves reported in figure 64 were found to fit a first order kinetic and were elaborated to get information on AmB dissociation rate. At 37°C, the disaggregation half-life time ($t_{1/2}$) was 194, 335, 463 and 618 s for unformulated AmB, Fungizone®, heated Fungizone® and AmB/PEG_{5kDa}-cholane micelles, respectively. The $t_{1/2}$ values calculated from disaggregation profiles obtained at 25ºC (figure 65) were 397, 507, 573 and 997 s for AmB in solution, Fungizone®, heated Fungizone® and AmB/PEG_{5kDa}-cholane micelles, respectively.

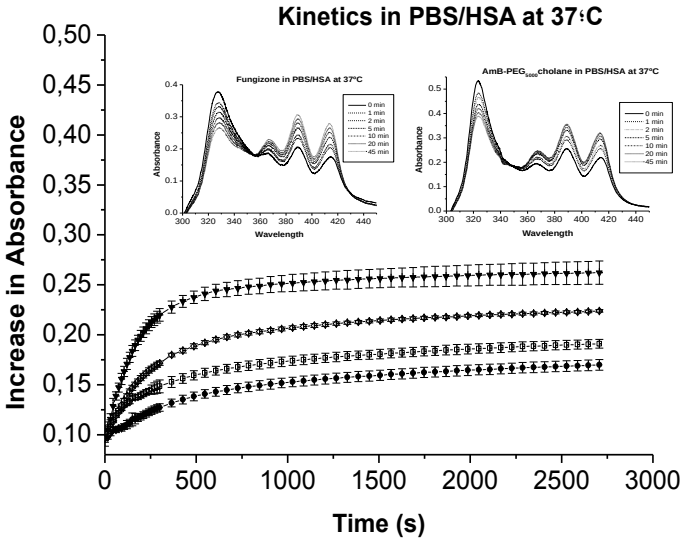

Figure 64. Disaggregation profiles at 37°C of AmB (-▼-), Fungizone® (-◊-), heated Fungizone® (-●-) and AmB/PEG_{5kDa}-cholane micelles (-□-) incubated with HSA.

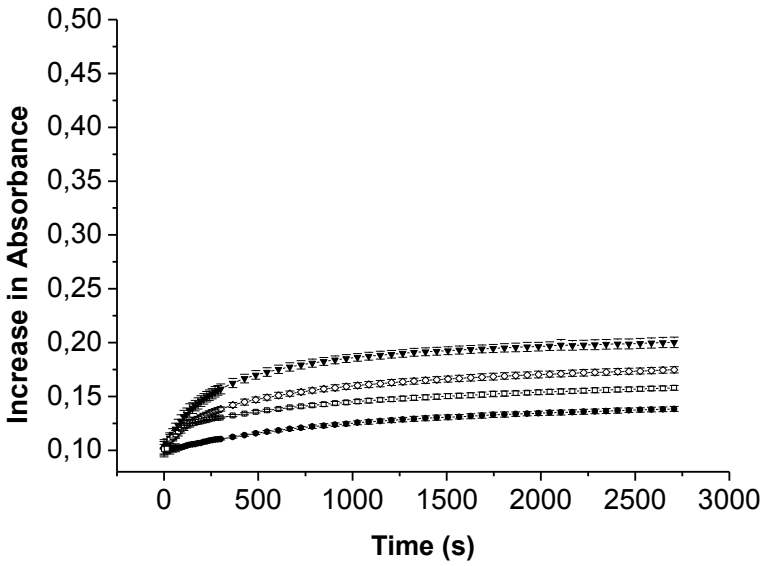

Figure 65. Disaggregation profiles at 25°C of AmB (-▼-), Fungizone® (-◊-), heated Fungizone® (-●-) and AmB/PEG_{5kDa}-cholanemicelles (-□-) incubated with HSA.

EXP2-2.3.9. Dialysis studies

The AmB release from the PEG_{5kDa}-cholane micelles was studied using dialysis. Figure 66 shows a biphasic profile where 70% AmB was released within 10 hours and 90% in 96 h.

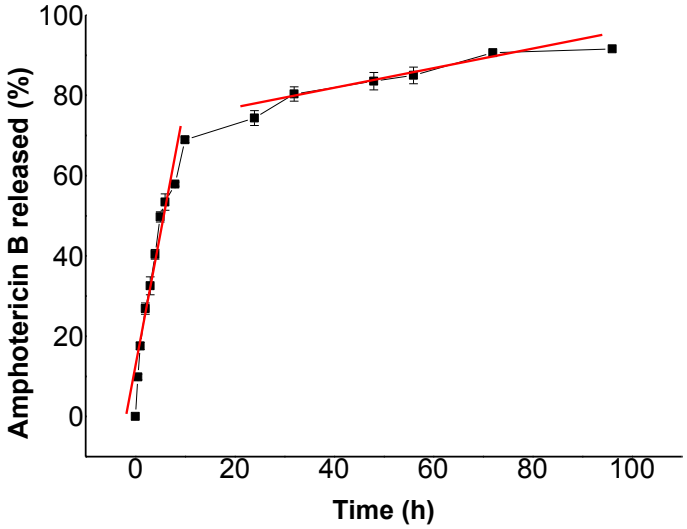

Figure 66. Percentage of AmB released from the PEG_{5kDa}-cholane micelle core over time.

In order to understand which mechanism (diffusion, erosion, relaxation of the polymer chains, etc.) governs the release of the AmB from the core of the PEG_{5kDa}-cholane micelles, the data obtained from the dialysis experiment was elaborated to find the best fit according to different mathematical methods (table 54).

Table 54. Results obtained with the different mathematical methods

Model	**AmB/PEG_{5kDa}cholane 0-10 h**		**AmB/PEG_{5kDa}cholane 24-96 h**	
	R^2	K	R^2	K
Zero order	0.887	1.344	0.867	0.002
First order	0.749	0.156	0.847	0.002
Hixon-Crowel	0.930	0.071	0.917	0.007
Higuchi	**0.988**	4.772	**0.923**	0.942
Baker-Lonsdale	0.598	0.033	0.767	0.001
Korsmeyer-Peppas (n=0.58)	**0.988**	0.156	**0.923**	0.038

As shown in table 54, the two steps of release were determined by diffusion. The differences found in the rate and in the K constant indicate that the structural conditions are different in the two moments of release.

EXP2-2.4. Stability studies

ICH Stability studies

This study is being currently on going and therefore no complete results are already generated. The results from the 2 months stability have been summarized in section EXP2-2.3.3.

Gastric mimicking fluid stability studies

AmB/PEG_{5kDa}-cholane micelles oral stability was studied as described in pharmacopoeia using simulated gastric mimicking fluid at pH 1.2 (see materials section EXP2-1.2.4). The aim of the study was to evaluate the integrity of the new formulation at low pH in the presence of pepsin during 4 hours. The assay was performed in triplicate.

The residence time of the drug in the stomach varies depending on many different factors but in general the mean residence time is around 1.5-2 h. As reported in table 55, after 90 minutes at pH 1.2, there was still a 51.75 ± 0.96% of intact AmB available to be absorbed. Figure 67 shows the behavior of the AmB included in PEG_{5kDa}-cholane micelles during all the assayed period.

As reported in table 56, the stability data in GMF was elaborated to find the best fit according to different mathematical models (zero, first and second order, Higuchi, Korsmeyer-Peppas, Baker Lonsdale and Hixon-Crowel). The AmB/PEG_{5kDa}-cholane micelles degradation kinetics was found to best fit to Higuchi and Korsmeyer-Peppas models with an r^2 of 0.996 and 0.994, respectively. The "n" value (n=0.392) in the Korsmeyer-Peppas fitting was calculated by plotting the log t versus log M_t/M_0 for those values with less than a 60% AmB degradation.

Table 55. AmB/PEG_{5kDa}-cholane micelles degradation in GMF at 37 ºC

Time (h)	Concentration [µg/mL]			Mean [µg/mL]	Mean % AmB	SD
	1	2	3			
0	31.483	30.173	33.048	31.568	100	0
0.5	32.849	33.740	35.487	34.025	67.83	1.37
1	29.762	30.096	29.655	29.838	60.27	0.46
1.5	25.598	26.106	25.150	25.618	51.75	0.96
2	22.516	22.029	21.408	21.984	44.41	1.11
2.5	18.517	18.473	17.900	18.297	36.96	0.69
3	16.117	15.943	15.457	15.839	31.99	0.69
3.5	14.013	13.674	13.658	13.782	27.81	0.42
4	11.798	11.250	11.710	11.586	23.40	0.59

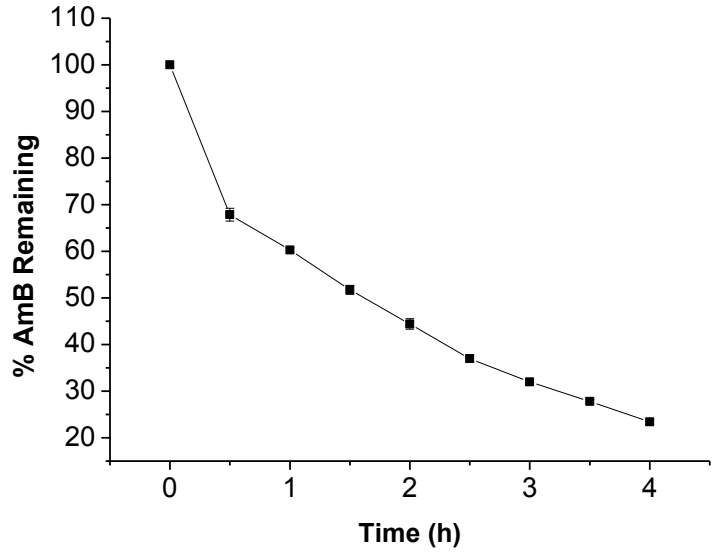

Figure 67. AmB/PEG_{5kDa}-cholane micelles stability in GMF at 37 ºC during 4 hours.

Table 56. AmB/PEG_{5kDa}-cholane micelles degradation kinetics adjusted to different mathematical models

Model	A-value	B-value	Correlation coeficient (r^2)
Zero order	17.43	16.59	0.888
First order	0.499	0.105	0.943
Second order	82.39	16.75	0.880
Higuchi	2.104	37.86	**0.996**
Korsmeyer-Peppas	0.019	0.447	**0.994**
Baker-Lonsdale	1.743	0.08	0.504
Hixon-Crowel	0.237	0.396	0.962

EXP2-2.5. *In vitro* toxicity studies

EXP2-2.5.1. Hemolysis

Prior to *in vivo* administration of AmB/PEG_{5kDa}-cholane micelles, the hemolytic effect of this new formulation was studied and referred to Fungizone®. It was referred to Fungizone® due to the structural similarities of both colloidal systems.

The results for the hemolysis study performed with AmB/DMSO, Fungizone®, AmB/PEG_{5kDa}-cholane micelles, AmB/PEG_{5kDa}-stearic, and AmB/PEG_{5kDa}-arachidonic are detailed on table 57 and figure 68.

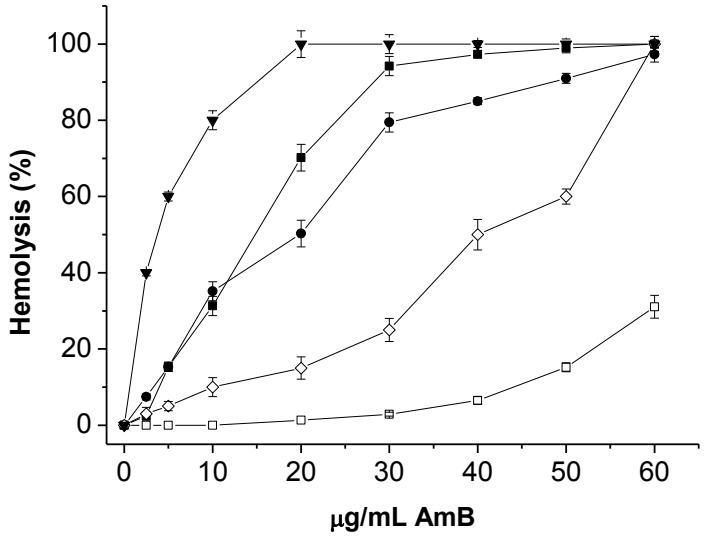

Figure 68. Hemolytic effect of AmB in DMSO (-▼-), Fungizone® (-◊-), AmB/ PEG_{5kDa}-arachidonic (-●-), AmB/ PEG_{5kDa}-stearic (-■-) and AmB/PEG_{5kDa}-cholane micelles (-□-) at different concentrations.

Table 57. Hemolytic effect of AmB included in different formulations at increasing concentrations.

AmB [μg/mL]	**% Hemolysis**				
	AmB in DMSO	**Fungizone®**	**AmB/PEG_{5kDa}-cholane**	**AmB/PEG_{5kDa}-stearic**	**AmB/PEG_{5kDa}-arachidonic**
0	0±0	0±0	0±0	0±0	0±0
2.5	40±0.8	3±1.7	0±0	2.46±0.8	7.45±1.1
5	60±1.2	5±1.2	0±0	15.3±1.2	15.3±1.2
10	80±2.5	10±2.5	0±0	31.28±2.5	35.17±2.7
20	100±3.5	15±2.9	1.3±0	70.2±3.5	50.3±3.3
30	100±2.5	25±3	2.87±0.5	94.22±2.5	79.44±2.1
40	100±0.9	50±4	6.50±1	97.3±0.9	85.03±1.0
50	100±1.3	60±2	15.2±1.2	99±1.3	91.09±1.6
60	100±2	100±1	31.07±3	100±2	97.29±2.3

The hemolytic effect was, as expected, concentration-dependent. Higher amounts of AmB caused higher hemolysis. At low AmB concentration (2.5 μg/mL) the AmB

dissolved in DMSO showed a 40% hemolysis while Fungizone® and AmB/PEG_{5kDa}-cholane micelles had barely hemolytic effect. At 10 µg/mL, AmB in DMSO produced an 80% hemolysis, Fungizone® a 10% and AmB/PEG_{5kDa}-cholane did not showed any hemolytic effect. At 40 µg/mL, AmB in DMSO caused 100% hemolysis, Fungizone® close to 50% and AmB/PEG_{5kDa}-cholane just an 8%. Finally, at 60 µg/mL both AmB in DMSO and Fungizone® produced 100% hemolysis while AmB/PEG_{5kDa}-cholane caused just 30% hemolysis.

The results from the hemolysis studies allowed for the *in vivo* administration of the AmB/PEG_{5kDa}-cholane micelles. This formulation was found to be less hemolytic than the already commercialized Fungizone®.

EXP2-2.6. *In vitro* efficacy studies

In vitro antifungal studies of AmB and AmB/PEG_{5kDa}-cholane micelles were performed against *C. albicans* [378]. The diameters of the inhibition halos were, for both formulations, higher than 15 mm (18.47±0.185 for AmB and 20.48±0.238 mm for AmB/PEG_{5kDa}-cholane micelles), indicating that they are active against *Candida albicans* [379-380]. The results reported in figure 69 show that AmB/PEG_{5kDa}-cholane micelles were 15% less active than the standard solution of AmB and 15% more active than AmB in buffer.

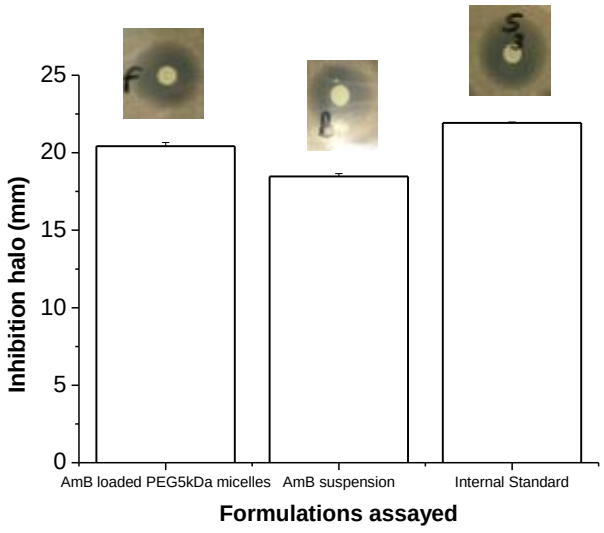

Figure 69. *C. albicans* inhibition in the presence of AmB/PEG_{5kDa}-cholane, AmB in buffer (suspension) and AmB in DMSO ($p<0.01$).

EXP2-2.7. *In vivo* studies

EXP2-2.7.1. Internal standard

Naproxen, widely used as internal standard, was prepared at different concentrations ranging from 3 ng/mL to 50 mg/mL and analyzed by RP-HPLC. Table 58 shows the results for the three calibration curves performed at 406 nm with this compound. The naproxen retention time was found to be 4.5 min and the peak was well resolved from the AmB peak.

As shown in Figure 70 the calibration curve was not linear in the assayed range ($y=5.601-0.618x$, $r^2=0.822$). The non-linearity was found to be related to the wavelength used in the analysis. Although at 406 nm naproxen was detected, when performing the same analysis at other wavelengths (300, 270 and 200 nm) the integration of the peaks eluted at 4.5 min was higher than that obtained at 406 nm with the same concentration.

Table 58. Concentration and area under the curve (AUC) of the different naproxen standards

Naproxen [mg/mL]	**AUC/1000**			**Mean AUC/1000**
	1	**2**	**3**	
50	32.141	32.009	32.208	32.12
25	24.89	25.02	25.63	25.18
12.5	18.442	18.26	18.54	18.41
6.25	14.784	15.18	14.92	14.96
3.125	12.432	12.64	12.59	12.55
1.5625	9.696	9.38	9.47	9.52
0.78125	6.237	6.99	6.71	6.65
0.3906	4.013	4.45	4.392	4.29
0.1953	2.429	2.54	2.46	2.48
0.09765	1.526	1.44	1.539	1.50
0.04882	0.932	0.904	0.924	0.92
0.02441	0.476	0.425	0.461	0.45
0.0122	0.357	No detection	No detection	x
0.0061	No detection	No detection	No detection	x
0.00305	No detection	No detection	No detection	x

.

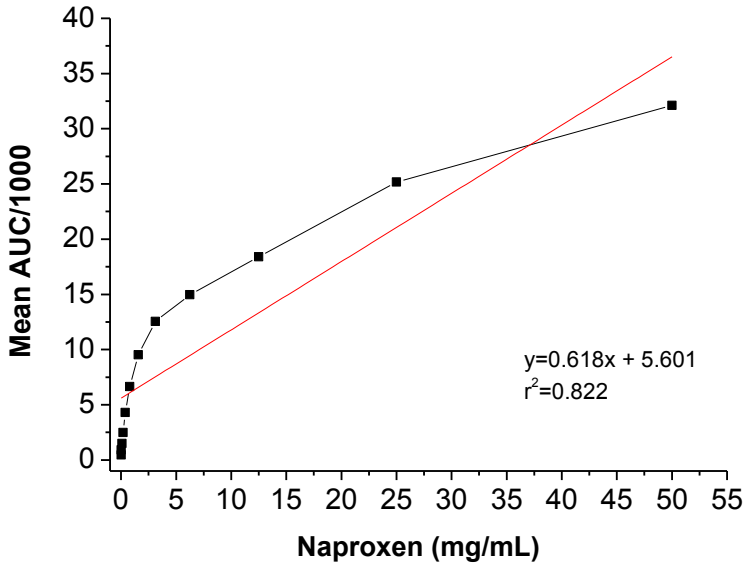

Figure 70. Calibration curve of naproxen at 406 nm.

As naproxen was discarded as internal standard, the recovery studies were then performed in order to have an indicator of drug loss during biological sample preparation.

EXP2-2.7.2. AmB recovery studies in plasma

AmB recovery studies from plasma were performed in order to calculate the AmB loss during sample preparation. AmB in DMSO and in dextrose (5% w/v), Fungizone®, Ambisome® and AmB/PEG_{5kDa}-cholane micelles were prepared and added of blood. Plasma samples were obtained as reported in methods (EXP2-1.2.7.2) and analyzed by RP-HPLC.

Tables 59-63 show the recovery values obtained for the different AmB formulations assayed orally and/or intravenously.

Table 59. AmB recovery in plasma from AmB/DMSO.

AmB [µg/mL]	Theoretical AmB [µg/mL]	Recovered in Blood AmB [µg/mL]	Recovered in Plasma AmB [µg/mL]
1	0.04761	0.2088	0.1148
2	0.09523	0.2982	0.1640
4	0.18957	0.3472	0.1909
6	0.28571	0.5388	0.2963
8	0.3809	0.6978	0.3837
10	0.47612	0.8221	0.4521

Table 60. AmB recovery in plasma from AmB/Dextrose (5% w/v).

AmB [µg/mL]	Theoretical AmB [µg/mL]	Recovered in Blood AmB [µg/mL]	Recovered in Plasma AmB [µg/mL]
1	0.04761	0.1834	0.1008
2	0.09523	0.2672	0.1469
4	0.18957	0.3781	0.2079
6	0.28571	0.4925	0.2708
8	0.3809	0.6732	0.3701
10	0.47612	0.8104	0.4457

Table 61. AmB recovery in plasma from Ambisome®.

AmB [µg/mL]	Theoretical AmB [µg/mL]	Recovered in Blood AmB [µg/mL]	Recovered in Plasma AmB [µg/mL]
1	0.04761	0.1337	0.0735
2	0.09523	0.2220	0.1221
4	0.18957	0.3111	0.1711
6	0.28571	0.4315	0.2373
8	0.3809	0.5380	0.2958
10	0.47612	0.8081	0.4444

Table 62. AmB recovery in plasma from Fungizone®.

AmB [µg/mL]	Theoretical AmB [µg/mL]	Recovered in Blood AmB [µg/mL]	Recovered in Plasma AmB [µg/mL]
1	0.04761	0.1509	0.0829
2	0.09523	0.2324	0.1278
4	0.18957	0.3701	0.2035
6	0.28571	0.4397	0.2418
8	0.3809	0.6433	0.3538
10	0.47612	0.7798	0.4288

Table 63. AmB recovery in plasma from AmB/PEG_{5kDa}-cholane micelles.

AmB [µg/mL]	Theoretical AmB [µg/mL]	Recovered in Blood AmB [µg/mL]	Recovered in Plasma AmB [µg/mL]
1	0.04761	0.1615	0.0882
2	0.09523	0.2895	0.1592
4	0.18957	0.4818	0.2649
6	0.28571	0.5093	0.2801
8	0.3809	0.6756	0.3715
10	0.47612	0.8229	0.4525

The % of AmB recovered in plasma from the different formulations was calculated by plotting the initial theoretical AmB concentration versus the AmB recovered in plasma. The slope of the curves, expressed as percentage, was assumed as the recovery value for each individual formulation.

Table 64 shows the regression curves and the percentages of recovery for all formulations assayed. The results showed that there were no significant differences between the recovery values obtained with the different AmB formulations. Therefore, a 79% (0.79) recovery was used for the determination of AmB concentration in biological samples regardless the formulation.

Table 64. Percentage of AmB recovered in plasma for each formulation.

Formulation	Equation	% Recovery
AmB in DMSO	$y=0.793x+0.071$, $r^2=0.984$	79.3%
AmB in dextrose (5% w/v)	$y=0.7932x+0.061$, $r^2=0.994$	79.32%
Fungizone®	$y=0.789x+0.045$, $r^2=0.987$	78.9%
Ambisome®	$y=0.79x+0.029$, $r^2=0.961$	79%
AmB/PEG_{5kDa}-cholane	$y=0.79x+0.075$, $r^2=0.969$	79%

EXP2-2.7.3. Oral pharmacokinetic studies

Study design

As described in methods, the oral pharmacokinetic studies of the different AmB formulations were performed on two non-consecutive days. On day 1, AmB/Dextrose and AmBisome® were tested and on day 2 Fungizone® and AmB/ PEG_{5kDa}-cholane were assayed.

Mice behavior

Independently of the formulation administered the mice behavior was almost exactly the same. For all the orally administered formulations the mice felt discomfort due to the insertion of a syringe directly into their stomach. After administration and for less than 3 minutes, the mice remained quiet and seemed afraid. Then, they started to move and act normally. At time 4 hours, the mice that have received 5 mg/kg of Fungizone® and Ambisome® showed signs of suffer and their hair was slightly frizzy while those receiving AmB/Dextrose and AmB/PEG_{5kDa}-cholane continued to act normally. It is worth pointing out that the mice that had received 5 mg/kg AmB/PEG_{5kDa}-cholane were moving faster and were more active than those receiving AmB/Dextrose.

Pharmacokinetic data treatment

- **General considerations**

A non-compartmental independent model was used to estimate the area under the curve between 0 and 24 h (AUC_{0-24}). The apparent elimination constant (Ke) was estimated with the last two plasma concentrations values available (8 and 24 h) for Fungizone®, Ambisome® and AmB/Dextrose formulations and with the last three points (4, 8 and 24 h) for the AmB/PEG_{5kDa}-cholane formulations. The half-life ($t_{½}$) was calculated as the ratio between 0.693 and Ke. Cmax and Tmax values were taken directly from the experimental data. The median of the Tmax values were used for comparative studies.

The area under the curve between 24 h and the infinite ($AUC_{24-\infty}$) was calculated as the ratio between the concentration at time 24 h (C_{24}) and the Ke. The area under the curve between 0 and the infinite ($AUC_{0-\infty}$) was estimated as the sum of AUC_{0-24} plus $AUC_{24-\infty}$. Absolute bioavailability (F) was obtained with the following equation:

$$F = 100 \times (AUC_{oral\ 0-24} \times Dose_{IV}) / (AUC_{iv\ 0-24} \times Dose_{oral})$$

The comparison of the results obtained with the different formulations assayed was performed using ANOVA and t-Student data treatments (Excel, Microsoft Office 2007).

- **Results**

Figure 71 shows the results of the four orally tested formulations (AmB/Dextrose, Ambisome®, Fungizone® and AmB/PEG_{5kDa}-cholane) after administration of a dose of 5 mg/kg of AmB.

Tables 65-68 show the pharmacokinetic parameters obtained on each mice after administration of AmB/Dextrose, Ambisome®, Fungizone® and AmB-PEG formulations, respectively.

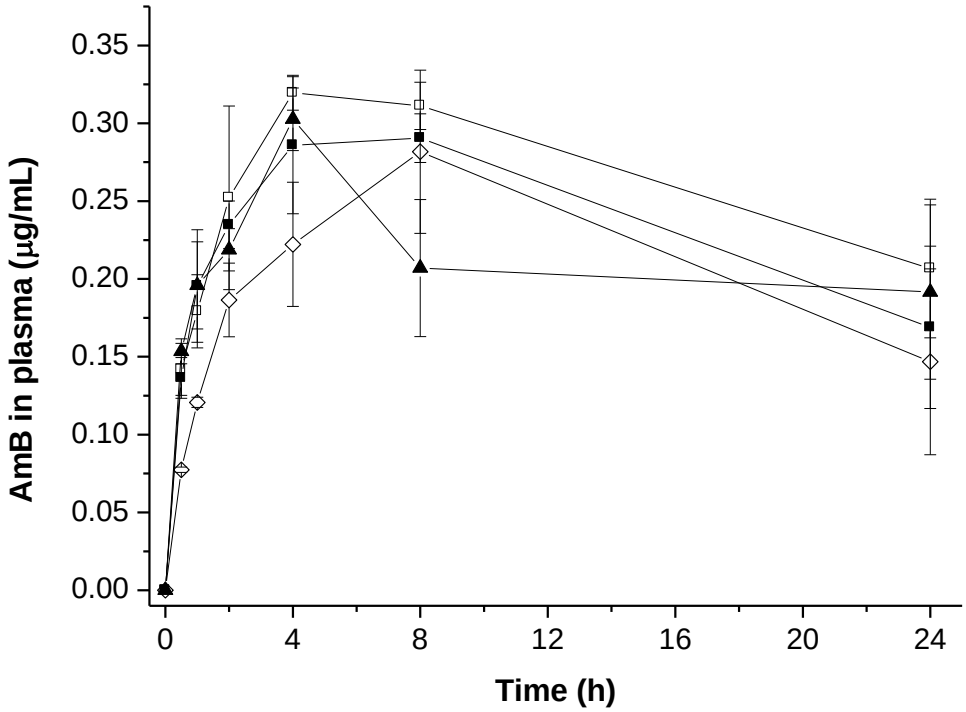

Figure 71. Mean and standard deviation of the plasma concentrations obtained after oral administration of AmB dextrose (-◊-), Ambisome® (-□-), Fungizone® (-■-), and AmB-PEG_{5kDa}-cholane (-▲-).

Table 65. Pharmacokinetic results obtained after oral administration of AmB/Dextrose at 5 mg/kg AmB.

AmB dextrose	**Mice**				**Mean**	**SD**
	1	**2**	**3**	**4**		
Ke (h)	0.04	0.07	0.04	0.03	**0.04**	0.02
t½ (h)	15.41	10.62	18.43	24.37	**17.21**	5.75
AUC0-24 (µg h/ml)	4.74	4.14	5.12	6.27	**5.07**	0.90
AUC24-infinite	2.90	1.22	4.08	7.86	**4.02**	2.82
AUC0-infinite	7.64	5.36	9.20	14.13	**9.08**	3.72
Extrapolation (%)	38.00	22.78	44.33	55.62	**40.18**	13.70
Cmax (µg/ml)	0.27	0.28	0.28	0.35	**0.30**	0.04
T max (h)	8.00	4.00	8.00	8.00	**8.00**	2.00

Table 66. Pharmacokinetic results obtained after oral administration of Ambisome® at 5 mg/kg AmB.

Ambisome®	**Mice**				**Mean**	**SD**
	1	**2**	**3**	**4**		
Ke (h)	0.02	0.04	0.03	0.01	**0.03**	0.01
t½ (h)	33.62	16.35	22.80	52.48	**31.31**	15.81
AUC0-24 (µg h/ml)	7.32	4.59	5.87	6.79	**6.14**	1.20
AUC24-infinite	11.62	3.68	6.02	18.82	**10.03**	6.74
AUC0-infinite	18.94	8.27	11.89	25.60	**16.18**	7.69
Extrapolation (%)	61.35	44.48	50.64	73.49	**57.49**	12.74
Cmax (µg/ml)	0.33	0.31	0.31	0.33	**0.32**	0.01
T max (h)	8	4	4	4	**4**	2
F (%)	8.42	5.28	6.75	7.81	**7.07**	1.37

Table 67. Pharmacokinetic results obtained after oral administration of Fungizone® at 5 mg/kg AmB.

Fungizone®	**Mice**				**Mean**	**SD**
	1	**2**	**3**	**4**		
Ke (h)	0.06	0.02	0.01	0.04	**0.04**	0.02
t½ (h)	10.84	28.91	52.11	15.69	**26.89**	18.47
AUC0-24 (µg h/ml)	5.14	6.11	5.89	5.60	**5.68**	0.42
AUC24-infinite	1.61	8.22	16.68	3..49	**7.50**	6.72
AUC0-infinite	6.75	14.32	22.57	9.08	**13.18**	7.02
Extrapolation (%)	23.88	57.36	73.91	38.38	**48.38**	21.85
Cmax (µg/ml)	0.29	0.35	0.27	0.31	**0.31**	0.03
T max (h)	8	4	8	8	**8**	2
F (%)	16.90	20.09	19.37	18.41	**18.69**	1.38

Table 68. Pharmacokinetic results obtained after oral administration of AMB/PEG_{5kDa}-cholane at 5 mg/kg AmB.

AMB/PEG_{5kDa}-cholane	**Mice**				**Mean**	**SD**
	1	**2**	**3**	**4**		
Ke (h)	0.01	0.01	0.02	0.04	**0.02**	0.01
t½ (h)	133.16	53.62	34.28	18.30	**59.84**	50.97
AUC0-24 (µg h/ml)	6.31	4.85	4.69	4.94	**5.20**	0.75
AUC24-infinite	51.32	14.79	8.74	3.48	**19.58**	21.66
AUC0-infinite	57.63	19.65	13.43	8.42	**24.78**	22.38
Extrapolation (%)	89.05	75.30	65.07	41.32	**67.69**	20.14
Cmax (µg/ml)	0.31	0.27	0.31	0.32	**0.30**	0.02
T max (h)	4.00	4.00	4.00	4.00	**4.00**	0.00
F (%)	10.94	8.42	8.13	8.57	**9.01**	1.30

Figures 72-76 show the mean half-life, AUC_{0-24}, Cmax, Tmax and Absolute bioavailability (F) obtained for the four orally tested formulations.

Due to the high $AUC_{24-infinite}$ values (higher than 5%) only AUC_{0-24} was used in the comparative studies.

Tables 69-73 show the results from the ANOVA tests performed on the different formulations. The half-lives ($t_{½}$), AUC_{0-24}, Cmax, Tmax and Absolute bioavailability (F) were studied.

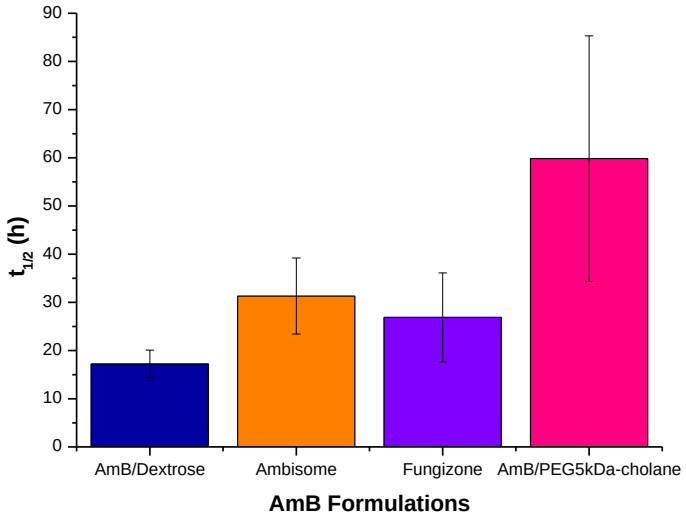

Figure 72. Mean and standard deviation of the half-lives ($t_{½}$) obtained after oral administration of AmB dextrose, Ambisome®, Fungizone® and AmB-PEG_{5kDa}-cholane.

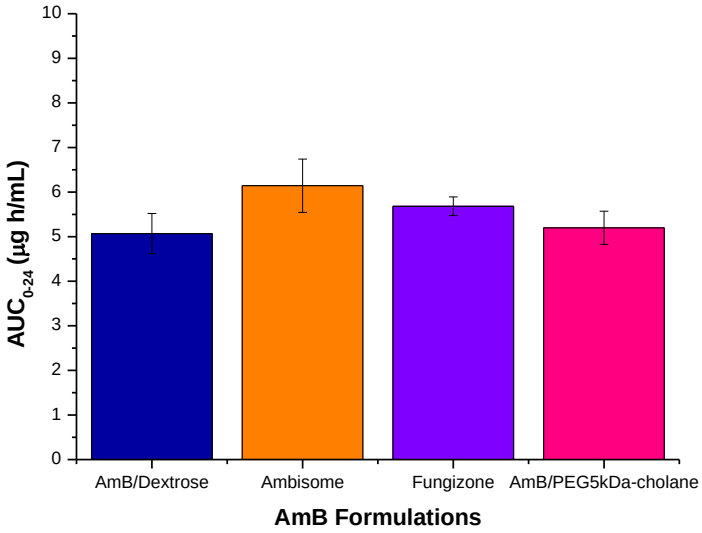

Figure 73. Mean and standard deviation of the $AUC_{0\text{-}24}$ values obtained after oral administration of AmB dextrose, Ambisome®, Fungizone® and AmB-PEG_{5kDa}-cholane.

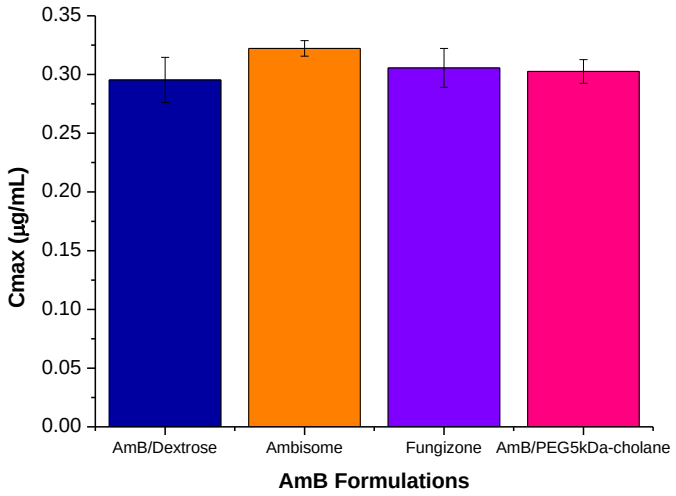

Figure 74. Mean and standard deviation of the Cmax obtained after oral administration of AmB dextrose, Ambisome®, Fungizone® and AmB-PEG_{5kDa}-cholane.

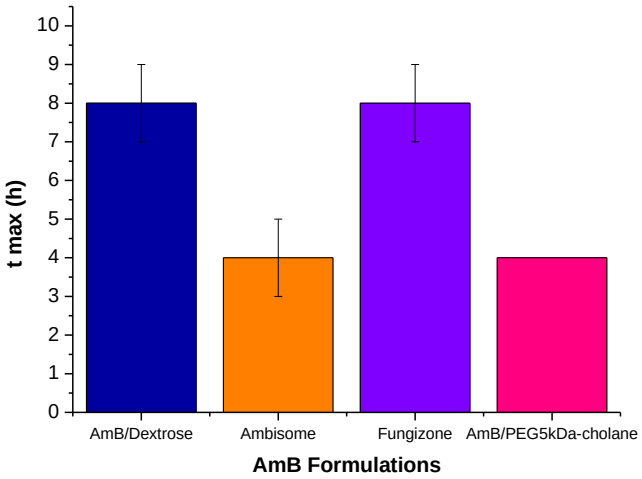

Figure 75. Mean and standard deviation of the t_{max} obtained after oral administration of AmB dextrose, Ambisome®, Fungizone® and AmB-PEG_{5kDa}-cholane.

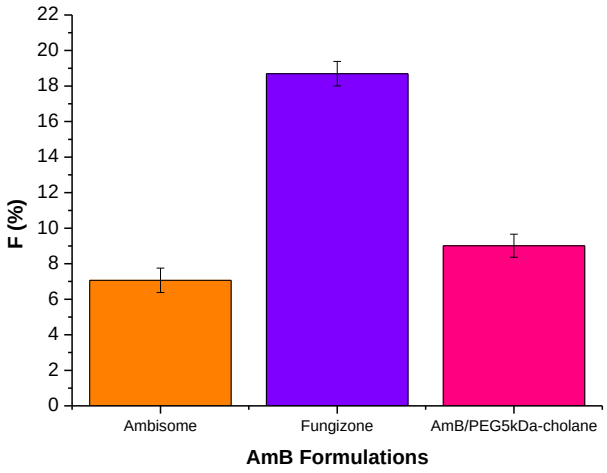

Figure 76. Mean and standard deviation of the Absolute Bioavailability (F) obtained after oral administration of Ambisome®, Fungizone® and AmB-PEG_{5kDa}-cholane.

Table 69. ANOVA test on the half-life constants of AmB Dextrose, Ambisome®, Fungizone® and AmB/PEG_{5kDa}-cholane. NS (P-value is higher than 0.05).

One-factor ANOVA

SUMMARY

Groups	*Counts*	*Sum*	*Mean*	*Variance*
AmB Dextrose	4	68.82	17.21	33.11
Ambisome®	4	125.25	31.31	249.90
Fungizone®	4	107.54	26.89	341.00
AmBPEG	4	239.36	59.84	2598.05

ANALYSIS OF VARIANCE

Variation origin	*Sum of squares*	*Degrees of freedom*	*Mean of squares*	*F*	*Probability*	*Critical value for F*
Between groups	4,029.59	3	1,343.20	1.67	**0.23**	3.49
In between groups	9,666.18	12	805.51			
					.	
Total	13,695.77	15				

Table 70. ANOVA test on the $AUC_{0\text{-}24}$ results of AmB Dextrose, Ambisome®, Fungizone® and AmB/PEG_{5kDa}-cholane. NS (P-value is higher than 0.05).

One-factor ANOVA

SUMMARY

Groups	*Counts*	*Sum*	*Mean*	*Variance*
AmB Dextrose	4	20.27	5.07	0.81
Ambisome®	4	24.57	6.14	1.43
Fungizone®	4	22.73	5.68	0.18
AmBPEG	4	20.79	5.20	0.56

ANALYSIS OF VARIANCE

Variation origin	*Sum of squares*	*Degrees of freedom*	*Mean of squares*	*F*	*Probability*	*Critical value for F*
Between groups	2.89	3	0.96	1.29	**0.32**	3.49
In between groups	8.92	12	0.74			
Total	11.80	15				

Table 71. ANOVA test on the Cmax results of AmB Dextrose, Ambisome®, Fungizone® and AmB/PEG_{5kDa}-cholane. NS (P-value is higher than 0.05).

One-factor ANOVA

SUMMARY

Groups	*Counts*	*Sum*	*Mean*	*Variance*
AmB Dextrose	4	1.18	0.30	0.00
Ambisome®	4	1.29	0.32	0.00
Fungizone®	4	1.22	0.31	0.00
AmBPEG	4	1.21	0.30	0.00

ANALYSIS OF VARIANCE

Variation origin	*Sum of squares*	*Degrees of freedom*	*Mean of squares*	*F*	*Probability*	*Critical value for F*
Between groups	0.00	3	0.0005	0.65	**0.60**	3.49
In Between groups	0.01	12	0.0008			
Total	0.01	15				

Table 72. ANOVA test on the tmax results of AmB Dextrose, Ambisome®, Fungizone® and AmB/PEG_{5kDa}-cholane. NS (P-value is higher than 0.05).

One-factor ANOVA

SUMMARY

Groups	*Counts*	*Sum*	*Mean*	*Variance*
AmB Dextrose	4	28	7	4
Ambisome®	4	20	5	4
Fungizone®	4	28	7	4
AmBPEG	4	16	4	0

Variation origin	*Sum of squares*	*Degrees of freedom*	*Mean of squares*	*F*	*Probability*	*Critical value for F*
Between groups	27	3	9	3	**0.07**	3.49
In between groups	36	12	3			
Total	63	15				

Table 73. ANOVA test on the Absolute Bioavailability (F) results of Ambisome®, Fungizone® and AmB/PEG_{5kDa}-cholane. S (P-value is lower than 0.001).

One-factor ANOVA

SUMMARY

Groups	*Counts*	*Sum*	*Mean*	*Variance*
Ambisome®	4	28.26	7.07	1.89
Fungizone®	4	74.78	18.69	1.91
AmBPEG	4	36.06	9.01	1.68

ANALYSIS OF VARIANCE

Variation origin	*Sum of squares*	*Degrees of freedom*	*Mean of squares*	*F*	*Probability*	*Critical value for F*
Between groups	310.27	2	155.13	84.89	**0.000001**	4.26
In between groups	16.45	9	1.83			
Total	326.72	11				

The above summarized statistic results show that only significant ($P<0.01$) differences were found among formulations in terms of the absolute bioavailability (F). The Fungizone® formulation had higher F values compared to Ambisome® and AmB-PEG_{5kDa}-cholane.

It is important to point out that all the oral AUC_{0-24} values were very similar regardless the formulation (figure 73).

EXP2-2.7.4. Intravenous pharmacokinetics studies

Study design

The intravenous pharmacokinetic studies of the different AmB formulations were performed on two non-consecutive days. On day 1, AmBisome® and Fungizone® were tested and on day 2, AmB/ PEG_{5kDa}-cholane was assayed. The number of sampling points (see study design on EXP2-1.2.7.4) together witht the number of operators did not allowed for the complete study in one day.

Mice behavior

The mice behavior was different depending on the formulation administered. The behavior of the female BALB/c after iv administration of 1 mg/kg Fungizone®, AmBisome® and AMB/PEG_{5kDa}-cholane is detailed below.

- **Fungizone®**

The intravenous administration of 1mg/kg Fungizone® caused discomfort and suffer on the mice. During the first 15 minutes after administration, the mice remained unmoved in a corner of the cage and in a position in which they seemed a ball. They were all together; really close ones to the others and even, ones over the others. Their hair got slightly frizzy . After 15 min, the mice started to move but the movements were slow and the mice seemed afraid.

This behavior is supported by the hemolysis found in most of the samples collected during the intravenous pharmacokinetic study.

- **Ambisome®**

The IV administration of Ambisome® caused less pain in the mice than the administration of Fungizone®. The mice showed signs of suffer but not so pronounced as for Fungizone®. Moreover, the mice recovery time after injection was shorter for Ambisome®. After 8 minutes, the mice started to move and behave normally, even though there were still some signs of suffer.

When preparing the samples for the HPLC analysis, some of them were found to be hemolyzed.

- **AmB/PEG$_{5kDa}$-cholane**

Immediately after Intravenous administration of 1 mg/kg AmB included in PEG$_{5kDa}$-cholane micelles, the BALB/c mice showed a normal behavior. They were active and continued to walk, jump, play, eat and wash themselves. There were no signs of suffer and their hair remained nice.

The mice just felt a little bit of pain when extracting the blood from the eye at each time point.

Pharmacokinetic data treatment

- **General considerations**

A non-compartmental independent model was used to estimate the area under the curve between 0 and 24 h (AUC_{0-24}). The initial concentration (C_0) was extrapolated using the first two plasma samples available adjusted to a fist-order kinetic.

The apparent elimination constant (Ke) was estimated with the last three plasma concentrations values available (4, 8 and 24 h). The regression coefficients calculated with those three values are reported in tables 74-76. The half-life ($t_{½}$) was calculated as the ratio between 0.693 and Ke.

The area under the curve between 24 h and the infinite ($AUC_{24-\infty}$) was calculated as the ratio between the concentration at time 24 h (C_{24}) and the Ke. The area under the curve between 0 and the infinite ($AUC_{0-\infty}$) was estimated as the sum of AUC_{0-24} plus $AUC_{24-\infty}$.

The results obtained with the different formulations assayed were compared using ANOVA and t-Student data treatments (Excel, Microsoft Office 2007).

- **Results**

Figure 77 shows the results of the three intravenously tested formulations (Ambisome®, Fungizone® and AmB/PEG$_{5kDa}$-cholane) after administration of a dose of 1 mg/kg of AmB.

Tables 74-76 summarize the pharmacokinetic parameters obtained on each mouse after iv administration of AmBisome®, Fungizone® and AmB-PEG formulations, respectively.

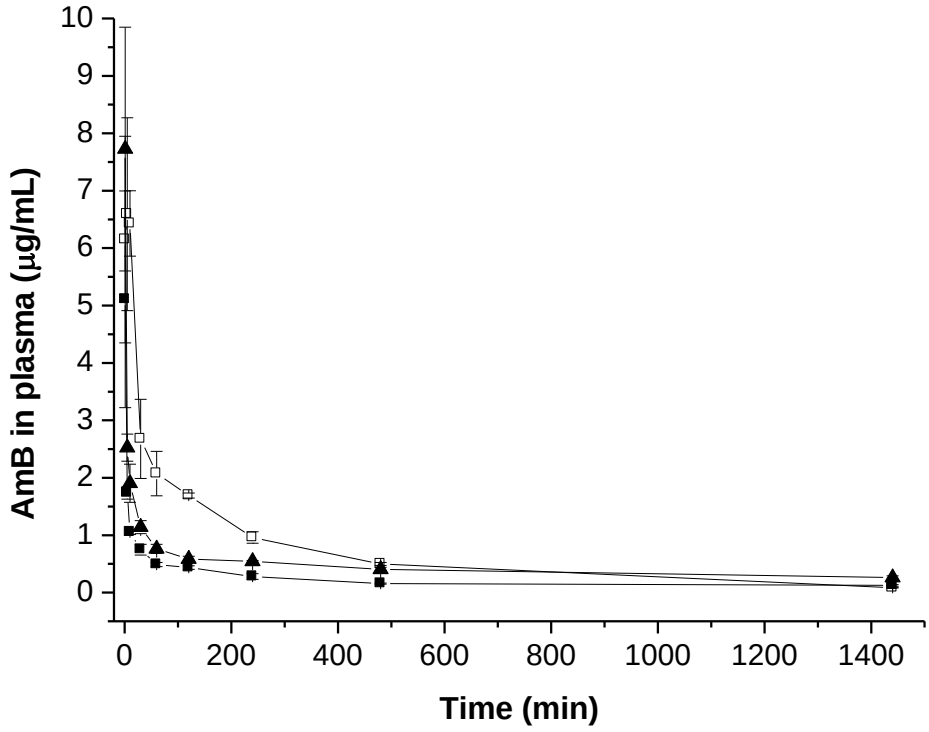

Figure 77. Mean and standard deviation of the plasma concentrations obtained after iv administration of Ambisome® (-□-), Fungizone® (-■-) and AmB-PEG$_{5kDa}$-cholane (-▲-)

Table 74. Pharmacokinetic results obtained after IV administration of Ambisome® at 1 mg/kg AmB.

AmBisome®	**Mice**						**Mean**	SD
	1	**2**	**3**	**4**	**5**	**6**		
Ke (h^{-1})	0.135	0.127	0.127	0.126	0.136	0.137	**0.131**	0.005
$t_{½}$ (h)	5.117	5.443	5.443	5.491	5.110	5.067	**5.278**	0.199
r	-0.987	-0.987	-0.990	-1.000	-0.991	-0.986	**-0.990**	0.005
AUC_{0-24} (μg h/ml)	16.179	16.486	18.164	17.853	18.476	17.155	**17.385**	0.931
$AUC_{24-\infty}$ (μg h/ml)	0.565	0.732	0.706	0.691	0.627	0.574	**0.649**	0.071
$AUC_{0-\infty}$ (μg h/ml)	16.744	17.219	18.869	18.544	19.103	17.730	**18.035**	0.951
Extrapolation (%)	3.373	4.253	3.740	3.726	3.281	3.240	**3.602**	0.386
C_{24} (μg/ml)	0.076	0.093	0.090	0.087	0.085	0.079	**0.085**	0.006

Table 75. Pharmacokinetic results obtained after IV administration of Fungizone® at 1 mg/kg AmB.

Fungizone®	**Mice**						**Mean**	SD
	1	**2**	**3**	**4**	**5**	**6**		
Ke (h^{-1})	0.055	0.057	0.038	0.048	0.056	0.048	**0.050**	0.007
$t_{½}$ (h)	12.491	12.153	18.346	14.551	12.362	14.449	**14.059**	2.356
r	-0.864	-0.877	-0.728	-0.932	-0.993	-0.888	**-0.880**	0.088
AUC_{0-24} (µg h/ml)	5.903	5.728	5.683	5.943	6.985	6.236	**6.080**	0.485
$AUC_{24-\infty}$ (µg h/ml)	2.005	1.909	3.748	2.739	2.157	2.887	**2.574**	0.699
$AUC_{0-\infty}$ (µg h/ml)	7.908	7.637	9.431	8.682	9.142	9.123	**8.654**	0.728
Extrapolation (%)	25.353	25.001	39.745	31.550	23.596	31.649	**29.482**	6.101
C_{24} (µg/ml)	0.111	0.109	0.142	0.130	0.121	0.138	**0.125**	0.014

Table 76. Pharmacokinetic results obtained after IV administration of AMB/PEG_{5kDa}-cholane at 1 mg/kg AmB.

AmB-PEG_{5kDa}-cholane	**Mice**							**Mean**	SD
	1	**2**	**3**	**4**	**5**	**6**	**7**		
Ke (h^{-1})	0.032	0.033	0.032	0.034	0.045	0.048	0.051	**0.039**	0.007
$t_{½}$ (h)	21.447	21.311	21.739	20.240	15.561	14.298	13.561	**18.308**	3.294
r	-0.931	-0.999	-0.960	-0.970	-0.999	-0.971	-0.984	**-0.973**	0.026
AUC_{0-24} (µg h/ml)	10.348	10.924	11.377	12.834	11.417	11.853	11.978	**11.533**	0.845
$AUC_{24-\infty}$ (µg h/ml)	8.277	7.971	9.302	9.015	5.221	4.970	4.560	**7.045**	1.895
$AUC_{0-\infty}$ (µg h/ml)	18.626	18.895	20.680	21.849	16.638	16.823	16.537	**18.578**	2.067
Extrapolation (%)	44.441	42.184	44.982	41.261	31.379	29.544	27.572	**37.337**	6.755
C_{24} (µg/ml)	0.267	0.259	0.297	0.309	0.233	0.241	0.233	**0.263**	0.030

Interestingly, AmB/PEG_{5kDa}cholane samples were the less hemolyzed of all tested formulations and the mice behavior was normal showing no signs of suffer.

Extrapolation of the $AUC_{24-\infty}$ for the Fungizone® and the AmB/PEG_{5kDa}cholane formulations was higher than 5%, and for this reason, only AUC_{0-24} was used for comparative purposes.

AmB pharmacokinetics is usually defined as multiexponential, non lineal and dependent on the drug formulation administered, even after simple *in bolus* administration [153].

.

Data reported in figure 77 and in tables 74-76 show that the pharmacokinetic behavior

of AmB depends on the type of formulation administered. Therefore, ANOVA tests were performed to study the possible statistically significant differences among the different formulations assayed.

It is reasonable that the apparent elimination constant and the half-life were found to be different depending on the drug formulation. Figures 78 and 79 show the mean apparent elimination constants and the half-lives associated to the three different formulations. In order to obtain a more reliable elimination constant value, more sampling points would be required. Nevertheless, as the aim of the present study was to test different AmB formulations and analyze their different pharmacokinetic behavior, the sampling points available are enough.

The apparent elimination constants were calculated with the last three available concentrations for each formulation and the regression coefficients are reported in tables 74-76.

Tables 77 and 78 summarize the results from the ANOVA tests performed on the three intravenously administered formulations. The statistical tests show significant differences among the formulations for the apparent elimination constants (Ke) and the half-life ($t_{½}$) parameters.

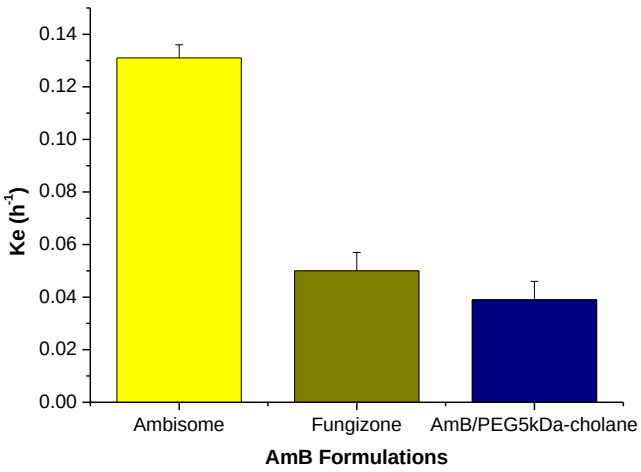

Figure 78. Mean apparent elimination constant (Ke) and standard deviation of Ambisome®, Fungizone® and AmB/PEG_{5kDa}-cholane after IV administration of 1 mg/kg AmB.

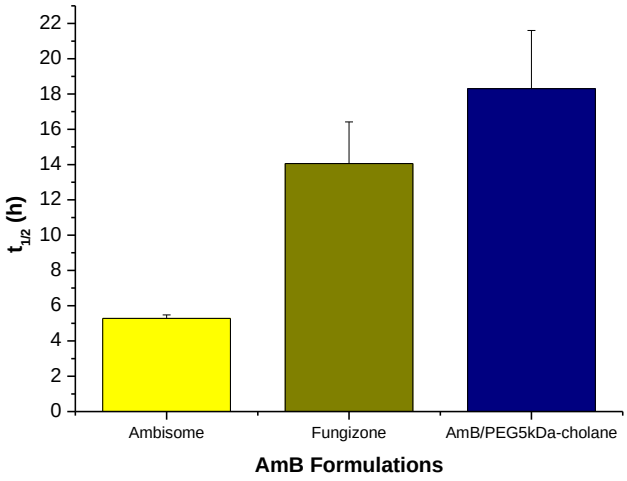

Figure 79. Mean half-life ($t_{½}$) (h) and standard deviation of Ambisome®, Fungizone® and AmB/PEG_{5kDa}-cholane after IV administration of 1 mg/kg AmB.

Table 77. ANOVA test on the apparent elimination constants (Ke) of AmBisome®, Fungizone® and AmB/PEG_{5kDa}-cholane. P-value is lower than 0.001.

One-factor ANOVA

SUMMARY

Groups	*Count*	*Sum*	*Mean*	*Variance*
AmBisome®	6	0.789	0.131	0.00002463
Fungizone®	6	0.302	0.050	0.00005494
AmB/PEG_{5kDa}-chlolane	7	0.275	0.039	0.00007104

ANALYSIS OF VARIANCE

Variation origin	*Sum of squares*	*Degrees of freedom*	*Mean of squares*	*F*	*Probability*	*Critical value for F*
Between groups	0.032	2.000	0.016	305.902	**$1.8\ 10^{-13}$**	3.634
In between groups	0.001	16.000	0.000			
Total	0.032	18.000				

Table 78. ANOVA test on the half-lives ($t_{½}$) of AmBisome®, Fungizone® and AmB/PEG_{5kDa}-cholane. P-value is lower than 0.001.

One-factor ANOVA

SUMMARY

Groups	*Counts*	*Sum*	*Mean*	*Variance*
AmBisome®	6	31.670	5.278	0.040
Fungizone®	6	84.352	14.059	5.549
AmB/PEG_{5kDa}-cholane	7	128.156	18.308	13.422

ANALYSIS OF VARIANCE

Variation origin	*Sum of squares*	*Degrees of freedom*	*Mean of squares*	*F*	*Probability*	*Critical value for F*
					$4.73\ 10^{-7}$	3.634
Between groups	561.272	2.000	280.636	41.394		
In between groups	108.474	16.000	6.780			
Total	669.746	18.000				

Figures 80 and 81 show the values of AUC_{0-24} and C_{24} for the different tested formulations. The concentration of AmB circulating in blood after 24 h was 0.263 μg/mL for the AmB-PEG_{5kDa}-cholane formulation, twice that of Fungizone® or Ambisome® (0.1252 μg/mL and 0.085 mg/mL, respectively). Tables 79 and 80 show the results from the ANOVA tests performed on both parameters (AUC_{0-24} and C_{24}).

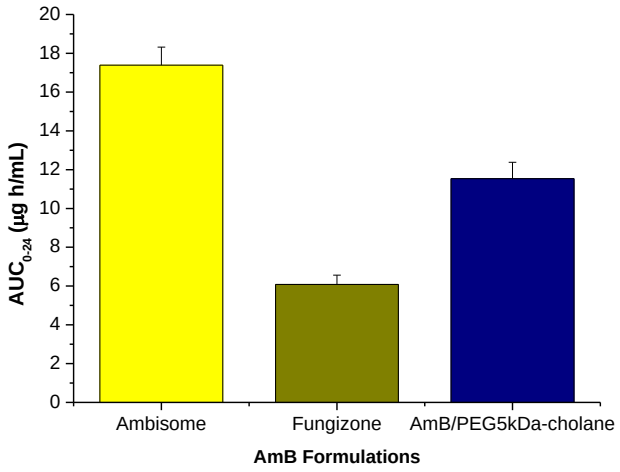

Figure 80. Mean AUC_{0-24} (μg h/mL) and standard deviation for the different tested formulations.

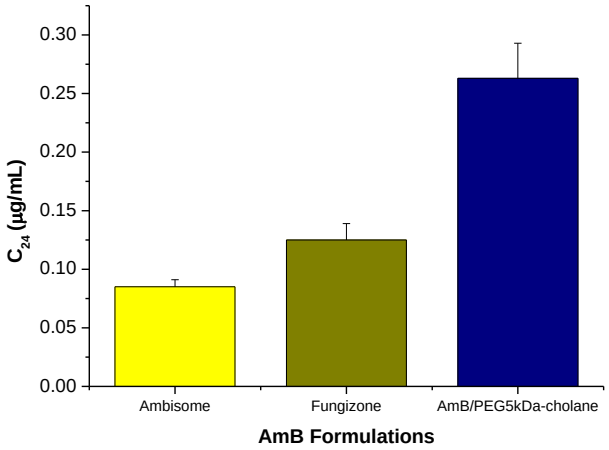

Figure 81. Mean C_{24} (µg/mL) and standard deviation for the different tested formulations.

Table 79. ANOVA test on the $AUC_{0\text{-}24}$ of AmBisome®, Fungizone® and AmB/PEG_{5kDa}-cholane. P-value is lower than 0.001.

One-factor ANOVA

SUMMARY

Groups	*Counts*	*Sum*	*Mean*	*Variance*
AmBisome	6	104.313	17.385	0.866
Fungizone	6	36.477	6.080	0.235
AmBPEG	7	80.732	11.533	0.634

ANALYSIS OF VARIANCE

Variation origin	*Sum of squares*	*Degrees of freedom*	*Mean of squares*	*F*	*Probability*	*Critical value for F*
					$9.9\ 10^{-14}$	3.634
Between groups	383.647	2.000	191.823	329.671		
In between groups	9.310	16.000	0.582			
Total	392.956	18.000				

Table 80. ANOVA test on the C_{24} of AmBisome®, Fungizone® and AmB/PEG_{5kDa}-cholane. P-value is lower than 0.001.

One-factor ANOVA

SUMMARY

Groups	*Counts*	*Sum*	*Mean*	*Variance*
AmBisome	6	0.510	0.085	0.000
Fungizone	6	0.752	0.125	0.000
AmBPEG	7	1.838	0.263	0.001

ANALYSIS OF VARIANCE

Variation origin	*Sum of squares*	*Degrees of freedom*	*Mean of squares*	*F*	*Probability*	*Critical value for F*
					$9.9\ 10^{-11}$	3.634
Between groups	0.114	2.000	0.057	1360.154		
In Between groups	0.007	16.000	0.000			
Total	0.121	18.000				

In order to study a possible relationship between the apparent elimination constant (Ke) with the AUC_{0-24} and the C_{24} a t-Student test was applied. The results are shown in tables 81 and 82 and figures 82 and 83.

Table 81. t-Student test with different variances for Ke and AUC_{0-24}.

	Ke (h^{-1})	AUC_{0-24} (µg h/ml)
Mean	0.071877004	11.6590439
Variance	0.00179644	21.8309061
Observations	19	19
Hypothetical difference between the means	0	
Degrees of freedom	18	
t-statistic	-10.8093683	
P(T<=t) one tail	**$1.3307\ 10^{-9}$**	
t-critical value (one tail)	1.734063592	
P(T<=t) two tails	**2.66141E-09**	
t-critical value (two tails)	2.100922037	

There is a significant relationship between both variables with a P-value lower than 0.001.

Table 82. t-Student test with different variances for Ke and C_{24}.

	Ke (h^{-1})	C_{24} (µg/ml)
Mean	0.071877	0.163168383
Variance	0.00179644	0.006732092
Observations	19	19
Hypothetical difference between the means	0	
Degrees of freedom	27	
t-statistic	4.308929837	
P(T<=t) one tail	**$9.73034\ 10^{-5}$**	
t-critical value (one tail)	1.703288423	
P(T<=t) two tails	**0.000194607**	
t-critical value (two tails)	2.051830493	

There is a significant relationship between both variables with a P-value lower than 0.001.

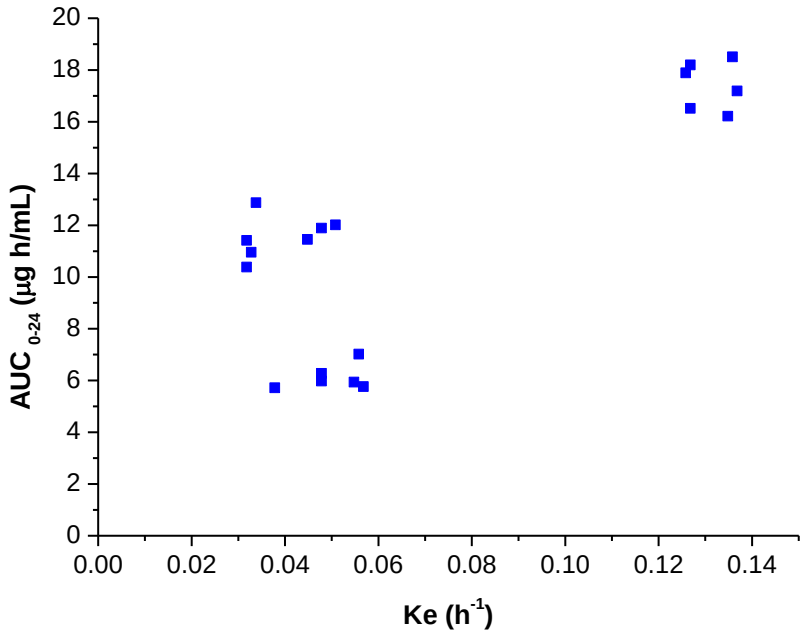

Figure 82. Significant relationship (P<0.01) between AUC_{0-24} and the apparent elimination constant (Ke).

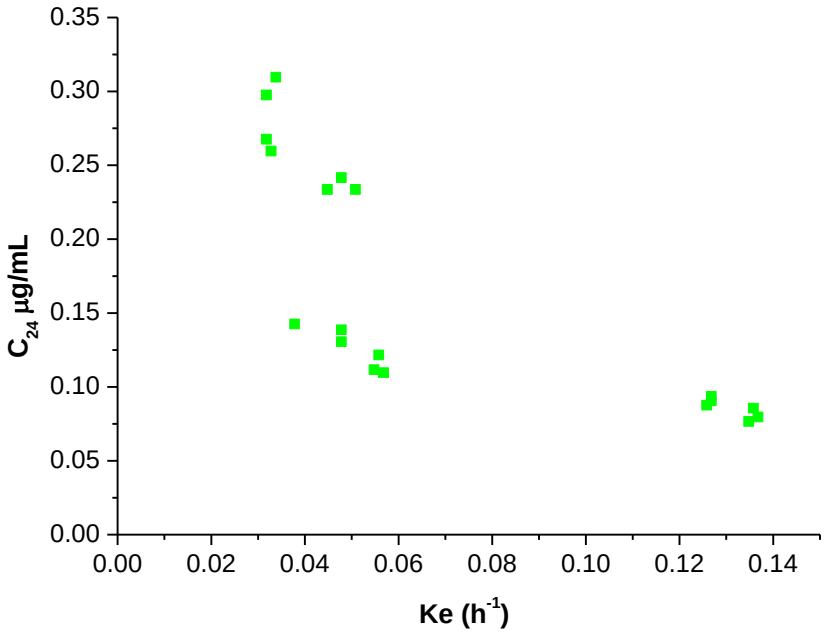

Figure 83. Significant relationship (P<0.01) between C_{24} and the apparent elimination constant (Ke).

KINETICS AMB/PEG$_{5KDA}$-CHOLANE FREE ENERGY CONJUGATION TEM FTIR HEMOLYSIS REFLUX GASTRIC MIMICKING FLUID RECOVERY NMR SYNCHROTON HSM DSC DISSOCIATION CONSTANT HSA PLASMA ISOTHERMAL TITRATION CALORIMETRY ENTROPY CIRCULAR DICHROISM ABSORBANCE DIMER TEA SIZE UNFORMULATED DRUG/POLYMER INTERACTION ΔS NANOAGGREGATES FUNGIZONE®

EXP.2-3. DISCUSSION

HEAT PPM ORAL/IV PHARMACOKINETICS STOMACH MOLAR RATIO AGGREGATION KD2 ANALYSIS NEUTRAL SURFACE CHARGE STOICHIOMETRY TMAX SYNTHESIS ΔH CM^{-1} Kd AMBISOME® AMORPHOUS MG/KG EXTRACTION POLARIZATION NEGATIVE-STAINING BENDING/STRETCHING VIBRATIONS TREATMENT ANTIBIOTIC PARTICLE SIZE ENTHALPY β-SHEET TAIL MICELLES COLLOIDAL DISPERSION

EXP2-3.DISCUSSION

The results reported in this thesis show that PEG_{5kDa}-cholane can increase more than 10^5 times the AmB solubility according to a linear [dissolved drug]/[polymer concentration] correlation. Solutions up to 12 mg/mL AmB (6 mg/mL PEG_{5kDa}-cholane) were obtained without significant change of buffer viscosity. Higher drug/polymer concentrations increased the viscosity, which prevented the accurate determination of the maximal AmB solubility. However, neither AmB separation nor inhomogeneity were observed up to 60 mg/mL AmB (30 mg/mL PEG_{5kDa}-cholane). PEG_{5kDa}-OH was not found to significantly affect the AmB solubility indicating that the drug solubility was due to the supramolecular PEG_{5kDa}-cholane self-association into micelles as previously reported [335].

The remarkable effect of PEG_{5kDa}-cholane on AmB solubility is due to a combination of effects, which include the ability of PEG_{5kDa}-cholane to form stable micelles with a low CMC [335] and the affinity of AmB for sterol molecules. AmB displays in fact its antifungal activity and cytotoxicity by interaction with ergosterol and cholesterol located in membranes of fungi and mammalian cells, respectively [168,381]. To note that a study reported in the literature showed that sterols in DSPE-PEG micelles favor the formation of soluble AmB aggregates [382].This study showed that either AmB solubility or aggregation depend on the chemical structure and content of sterols in the DSPE-PEG vesicles.

The high AmB solubility obtained by using little amounts of excipients, namely solubilizing agents, is an important requisite for the development of safe products easily manageable in clinical practice. The use of high amounts of excipients may in fact be associated to toxic effect, in particular in parenteral administrations, namely infusion. Little amounts of PEG_{5kDa}-cholane yielded very high AmB concentration solutions whilst commercial products, namely Fungizone® and Ambisome®, and other formulations described in the literature contain high amounts of solubilizing excipients [155]. In Fungizone® and Ambisome®, for example, 50 mg AmB are formulated with 41 mg sodium deoxycholate and 350 mg phospholipids/cholesterol/tochopherol, respectively [362], which are re-constituted in 15 mL saline solution resulting in 3.33 mg/mL AmB. The same amount of AmB could be dissolved with 25 mg of PEG_{5kDa}-

cholane in about 4 mL buffer to yield 12.5 mg/mL AmB. It is worth to note that previous cell culture studies showed that PEG_{5kDa}-cholane has negligible toxicity even at high doses. Furthermore, preliminary studies showed that, oppositely to sodium deoxycholate used in Fungizone®, PEG_{5kDa}-cholane does not display significant hemolytic effect [335].

The different capability of PEG_{5kDa}-cholane to solubilize AmB observed with different dissolution methods can be explained by the effect of the dissolution conditions in the formation of monomeric and multimeric soluble species, typically dimers and tetramers [145]. According to the UV and CD spectrometric data, the direct AmB dissolution process produces low drug concentrations where AmB is mainly associated in the monomeric form with PEG_{5kDa}-cholane. On the contrary, the spectra obtained with AmB/PEG_{5kDa}-cholane prepared by co-solvent dissolution or by dissolution/pH change showed the typical profile of aggregated AmB. Therefore, the high drug concentration obtained by these methods can be ascribed to the formation of AmB nanoaggregates, which are promptly stabilized by the polymer interaction.

Dynamic light scattering (DLS) and transmission electron microscopy (TEM) confirmed that the AmB/PEG_{5kDa}-cholane association forms micelles with homogeneous size. The particles size was similar to other nanoformulations such as nanosomal AmB (34.6 nm) [269] or Ambisome® (35-70 nm) [106,156,362]. The structure of the AmB/PEG_{5kDa}-cholane micelles was confirmed by the TEM analyses, which showed the polymeric chains exposed on the vesicle surface, while the hydrophobic cholane moieties are localized inside the micelles. The similar zeta-potential of AmB free and AmB loaded micelles indicates that the AmB ionization does not affect the overall surface charge of the micelle confirming that the drug was localized in the micelle core.

The high affinity of AmB for PEG_{5kDa}-cholane observed by isothermal calorimetry (ITC) is in agreement with the high affinity of this drug for steroidal polycycles described in the literature, which is responsible for its antifungal activity and cytotoxicity [168,381]. However, the isothermal calorimetry (ITC) highlighted the complexity of the PEG_{5kDa}-cholane interaction with AmB, which takes place with different AmB soluble species, namely monomers, dimers, tetramers, and other multimeric nanoaggregates, of which abundance depends on the pH. It has been

reported that the presence of a net charge in the antibiotic molecule is the main factor that induces the solubility of AmB through the formation of the monomeric specie. AmB pKa values are 5.7 for the carboxyl group and 10.0 for the amino group. Therefore, at pH 11.0 AmB is mainly in the monomeric highly soluble anionic form [145]. As the pH decreases to the isolectric point, the AmB anionic form and the drug solubility decrease with concurrent formation of less soluble nanoaggregates. At pH 3.5 the AmB solubility slightly increases with the increase of the cationic specie, which was found to be less soluble than the anionic form. The similar thermal profile obtained at pH 5.5 and 7.2 and the similar ones obtained at 3.5 and 8.5 seem to indicate that the polymer interaction with the drug is strictly related to the solubility of AmB and hence to the relative abundance of the mono- or multimeric species.

The three different binding sites calculated by ITC analyses reasonably result from the PEG_{5kDa}-cholane interaction with different AmB species through hydrophobic interactions between the cholane moiety and the heptaene side of the drug molecule to form different supramolecular structures. These results are in agreement with studies reported in the literature, which showed that the aggregation state of AmB depends on the sterol content physically incorporated in DSPE-PEG micelles. However, in all cases, the AmB/PEG_{5kDa}-cholane interaction is enthalpically favored, regardless the binding site and the pH, indicating that the cholane interaction with AmB is thermodynamically favored as expected by the interaction of hydrophobic moieties in aqueous solution.

The first and second bindings are also strongly entropically contributed suggesting that in these steps the polymer interaction with the drug provokes the disruption of ordered structures, namely AmB nanoaggregates, dimers and tetramers or by displacement of water molecules coordinated with the polymer and the drug. We hypothesize that these interactions occur by insertion of the cholanic moiety in between the heptaenic sides of coupled molecules in multimeric forms, dimers and tetramers.

The affinity constant for the third binding site (K3) was remarkably lower than that calculated for the other sites. Despite the strongest enthalpic contribution, the entropic contribution to this interaction was lower than the first two interactions, especially at high and low pHs. At pH 11.0, the ΔS was negative indicating that this interaction can occur with the formation of ordered structures. This seems to be in agreement with the RDX spectra, which showed that the AmB incorporation into the polymer micelles

occurs with the destruction of the typical crystalline form of AmB while novel ordered structures are formed.

Importantly, the AmB/PEG_{5kDa}-cholane formulation was found to be pharmaceutically stable. The lyophilization process produced a fluffy powder with low moisture content without cake formation. The lyophilized product was stable throughout the time as AmB/PEG_{5kDa}-cholane solutions could be perfectly reconstituted by physiological buffer addition in few seconds, even without shaking, to yield a colloidal dispersion with the same physicochemical features of the freshly prepared formulation. It is worth to note that the reconstituted formulation was physically and chemically stable over 1 month at room temperature.

The spectrometric and thermal analyses performed on lyophilized AmB/PEG_{5kDa}-cholane provided information about the physical structure of the dried formulation. The Fourier transform infrared (FTIR) analysis showed new signals for the AmB/PEG_{5kDa}-cholane micelle formulations, while the AmB/PEG_{5kDa}-cholane physical mixture showed all the signals corresponding to the drug and the polymer. Similarly, the differential scanning calorimetry and X-ray diffraction (XRD) analyses evidenced the intimate AmB/PEG_{5kDa}-cholane interaction with the disappearance of the typical thermal and diffraction signals of crystalline AmB and PEG_{5kDa}-cholane. On the contrary, the AmB/PEG_{5kDa}-cholane physical mixture showed all signals of drug and polymer. However, it should be noted that as reported above the XRD spectrum of the lyophilized AmB/PEG_{5kDa}-cholane micelles showed new signals suggesting that novel non-amorphous species are formed.

The CD studies showed that, similarly to Fungizone® and heated Fungizone®, AmB/PEG_{5kDa}-cholane micelles did not induce structural alterations of human serum albumin (HSA). This indicates that the formulation shouldn't have detrimental effect on native proteins after administration. In the presence of HSA, the AmB nanoaggregates in the PEG_{5kDa}-cholane micelles are more stable and less rapidly disaggregated than in non-heated Fungizone®, which can result in lower toxicity. The AmB displacement from the PEG_{5kDa}-cholane micelles is higher than from heated Fungizone®. Actually, heated Fungizone® was reported to contain higher amount of aggregated AmB compared to normal Fungizone®, which results in a more stable and less toxic product [383,384,385]. Nevertheless, the therapeutic effect of heated Fungizone® is less

reproducible than non-heated Fungizone® [386]. Therefore, the aggregation results seem to indicate that PEG_{5kDa}-cholane formulation can yield a product with higher AmB stability and lower toxicity compared to Fungizone® and enhanced reproducibility compared to heated Fungizone®.

The dialysis results showed a biphasic pattern where 70% of the drug was release in 10 h and 90% in 96h. Both steps of release were controlled by diffusion (the best fittings were obtained with the Higuchi and Korsmeyer-Peppas model) but the rate and the K constant showed that the structural conditions were different for each step of release.

The AmB stability in gastric mimicking fluid demonstrated that after 1.5 h at pH 1.2 in the presence of pepsin there is still a 51.7% AmB available to be absorbed. This study was performed in order to demonstrate that the oral administration of AmB/PEG_{5kDa}-cholane could lead to systemic adsorption of AmB. Even though the absorption values are not expected to be high, the oral administration of AmB would avoid the problems related to the parenteral treatment compliance and parenteral treatment cost.

The use of naproxen as internal standard in the treatment of blood samples was discarded. Although naproxen is detected at 406 nm and eluted near the AmB but well-resolved from it, there was non linearity between its concentration and its absorbance at 406 nm. Therefore, the recovery studies in plasma were performed.

The AmB recovery studies in plasma showed similar values for all the formulations studied (AmB in DMSO, AmB in dextrose, Fungizone®, Ambisome® and AmB/PEG_{5kDa}-cholane). The percentage of AmB recovered was 79% regardless the formulation. When manipulating the blood samples containing the AmB for obtaining the plasma there was a 20% AmB loss. This loss can be explain by the high binding affinity of AmB to proteins. The protocols for blood sample preparations include several steps (centrifugation and precipitation) where the AmB can be lost. If during sample preparation the AmB joins the proteins contained in the blood, the solvents add to precipitate those proteins could led to AmB loss. This 79% recovery value is in agreement with previously reported values (74% recovery) [387].

The hemolysis studies confirmed that the AmB/PEG_{5kDa}-cholane micelles were less hemolytic than Fungizone®. Even at concentrations in which the Fungizone® caused 100% hemolysis, the new formulation produced not more than 30% hemolysis. These

results are in fair agreement with the toxicity studies performed with PEG_{5kDa}-cholane by Salmaso *et al*. [335]. The lower hemolytic effect of AMB/PEG_{5kDa}-cholane compared to Fungizone® is explained by the solubilizer agent. The sodium deoxycholate found in Fungizone® produces hemolytic effects itself [134,148, 152 259]. Moreover, its CMC value (10^{-3}) makes the micelles susceptible to *in vivo* dilution processes when being intravenously administered. Dilution with plasma, which may happen in a time-scale of µsec, lead to the disappearance of the deoxycholate micelles, the continuous loss of deoxycholate from the AmB-deoxycholate aggregates and consequently, the rapid release and reaggregation of the AmB [148,253]. These AmB aggregates are not selective against fungal cells damaging either fungal or mammalian cells and being therefore, responsible for the higher hemolytic effect of Fungizone®.

The biological *in vitro* studies showed that the AmB formulated with PEG_{5kDa}-cholane maintains high antimicrobial activity, which is very close to AmB in solution. This confirms that the drug is released from the micelles to interact with the cell membrane. The slightly lower activity of AmB/PEG_{5kDa}-cholane compared to the standard may be ascribed to the drug release process from the micelles while the drug in solution is immediately available. Similarly, the higher activity of the micelle formulation compared to the AmB suspension may be attributed to the fastest drug release from the former than the dissolution from the solid dispersion. Moreover, considering that the mechanism for AmB activity seems to be related to the formation of multimeric drug associations, it could possible that the drug released from the micelles is partially in the conformation for the interaction with the target. Furthermore, AmB in solution is obtained with DMSO, a solvent and absorption enhancer that also has irritant effects. The new formulation of AmB presented in this work shows a similar antimicrobial activity without DMSO suggesting interesting practical applications.

The oral administration of 5 mg/kg AmB demonstrated that the new formulation developed had the highest half-life of all assayed formulations. While the $AUC_{0\text{-}24}$ values were similar for all tested formulations the oral absolute bioavailability (F) was dependent on the formulation and varied in between 7-19%.

Finally, The IV administration of 1 mg/kg AmB in Ambisome®, Fungizone® and AmB/PEG_{5kDa}-cholane showed that the new formulation developed had a significantly ($P<0.01$) lower apparent elimination constant and consequently, a higher half-life

compared to the marketed formulations Ambisome® and Fungizone®. This higher "$t_{1/2}$" value is in agreement with the fact that the PEGylated polymers used as carriers, prolong the drug circulation time in blood. The PEGylation decreases the uptake, and therefore the accumulation in RES organs, liver and spleen. This is due to the steric stability impart by the PEG chains which minimize protein adsorption to hydrophibic surfaces, avoiding renal clearance [288,310,317,331,335,388-390], The PEG-cholane acts as a nanoscopic carrier capable of releasing the AmB slower over the time, which is supported by the higher C_{24} value obtained for AmB/PEG_{5kDa}-cholane compared to Fungizone® and Ambisome®. The higher AmB concentration found in blood after 24 h is due to the longer time-dependent relaxation effects of PEG-cholane compared to other low molecular weight surfactants as sodium deoxycholate (Fungizone®) [329].

DRUG UNIPD AMPHOTERICIN B PEG_{5KDA}-CHOLANE FTIR HSM HEMOLYSIS ORAL UCM MONOMER POLYAGGREGATES ITC *IN VITRO* INTRAVENOUS Ke SYNTHESIS mV TNBS RESISTANCE $T_{1/2}$ NMR XRD FORMULATION ACTIVATION IR CANDIDA HPLC 1959 EFFICACY SYNCHROTRON CHOLESTEROL pH CMAX DIMER ORAL NAIL CHARACTERIZATION ΔH 924Da CRITICAL AGGREGATION CONCENTRATION MIC CMC

4. APPENDIX

CIRCULAR DICHROISM ONYCHOMYCOSIS STABILITY RELEASE UV TOXICITY TEA HSA C24 TOPICAL ADMINISTRATION AMORPHOUS CONJUGATION AUC MIXED INFECTIONS MEMBRANE ΔS PENETRATION EXCIPIENTS BETA-SHEET $C_{47}H_{73}NO_{17}$ KD2 CM^{-1} ALPHA-HELIX EF ERGOSTEROL FILM-FORMING DERMATHOPHYTE MOLDS AMPHOTERIC PKA DISSOCIATION CRYSTALLINE INTERACTION BALB/C

4.1. COMPLEMENTARY INFORMATION

4. APPENDIX

4.1. COMPLEMENTARY INFORMATION

Note

Appendix 1 includes complementary information on the amphotericin B nail lacquer developed for the treatment of onychomycosis.

Section AP1.1 contains a general introduction of the onychomysis. The etiology, indicence, prevalence, predisposition factors, pathophysiology, clinical types of onychomycosis, the nail permeability as well as the possible treatments are discussed in this section.

Section AP1.2 includes the detailed description of the excipients studied during formulation development.

Section AP1.3 comprises the composition of the formulations developed

Ansd finally, Section AP1.4 details the troubleshooting found during formulation preparation.

AP1.1. ONYCHOMYCOSIS INTRODUCTION

AP1.1.1. General Considerations

Onychomycosis, also known as tinea *ungium,* is an infection of the fingernails or toenails caused by dermatophytes, yeasts or non-dermatophyte molds. It is responsible for approximately 50% of consultations for nail disorders [391-393] and represents about 30% of diagnosed superficial fungal infections [394]. Even though the onychomycosis can affect both finger and toenails, the later are more commonly affected [391,395] (the onychomycosis in the toenails are 4-25 times more widespread than the infections located in the fingernails [396] . The infections may involve other components of the nail including the matrix, the nail bed or the nail plate [396]. Onychomycosis is the most common nail disorder and it is reported to be age and gender-related. The prevalence of onychomycosis is higher in men, in the younger age, but this prevalence increases with age in both genders [391,392,395-399]

AP1.1.2. Etiology

The etiology of the onychomycosis varies depending on the zone affected (toe or fingernails) [395]. In most cases, the pathogens responsible for the toenail infections are dermatophytes. Between all the dermatophytes, *Trichophyton rubrum is* the most common cause of onychomycosis worldwide (causing 60% of the dermatophyte onychomycosis) followed by *Trichophyton mentagrophytes* (that causes 20% of the infections) and *Epidermophyton floccosum* (responsible for the 10%) [391,392,398,399]. Apart from the dermatophytes, the non-dermatophyte molds such as *Aspergillus sp*. and *Scopulariopsis brevicaulis,* can be also involved in the nails infections as main responsible (primary pathogens) or as secondary pathogens (contaminant agents) [391,400,401]. Other molds that have been isolated from the infected nails, although are not commonly found in the affected areas, are *Fusarium* spp., *Acremonium* spp., *Alternaria* spp. and *Neoscytalidium* sp [391, 402]. An estimated 2-15% of the nails infections are due to non-dermatophyte molds [391,403-405]. Yeast, such as *Candida albicans* and *Candida parapsilosis, glabrata, C. guillermondii, C. krusei,* and *C. tropicalis* represent the third cause of fungal toenail infection [406]. Infections caused by *Candida spp*. occur almost only when predisposing factors are

present (diabetes or immunosuppression), as *Candida* is just able to penetrate the toenail if there is an altered immune response [394].

Conversely, the onycohomycosis located in the fingernails are mainly caused by yeasts belonging to the genus *Candida* (*C. albicans, parapsilosis and tropicalis*) [395, 407]. These being responsible for the 60% of the infections located at this level [408,409, 410]. Nevertheless, the fingernail infections can also be produced by dermatophytes (*Trichophyton rubrum* and *mentagrophytes*) and non-dermatophytes molds (*Scopulariopsis brevicaulis* and *Mucor spp).*

AP1.1.3. Incidence

The incidence of the onychomycosis has increased during the last years owing to factors such as ageing of the population, increased number of immunocompromised patients and increase in sports participation [391,394,395,397,399]. Firstly, as the population ages, there is a parallel increase in chronic health problems (diabetes) and poor peripheral circulation. Secondly, the number of persons that are immunocompromised due to infections with HIV and the use of immunosuppressive therapy, cancer chemotherapy or antibiotics, continue to expand. Finally, the rise in sport participations has increased the use of health clubs, commercial swimming pools and occlusive foot wears for exercise [400]. Just in a small percentage of people, onychomycosis may be caused by a genetic defect that causes an alteration in the immune function.

AP1.1.4. Prevalence

Not only the incidence of onychomycosis has increased in the last decade but also the prevalence of the infections has changed. Even though, *Trichophyton rubrum* is known to be the main ethological agent responsible for the onychomycosis, the nail infections caused by yeasts, and in particular by *Candida* spp, are actually in increase [410]. *Candida* genus is not only responsible for approximately 51-70% of the fingernails infections, but also for many of the toenails onychomychosis. Moreover, the incidence of concomitant infections caused by dermatophytes or non-dermatophytes and *Candida* spp (figure 84) [411], or by different species of Candida at the same time, has raised

during the last years. These concomitant infections are an important healthy issue as most of the commercialized treatments are not effective against mixed infections.

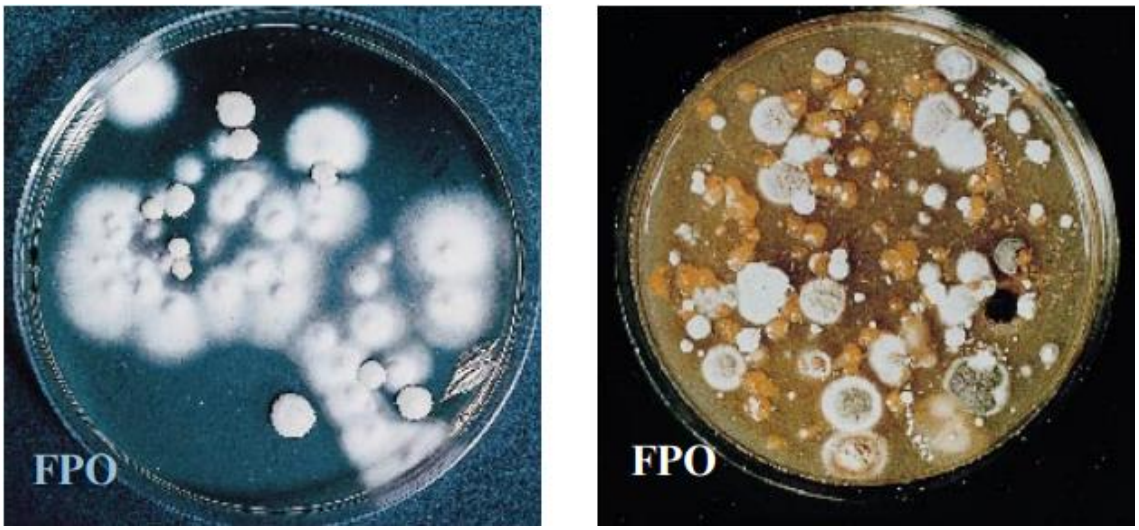

Figure 84. Mixed cultures of different infections caused by dermatophytes/non-dermatophytes and *Candida* spp. Culture of infected nails by *T. mentagrophytes* and *Candida* spp. (left), and by *T. rubrum*, *Scopulariopsis* and yeasts (right). Image taken from [411].

AP1.1.5. Predisposing factors

Onychomycosis predisposing factors can be classified into personal or environmental factors. The first group includes nail trauma, male gender (men are 1.7 to 3 times more likely to have a fungal nail infections compared to women); age (the prevalence of onychomycosis in patients younger than 19 years of age is 0.7%, in patients ranging 20-39 years of age is 3.1%, in patients ranging 40-59 years of age is 9.5% and in patients above 60 years is 18.32%) [412]; genetic predisposition; hyperhydrosis, peripherical vascular diseases (lower extremity venous disease); microcirculatory disorders; Raynaud's phenomenon; collagen diseases; diabetes; HIV; finger deformities; dystrophic nails; chronic skin diseases such as psoriasis, ichthyosis and atopic dermatitis; cancer; monocutaneous candidiasis; long-term use of antibiotics and immunosuppressors; poor hygiene and tinea pedis [391,392,394-396,413]. Regarding the second group, the environmental factors, the most important risk factors are tropical or subtropical climate; occlusion and excessive sweating on the hands or feet; repeated trauma; detergents; abrasive liquids and food handling; wearing boots and closed shoes; contact with contaminated tools and equipment for cosmetic treatment of the hands and

finger/toenails (manicure and pedicure); smoking and contact with animals such as family pets [402]. The increasing exposure to the pathogens in public bathrooms and swimming pools, together with the habit of wearing other people's shoes, increases the risk of contracting onychomycosis.

In order to understand the different clinical types of onychomycosis, a brief description of the pathophysiology of this infection is included below.

AP1.1.6. Pathophysiology of onychomycosis

As detailed in figure 85, the nail structural components include the proximal and lateral folds, cuticle, matrix, plate, bed and hyponichium [412].

The ***proximal fold*** refers to the skin folded over the part of the nail plate attached to the finger while the ***lateral fold***, scientifically known as *paronychium*, is the soft tissue surrounding the border of the nail [414].

The ***cuticle*** is the semi-circular layer of non-living skin cells that cover the back of the visible nail plate. It consists of modified stratum corneum that is originated at the junction of the dorsal and ventral epithelial surfaces and proceeds along the nail surface [415]. The main function of the cuticle is to protect the matrix from infections caused by microorganisms [412].

The ***matrix***, commonly known as the growth center of the nail, is located under the cuticle at the proximal end [415-417]. It contains nerves, lymph, blood vessels and basal cells that migrate into the nail plate, where they divide and differentiate, forming the hard, keratinized component of the nail plate. The length, size and thickness of the matrix determine the width and the thickness of the nail plate. The matrix would continue to grow as long as it would received nutrition.

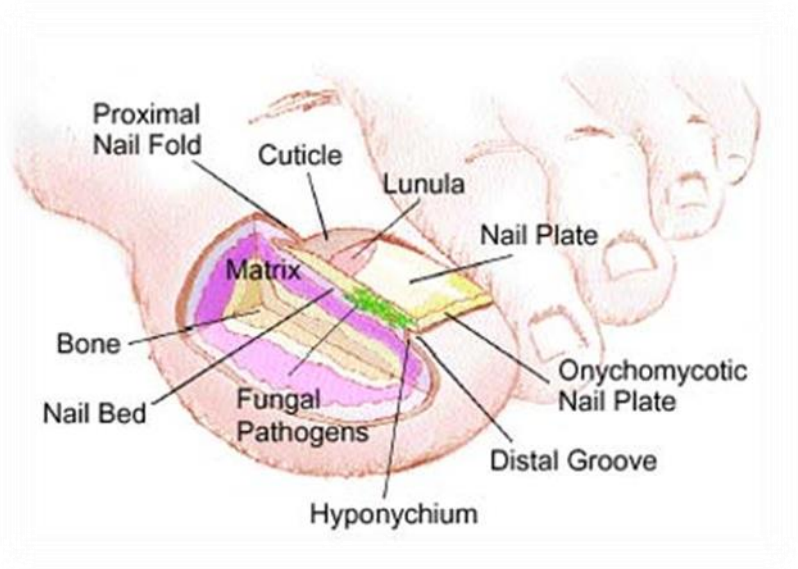

Figure 85. Nail structural composition (taken from [412]).

The ***nail plate*** is the largest structure of the nail unit and it is attached to the top of the nail bed [415]. It is a transparent structure that is gradually replaced as it grows. It is composed by several layers of dead, compacted cells that confers the nail strength and flexibility [418] This structure is completely renewed every 6 months on fingers and every 10-18 months on toes [412]. The growth speed is usually faster on the longer digits which are the ones usually involved in the trauma.

The ***nail bed***, located under the nail plate, consists of epidermal grooves and ridges that contain small blood vessels [419]. Due to its location, a bacterial infection in the nail bed increases the possibilities of developing osteomyelitis [275,412].

Finally, the ***hyponychium*** is the epithelium located beneath the nail plate at the junction between the free edge and the skin of the fingerprint fingerprint [412,420].

AP1.1.7. Progression of fungal infection

There are some studies suggesting that the skin is the main source of fungal organisms that infect the nail [421-423]. Initially the fungal microorganisms invade the part

located in between the nail plate and the nail bed through an opening in the subungual space of the hyponychium, close to the distal groove. The infection usually starts distally and then progresses proximally except in those cases in which there is a nail trauma. The trauma would allow for the direct entry of the microorganisms. Onychomycosis is usually considered as a superficial infection as the growth of fungal hyphae occur on the nail bed (below the nail plate) [412].

The susceptibility to the onychomycosis as well as the progression of the disease, once the nails have been infected, depends on the interaction of several factors (fungal agent, host and environmental factors) [424]. Even though the disease has a low overall prevalence, this is much higher in certain groups of population such as older people and immunocompromised patients. The onychomycosis, usually considered as a nuisance but not really important health problem, can cause morbidity in all population groups but mainly in high-risk patients (diabetics, HIV, patients with acquired immunodeficiency syndrome [AIDS] and patients with other types of immunosuppression [i.e. long-term corticosteroid therapy and transplant recipients]. The impact of the onychomycosis in these types of patients may be really significant. For example, in the case of the diabetic patients, if the infection is not treated and the natural course of this process continues, a cellulitic or osteomyelitic stage can take place. This can be followed by necrosis and finally, major lower-limb amputation.

Figure 86 shows the natural course of the onychomycosis in non-treated high-risk patients.

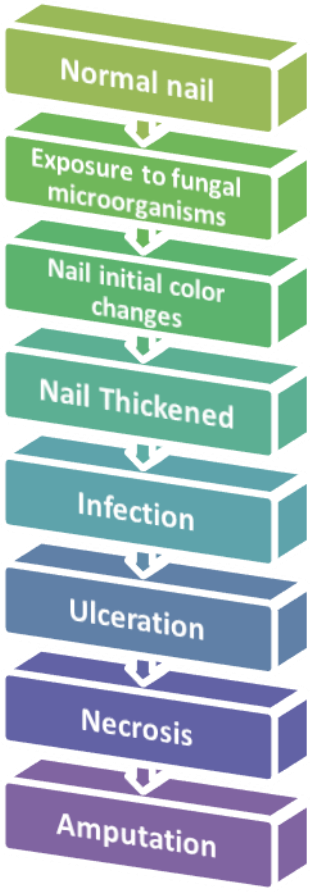

Figure 86. Natural course of onychomycosis and potential sequelae in non-treated high-risk patients.

AP1.1.8. Clinical types of onychomycosis

There are different clinical types of onychomycosis depending on the area that is affected and on the modality of the nail invasion. The patients can be affected by one subtype of onychomycosis or a combination of various subtypes.

The most commonly detected clinical types of onychomycosis are the distal lateral subungual onychomycosis (DLSO); the white superficial onychomycosis (WSO); the proximal subungual onychomycosis (PSO); the endonyx onychomycosis (EO); the total dystrophic onychomycosis (TDO) and the candidal onychomycosis (CO).

Below there is a brief description of each of the subtypes.

- **Distal lateral subungual onychomycosis (DLSO)**

The distal subungual onychomycosis is the most common variant of the infection (in a case study performed by Kolonchenko *et al* in 2013, approximately the 89% of the patients included in the trial presented DLSO [425]. It is characterized by an invasion of the nail bed where fungi reach the nail through the hyponychium and invade the undersurface of the nail unit plate being spread proximally [400]. This invasion results in subungual hyperkeratosis (thickening of the nail plate) and onycholysis (separation of the nail plate from the nail bed) [407,423]. The nail plate appears yellow-white as a consequence of the onycholysis, the nail becomes cornified and the normal nail contour is lost [394]. Not so frequently, a brown, black or orange discoloration of the onycholytic nail can be detected. DLSO can be associated to black pigmentation of the nail when the pathogen responsible for the infection is the Melanoids variant of *Trichophyton rubrum* or other melanin-producer fungi such as *Aspegillus niger* or *Neoscytalidium dimidiatum* [391]. DLSO usually affects one or both of the great toenails and it is usually associated to *tinea pedis*.

Even though DLSO is the most common presentation of dermatophyte nail infection [395], it can be also produced by non-dermatophytes [411]. DLSO is usually caused by the dermatophyte *T. rubrum*, although *T. mentagrophytes*, *T. tonsurans* and *E. floccosum* are also known to be causative [415]. The DLSO associated with non-dermatophytes is usually characterized by a marked periungual inflammation [403].

- **White superficial onychomycosis (WSO)**

The white superficial onychomycosis is less common than the DLSO (10% estimated number of onychomycotic patients) [423]. It appears when fungi directly invade the superficial layers of the nail plate. Fungi invade the dorsal nail plate and form colonies that appear as white opaque formations easily scraped away [391]. These colonies, located on the surface of the nail, has the appearance of white patches ("white islands") with distinct edges [394,396].

The classical WSO, non-invasive infection, is the most detected onychomycosis in children [395] and it is caused by dermathophytes (*Trichophyton interdigitale, T. mentagrophytes*) which colonize the most superficial layers of the nail plate without penetrating the nail (the fungal microorganisms initially grow on the top of the nail

plate) [412]. On the contrary, the molds (*Fusarium*, *Acremonium* and *Aspergillus* spp) usually cause a WSO with a deeper nail invasion [399,400].

- **Proximal subungual onychomycosis (PSO)**

In the proximal subungual onychomycosis the infections begins by the fungi invasion of the cuticle and the ventral portion of the proximal nail fold and spreads to the newly forming nail plate which results in subungual hyperkeratosis, proximal onycholysis and destruction of the proximal nail plate [394]. PSO caused by dermatophytes is very strange and it appears as a white area under the proximal nail plate, in the lunula area [426]. Although it is the less common presentation of dermatophyte onychomycosis in general population, it is common in persons with AIDS (it has been sometimes considered an useful marker of HIV infection [395,411, 412]. PSO is usually associated to non-dermatophyte mold infections caused by *Aspergillus* spp and *Fusarium* spp in which the nail plate presents discoloration that might be associated with acute periungual inflammation, and in some cases with purulent discharge [403].

- **Endonyx onychomycosis (EO)**

The endoxyn onychomycosis could be considered as a variant of the DLSO in which the fungi nail plate invasion takes place directly via the skin (the fungus immediately penetrates the nail plate keratin) [395,425]. It is characterized by a massive nail plate invasion in the absence of nail bed involvement. Clinically, the nail plate show lamellar splitting, a milky-white discoloration [394] and, conversely to DLSO, there are no signs of subungual hyperkeratosis or onycholysis [391]. It is produced by microorganisms that usually produce endothrix scalp infections (e.g. *T. soudanense or violaceum*).

- **Candidal onychomycosis (CO)**

The candidal onychomycosis usually occurs in patients with chronic monocutaneous candidiasis [415] and in the 70% of the cases it is caused by *C. albicans* [400]. Both toenails and fingernails can be involved. *Candida* sp invade directly the nail plate and produce *C.* paronychia, *C.* granuloma or *C.* onycholysis. In between all, *Candida* paronychia is the predominant variant and it is characterized by swelling and erythema of the proximal and lateral nail folds. This variant is also known as whitlow. *Candida granuloma* is really uncommon and is characterized by direct invasion and thickening of the nail plate with associated paranonychia. Finally, *Candida* onycholysis occurs

when the nail plate separates from the nail bed. The distal subungual hyperkeratosis can be appreciated as a yellowish-grey mass lifting of the nail plate [394].

- **Total dystrophic onychomycosis (TDO)**

Finally, the total dystrophic onychomycosis is considered as the most severe stage of onychomycosis and it can be a result of long-standing DLSO or PSO. It consists of the total destruction of the nail plate [395]. The nail plate is diffusely thickened, friable and yellowish. There are two main forms of TDO: secondary total dystrophic onychomycosis and primary total dystrophic onychomycosis [427]. The secondary TDO results from a complete progression of any of the previously mentioned destructive nail dystrophies, while the primary TDO occurs in those cases of chronic monocutaneous candidiasis where all tissues of the nail apparatus may be involved simultaneously, including the nail folds [428].

Once the clinical types of onychomycosis have been described and before considering the possible treatments, one should take into account which factors influence the drug transport through the nail plate and which techniques are currently available to enhance the drug penetration.

AP1.1.9. Nail permeability

AP1.1.9.1. Factors that influence the drug transport into and through the nail plate

There are many factors that should be considered before designing a treatment helpful for the onychomycosis therapy. The molecular size of the drug, the hydrophilicity and lipophilicity, the nature of the vehicle as well as the pH of the vehicle and the solute charge, are the most relevant factors [429].

AP1.1.9.1.1. Molecular size of diffusing drug

The molecular size of the drug is really important for the topical treatment of onychomycosis. There is an inverse relationship between the size of the drug and the

penetration into the nail plate. The larger the molecule size, the harder the molecule diffusion through the keratin [395,430,431].

AP1.1.9.1.2. Hydrophilicity/Lipophilicity of the diffusing molecule

The use of nail lacquers containing alcohols, that allow to obtain systems that rapidly dry once applied to the nail, is well known. The increased lipophilicity of a diffusing alcohol molecule reduces the permeability coefficient until a certain point after which further increase in lipophilicity results in increased permeation. Nevertheless, except for methanol, the permeability coefficient of net alcohols (water-free) is approximately five times smaller than the permeability coefficient of diluted alcohols [432]. When an aqueous solution is used, the nails swell as water is taken up into the nail plates. As a consequence, the keratin network expands which leads to the formation of larger pores through which diffusing molecules can permeate more easily [416,429]

AP1.1.9.1.3. Nature of the vehicle

Water hydrates the nail plate which consequently swells. Considering the nail plate to be an hydrogel, swelling results in increased distance between the keratin fibers, the formation of larger pores through which permeating molecules can diffuse and hence, increased permeation of the molecules. Replacing water with non-polar solvents, which do not hydrate the nail, is therefore expected to reduce drug permeation into the nail plate [416,429,432].

AP1.1.9.1.4. pH of the vehicle and solute charge

It seems that the pH of the formulation has a distinct effect on the drug permeation through the nail plate. Uncharged species permeate to a greater extent compared to charged ones [416,432].

AP.1.1.9.2. Techniques for enhancing transungual drug delivery

Nail is said to be composed by approximately 25 layers of tightly bound keratinized cells. It is approximately 100 folds thicker than subcutaneous and therefore, the trans-nail penetration of drugs is really challenging. In order to overcome the nail barrier and to be able to transport the antifungal drugs above the minimal inhibitory concentration (MIC), different chemical, physical and mechanical methods have been used [429,433].

AP1.1.9.2.1. Chemical methods to enhance drug penetration

From a chemically point of view, drug permeation into the nail plate, can be assisted by breaking the physical and chemical bounds responsible for the stability of nail keratin which would destabilize the keratin, compromise the integrity of the nail barrier and allow penetration of drug molecules. Some potential targets of the chemical enhancers are the disulphide, peptide, hydrogen and polar bonds in keratin.

- **Keratolytic enhancers or nail softening agents**

In 1998, the paper published by Quintanar-Guerrero *et al*., described the effect of some keratolytic agents (urea, salicylic acid and papain) on the permeability of three imidazole antifungal drugs (miconazole, ketoconazole and itraconazole). Both urea and salycilic acid were found not only to hydrate and soften the nail plate but also to damage the surface of the nail plates, resulting in fractured surfaces. The use of urea followed by an oxidizing agent (H_2O_2) dramatically improved the human nail penetration. All three, urea, papain and salicylic acid, act via disruption of the keratin disulphide bonds resulting in the formation of pores that provide "open" drug transport channels [434,435].

- **Compounds containing sulfhydryl groups**

Compounds which contain sulfhydryl (-SH) groups such as acetylcysteine, cysteine or mercaptoethanol, can reduce and, therefore cleave the disulphide bonds in nail proteins. These chemicals have been found to produce structural alterations in nail plate by breaking the disulphide bounds which are responsible for nail integrity and therefore influence drug transport. However, post-treatment barrier integrity studies performed in the nails treated with these enhancers have demonstrated that the changes induced in the nail keratin matrix are irreversible. The disulphide broken bonds produce irreversible structural changes in the nail plate [436].

- **Keratinolytic enzymes**

Due to the great abundance of keratin filaments, the use of keratinase for the hydrolysis of keratinic tissues such as the stratum corneum (SC), has been considered as an alternative for drug penetration enhancement. Mohorcic *et al* described for the first time the efficacy of keratinase administration over the nail plate. These authors designed permeation studies using modified Franz diffusion cells and metformin hydrochloride as

a model of drug, and they found that the keratinase markedly enhanced the drug penetration [433,437]

AP1.1.9.2.2. Physical methods to enhance nail penetration

The physical methods for drug penetration enhancement are usually preferred to the chemical methods in the delivery of hydrophilic and macromolecular drugs (these methods obtain a higher drug permeation).

- **Iontophoresis**

This method involves the delivery of a compound across a membrane using an electric field. Several are the factors that enhance the drug diffusion through the hydrated keratin of the nail: electrorepulsion/electrophoresis; interaction between the electric field and the charge of the ionic permeant; electroosmosis; convective solvent flow in preexisting and newly created charged pathways; and permeabilization/electroporation, electric field-induced pore induction. The type of transport varies depending on the charge of the molecule. If the transport of a neutral drug has to be enhanced, the permeation will rely on an electroosmotic process. On the contrary, if there is the need to enhance the permeation of a charged molecule, the transport will rely on electrophoresis and electroosmosis. In all cases, the iontophoresis has a reversible effect on the nails [438-440].

- **Etching**

The "etching" basically consists on the formation of profuse microporosities. These microporosities are known to increase the wettability and the surface area and to decrease the contact angle. As stated by Repka *et al.* the presence of microporosities improves the interpenetration and bonding of a polymeric delivery system and facilitates the interdiffusion of a therapeutic agent [441]. Once the nail plate surface has been "etched", a sustained release, hydrophilic, polymer film drug delivery system can be applied. This "etching" or roughness of the nail plate results in increased surface area which improves the polymer chains inter-diffusion, increasing the bioadhesion and the retention of the delivery system.

- **Carbon dioxide laser**

The use of carbon dioxide as a penetration enhancer can produce positive but unpredictable results. This method enhances the nail plate penetration and therefore the laser nail radiation has to be followed by daily topical antifungal treatment [442].

- **Hydration and occlusion**

The hydration of the nail plate results in an increase of the pore size of the nail matrix and consequently in enhanced drug permeation [431] Hydrated nails are well known to be more elastic and permeable. Sometimes, due to the onychomycosis, there is a decrease in transonychial water loss, ceramide concentration and water binding capacity. In these cases, and in order to enhance the drug transport, the occlusion could be an option. The reconstitution of water and lipid homeostatisis in distrophic nails would allow for a higher drug permeation [416,429,432,443].

AP1.1.9.2.3. Mechanical methods to enhance drug penetration

The mechanical methods include nail abrasion and nail avulsion. Even though these methods have been widely used by dermatologists and podiatrists over the last decades, they are considered invasive and potentially painful [432]. The reason why we have reserved these enhanced penetration methods for the end relies on the fact that they should only be used if none of the previously described chemical or physical penetration methods work.

- **Nail abrasion**

The nail abrasion implies the sanding of the nail plate in order to reduce its thickness or to completely destroy it. Sanding, using sandpaper number 150 or 180, must be done on the edges of the nail in order not to cause discomfort. Nail abrasion thins the nail plate which decreases the fungal mass onychomycosis and exposes the nail bed, enhancing consequently the action of the drug.

- **Nail avulsion**

Nail avulsion, total or partial, involve surgical removal of the entire or partially affected nail plate. The avulsion has to be done under local anesthesia. A chemical/non-surgical

nail avulsion can be also performed using urea or a combination of urea and salicylic acid at high concentrations.

Onychomycosis is an infectious disorder that deserves prompt and appropriate care. As onychomycosis management remains a clinical challenge from the medical point of view, the treatment plan has to be carefully chosen in order to provide the best potential for cure [444]. Before initiating the onychomycosis therapy several factors might be taken into account; the pathogen agent responsible for the infection, its susceptibility to the antifungal drugs, the patient co-morbidities, the possible interaction with other drugs or diet, the side effects derivate from the antifungal administration, the patient's age and the cost of the therapy. An evaluation of the extension and the severity of the disease would be also helpful [399].

AP1.1.10. Treatment

Onychomycosis treatments are mainly classified into: pharmacological treatments, which include topical and systemic antifungal therapies; and non-pharmacological treatments, which include laser and photodynamic therapy, chemical or surgical abrasion and mechanical debridement.

AP1.1.10.1. Pharmacological therapies

As stated above, the pharmacological treatment encompasses the topical and oral antifungal therapies (figure 87). As the topical administration is usually considered as first line treatment, it would be the first described.

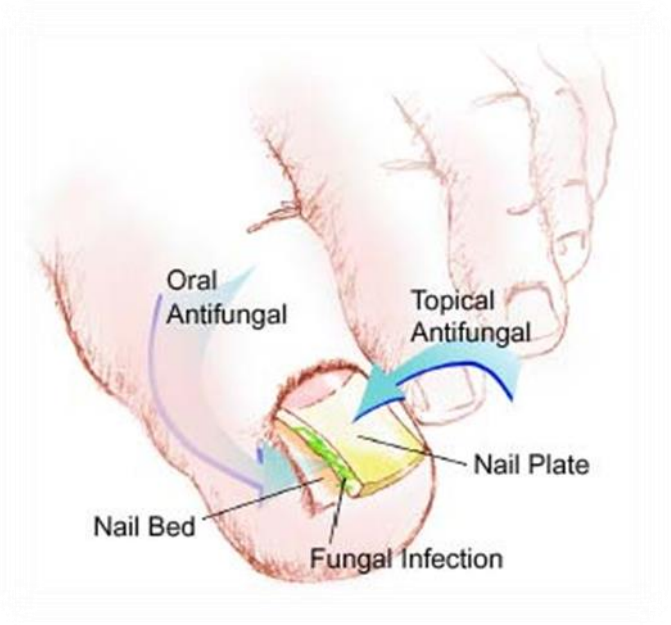

Figure 87. Pharmacological treatments of onychomycosis

AP1.1.10.1.1. Topical treatment

The topical therapy aims to apply the drug directly into the nail. The administration of different antifungal drugs included in a matrix (usually a nail lacquer) into the nail plate are the bases of this treatment.

Penetration of topical antifungals through the nail plate requires a vehicle that is specifically formulated for transungual delivery. The poor nail unit penetration limits the use of topical antifungal agents and therefore, relapses and re-infections are common, occurring in at least 20-25% of the patients.

The topical antifungal therapy is basically focused on the application of nail lacquers. The nail lacquers are effective, when used in monotherapy, in the treatment of WSO and DLSO limited to the distal nail. These lacquers should only be used in those cases in which the infection involves less than half of the distal nail plate or in patients unable to tolerate systemic treatment.

The possible topical treatments include:

- **Amorolfine**

The amorolfine, a morpholine-derived antifungal drug (figure 88) with a broad spectra of action acts blocking the delta 14 reduction and delta 7-8 isomerization, resulting in

the depletion of ergosterol and the accumulation of ignosterol in the fungal cytoplasmatic membrane. The cell wall becomes thicker and chitin deposits are formed inside and outside the fungal cell wall. The amorolfine has fungistatic and fungicidal properties against dermatophytes, non-dermatohytes molds and yeasts. Amorolfine 5% (w/vol) nail lacquer is recommended for onychomycosis without matrix involvement and mild cases of distal and lateral subungual onychomycosis that affect up to two nails [396,398,399,433,445,446].

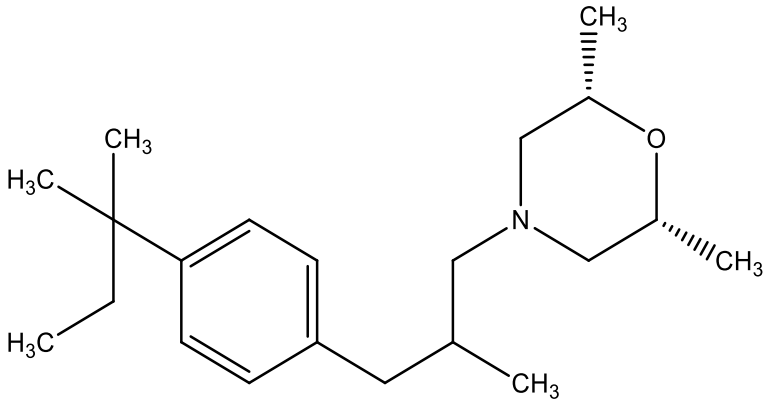

Figure 88. Chemical structure of amorolfine

Amorolfine 5% in non-water soluble nail lacquer is applied once a week. The film, a water-insoluble film-forming polymer, seals the drug, which remains in the nail until next application. The treatment with amorolfine lasts until the nail has grown, approximately 9-12 months in toenails and 6 months in fingernails.

- **Ciclopirox**

Ciclopirox is a drug that structurally belongs to the hydroxypyridine family (figure 89). Its mechanisms of action is related to the inhibition of metal-dependent enzymes by chelating of polyvalent cations (Fe^{3+}, Al^{3+}) which affects the intracellular energy production and produce toxic peroxide degradation. It also acts inhibiting the fungal nutrient uptake, resulting in a decrease in nucleotides and a reduction in protein synthesis. Ciclopirox has fungicidal, anti-inflammatory and anti-allergic activity.

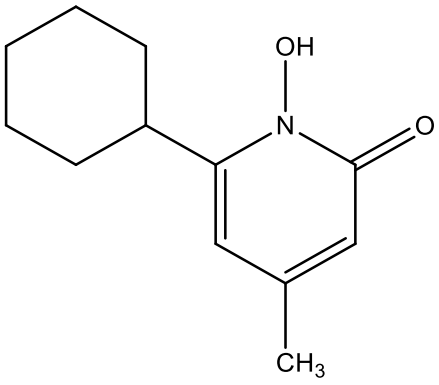

Figure 89. Chemical structure of ciclopirox

Ciclopirox olamine 8% (w/vol) in non-water and water soluble nail lacquer solutions should be applied daily covering the total nail plate surface and 5 mm of the surrounding skin. The treatment usually lasts 12 months [395,398,433,445-448].

- **Tioconazole**

Tioconazole is one of the antifungal derived imidazoles agents (figure 90) first developed by Pfizer. It is effective against dermatophytes and yeasts (*T. rubrum* and *Candida albicans*). It is marketed as Trosyl® nail solution which contains 28% w/w tioconazole in a solution of ethylacetate and undecylenic acid [449]. Nowadays, the use of tioconazole 28% is limited, as the amorolfine and ciclopirox has demonstrate better treatment success and avoidance of the allergic contact dermatitis derived from its application [395,396].

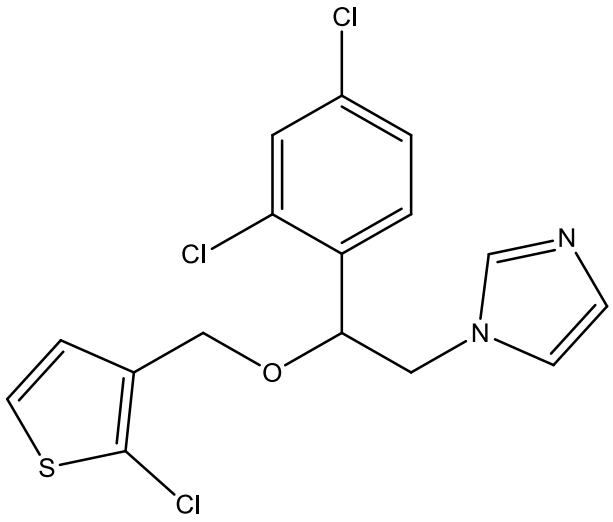

Figure 90. Chemical structure of tioconazole

- **Efinaconazole**

Efinaconazole was the first topical triazole (figure 91) developed specifically for the treatment of onychomycosis and approved by the FDA. It was approved in June 2014 for the topical treatment of dermatophyte-induced toenail onychomycosis. Its mechanism of action is based on the inhibition of lanosterol 14α-demethylase, an enzyme involved in the ergosterol biosynthesis. It is believed that the accumulation of 14α-methyl sterols and the consequent lost of ergosterol (which affects membrane function and integrity and therefore inhibits grow leading to cell death) might be responsible for the fungicidal and fungistatic activity seen in this molecule. The efinaconazole has demonstrated to be more effective than itraconazole against *T. mentagrophytes* and than clotrimazole against *C. albicans* [395,450-452].

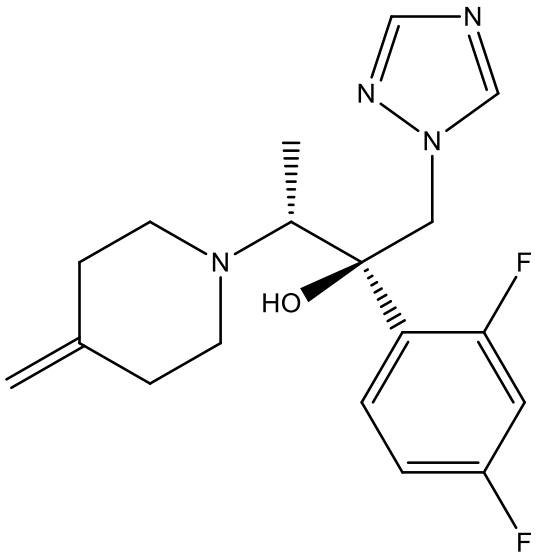

Figure 91. Chemical structure of efinaconazole

This new triazole, in a 10% (w/vol) topical solution applied once daily, was developed for the treatment of mild to moderate DLSO and it has shown to be effective avoiding nail debridement.

- **Tavaborole**

Tavaborole is the first member of a new class of pharmaceutical antifungal agents with a novel chemical structure (boron-liked) (figure 92) and mechanism of action [453]. It is an oxaborole compound that has been designed to be a lightweight, highly water soluble compound that maintains a broad-spectrum antifungal activity in the presence of keratin. It has been shown to retain its pharmacological antifungal activity in the presence of keratin which suggests that it would be effective after permeating the nail plate. Compared to other antifungals, tavaborole mechanism of action is completely different. It acts on aminoacyl-transfer RNA (tRNA) synthetases by specially binding to the editing site of the tRNA. This binding prevents the synthesis of leucine-charged tRNAs and consequently, the fungal activity is suppressed [453].

.

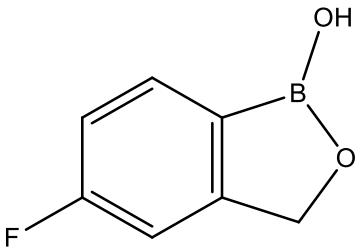

Figure 92. Chemical structure of tavaborole

This compound has demonstrated a great ability to penetrate the nail (its low molecular weight allows for a high amount of penetration through full-thickness human nail plates) which avoids the aggressive debridement required with other lacquers. Due to its broad spectrum antifungal activity against dermatophytes, molds and yeasts it is indicated in the topical treatment of toenail onychomycosis. In July 2014, it has been approved as a 5% topical solution by the FDA [454].

- **Antifungal drugs under clinical trial**

Other possible topical treatments include the terbinafine (figure 93) nail solution and spray (TDT 067) and other two terbinafine formulations (MOB-015 and TMI-358) which are under clinical trials. The topical application of luliconazole 10%, an imidazole molecule (figure 94) with fungicide and fungistatic activity, has already completed phase 1 and phase 2a for the treatment of moderate to severe distal subungual onychomycosis with excellent tolerability and safety profile [391,392,455].

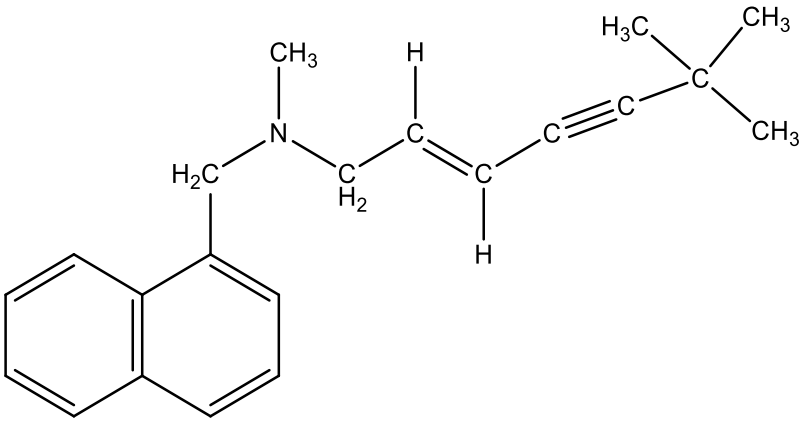

Figure 93. Chemical structure of terbinafine

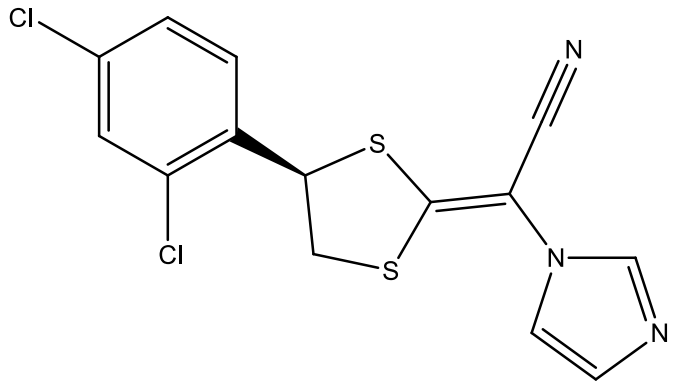

Figure 94. Chemical structure of luliconazole

The topical treatment of onychomycosis requires several months (from 6 to 12 months), as the nail growth is very slow. Even though the treatment lasts long, in most of the cases, and more in the elderly, the topical treatment is the first line treatment for patients presenting DLSO due to dermatophytes involving one or two of the great toe nails. In these particular cases, the topical antifungal administration is recommended to be associated, whenever possible, with periodic removal of the affected nail plate.

The indications for topical treatment of onychomycosis were summarized by Iorrizo *et al* [446] as follows:

- Distal subungual onychomycosis affecting <50% of the nail without matrix area involvement, without the presence of yellow streaks along the lateral margin of the nail and without yellow onycholytic areas in the central portion of the nail (dermatophytoma)
- "Classical" white superficial onychomycosis (WSO) (excluding cases of deep WSO)
- Onychomycosis due to molds (except for those caused by *Aspergillus* sp.). This onychomycosis usually do not respond to systemic antifungal administration.
- Patients unwilling or unable to tolerate oral therapy.
- Patients requiring maintenance therapy after the course of an oral therapy. The topical treatment administration after a systemic therapy is sometimes also considered as an alternative useful for avoiding recurrence in patients cured by these oral therapies [398].

Even though the topical treatment of onychomycosis is widely spread, there are some infections in which a systemic administration is highly recommended. The DLSO extending to the proximal nail, the PSO due to dermatophyte and the deeply infiltrating WSO are some of the onychomycosis that require a drug systemic administration.

AP1.1.10.1.2. Systemic treatment

The systemic therapy of onychomycosis consists on the oral administration of antifungal drugs during several months. Usually, the drug is administered until cure is achieve or side effects and/or resistant appear. The drugs commonly included in the systemic therapy belong to the family of the azoles and alkylamines and they can be administered continuously or in pulse manner [399].

The drugs usually administered in the systemic therapy include the terbinafine, itraconazole and fluconazole. It has been demonstrated that the systemic administration of these drugs has a good safety profile and produce 90% of mycological cure in the fingernails infections and 80% in the toenails infections [391].

- **Terbinafine**

The terbinafine is an alkylamine drug first synthesized in 1979 (figure 95), that acts blocking the biosythesis of ergosterol and therefore, damaging the fungal cell wall integrity. It is a strong lipophilic molecule that has demonstrated to be well distributed in the skin, fat and nails. This fungicidal drug penetrates the nail through the nail matrix and the nail bed. Terbinafine is generally well tolerated and has fewer interactions with other drugs than azoles [395].

The terbinafine can be administered at a dose of 250 mg/day in a continuous treatment of 12 weeks or as pulse therapy in which the first 4 weeks the patient would receive 500 mg/day and then the following 4 weeks the patient would not receive any treatment [393].

- **Itraconazole**

Itraconazole is an azole compound (figure 97) developed in the late 1980s that is effective against dermatophytes, yeasts and other fungal infections. It acts differently to terbinafine. In this case, the drug inhibits the fungal cell CYP450 enzyme, 14-α-demethylase which is responsible for the transformation of lanosterol to ergosterol, affecting the synthesis of the fungal cells wall. It is a highly lipophilic drug that is well absorbed in the presence of food and acidic pH.

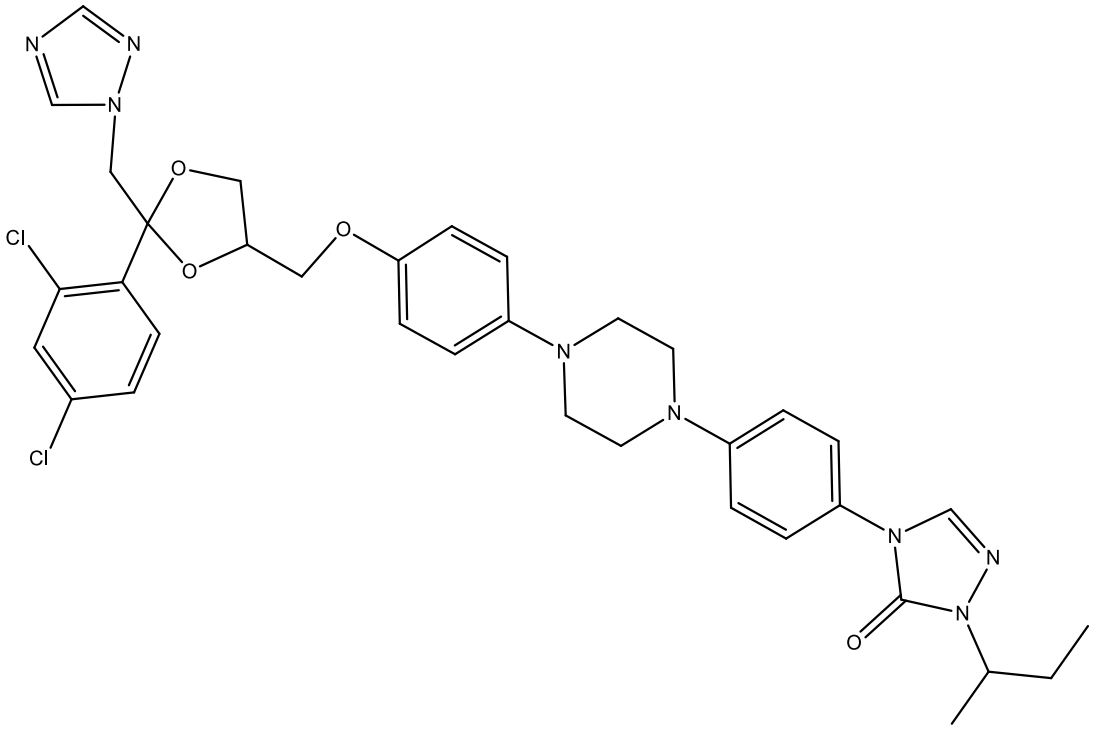

Figure 95. Chemical structure of itraconazole.

It is usually administered at a dose of 200 mg/daily for 6 weeks in the fingernails and for 12 weeks in the treatment of the toenails onychomycosis. It can also be administered in pulse therapy at 400 mg/day (200 mg twice a day) during one week per month. A total of two pulses (2 months treatment) and three pulses (three months treatment) are necessary for the fingernails and toenails treatment, respectively [395,398,403,415,444,456].

- **Fluconazole**

Fluconazole is a hydrophilic and keratoniphilic bistriazole (figure 96) that acts similarly to itraconazole, affecting also the synthesis of ergosterol. Nevertheless, in this case, the flucanozole has almost no effect on human sterol byosynthesis and its absorption is not related to food uptake or pH. It has demonstrated to be effective against dermatophyte and many *Candida* spp but its administration is limited due to the important interactions with other drugs (it acts at the level of the CYP450) [395,444,457].

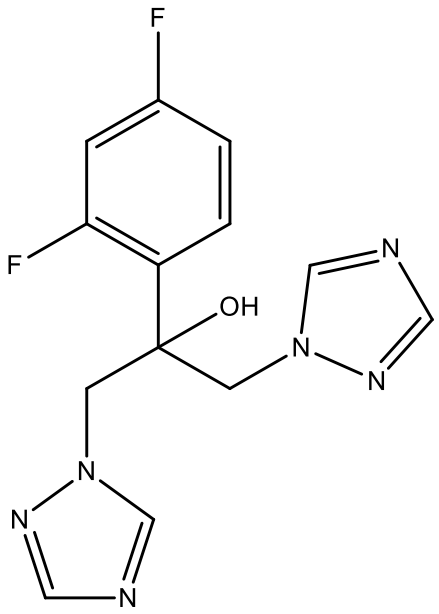

Figure 96. Chemical structure of fluconazole.

It is used in the treatment of dermatophyte onychomycosis at a dose of 150-300 mg/week during at least 6 months.

The continuous terbinafine and the pulse itraconazole therapies have demonstrated to be effective in the treatment of toenails onychomycosis in patients with diabetes. Treatment with fluconazole is less effective than the treatments with terbinafine and itraconazole and therefore, these two are preferred in the systemic administration.

Apart from the drugs already described, the voriconazole, posaconazole, ravuconazole and albaconazole are new drugs with similar efficacy to terbinafine. Some of these azoles are still on clinical trials but there is a lot of interest focused on them as new possible onychomycosis systemic therapies.

- **Voriconazole**

Voriconazole is a molecule which structure is really similar to that of fluconazole (figure 97). It was approved by the FDA in 2002 and it can be found as suspension for oral administration (40 mg/mL), as tablets (200 mg) or as intravenous infusion (50 mg). It has been reported to be effective against *Scopulariopsis brevicaulis*, *Fusarium* spp. and S*cytalidium dimidiatium*. It might be useful in resistant cases of onychomycosis but it has not been yet studied in clinical trials of nail fungal infections infections [395,396,399,446,458,459].

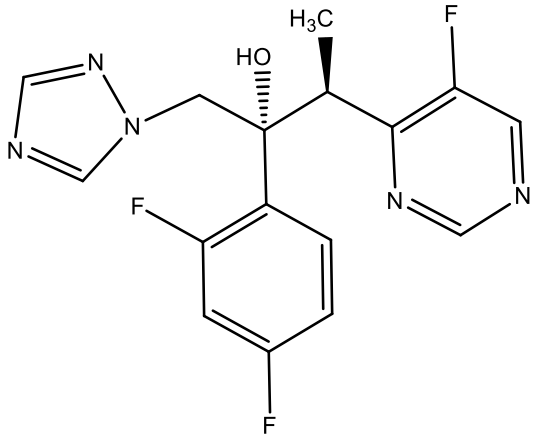

Figure 97. Chemical structure of voriconazole

- **Posaconazole**

As well as the other azoles compounds, posaconazole (figure 98), inhibits the CYP450 14-α-demethylase but its enzyme's inhibition is stronger than that produced by itraconazole, especially in the infections caused by *Aspergillus* spp. It is available as an oral suspension (40 mg/mL) and not only its spectrum of action is broader than that of fluconazole but also it is more active than the latest. It is effective against *Zygomycetes*, *Candida* spp and molds. A comparative blinded clinical trial carried out with posaconazole and terbinafine showed that the number of patients receiving posaconazole at 200 mg/24weeks and 400 mg/24 weeks with complete cure and treatment success was higher than for terbinafine 250 mg/12 (393,395,396,399,403,446,460). Even though the success was greater, the cost of the

treatment and the dose might be considered before this drug would be approved for the treatment of onychomycosis.

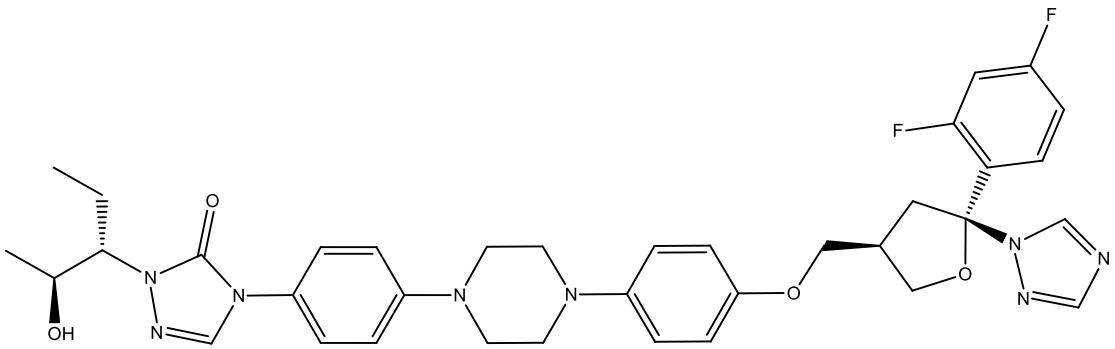

Figure 98. Chemical structure of posaconazole

- **Ravuconazole**

Ravuconazole, which is structurally similar to fluconazole and voriconazole (figure 101), acts also inhibiting the 14-α-demethylase. Its potency is similar to that of itraconazole and it is active against Candida spp, *Cryptococcus neoformans*, *.A fumigatus*, dermatophytes and dematiaceous fungi. Its spectra of action as well as its success in the treatment of onychomycosis is still under study [395,399,461].

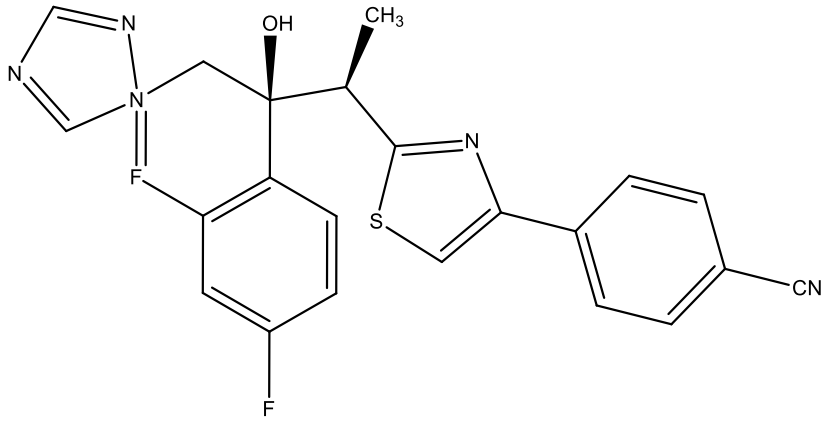

Figure 99. Chemical structure of ravuconazole

Several new azoles such as isavuconazole (figure 100) (which has similar activity to terbinafine), pramiconazole (figure 101) (which has shown to have a long half-life and its posology could be possibly once/daily) and albaconazole (figure 102) (new azole with broad spectra of action and excellent oral bioavailability) are being studied as

possible alternatives to flucanozole and itraconazole when there is a resistance to *Candida* spp and in the infections caused by non-dermatophytes molds.

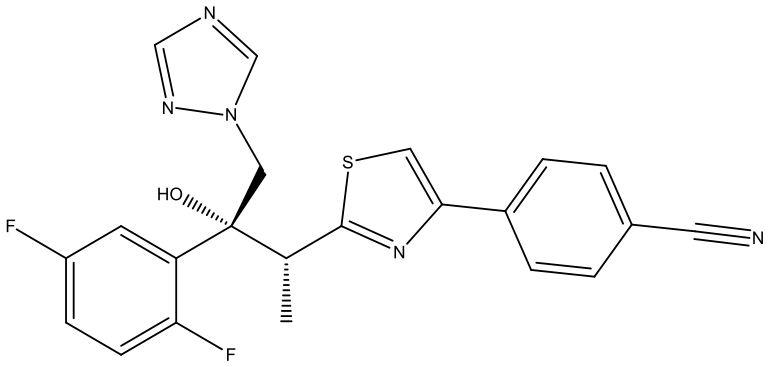

Figure 100. Chemical structure of isavuconazole.

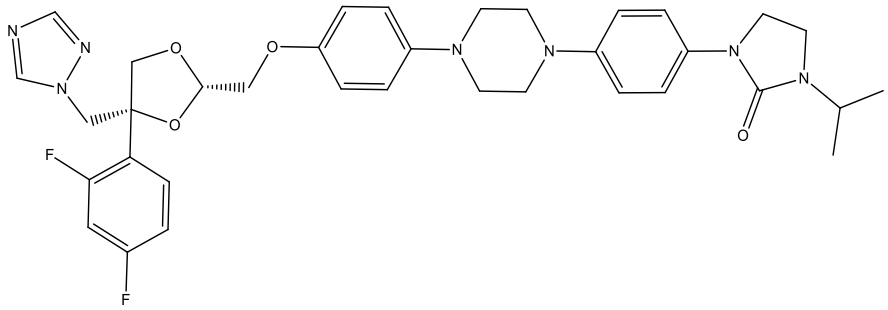

Figure 101. Chemical structure of pramiconazole.

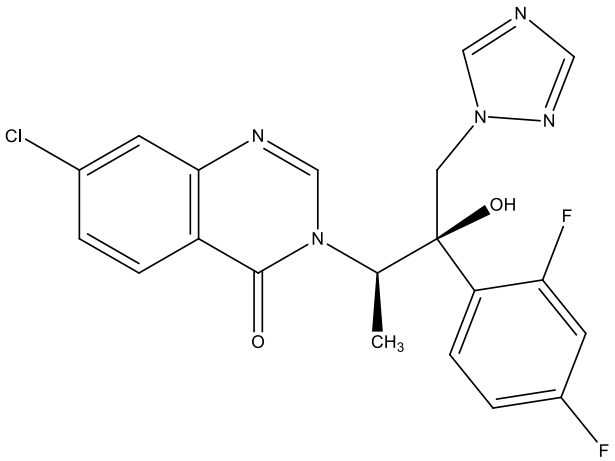

Figure 102. Chemical structure of albaconazole.

Before systemically administering an antifungal, the diagnosis should be clear as the non-dermatophyte molds are usually not susceptible to systemic therapies and therefore, the best treatment would imply the topical therapy combined with the periodical removal of the nail plate affected area. In the case of onychomycosis caused by *Candida* spp it should be taken into account that these infections usually appears in diabetic patients and in immunodepressed patients and that some systemic drugs, as terbinafine, are not active against yeasts.

The systemic therapy is in general successful but there are still some treatment failures. These can be related to the clinical characteristics of the onychomycosis (the drug is unable to reach the affected area in active concentration in the total onychomycosis, in the very thick subungual onychomycosis and in the dermatophytoma), to the etiological agents involved (some non-dermatophyte such as *Neoscytalidium, Scopulariopsis* and *Fusarium* sp. do not respond to systemic antifungals) and to the patients concomitant infections or immunodepressions (other drugs that these patients might take would reduce the antifungal blood levels and therefore the drug wouldn't be any more effective).

In order to reduce the number of treatment failures, combined therapies of systemic and topical antifungals are usually administered (even though there are almost no studies showing the greater efficacy of this combined therapy).

Despite all the efforts and the combined therapies, the onychomycosis recurrence and reinfections are really common. Up to 20% of the cured patients are estimated to have recurrence infections.

AP1.1.10.2. Non-pharmacological treatment

The non-pharmacological treatment approaches include the laser treatment, the photodynamic therapy, the chemical or surgical nail avulsion and the mechanical debridement. The use of these treatments is usually limited and reserved to those cases in which the pharmacological therapies are not effective or to those situations in which the combination of pharmacological and non-pharmacological treatments has shown to be more effective than the use of those therapies separately.

AP1.1.10.2.1. Laser treatment

The laser therapy can be used as a primary treatment for the onychomycosis due to its ablative properties or as a adjunct to topical treatments providing a higher drug penetration through the nail plate to the nail bed where the fungal growth is located [397]. The laser therapy involves the use of carbon dioxide laser, the Nd:YAG laser [398] and the diode 870 nm, 930 nm laser. All these lasers have been approved by the FDA due to their low-invasive nature [425] and the reduce number of sessions requested (the dual wavelength laser 870/930 nm has demonstrated a 100% eradication of bacteria, fungi and yeast [395,462]. The laser therapy is considered as a safe and cost-effective treatment modality in which the side effects of the drugs are avoided. The inhibitory effects of laser on fungal growth have been widely studied [463].

AP1.1.10.2.2. Photodynamic therapy (PDT)

Photodynamic therapy (PDT) is the most studied light therapy for onychomycosis. It involves the use of a photosensitizer and a light source [432]. When using PDT for onychomycosis, the pathogen absorbs the photosensitizing agent, making it more susceptible for destruction [397]. The use of both, the photosensitizer and the light source, generate reactive oxygen species that lead to chemical destruction of nail fungi. The photosensitizers that are more commonly used are the 5-aminolevulanic acid (ALA) [433], the methyl-aminolevulinate (MAL), the porphyrins and the phenothiazine dyes (methylene blue or toluidine blue). This treatment has shown to be effective against many fungi (e.g. *T. rubrum*) [398] but the high number of sessions that it implies (3 to 12) is an important inconvenience and raises the cost of the therapy [391].

The PDT is indicated for those patients with a contraindication for systemic therapy [399].

AP1.1.10.2.3. Chemical or surgical nail avulsion

Nail avulsion involves the removal of the affected nail plate which can be performed either surgically or chemically using 40% urea, 30% salicylic acid or 50% potassium iodide [412,428]. Those solutions have to be applied over the affected nail and keep under occlusion during 7 to 14 days [399,445]. After those days, the nail becomes softer and it is more easily removable. After nail removal, a topical antimycotic agent, such as bifonazole, is applied for 4 weeks in order to treat the zone. Apart from bifonazole,

other topical agents such as tioconazole 28%, amorolfine, ciclopirox 8% lacquer or terbinafine gel (this last under study) could be applied once removed the nail for 6 to 12 months.

The nail plate removal causes discomfort to the patient and therefore it is restricted to cases in which the treatment success depends on the removal of the nail plate.

AP1.1.10.2.4. Mechanical debridement

The aim of this technique is to reduce pressure and fungal load by mechanically reducing nail thickness [398]. As the mechanical debridement removes a large amount of onychomycotic material from the nail, this technique is useful since it enhances the effectiveness of other therapies, mainly those ones involving the use of antifungal agents [449,464].

Event though there exist a wide variety of possible treatments for the onychomycosis, most of them are not effective against concomitant infections.

The raise of mixed infections caused by dermatophytes or non-dermatophytes and *Candida* sp., together with the increase appearance of resistance and the long duration of the treatments, make the development of new antimycotic formulations a neccesity.

In this sense, the development of new formulations including antifungal agents with broad spectra of action, high potency and reduced resistances (such as amphotericin B) will be an alternative to the conventional treatments. The reduction of treatment duration will also increase patient compliance.

AP1.2. Description of the excipients assayed for the AmB nail lacquer.

The composition, properties and structure of the film-forming agents, plasticizers, solvents, AmB solubilizers and cosolvents used in the nail laquer matrix is detailed below.

AP1.2.1. Film-forming agents

- **Plasdone K90®**

Plasdone® is the commercial name of povidone. It is a synthetic homopolymer containing 1-vinyl-2-pirrolidinone as a monomer (figure 103). The degree grade of polymerization (n) results in a wide range of different molecular weight polymers.

It is a white (or creamy) colored, odorless and hygroscopic powder that in solution produces viscous media. It is soluble in water although its solubility is limited to the viscosity of the resulting solution; it is soluble in acids, chloroform, ethanol, ketones and methanol. It is an amphiphilic polymer that is widely used as film-former, adhesive, binder, solvent, suspensor, stabilizer and viscosity increasing agent.

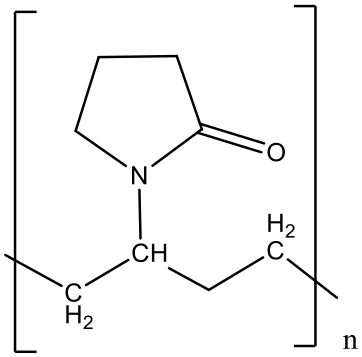

Figure 103. Chemical structure of povidone

- **Eudragit L100®**

Eudragit L100® is an anionic copolymer of methacrylic acid and methyl acrylate in a ratio 1:1 (carboxyl groups:ester groups) (figure 104). It is commercially available as a white redispersable powder. It is freely soluble in acetone, ethanol, isopropyl alcohol and methanol, and insoluble in water. When dissolved, and in contact with water it precipitates, forming white plastic films.

It is mainly used as film-forming agent, binder and diluent.

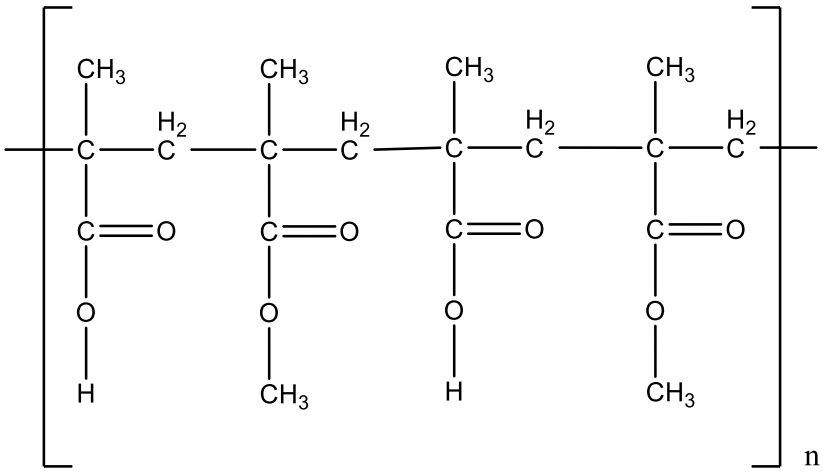

Figure 104. Chemical structure of Eudragit L100®

- **Cellulose acetate phthalate**

Cellulose acetate pthalate (CAP) (figure 105) is a hygroscopic, tasteless and odorless white powder, granule or flake. It is insoluble in water, alcohols and chlorinated and unchlorinated hydrocarbons, but soluble in some ketones, esters, ether alcohols, cyclic ethers and in certain mixtures of solvents. It is widely used as a film coating agent or as a matrix binder.

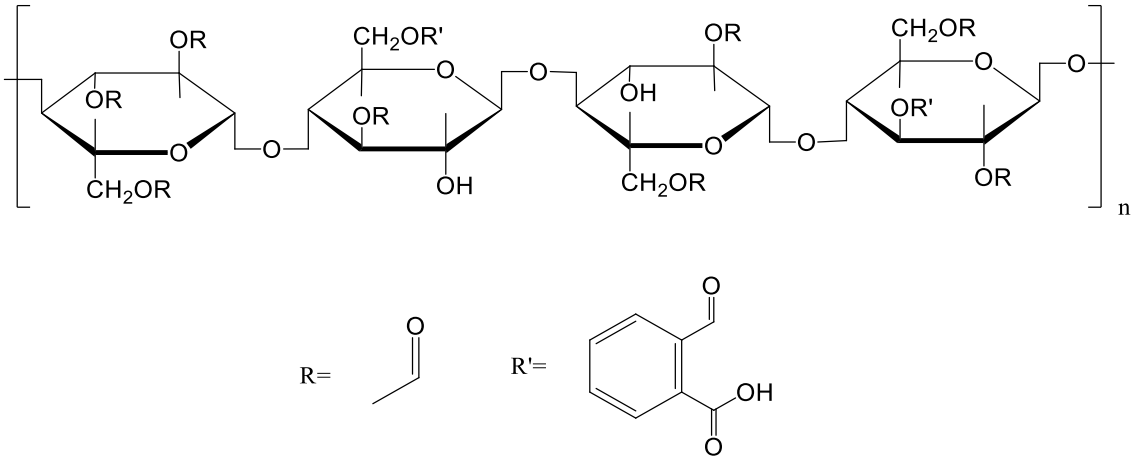

Figure 105. Chemical structure of cellulose acetate phthalate.

- **Pluronic F127®**

Pluronic®, also known as poloxamer, is a block copolymer of ethylene oxide and propylene oxide (figure 106). The two ethylene blocks are repeated 101 times and the propylene block 56 times. It is a white solid, freely soluble in water, in ethanol and in 2-propanolol.

It is a nonionic polyol surfactant used as film-forming, dispersing, emulsifying, solubilising, lubricant and wetting agent.

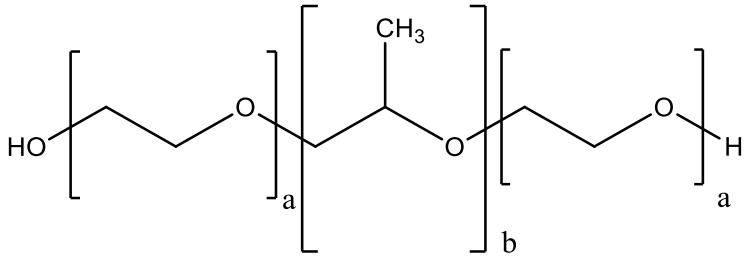

Figure 106. Chemical structure of poloxamer.

AP1.2.2. Plasticizers

- **Polyethylene glycol**

Polyethyleneglycols (PEGs) (figure 107) are stable and hydrophilic substances that are non irritant to the skin. According to the molecular weight (M_w), there exist a wide variety of PEGs.

PEGs with molecular weights ranging between 200-600 Da (M_w) are clear, colorless or pale yellow, viscous liquids; PEGs in the range 1000-5000 Da (M_w) are white pastes or waxy flakes depending of the molecular weight, and PEG above 6000 can be found as white powders. All grades of PEGs are water soluble and miscible in all proportions with other PEGs. Liquid PEGs are soluble in alcohols, acetone, benzene, glycerin and glycols; while solid PEGs are soluble in acetone, dichloromethane, ethanol and methanol, and slightly soluble in aliphatic hydrocarbons and ether. They are mainly used as plasticizers, solvents, lubricants and suspensors.

The PEGs used in the nail polish composition were PEG_{400}, PEG_{600} and PEG_{6000} in a proportion ranging between 2-10%

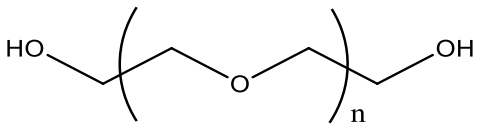

Figure 107. Chemical structure of polyethylene glycol.

- **Propylene glycol**

Propylene glycol (PPG) (figure 108) is a hygroscopic, colorless, odorless, clear and viscous liquid that is stable up to 40 ºC. It is miscible with acetone, chloroform, ethanol, glycerin and water. It is commonly used as plasticizer in aqueous film-forming formulations but it also acts as antiseptic, disinfectant, humectant, solvent, stabilizing agent and water-miscible cosolvent. It has been widely used in different pharmaceutical dosage forms including the topicals and parenterals.

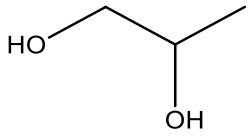

Figure 108. Chemical structure of propylene glycol.

- **Glycerin triacetate**

Glycerin triacetate (GT) (figure 109) also known as triacetin, is a colorless viscous liquid with a slightly fatty odor. It is miscible with chloroform, ethanol, ether, and toluene and with water in a ratio 1:14. It is used as hydrophilic plasticizer, solvent or fixative.

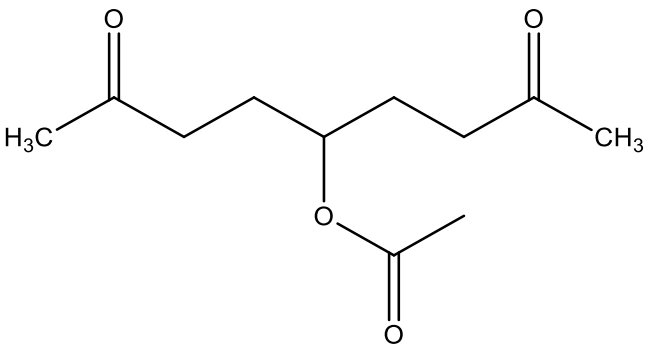

Figure 109. Chemical structure of glycerin triacetate.

- **Diethyl phthalate**

Diethyl phthalate (DEP) (figure 110) is a compound included in the group of the low molecular weight (<250 Da) esters of phthalic acid which have low viscosity and high volatility. It is a clear, colorless, practically odorless oily liquid that is insoluble in water but miscible with ethanol, ether and other organic solvents. It is used as plasticizer but also as film-forming agent, solvent, vehicle and alcohol denaturant.

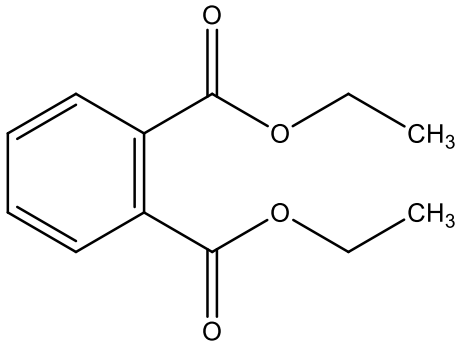

Figure 110. Chemical structure of diehtyl phthalate.

- **Castor Oil**

Castor oil (CO) (figure 111) also known as *ricini oleum* is a triglyceride of fatty acids composed by 87% ricinoleic acid, 7% oleic acid, 3% linoleic acid, 2% palmitic acid, 1% stearic acid and by traces of dyhydroxystearic acid. It is a colorless or light yellow viscous oil with a slight odor. It is insoluble in water, soluble in ethanol and miscible with chloroform, diethyl ether, ethanol, glacial acetic acid and methanol. CO is used as plasticizer and as solvent.

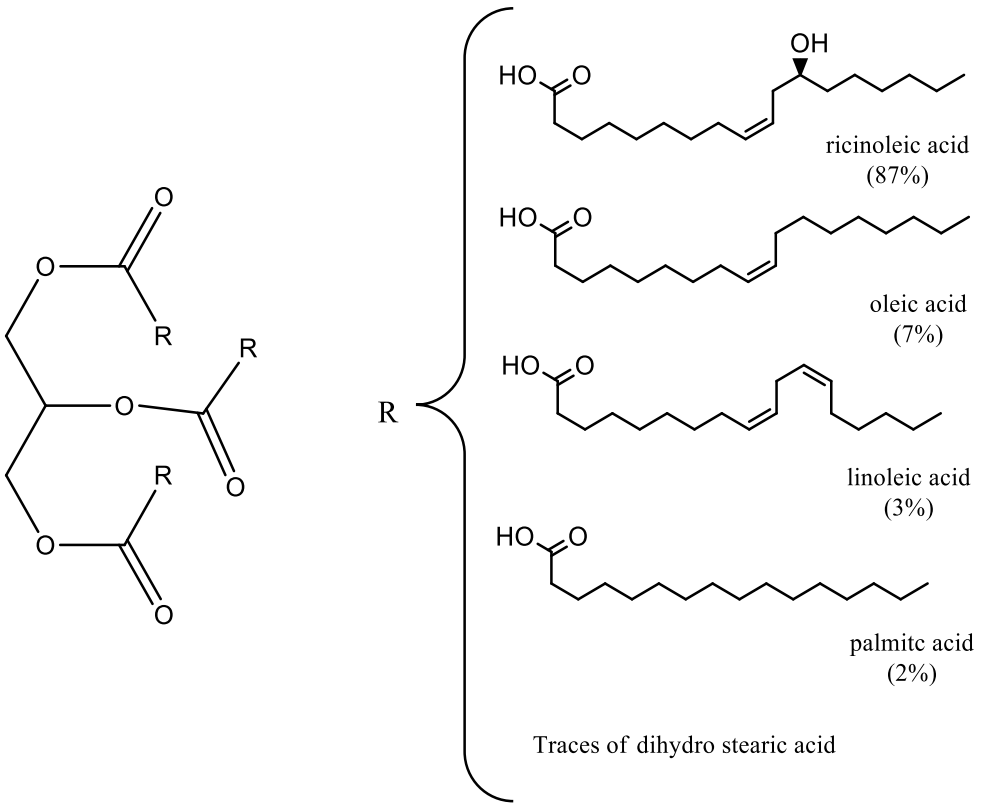

Figure 111. Chemical structure of castor oil.

- **Dibutyl Sebacate**

Dibutyl Sebacate (DBS) (figure 112) is a colorless, clear oily liquid with a slight butyl odor that is practically insoluble in water but soluble in ethanol, ether, mineral oils and toluene. It is used as plasticizer together with film-forming agents.

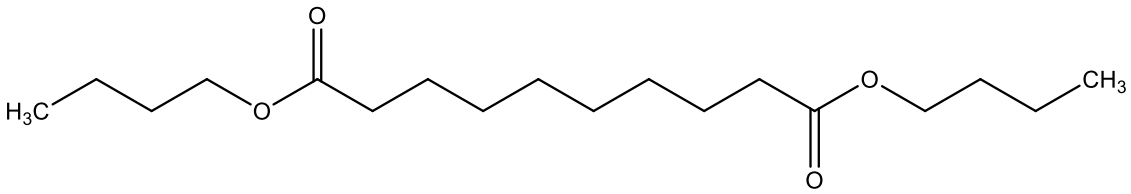

Figure 112. Chemical structure of dibutyl sebacate.

AP1.2.3. AmB solubilizers

- **Sodium deoxycholate**

Sodium deoxycholate (DocNa) (figure 113) is a water soluble anionic detergent commonly used as surfactant. It is a secondary bile acid produced by the action of the bacterial enzymes over glycocholic and taurocholic acid, salts released in the bovine intestine. This chemical is not only used as surfactant but also as intermediate in the production of corticosteroids; in the preparation and formulation of certain microbiological diagnostic media, and as biological detergent to lyse cells and to solubilize cellular and membrane components.

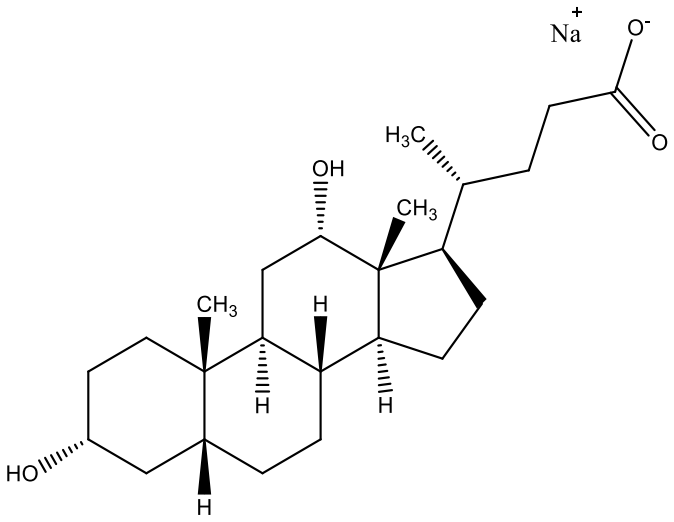

Figure 113. Chemical structure of sodium deoxycholate.

It has the ability to self-assembly in solution and form mixed aggregates with hydrophobic drugs. This effect together with its physiological compatibility resulted in its wide application as controlled drug delivery carriers. The micelle structure formed by sodium deoxycholate and other bile salts, differs from one generated with the typical micelle-forming surfactants. Bile salts have a rigid hydrophobic moiety of a steroid nucleus with hydrophilic parts of two or three hydroxyl groups and an anionic head of a carboxylate group. The spatial arrangement of hydrophilic and hydrophobic groups determines the facial amphiphilicity of the molecules of these compounds since they have convex hydrophobic and concave hydrophilic surfaces. The critical micelle concentration (CMC) of the bile salts is in the range $1\text{-}10.10^{-3}$ M having sodium deoxycholate a CMC value of $2x10^{-3}$ M.

Sodium deoxycholate has been widely used as amphotericin B solubilizer for many years. Thus, Fungizone®, was the first amphotericin B commercialized product in which sodium deoxycholate was used as AmB solubilizer and as carrier.

- **Gamma cyclodextrins**

Gamma cyclodextrin (γ-CD) (figure 114), is a cyclic alpha-(1-4)-linked oligosaccharide composed by eight molecules of glucose. It is a white, almost odorless, fine crystalline powder with a slightly sweet taste. It solubility in water is limited; 1part of γ-CD in 4.4 parts of water at 20ºC and 1 in 2 parts of water at 45ºC. γ-CD, as well as other cyclodextrins, is able to form inclusion complexes with a large variety of molecules, resulting in improvements to dissolution and bioavailability owing to enhanced solubility and improved chemical and physical stability. Its ability to form these complexes is explained by the less polarity of the inner side of the torus-like molecule compared to outer side [465]. This is due to the arrangement of hydroxyl groups within the molecule. This arrangement allows the γ-cyclodextrin to accommodate a guest molecule within the cavity, forming an inclusion complex. The cavity diameter of the γ-CD is in the range 7.5-8.3 A.

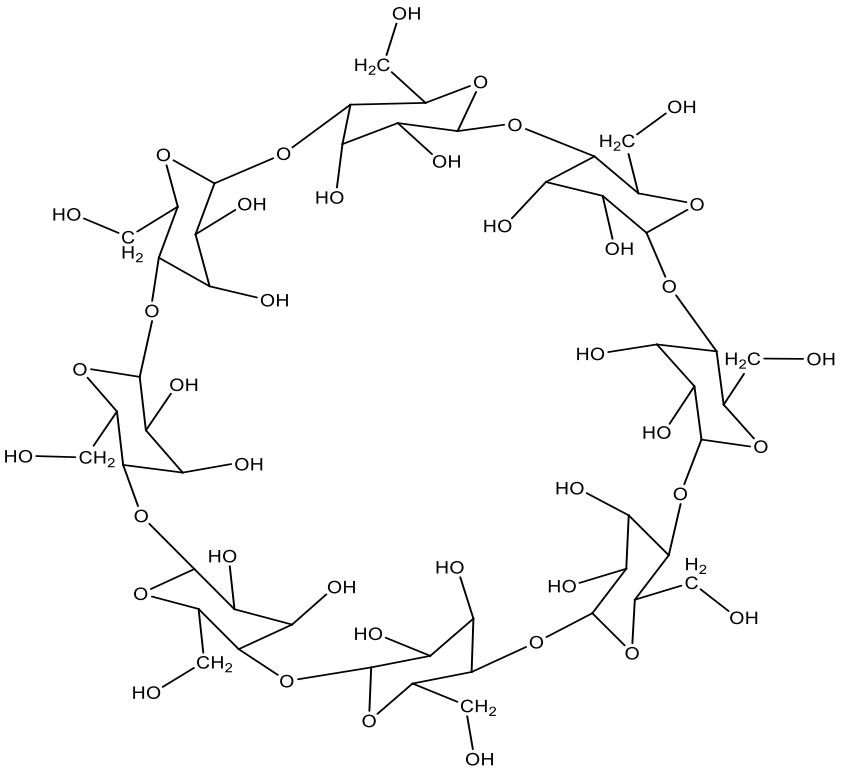

Figure 114. Chemical structure of γ -cyclodextrin

Gamma cyclodextrins are widely used in oral, topical and parental formulations due to their great solubilizing properties. Its solubilizing effect on amphotericin B was first described on 1985 [466] and from this date, this molecule has been used in many different AmB formulations such as vaginal gels, ointments, eye drops and solutions (AmB forms a soluble inclusion complex with γ-CD in which the AmB solubility can be enhanced up to 200-fold) . γ-CD has shown a synergistic effect on membrane destabilization with AmB. The combination of AmB- γ-CD in topical formulations have shown a greater antifungal activity than AmB dissolved in other solvents [290].

- **N-methyl-2-pyrrolidone**

N-methyl-2-pyrrolidone (NMP) (figure 115) is a hygroscopic colorless organic solvent with a mild amine odour, miscible with ethanol, propanol and water. It is also miscible with organic solvents such as benzene, carbon disulfide, chloroform, ether and ethyl acetate. Its high stability is only decreased by a slow oxidation process when it contacts with air [467]. This polar aprotic solvent is used as penetration enhancer (NMP increases partiotioning of drugs into the skin), plasticizer, solvent and as solubilizer agent. It has microbiological activity against Gram positive (G+) and Gram negative (G-) bacteria and some molds.

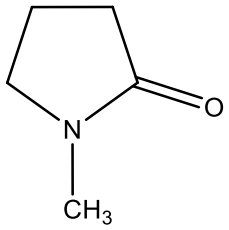

Figure 115. Chemical structure of N-methyl-2-pirrolidone

Its ability to penetrate the tissues is based on the modification of the solvent nature of the membranes. For this reason, it has been used to generate reservoirs within skin membranes. NMP dermal penetration through human skin has been shown to be fast [468]. Its use as penetration enhancer in many topical formulations at concentrations up to 40% has been reported not to generate any skin sensitization [469]. Due to the solvent effects and to its permeability properties, this molecule was assayed for the first time as a possible AmB solubility enhancer.

- **Plasdone K90®**

Plasdone K90®, previously described, it is not only used for its film-forming properties but also for its amphiphilic character. At basic pH (pH=12) it interacts with the charged AmB, forming a complex in which the drug remains soluble even after neutralization (pH 5-7).

AP1.2.4. Cosolvents

- **Ethanol**

The ethanol was used either as solvent or cosolvent in all the below described formulations. This is due to its fast dryness which confers the nail lacquers the capacity of generating homogenous films in just a few minutes (≤ 5 minutes). The ethanol incorporated was ethanol 96%.

AP1.3. Nail lacquer formulations

AP1.3.1. Water soluble nail lacquers

Due to the film forming properties of the polyvinyl pyrrolidone molecule, the first matrix formulation (without drug incorporation) was prepared using Plasdone® K90 as film forming agent. The choice of this polymer was based first, on the information obtained from different patents (i.e [470] and secondly, on the possibility of having a system in which the AmB solubilization did not imply the addition of extra-excipients. The AmB solubility in Plasdone® was assayed.

AP1.3.1.1. Preparation of a water soluble matrix

- ✓ **Formulation 1**

This formulation implies the preparation of a water soluble matrix able to constitute a nail lacquer.

Composition

Plasdone K90®……....20 %
Urea……..10 %
Glycerin triacetate…….4 %
Ethanol…….20 %
Water……46 %

Protocol followed for preparation

5 g formulation was prepared by adding 1 g of Plasdone K90® to 2.3 mL of deionized water containing 0.5 g of urea. Once dissolved, 0.2 g of glycerin triacetate and 1 g of ethanol were supplied. The formulation was stored in a sealed glass vial to avoid ethanol evaporation.

Evaluation

Using a scale from 1 to 5 (1 is the minimum value and 5 the maximum), the following parameters were evaluated.

- water permeability of the film formed,
- viscosity of the formulation,
- brightness of the formulation and film formed,
- film drying time over the nail,
- stickiness of the film once dried,
- extensibility of the formulation,
- homogeneity of the film formed and
- pH of the formulation

These parameters were evaluated in all the formulations prepared (1-20)

- ✓ **Formulation 2**

Formulation 1 was found to be highly viscous. In order to decrease the overall viscosity of this formulation the amount of polymer was decreased and the urea was removed.

Composition

Plasdone K90®……....10 %
Glycerin triacetate…….4 %
Ethanol…….36 %
Water……50 %

Protocol followed for preparation

5 g formulation was prepared as reported in formulation 1 without the addition of urea. The formulation was stored in a sealed glass vial to avoid ethanol evaporation.

AP1.3.1.1.1. Incorporation of amphotericin B in the water soluble nail lacquers using Plasdone® K90 as film forming agent.

- ✓ **Formulation 3**

The incorporation of AmB into the water permeable nail lacquer, was assayed for the first time with NMP.

Composition

AmB…….0.3 %
NMP……..10 %
Plasdone K90®……..…....10 %
Glycerin triacetate……..…….5 %
Ethanol…….……..24.7 %
Water……50 %

Protocol followed for preparation

15 mg AmB were added of 0.5 g NMP (A) and left under magnetically stirring for 15 min. Meanwhile, 0.5 g of Plasdone K90® were dissolved with 2.5 mL deionized water and added of 0.25 g of glycerin triacetate (B). Then, A was added to B and 1.235 g ethanol was incorporated. The formulation was stored as described above.

- ✓ **Formulation 4**

The AmB solubility with γ-CD (instead of NMP) was assayed in formulation 4. It is important to consider that the γ-CD maximum solubility in water is 23.3 g/100 mL [471]. When a formulation contains γ-CD, its solubility value limits the amount of the other components that can be included in the formulation.

Composition

AmB…….0.3 %
γ-CD……9 %
Plasdone K90®…….....10 %
Glycerin triacetate……..….5 %
Ethanol…….…..25.7 %
Water…….…50 %
NaOH 0.1 M……..……...c.s.
Orthophosphoric acid 0.1 M…….....…...c.s.

Protocol followed for preparation

The first step was the AmB dissolution. For this purpose, the γ-CD in a ratio 30:1 (CD:AmB) was used as solubiliser. 0.45 g of γ-CD dissolved in 2.5 mL purified water were added of NaOH 0.1 M. When the pH was 12, 15 mg AmB were dissolved and the pH was immediately decreased to 5.5 using orthophosphoric acid 0.1 M. Then, 0.5 g of Plasdone K90® were added to the AmB-CD complex and left under magnetically stirring for 15 min. Finally, 0.25 g of glycerin and 1.285 g ethanol were incorporated.

The formulation was stored as above indicated

Formulation 4, both in the presence and in the absence of AmB, showed a precipitate after two days preparation. In order to study the factors responsible of this effect, different changes in the composition were performed.

- ✓ **Formulation 5**

Due to the precipitation observed at 48 h and to overcome this problem, some changes in F4 were done.

Composition

AmB…….0.3 %
γ-CD……..15 %
Plasdone K90®…….....10 %
PEG400…….…….5 %
Water…….….69.7 %
NaOH 0.1 M……..……...c.s.
Orthophosphoric acid 0.1 M…….....c.s.

Protocol followed for preparation

The same protocol described in formulation 4 was used to prepare 5 g of this formulation. In this case, a higher amount of γ-CD and water was used. The formulation was prepared without the addition of ethanol.

- ✓ **Formulation 6**

In formulation 6, the solubilizing effect of Plasdone® K90 on AmB was studied.

Composition

AmB…….0.3 %
Plasdone K90®……..……....10 %
PEG 400…….…….5 %
Water……...…….……..84.7 %
NaOH 0.1 M……..……...c.s.
Orthophosphoric acid 0.1 M…….....c.s.

As described in the literature, the polyvinylpyrrolidone (Plasdone®) is an amphiphilic molecule. In this formulation, the Plasdone® was not only used as film-forming agent but also as a possible AmB solubilizer.

Protocol followed for preparation

0.5 g of Plasdone K90® were dissolved in 4.235 mL of deoinized water at pH 5.5. The pH was increased up to 12 with NaOH 0.1 M and then 15 mg of AmB were added.

When dissolved, the pH was decreased again to 5.5 with orthophosphoric acid. Finally, 0.25 g of PEG400 was added.

- ✓ **Formulation 7**

As the drying time for F6 (once applied to the nail) was longer than expected, some modifications were done on F6 to obtain a formulation with a shorter drying time (F7).

Formulation 6 showed that although Plasdone K90® interacts with the AmB at pH 12 and maintain the molecule in solution at lower pHs, the formulation had some disadvantages that had to be improved. The drying time when applied to the nail was too long due to the high water content. In this formulation, approximately a 20% of the water was replaced by ethanol.

Composition

AmB…….0.3 %
Plasdone K90®……..……....10 %
Glycerin triacetate……..…….4 %
Ethanol……..…….20 %
Water……...…….……..65.7 %
NaOH 0.1 M……..……...c.s.
Orthophosphoric acid 0.1 M…....…….....c.s.

Protocol followed for preparation

15 mg AmB dissolved in 3.285 mL of deionized water at pH 12 (NaOH 0.1M) were added of 0.5 g of polymer. The pH was then decreased to 5.5 (orthophosphoric acid 0.1M) and the rest of the components (ethanol and plasticizer) were added. Following this protocol, AmB was found to be totally soluble. The formulation was stored in a sealed glass vial hermetically as reported elsewhere.

- ✓ **Formulation 8**

F8 was designed to improve the drying problems still found on F7.

Composition

AmB…….…….0.3 %
Plasdone K90®……...…....10 %
Glycerin triacetate……..…….4 %
Ethanol……..…...…….30 %
Water……...……..……..55.7 %
NaOH 0.1 M……...……...c.s.
Orthophosphoric acid 0.1 M…....……....c.s.

Although the modifications performed on formulation 7 improved the drying properties of formulation 6, there were still some aspects to be improved. The drying time in the nail was shorter than before, but not short enough to constitute a nail lacquer. For this reason, the percentage of water was decreased and the amount of ethanol increased.

Protocol followed for preparation

The formulation was prepared as described for formulation 7.

- ✓ **Formulation 9**

The Amb solubility as simile of Fungizone® that is, dissolved with sodium deoxycholate was studied in F9.

Composition

AmB…….0.3 %
DocNa…….…….0.246 %
Plasdone K90®……..……....10 %
PEG 400…….…….5 %
Water……...……..…….....84.454 %
NaOH 0.1 M……..……...c.s.
Orthophosphoric acid 0.1 M....……....c.s.

In order to check the improved stability and the physichochemical properties of the nail lacquer with the AmB incorporated as simile of Fungizone®, the formulation detailed above was prepared. The ratio DocNa:AmB used was the one described for Fungizone® (0.82:1) [325].

Protocol followed for preparation

12.3 mg of DocNa were dissolved in 2 mL of deionized water and the pH was checked (pH 7.6). Then, 20 µL of NaOH 0.1 M were added (pH 12) and 15 mg of AmB were dissolved. Just after solubilization, 40 µL of orthophosphoric 0.1 M acid were used to decrease the pH to 7.5 (pHs lower than 7 makes the DocNa precipitate). The water volume was completed to 4.227 g and 0.5 g of Plasdone K90® were added. A slightly viscous solution was obtained. Finally, 0.25 g of PEG400 were incorporated.

Formulation 9 was modified in order to add a keratolytic agent to the composition (see Formulation 10)

- ✓ **Formulation 10**

The previously developed formulation (F9) showed adequate physicochemical properties as nail lacquer (even though the drying time was not as short as expected). In order to increase its permeation through the nail, a 10% (weight) urea was added as keratolytic agent.

Composition

AmB…….…….0.3 %
DocNa……..….0.246 %
Plasdone K90®……...……....10 %
PEG 400……..……5 %
Urea……..……..10 %
Water……...……...…....74.454 %
NaOH 0.1 M……...……...c.s.
Orthophosphoric acid 0.1 M…....……....c.s.

In this formulation a 10% urea was added. At this % or at higher concentrations the urea has keratolytic effect. It softens the tissues and enhances the drug penetration through the nail [472].

Protocol followed for preparation

The formulation was prepared as described in formulation 9. The addition of urea was performed right after polymer dissolution.

- ✓ **Formulation 11**

Formulation 11 was designed as an alternative to Formulation 9. This formulation aims in decreasing the drying time over the nail. For this purpose, approximately a 35% of water content was replaced by ethanol.

Composition

AmB…….…….0.3 %
DocNa……..…….0.246 %
Plasdone K90®……...……....10 %
PEG 400.....……....……4 %
Ethanol……...……..…35.454 %
Water……..……..….....50 %
NaOH 0.1 M…….....……...c.s.
Orthophosphoric acid 0.1 M…….....…...c.s.

Protocol followed for preparation

12.3 mg of DocNa were dissolved in 2 mL of deionized water and the pH was checked (pH 7.6). Then, 20 µL of NaOH 0.1 M were added (pH 12) and 15 mg of AmB were dissolved. Immediately after solubilization, 40 µL of orthophosphoric 0.1 M acid were used to decrease the pH to 7.5, and the water volume was completed to 2.5 mL. Then, 0.5 g of Plasdone K90® were incorporated to the previous solution and, once dissolved, 1.772 g of ethanol were added. Finally, 0.20 g of PEG400 were incorporated. The formulation was stored in a sealed glass vial hermetically to avoid ethanol evaporation.

- ✓ **Formulation 12**

The amount of ethanol added on formulation 11 was enough to get the required drying times over the nails. Therefore, the incorporation of urea was assayed in F12.

A 10% urea was incorporate to formulation 11. For this purpose, the amount of ethanol was decreased in the same proportion (10%).

Composition

AmB…….0.3 %
DocNa…….0.246 %
Plasdone K90®……..……....10 %
PEG 400.....……...…….4 %
Urea……..……..10 %
Ethanol……..……..…25.454 %
Water……...……...…….....50 %
NaOH 0.1 M……...……...c.s.
Orthophosphoric acid 0.1 M…….....…....c.s.

Protocol followed for preparation

The formulation was prepared as reported for formulation 11. The urea was added before the polymer.

- ✓ **Formulation 13**

The high decrease in the ethanol content in F12 caused longer dryings times. To avoid the problems with the drying, in the new formulation (F13), both water and ethanol were decrease in a similar proportion (5%).

Composition

AmB…….…….0.3 %
DocNa……..….0.246 %
Plasdone K90®……...…….....10 %
PEG 400.....……...…….4 %
Urea……...……..10 %
Ethanol……..…..…30.454 %
Water……...……...…….....45 %
NaOH 0.1 M……...……...c.s.
Orthophosphoric acid 0.1 M…….....…....c.s.

Protocol followed for preparation

The formulation was prepared as reported for formulation 12.

AP1.3.1.1.2. Incorporation of amphotericin B in the water soluble nail lacquers using Pluronic® F127 as film forming agent.

- ✓ **Formulation 14**

In addition to Plasdone® K90, the efficacy of Pluronic® F127 on the generation of a water soluble film was also studied.

Composition

AmB…….0.3 %
DocNa…….…….0.246 %
Pluronic F127®……..…….....20 %
Glycerin triacetate……..……4 %
Ethanol……..……..…30.454 %
Water……...……...…….....45 %

The use of Pluronic F127 (poloxamer) as film-forming agent has been previously reported elsewhere. (i.e. [473]).

Protocol followed for preparation

The simile of Fungizone® was prepared as previously described. Then, half of the Pluronic F127® (0.5 g) was added. As the polymer took long to dissolve (approximately 45 minutes), the ethanol (1.523 g) was added to the solution prior to the other 0.5 g of polymer in order to have more volume to dissolve the polymer. Finally, 0.2 g of glycerin triacetate were incorporated. The formulation was stored in a sealed glass vial to avoid the ethanol evaporation.

- ✓ **Formulation 15**

The feasibility of the new water permeable lacquer containing Pluronic F127, was studied after addition of a 10% urea as keratolytic agent.

AmB…….0.3 %
DocNa……..0.246 %
Pluronic F127®…….……..20 %
Glycerin triacetate……..……4 %
Urea……..……..10 %
Ethanol…….…..…25.454 %
Water……...……..…….....40 %

Protocol followed for preparation

The formulation was prepared as detailed in formulation 14. The addition of urea was performed just after the simile preparation.

- ✓ **Formulation 16**

Formulation 16 was prepared as an alternative to F14 and F15. The aim of this formulation was to improve the stability problems detected on F14 and F15.

Composition

AmB…….0.3 %
DocNa…….….0.246 %
Pluronic F127®……..……....20 %
Glycerin triacetate……..……4 %
Water……...……..….....75.454 %

Aiming to solve the stability problems found on formulations 14 and 15, the removal of ethanol and urea were considered as an alternative to improve the stability of the formulations.

Protocol followed for preparation

The formulation was prepared as reported in formulation 14. All the water was added at the beginning.

- ✓ **Formulation 17**

To improve the stability of F16, the AmB was dissolved with γCD and the ethanol was removed from the formulation.

The stability problems associated to formulations 14 and 15 were not solved with the modifications applied on formulation 16. For this reason, the replacement of DocNa for γ-CD and the elimination of ethanol were considered as good alternatives.

Composition

AmB…….0.3 %
γCD…….…...15 %
Pluronic F127®……..…....20 %
Glycerin triacetate……..…….4 %
Water…….……..…70.7 %

Protocol followed for preparation

AmB (15 mg) was added to 0.75 g of γ-CD in 3.25 mL of deionized water at pH 12 (NaOH 0.1 M). When the AmB was dissolved, the pH was decreased to 5.5 with orthophosphoric acid 0.1 M and the amount of water was adjusted to 3.535 mL. 1 g poloxamer was then dissolved on this solution and finally, 0.2 g of plasticizer was added.

AP1.3.2. Water insoluble nail lacquers

AP1.3.2.1. Preparation of a water insoluble nail matrix and incorporation of AmB

Considering the fact that the topical treatment against onychomycosis implies the administration of the antifungal lacquer not more than once daily, the preparation of a water impermeable nail lacquer will improve the efficacy of the treatment. With a non-water soluble lacquer, the patient would not have to be worried about being in prolonged contact with water.

- ✓ **Formulation 18**

F18 was designed based on an already patented formulation [474] in which the Eudragit® (water impermeable film-forming polymer) was used as film forming agent.

The AmB solubility results reported in EXP1-2.1 showed that NMP was able to solubilize this drug. NMP is considered as a penetration enhancer suitable for topical and intravenous administration. For this reason, the NMP was assayed as solvent for both the polymer and the AmB in this formulation.

Composition

AmB…….…….0.3 %
Eudragit L100®……..…....15 %
PEG 400……..…….5 %
NMP…….……...79.7 %

Protocol followed for preparation

15 mg of AmB were dissolved in 3.985 g of NMP. Then, 0.75 g Eudragit were added and the resulted solution was left stirring for 1 h. After 60 min, 0.25 g of PEG_{400} were added and the final formulation was stored in a sealed glass vial to avoid NMP hydration.

- ✓ **Formulation 19**

F19 was designed to avoid the drying problems found with F18. Formulation 18, containing only NMP as solvent, was not getting dried once applied to the nail. In order to solve this problem, ethanol was included in formulation 19 as polymer solubiliser. The ethanol evaporates easily assuring the film formation.

Composition

AmB…….…….0.3 %
NMP……..……...10 %
Eudragit L100®……..…….....15 %
PEG 400……...…...…….5 %
Ethanol……...……..69.7 %

Protocol followed for preparation

0.75 g of Eudragit L100® were left stirring 30 min in a close vial containing 3.485 g ethanol (A) (it took quite a long time to dissolve all the Eudragit). Meanwhile, 15 mg of AmB were dissolved with 0.5 g NMP (B). This solution was vortex for 15 min until final dissolution of AmB. Once it was dissolved in NMP, the resultant AmB solution turned orangish transparent and the AmB molecules were found in its monomeric state.

Then, B was added of A while stirring. Finally, 0.25 g of PEG400 were supplied and vortex for 1 min. The formulation was stored as previously described.

- ✓ **Formulation 20**

Taking into account that formulation 19 showed adequate properties for nail administration, the incorporation of urea as keratolytic agent was studied.

Although urea is known to be insoluble in ethanol, the solubilization in a mixture of ethanol and NMP was assayed.

Composition

AmB…….0.3 %
NMP……..10 %
Eudragit L100®…….……....15 %
PEG 400…….…….5 %
Urea……..……..10 %
Ethanol…….……..59.7 %

Protocol

15 mg of AmB were dissolved in 0.25 g of NMP and left under magnetically stirring for 15 min (A). Then, 0.5 g of urea and 0.75 g of Eudragit L100® were added to a mixture of ethanol and NMP (12:1) (B). A was added of B while stirring and finally, 0.25 g of PEG_{400} were incorporated. The formulation was stored as reported elsewhere.

AP1.4. Formulation preparation and troubleshooting

AP1.4.1. Water soluble nail lacquers

AP1.4.1.1. Preparation of a water soluble matrix

- ✓ **Formulation 1**

The first formulation was selected according to the patents ES 2 260 093 T3 published in 2006 entitled "Preparados para la eliminación ungueal atraumática" and the patent USP00746396B2 published in 2009 and titled "Composition for removing abnormal keratinous material". In both patents the authors used polyvinylpyrrolidone (PVP) as film forming agent. Just by the addition of water, the polymer was completely dissolved generating an homogenous solution that once applied to the nail formed a film. The polymer concentrations detailed in these patents were 10% and 20% respectively, and the molecular weights of the PVPs used were 11.5 kDa and 25 kDa for the Spanish patent and 11.5 kDa for the American.

Taking into account these patents, the first polymer used as film forming agent was polyvinylpyrrolidone (PVP). Between all the PVPs available, Plasdone K90® with a molecular weight of 1,300 kDa was the one selected. As detailed in its technical data sheet, this polymer is biocompatible and can be used as an hygroscopic, adhesive, amphiphlic, binder and film forming agent.

For this fist formulation the concentration of Plasdone K90® used was 20%. Based on the patents, the urea was added as keratolytic agent, the glycerin triacetate as plasticizer, the ethanol (added in order to reduce the amount of water in the formulation and, to favor and speed up the drying process) as cosolvent and the water as polymer solvent.

Plasdone K90®……....20 %
Urea……..10 %
Glycerin triacetate…….…….4 %
Ethanol…….20 %
Water……46 %

As detailed in materials and methods, the formulation was prepared by the dissolution of the polymer in the water containing the keratolytic agent and the subsequent addition of the other components.

Once the polymer was dissolved, the solution obtained was really viscous. It seemed more a gel than a solution. When applied to the nail it did not formed an homogenous film. As a consequence of the high viscosity of the solution, the drying time was over 5 minutes, which was our upper limit.

Table 83 details the results from the parameters evaluated for this first formulation where 1 is the minimum and 5 is the maximum.

Table 83. Evaluation of the physicochemical properties of formulation 1 (scale 1-5)

Parameter	**Evaluation (1 minimum; 5 maximum)**	**Observations**
Water permeability	5	In contact with water the film is completely removed
Viscosity	5	The solution is highly viscous
Brightness	3	N/A
Drying time in the nail	≥ 5 min	7 min
Stickiness	4	4 when applied and 2 when it gets dried
Extensibility	2	The viscosity difficults the extensibility
pH	5.5-6	Measured with paper bands

- ✓ **Formulation 2**

The composition of formulation 2 differs to 1 not only in the percentage of polymer used but also in the absence of urea. The percentage of polymer was decreased up to 10% in order to obtain a low viscous solution.

It was decided not to go ahead with the urea since it is a component that might not be included in our final lead formulations for AmB delivery. As it is not a basic component on the nail lacquer matrix, the urea was not included in formulation 2.

Plasdone K90®……....10 %
Glycerin triacetate…….4 %
Ethanol…….36 %
Water……50 %

The reduction on polymer concentration and the elimination of urea, resulted in an increase of 4% water and 16% ethanol in formulation 2 compared to 1. The increase on ethanol respect to water is a strategy to decrease the drying time over the nail.

When preparing the formulation, we realized that after the addition of glycerin triacetate there were some oily drops remaining on the surface of the solution. Those drops completely disappeared after ethanol incorporation. The final solution was transparent.

As for formulation 1, table 84 summarizes the results from the evaluation of formulation 2.

Table 84. Evaluation of the physicochemical properties of formulation 2 (scale 1-5)

Parameter	**Evaluation (1 minimum; 5 maximum)**	**Observations**
Water permeability	5	In contact with water the film is completely removed
Viscosity	2-3	The solution has an appropriate viscosity
Brightness	3	N/A
Drying time in the nail	≤ 5 min	4 min
Stickiness	3	3 when applied and 1 when it gets dried
Extensibility	4	It is easily extensible
pH	5.5-6	Measured with paper bands

AP1.4.1.1.1. Incorporation of amphotericin B in the water soluble nail lacquers using Plasdone® K90 as film forming agent.

- ✓ **Formulation 3**

Once obtained an appropriate matrix for the AmB lacquer, a first attempt to include the amphotericin B was performed.

In formulation 3, the amphotericin B (0.3%) and N-methyl-2-pyrrolidone (NMP) (10%) were included. The addition of those components implies a reduction of the percentage of ethanol up to 24.7%.

To improve the elasticity of the film, glycerin triacetate (plasticizer) was increased up to 5%.

AmB…….0.3 %
NMP……...10 %
Plasdone K90®……..……....10 %
Glycerin triacetate……..…….5 %
Ethanol……..……..24.7 %
Water…….……50 %

Formulation 3 was prepared as detailed in Materials and Methods. Briefly, the AmB was first dissolved in NMP and then added to the polymer water solution containing the plasticizer. It is worth noting that the AmB dissolution in NMP is not an immediate process, it can last up to 15 min. At the beginning of the dissolution process the solution had a yellowish opaque aspect and, when vortexing for some minutes, the solution turned orangish transparent. The aspect of the final AmB dissolved in NMP was the same as for the AmB in DMSO (figure 37). The AmB aggregation state on NMP was also checked by UV finding the AmB as monomers (figure 36).

The aspect of the final formulation (after addition of ethanol) was yellow-orangish translucent even though the solution seemed perfectly dispersed. When applied to the nail, the solution left an orangish film.

In order to determine what was producing the change from the transparent to the translucent solution, an aliquot of NMP containing AmB was added of water. The NMP solution which was initially transparent turned slightly translucent after water addition. The addition of water to the mixture AmB-NMP was responsible for this change.

Table 85 summarizes the results from the evaluation of formulation 3.

Table 85. Evaluation of the physicochemical properties of formulation 3 (scale 1-5)

Parameter	Evaluation (1 minimum; 5 maximum)	Observations
Water permeability	5	In contact with water the film is completely removed
Viscosity	2-3	The solution has an appropriate viscosity
Brightness	3	N/A
Drying time in the nail	≤ 5 min	4 min
Stickiness	3	3 when applied and 1 when it gets dried
Extensibility	4	It is easily extensible
pH	5.5-6	Measured with paper bands

- ✓ **Formulation 4**

In formulation 4, the nail lacquer matrix described above was used but in this case, instead of dissolving the AmB in NMP, it was dissolved using gamma cyclodextrins (γ-CD) in a ratio 1:30 (AmB: γ-CD). Thus, the percentage of γ-CD used was 9%.

AmB…….0.3 %
γ-CD……9 %
Plasdone K90®…….....10 %
Glycerin triacetate……...…….5 %
Ethanol……..……..25.7 %
Water……..……50 %
NaOH 0.1 M……...……...c.s.
Orthophosphoric acid 0.1 M…….....c.s.

In order to form the complex AmB: γ-CD, 0.1 M sodium hydroxide and orthophosphoric acid solutions were used. The complex was formed by the addition of AmB to a γ-CD water solution at pH 12 (NaOH 0.1 M). The subsequent decrease of the pH value to 5.5 was achieved with orthophosphoric acid. The polymer and plasticizer were added to this AmB- γ-CD complex resulting in a transparent solution that turned translucent immediately after ethanol addition.

Once applied to the nail, the drying time compared to formula 3, was increased up to 7 minutes. Moreover, the film formed was not homogenous since the AmB was not uniformly distributed within the lacquer.

Table 86 summarizes the results from the evaluation of formulation 4.

Table 86. Evaluation of the physicochemical properties of formulation 4 (scale 1-5)

Parameter	**Evaluation (1 minimum; 5 maximum)**	**Observations**
Water permeability	5	In contact with water the film is completely removed
Viscosity	2-3	The solution has an appropriate viscosity
Brightness	2	N/A
Drying time in the nail	≥ 5 min	7 min
Stickiness	3	3 when applied and 1 when it gets dried
Extensibility	3	It is easily extensible
pH	5.5-6	Measured with paper bands

- ✓ **Formulation 5**

Taking into account that the ratio 1:30 AmB: γ-CD did not generate an homogenous AmB dispersion on the nail lacquer, we decided to increase the amount of γ-CD up to 50% having a ratio 1:50. The amount of γ-CD that can be used in the formulation is limited by its solubility in water (2.32 g in 10 mL). For this reason, a maximum of 1.5% γ-CD can be included in the formulation.

The increase on the percentage of γ-CD was accompanied by an increase on the water content in order to cover the cyclodextrins solubility. The ethanol was removed from the formulation due to the increase of both water and γ-CD. The glycerin triacetate was replaced for another plasticizer (PEG_{400}) that does not generate oily drops in water. As previously stated, those drops disappeared after the addition of ethanol. In this case, since the formulation does not contain ethanol, the plasticizer was changed.

AmB…….0.3 %
γ-CD……..15 %
Plasdone K90®……..……....10 %
PEG400…….…….….5 %
Water……..……69.7 %
NaOH 0.1 M……...……...c.s.
Orthophosphoric acid 0.1 M…….....…...c.s.

The formulation was prepared following the same protocol used for formulation 4. In this case, the solution obtained was highly viscous in such a way that it could be considered more a gel than a solution. When applied to the nail, due to its high viscosity, it did not leave an homogenous film. Furthermore, once it got dried, the film surface was rough.

Table 87 summarizes the results from the evaluation of formulation 5.

Table 87. Evaluation of the physicochemical properties of formulation 5 (scale 1-5)

Parameter	**Evaluation (1 minimum; 5 maximum)**	**Observations**
Water permeability	5	In contact with water the film is completely removed
Viscosity	5	The solution is highly viscous
Brightness	2	N/A
Drying time in the nail	≥ 5 min	10 min
Stickiness	3	3 when applied and 1 when it gets dried
Extensibility	1	It is not easily extensible
pH	5.5-6	Measured with paper bands

From the first five formulations the following conclusions can be drawn:

- Plasdone K90® produces homogenous films when used at 10%.
- The best solvent to dissolve AmB is NMP.
- The drying time depends on the formulation composition. The longest times were found in those formulations containing γ-CD.
- The addition of ethanol to the above formulations made the solutions turned slightly translucent.

✓ **Formulation 6**

In this formulation the AmB dissolution was performed with Plasdone K90®. As detailed on Materials and Methods, this polymer is an amphiphilic molecule that may behaves as AmB solubilizer without the need of any other solubilizing agent. In order

to check whether Plasdone® was able to solubilize the AmB or not, the following formulation was prepared.

AmB…….0.3 %
Plasdone K90®……..……....10 %
PEG 400…….…….5 %
Water……...…….……..84.7 %
NaOH 0.1 M……..……...c.s.
Orthophosphoric acid 0.1 M…….....…....c.s.

Briefly, the polymer water solution adjusted at pH 12 (0.1M NaOH) was added of AmB. Once the solution was transparent, the pH was shifted down to 5.5 and the plasticizer was then added. The solution was slightly translucent but it seemed well-dispersed. Once applied to the nail it dried but it took longer than the formulations containing ethanol.

This formulation remained stable after 1 month storage at 20ºC. There existed an interaction between the polymer and the drug which made the amphotericin B remained stable in solution for long periods of time.

Table 88 summarizes the results from the evaluation of formulation 6.

Table 88. Evaluation of the physicochemical properties of formulation 6 (scale 1-5)

Parameter	**Evaluation (1 minimum; 5 maximum)**	**Observations**
Water permeability	5	In contact with water the film is completely removed
Viscosity	2-3	The solution has an appropriate viscosity
Brightness	2	N/A
Drying time in the nail	≥ 5 min	10 min
Stickiness	3	3 when applied and 1 when it gets dried
Extensibility	4-5	It is easily extensible
pH	5.5-6	Measured with paper bands

- ✓ **Formulation 7**

Formulation 7 has almost the same composition than Formulation 6 but in this case the water content was decreased because of the ethanol addition. The ethanol is necessary to decrease the dying time when applied to the nail.

AmB…….0.3 %
Plasdone K90®……..……....10 %
Glycerin triacetate……..……4 %
Ethanol…….……20 %
Water……...…….…..65.7 %
NaOH 0.1 M……..……...c.s.
Orthophosphoric acid 0.1 M…….....…....c.s.

As expected, the drying time was decreased from 10 to 7 min. Even though there was a considerably reduction on the drying time, 7 minutes was still above the defined upper limit of 5 min.

Table 89 summarizes the results from the evaluation of formulation 7.

Table 89. Evaluation of the physicochemical properties of formulation 7 (scale 1-5)

Parameter	**Evaluation (1 minimum; 5 maximum)**	**Observations**
Water permeability	5	In contact with water the film is completely removed
Viscosity	2-3	The solution has an appropriate viscosity
Brightness	2	N/A
Drying time in the nail	≥ 5 min	7 min
Stickiness	3	3 when applied and 1 when it gets dried
Extensibility	4-5	It is easily extensible
pH	5.5-6	Measured with paper bands

- ✓ **Formulation 8**

Formulation 8 differs from formulation 7 on the percentage of ethanol. In this formulation the ethanol was increased in a 10% and the water content was decreased in the same percentage.

AmB…….0.3 %
Plasdone K90®…….....10 %
Glycerin triacetate……..….4 %
Ethanol……...30 %
Water……..……....55.7 %
NaOH 0.1 M…….....c.s.
Orthophosphoric acid 0.1 M…….....c.s.

The film formed by Formulation 8 got dried within 4 minutes once applied to the nail.

Table 90 summarizes the results from the evaluation of formulation 8.

Table 90. Evaluation of the physicochemical properties of formulation 8 (scale 1-5)

Parameter	**Evaluation (1 minimum; 5 maximum)**	**Observations**
Water permeability	5	In contact with water the film is completely removed
Viscosity	2-3	The solution has an appropriate viscosity
Brightness	1-2	N/A
Drying time in the nail	≤ 5 min	4 min
Stickiness	3	3 when applied and 1 when it gets dried
Extensibility	4-5	It is easily extensible
pH	5.5-6	Measured with paper bands

- ✓ **Formulation 9**

In formulation 9 the AmB was dissolved using sodium deoxycholate (DocNa). The ratio used for the AmB dissolution was the same as for Fungizone®, that is 1:0.82 AmB:DocNa.

AmB…….0.3 %
DocNa…….…….0.246 %
Plasdone K90®……..……....10 %
PEG 400…….…….5 %
Water……...…….....84.454 %
NaOH 0.1 M……..……...c.s.
Orthophosphoric acid 0.1 M……....…...c.s.

The sodium deoxycholate has the ability of complexing the AmB inside the micellar system tha it is formed in contact with water. DocNa is able to maintain the AmB in solution even after pH decrease (pH 7.4). The only disadvantage related to the use of DocNa is its poor stability at pHs lower than 7.4. Below pH 7.4 this bile salt is not anymore stable and it starts to precipitate.

This formulation was stable at pH 7.4 for at least 4 weeks. During the assayed period the solution remained transparent.

Table 91. Evaluation of the physicochemical properties of formulation 9 (scale 1-5)

Parameter	**Evaluation (1 minimum; 5 maximum)**	**Observations**
Water permeability	5	In contact with water the film is completely removed
Viscosity	2-3	The solution has an appropriate viscosity
Brightness	2-3	N/A
Drying time in the nail	≥ 5 min	≥ 10 min
Stickiness	2	2 when applied and 1 when it gets dried
Extensibility	4	It is easily extensible
pH	7.4	Measured with paper bands

- ✓ **Formulation 10**

Even though formulation 9 took long to get dried over the nail, its aspect and long stability made us consider it as a good candidate for AmB delivery. In order to improve the drying time some modifications were performed on formulation 9.

The first modification was based on the addition of a keratolityc agent, the urea, at a 10%. As previously stated, at 10% or higher concentrations the urea is able to soften the tissues and enhance the drug penetration.

AmB…….0.3 %
DocNa…….…….0.246 %
Plasdone K90®……..…...10 %
PEG 400…….…….5 %
Urea…….…..10 %
Water……...…….....74.454 %
NaOH 0.1 M……..…...c.s.
Orthophosphoric acid 0.1 M…….....c.s.

The preparation protocol for Formulation 10 is detailed on Materials and Methods. It is worth pointing out that during preparation we realized that the addition of urea made the solution turned translucent.

Table 92. Evaluation of the physicochemical properties of formulation 10 (scale 1-5)

Parameter	**Evaluation (1 minimum; 5 maximum)**	**Observations**
Water permeability	5	In contact with water the film is completely removed
Viscosity	3	The solution has an appropriate viscosity
Brightness	2	N/A
Drying time in the nail	≥ 5 min	≥ 10 min
Stickiness	2	2 when applied and 1 when it gets dried
Extensibility	4	It is easily extensible
pH	7.4	Measured with paper bands

- ✓ **Formulation 11**

The second modification performed on formulation 9, which was focused on the addition of ethanol, made us considered formulation 11 as a lead candidate for AmB delivery.

AmB…….0.3 %
DocNa…….…….0.246 %
Plasdone K90®……..……....10 %
PEG400.....……...…….4 %
Ethanol……...…35.454 %
Water……..…….....50 %
NaOH 0.1 M……..……...c.s.
Orthophosphoric acid 0.1 M……...…...c.s.

The addition of ethanol was performed in order to decrease the drying time.

Table 93. Evaluation of the physicochemical properties of formulation 11 (scale 1-5)

Parameter	**Evaluation (1 minimum; 5 maximum)**	**Observations**
Water permeability	5	In contact with water the film is completely removed
Viscosity	3	The solution has an appropriate viscosity
Brightness	2	N/A
Drying time in the nail	≤ 5 min	3-4 min
Stickiness	1	N/A
Extensibility	4	It is easily extensible
pH	7.4	Measured with paper bands

- ✓ **Formulation 12**

Formulation 12 came out from the combination of the two modifications carried out on formulation 9 and 11. Those are the incorporation of urea and the addition of ethanol. The percentage of ethanol was decreased in a 10% (from 35.454% to 25.454%) due to the incorporation of urea in the formulation.

AmB…….0.3 %

DocNa…….0.246 %

Plasdone K90®……..……....10 %

PEG 400.....……...……4 %

Urea…….……..10 %

Ethanol…….…..…25.454 %

Water……..……..….....50 %

NaOH 0.1 M……...……...c.s.

Orthophosphoric acid 0.1 M…….....…....c.s.

Both, the addition of ethanol and the urea produced a changed in the aspect of the formulation. The formulation, initially transparent, turned slightly translucent after addition of ethanol and/or urea, but it remained stable without signs of precipitation at least during 2 weeks.

The drying time with formulation 12 was increased approximately 1 minute compared to formulation 11 due to the reduction on ethanol percentage.

Table 94. Evaluation of the physicochemical properties of formulation 12 (scale 1-5)

Parameter	**Evaluation (1 minimum; 5 maximum)**	**Observations**
Water permeability	5	In contact with water the film is completely removed
Viscosity	3	The solution has an appropriate viscosity
Brightness	2	N/A
Drying time in the nail	≤ 5 min	4-5 min
Stickiness	1	N/A
Extensibility	4	It is easily extensible
pH	7.4	Measured with paper bands

- ✓ **Formulation 13**

In order to decrease the drying time to 3-4 minutes, formulation 12 was modified. The ethanol was increased in a 5% and the water content was decreased in the same percentage. In this way, and compared to formulation 11, the amount of solvent and cosolvent (water and ethanol) were decreased in the same proportion (5%) and a 10% urea was added.

AmB…….0.3 %
DocNa…….0.246 %
Plasdone K90®……..…....10 %
PEG 400.....……...…….4 %
Urea…….…..10 %
Ethanol……...…30.454 %
Water……..…….....45 %
NaOH 0.1 M……...…....c.s.
Orthophosphoric acid 0.1 M…….....c.s.

The readjustment on the amount of ethanol and water on formulation 13 reduced, just slightly, the drying time over the nail (from 4.5 minutes to 4 minutes).

Table 95. Evaluation of the physicochemical properties of formulation 13 (scale 1-5)

Parameter	**Evaluation (1 minimum; 5 maximum)**	**Observations**
Water permeability	5	In contact with water the film is completely removed
Viscosity	4	The viscosity is slighter higher
Brightness	2	N/A
Drying time in the nail	≤ 5 min	4 min
Stickiness	1	N/A
Extensibility	4	It is easily extensible
pH	7.4	Measured with paper bands

AP1.4.1.1.2. Incorporation of amphotericin B in the water soluble nail lacquers using Pluronic® F127 as film forming agent.

- ✓ **Formulation 14**

For this formulation a new polymer was used as film forming agent. Based on the data reported by Nogueiras-Nieto *et* al. [473] we decided to design a nail lacquer containing Pluronic® F127 as film forming agent. The percentage of Pluronic® F127 used was 20% and the AmB was dissolved using DocNa.

AmB…….0.3 %
DocNa……..0.246 %
Pluronic F127®…….....20 %
Glycerin triacetate……..….4 %
Ethanol……..….30.454 %
Water……...…….....45 %

The dissolution of Pluronic® F127 during sample preparation took around 45 minutes, which slowed down and difficulted the formulation process. The aspect of the solution obtained after the addition of all the components was yellowish translucent.

The application of Formulation 14 over the nail, left a non homogenous film which dried slowly (9 minutes).

Table 96. Evaluation of the physicochemical properties of formulation 14 (scale 1-5)

Parameter	**Evaluation (1 minimum; 5 maximum)**	**Observations**
Water permeability	5	In contact with water the film is completely removed
Viscosity	3	The solution has an appropriate viscosity
Brightness	4	N/A
Drying time in the nail	≥ 5 min	9 min
Stickiness	1	N/A
Extensibility	5	It is easily extensible
pH	7.4	Measured with paper bands

- ✓ **Formulation 15**

In order to check if there were some improvements on the film formed by F14 with the additon of a keratolytic agent, a 10% urea was included. The amount of ethanol and water were decreased in the same proportion, 5% each.

AmB…….0.3 %
DocNa……..0.246 %
Pluronic F127®…….....20 %
Glycerin triacetate…….…….4 %
Urea…….……..10 %
Ethanol……...…25.454 %
Water……..…….....40 %

The film formed with this new formulation did not present any advantage compared to Formulation 14, even more, the drying time was increased in almost 1 minute.

Table 97. Evaluation of the physicochemical properties of formulation 15 (scale 1-5)

Parameter	**Evaluation (1 minimum; 5 maximum))**	**Observations**
Water permeability	5	In contact with water the film is completely removed
Viscosity	3	The solution has an appropriate viscosity
Brightness	3	N/A
Drying time in the nail	≥ 5 min	10 min
Stickiness	1-2	N/A
Extensibility	5	It is easily extensible
pH	7.4	Measured with paper bands

Formulations 14 and 15 precipitated after two days storage at 20ºC and consequently, they were discarded.

- ✓ **Formulation 16**

The stability problems found with formulations 14 and 15 were managed through the removal of ethanol from the composition. Even though that decision would carried out a longer drying time, we wanted to check whether or not the formulation stability was improved.

AmB…….0.3 %
DocNa…….….0.246 %
Pluronic F127®……..……....20 %
Glycerin triacetate……..……4 %
Water……..……..….....75.454 %

The elimination of ethanol from the formulation did not only resulted in longer drying times (≥10 min) but also in a highly viscous solution. In the absence of ethanol the polymer solubility took even longer (approximately 60 min).

Table 98. Evaluation of the physicochemical properties of formulation 16 (scale 1-5)

Parameter	**Evaluation (1 minimum; 5 maximum)**	**Observations**
Water permeability	5	In contact with water the film is completely removed
Viscosity	5	The solution was highly viscous
Brightness	3	N/A
Drying time in the nail	≥ 5 min	≥ 10 min
Stickiness	1-2	N/A
Extensibility	5	It is easily extensible
pH	7.4	Measured with paper bands

- ✓ **Formulation 17**

The stability problems found on formulations 14 and 15 can be explained by an incompatibility between the sodium deoxycholate and the polymer. For this reason, in formulation 17, the AmB was dissolved using γ-CD. The ratio AmB: γ-CD used was 1:50.

AmB…….0.3 %
γCD…….…..15 %
Pluronic F127®…….....20 %
Glycerin triacetate…….……4 %
Water……..…70.7 %

In this case, the pH of the formulation was decreased up to 5.5 as the γ-CD are stable over a wide range of pHs. The resulting formulation was extremely viscous. It did not

almost have mobility within the vial in which it was prepared. At pH 12 there was an interaction between the γ-CD and the poloxamer that made the polymer jellify when neutralizing the solution.

Table 99. Evaluation of the physicochemical properties of formulation 17 (scale 1-5)

Parameter	**Evaluation (1 minimum; 5 maximum)**	**Observations**
Water permeability	5	In contact with water the film is completely removed
Viscosity	5*	The solution extremely viscous. It jellified.
Brightness	3	N/A
Drying time in the nail	≥ 5 min	The gel did not get dried
Stickiness	4-5	N/A
Extensibility	1	It is hard to extend due to its high viscosity
pH	5.5	Measured with paper bands

The above formulations (formulations 1 to 17) have in their composition a water soluble polymer. The polymers used, Plasdone K90® and Pluronic F127® form a film that it is immediately dissolved when in contact with water. This water solubility is a great advantage as the lacquer can be easily removed from the nails without the need of organic solvents. Nevertheless, there is an important disadvantage associated to the use of these water soluble lacquers which can lead to treatment failure. Once the lacquer is applied and dried over the nail (overall when applied to the fingernails), if the patients wash their hands, or the nails are exposed to high humid ambients, the film can be broken without leaving enough time for the amphotericin B to penetrate the nail and therefore, to make its therapeutic action.

The development of an AmB water impermeable lacquer is, therefore, an important issue for the treatment of onychomycosis and patient therapeutic compliance.

The following formulations, Formulations 18 to 20 have in their composition a water impermeable polymer that assures the film integrity over the nail even in contact with water.

AP1.4.2. Water insoluble nail lacquers

Based on a deep bibliographic research including papers and patents (i.e. US20110200544 A1 (2009) patent entitled "Urea-based film forming solution for treating nail psoriasis"), a water impermeable nail lacquer was prepared. Following what is described in those publication (the use of different types of Eudragits in a percentage ranging 5-15% as film forming agent), the Eudragit L100® was selected as film forming agent for the development of a water impermeable nail lacquer.

- ✓ **Formulation 18**

Apart from Eudragit L100® as film forming agent, in the composition of this formulation, the PEG_{400} was used as plasticizer and the NMP as solvent, AmB solubilizer and penetration enhancer.

Even though, the use of NMP as Eudragit L100® solubilizer had not been previously reported, it was decided to assay the polymer solubility on this solvent. As reported in section AP4.1.2, the NMP was the solvent in which the AmB showed its highest solubility. The NMP has been widely used in different pharmaceutical formulations as penetration enhancer, providing the drug to reach its site of action.

AmB…….0.3 %
Eudragit L100®……..…....15 %
PEG 400……..…….5 %
NMP……....79.7 %

As detailed in materials and methods, the NMP was first used to dissolved the AmB and then the polymer. Once both were dissolved, the PEG_{400} was added. The final solution had a yellowish-transparent aspect and was slightly viscous. When applied to the nail, the film did not got dried due to the long evaporation time of the NMP.

Table 100. Evaluation of the physicochemical properties of formulation 18 (scale 1-5)

Parameter	Evaluation (1 minimum; 5 maximum)	Observations
Water permeability	1	In contact with water the film remains intact
Viscosity	3	The solution was slightly viscous
Brightness	3-4	N/A
Drying time in the nail	≥ 5 min	It did not get dried
Stickiness	NA	Not evaluable as the film is not getting dry
Extensibility	5	It is easily extendible
pH	5.5-6	Measured with paper bands

- ✓ **Formulation 19**

The drying problems associated to the use of NMP as unique solvent for both AmB and polymer, were resolved by the addition of ethanol as Eudragit L100® solvent.

AmB…….0.3 %
NMP……..10 %
Eudragit L100®……..……....15 %
PEG 400……..…….5 %
Ethanol……..…..69.7 %

Briefly, the formulation was prepared by the addition of the AmB dissolved in NMP to the ethanol solution containing the Eudragit L100®. The last step was the PEG_{400} incorporation.

The solution obtained was yellow-orangish translucent and when applied to the nail using a brush it quickly dried (within 3 minutes) forming a colored film.

Table 101. Evaluation of the physicochemical properties of formulation 19 (scale 1-5)

Parameter	**Evaluation (1 minimum; 5 maximum)**	**Observations**
Water permeability	1	In contact with water the film remains intact
Viscosity	2-3	The solution extremely viscous. It jellified.
Brightness	3	N/A
Drying time in the nail	2-3 min	It quickly dries
Stickiness	2	1 when it gets dry
Extensibility	5	It is easily extendible
pH	5.5-6	Measured with paper bands

- ✓ **Formulation 20**

Even though formulation 19 showed great properties as impermeable nail lacquer, we considered to improve the formulation by the addition of a queratolytic agent, the urea. The urea is well known to be insoluble in ethanol but we wanted to check whether or not we were able to include it in the formulation using the mixture ethanol-NMP.

In order to include the urea in the formulation, the percentage of ethanol was decreased in a 10%.

AmB…….0.3 %
NMP……..10 %
Eudragit L100®……..…....15 %
PEG 400……..…….5 %
Urea……..…..10 %
Ethanol…….....59.7 %

As expected, the urea was not getting dissolved in the mixture ethanol-NMP. Therefore, this formulation was not considered as a candidate.

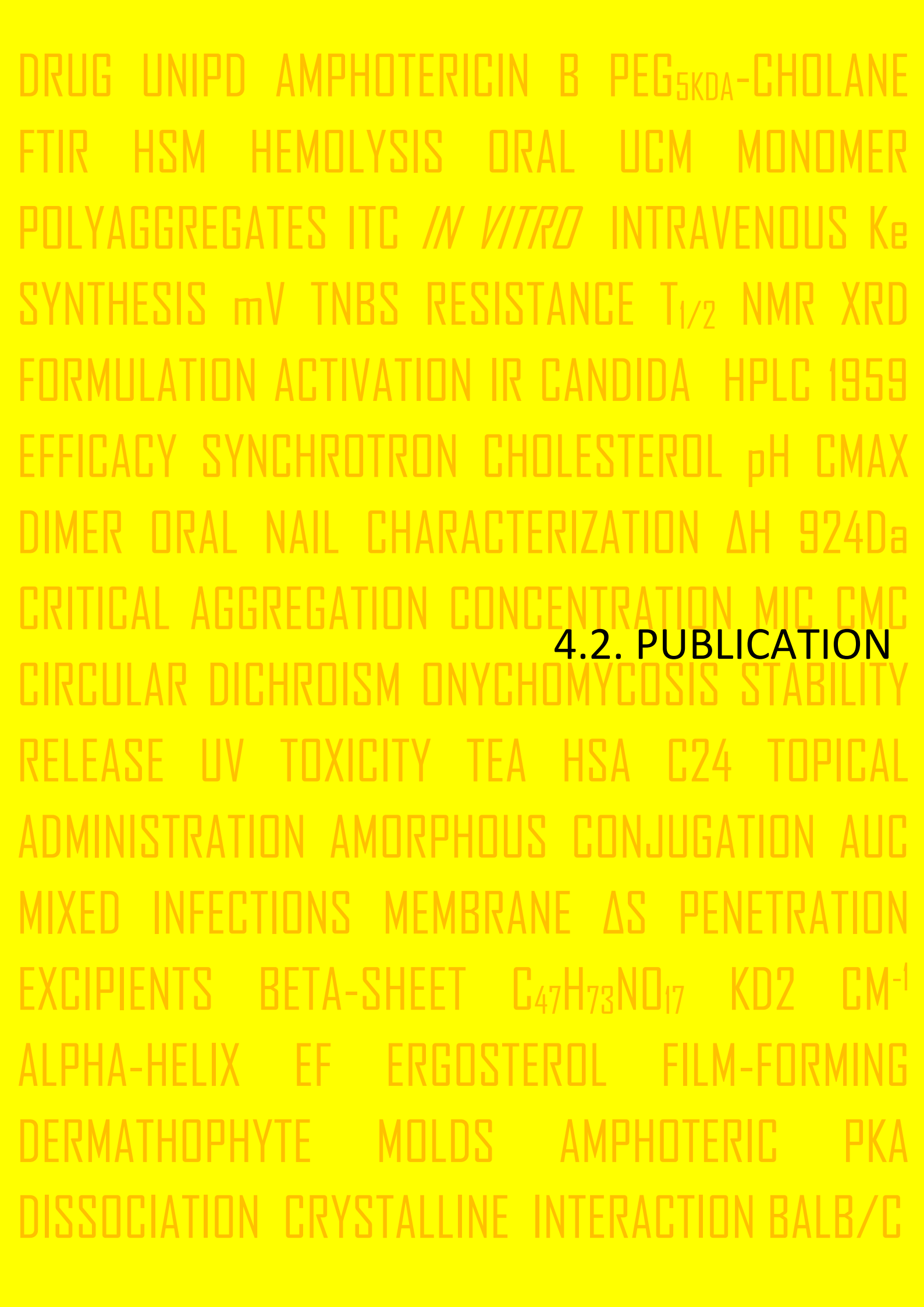
DRUG UNIPD AMPHOTERICIN B PEG5KDA-CHOLANE
FTIR HSM HEMOLYSIS ORAL UCM MONOMER
POLYAGGREGATES ITC IN VITRO INTRAVENOUS Ke
SYNTHESIS mV TNBS RESISTANCE T1/2 NMR XRD
FORMULATION ACTIVATION IR CANDIDA HPLC 1959
EFFICACY SYNCHROTRON CHOLESTEROL pH CMAX
DIMER ORAL NAIL CHARACTERIZATION ΔH 924Da
CRITICAL AGGREGATION CONCENTRATION MIC CMC
4.2. PUBLICATION
CIRCULAR DICHROISM ONYCHOMYCOSIS STABILITY
RELEASE UV TOXICITY TEA HSA C24 TOPICAL
ADMINISTRATION AMORPHOUS CONJUGATION AUC
MIXED INFECTIONS MEMBRANE ΔS PENETRATION
EXCIPIENTS BETA-SHEET C47H73NO17 KD2 CM-1
ALPHA-HELIX EF ERGOSTEROL FILM-FORMING
DERMATHOPHYTE MOLDS AMPHOTERIC PKA
DISSOCIATION CRYSTALLINE INTERACTION BALB/C

4.2. PUBLICATION

International Journal of Pharmaceutics 495 (2015) 41–51

Contents lists available at ScienceDirect

International Journal of Pharmaceutics

journal homepage: www.elsevier.com/locate/ijpharm

A novel performing PEG-cholane nanoformulation for Amphotericin B delivery

Claudia Luengo-Alonso[a,b], Juan José Torrado[b], Maria Paloma Ballesteros[b], Alessio Malfanti[a], Sara Bersani[a], Stefano Salmaso[a], Paolo Caliceti[a,*]

[a] Department of Pharmaceutical and Pharmacological Sciences, University of Padova, Via F. Marzolo 5, 35131, Italy

[b] Department of Pharmacy and Pharmaceutical Technology, School of Pharmacy, University Complutense of Madrid, Plaza Ramon y Cajal S/N, 28040 Madrid, Spain

ARTICLE INFO

Article history:
Received 17 July 2015
Received in revised form 20 August 2015
Accepted 21 August 2015
Available online 28 August 2015

Keywords:
Amphotericin B
Poly(ethylene glycol)
PEG_{5kDa}-cholane
Micelles
Cholanic acid

ABSTRACT

A novel formulation for amphotericin B (AmB) delivery has been developed using micelle-forming 5 kDa monomethoxy-polyethylene glycol functionalized with cholanic acid (PEG_{5kDa}-cholane). This polymer was found to increase 10^3 times the AmB solubility witha12:1AmB/PEG_{5kDa}-cholane molar ratio (2:1 w/wratio). Dynamic light scattering and transmission electron microscopy analyses showed that PEG_{5kDa}-cholane associated with AmB to form 30 nm micelles. Isothermal titration calorimetry analyses performed at different pH showed that PEG_{5kDa}-cholane interacts with AmB according to multiple-site association profiles. Affinity constants and enthalpy and entropy changes were found to depend on pH, suggesting that the polymer interaction depends on the AmB ionization and aggregation. The freeze-dried product could be promptly re-dispersed forming a colloidal dispersion with the biopharmaceutical features of the freshly prepared micelles, namely AmB solubility and micelle size. The dispersion was stable over one month incubation at room temperature. FT-infrared spectrometry, differential scanning calorimetry and X-ray diffractometry showed that in the freeze-dried product, AmB intimately interacts with PEG_{5kDa}-cholane. In presenceofserum albumin, AmB formulatedwith PEG_{5kDa}-cholane wasfoundto undergo less extensive and slower disaggregation than in Fungizone[1]. Antifungal activity studies performed using Candida albicans showed that AmB/PEG_{5kDa}-cholane was 15% more active than AmB in buffer.

1. Introduction

Amphotericin B (AmB) is a macrolide antibiotic with broad spectra of action widely used in the treatment of systemic fungal infections since more than 40 years (Gray et al., 2012; Gagos and Arczewska, 2010). Even though several new antifungal drugs have been developed, AmB remains the drug of choice for treatment of severe systemic fungal diseases as it does not cause microbial resistance (Gray et al., 2012), and for treatment of visceral leishmaniasis when the parasite develops resistance to antimonial compounds (Larabi et al., 2003; Brajtburg and Bolard, 1996; Volmer et al., 2010). Nevertheless, AmB administration is often associated with severe dose-limited toxicity, namely nephrotoxicity, anemia, phlebitis and general malaise side effects,which strongly limititsuse (Lemke et al., 2005; Yu et al., 1998b). Furthermore, the AmB aggregation is responsible of unspecific cytotoxic effects towards cells with ergosterol/cholesterol rich membranes (Gaboriau et al., 1997).

The poor AmB solubility is the main drawback to the development of pharmaceutical formulations. So far, many attempts have been made to develop AmB formulations with enhanced therapeutic profiles, including solid lipid nanoparticles, polymeric nanoparticles, liposomes, micelles and polymer bio-conjugates (Vandermeulen et al., 2006; Elgart et al., 2010).

Fungizone[1], in which micelle forming sodium deoxycholate was used as solubilizer, is the first commercialized AmB formulation (Rajagopalan et al., 1986; Oka and Kamimori, 2013; Fukui et al., 2003). However, the intrinsic toxicity of this low molecular weight surfactant was found to enhance the nephrotoxic and hemolytic effects of AmB (Yu et al., 1998a; Oka and Kamimori, 2013). Moreover, the high critical micelle concentration (CMC) of sodium deoxycholate is responsible for in vivo micelle instability that results in AmB release and aggregation with consequent non-selective channel formation damaging cells with high content of ergosterol or cholesterol (Brajtburg and Bolard, 1996).

* Corresponding author at: Department of Pharmaceutical and Pharmacological Sciences, University of Padova, Via F. Marzolo 5, 35131, Italy. Fax: +39 49 8275366.
E-mail address: paolo.caliceti@unipd.it (P. Caliceti).

http://dx.doi.org/10.1016/j.ijpharm.2015.08.070 0378-5173/

Lipidic systems, namely Ambisome®, Abelcet® and Amphotec® do not display the high toxicity of Fungizone®. Nevertheless, high cost and biopharmaceutical instability are important limiting factors to their use (Das and Suresh, 2011; Chakraborty and Naik, 2003). Abelcet® is formed by large size particles that are rapidly taken up by macrophages thus cumulating in liver and spleen, which on one side shortens the circulating and on the other increases its volume of distribution and clearance. Ambisome® substantially escapes recognition and uptake by the mononuclear phagocyte system (MPS) but tends to accumulate in high amount in the liver and spleen. Finally, Amphotec® exhibits dose-limiting infusion-related toxicities. Interestingly, clinical trials showed that despite the lipid-associated formulations were significantly less nephrotoxic than AmB/deoxycholate, they were not significantly better than the latter for treatment of several diseases, including AIDS-associated acute cryptococcal meningitis (Hamill, 2013).

Polymeric micelles have some advantages over lipid-based systems such as easy preparation process, higher thermodynamic and kinetic stability, which confers higher stability towards dilution in vivo, and prolonged blood circulation due to a lower uptake from the MPS (Adams et al., 2003). A few PEG containing polymers have been used to produce AmB pharmaceutical products. PEG is a soluble non-toxic, low immunogenic and low antigenic polymer widely applied for preparation of hybrid macromolecules controlled drug delivery systems such as PEG-cyclodextrins (He et al., 2013; Salmaso et al., 2007). PEG prolongs the circulation of colloidal drug delivery systems as it prevents their massive accumulation in MPS rich organs, namely liver and spleen (Jung et al., 2009; Schreier et al., 2000), reduces the kidney elimination and the capillary penetration (Croy and Kwon, 2006; Yu et al., 1998a,b; Lukyanov and Torchilin, 2004). Micelle formulations obtained using poly(ethylene glycol)-block-poly (-caprolactone-co-trimethylenecarbonate) and PEG–DSPE showed that the AmB solubility could increase of 2 order of magnitude (Vandermeulen et al., 2006). Interestingly, the physical combination of PEG–DSPE with sterol molecules was found to determine both the solubility and the aggregation state of AmB.

Monomeric AmB is known to selectively interact with ergosterol in fungal cell membranes, forming channels by the classic barrel stave motif, while aggregated AmB preferentially associates with cholesterol, which causes toxicity in mammalian cells. Therefore, polymers containing sterol molecules have been hypothesized to be suitable materials for preparation of stable AmB colloidal formulations. Typically, PEG-cholesterol type polymers have been found to produce micelles with about 10 ^{6} M CMC (Croy and Kwon, 2006; Lukyanov and Torchilin, 2004; Li et al., 2010), which are much more stable compared to sodium deoxycholate (CMC 2–6 10 ^{3} M) (Li et al., 2010). Recently, self-assembling polymers obtained by end-conjugation of cholanic acid to monomethoxypoly(ethylene glycol) chains have been investigated for the delivery of proteins and low mol. wt. drugs (Salmaso et al., 2012, 2014). These PEG-cholane polymers were found to associate with proteins by cholanic moiety docking into the hydrophobic clefts and interaction with hydrophobic surfaces of proteins yielding novel supramolecular systems for protein delivery.

Due to the strong affinity of sterol moieties for AmB and the ability of PEG-cholane to dissolve hydrophobic drugs by forming micelles, these polymers seem to possess the requisites for obtaining new efficient colloidal systems for delivery of this antifungal drug. Accordingly, a dissolution study was carried out and spectrometric analyses were performed to evaluate the physical and biopharmaceutical properties of the new micelle formulation, namely drug aggregation and stability. Finally a biological study was carried out to evaluate the antifungal activity of the novel formulation.

2. Materials and methods

Amphotericin B (AmB) was purchased from Azelis (Barcelona, Spain) and Fungizone® from Bristol-Myers Squibb (Madrid, Spain). Globulin free human serum albumin and 5b-cholanic acid were supplied by Sigma–Aldrich (Milan, Italy). 5 kDa amino-terminating monomethoxy-terminating poly(ethylene glycol) (PEG_{5kDa}-NH_2) and hydroxyl-terminating monomethoxy-terminating poly(ethyl-ene glycol) (PEG_{5kDa}-OH) were supplied by Iris Biotech GmbH (Marktredwitz, Gemany). Certified Candida albicans strain (CECT1394) was a gift of Dr. Pérez Carrasco from Centro de Análisis Químico y Microbiológico (CAQYM), Universidad Alcalá de Henares (Madrid, Spain). Culture media were purchased from Pronadisa-Conda Lab (Madrid, Spain). Technical grade and HPLC grade solvents and salts were purchased from Merck (Milan, Italy).

2.1. Synthesis of monomethoxy-poly(ethylene glycol)-cholane (PEG_{5kDa}-cholane)

Monomethoxy-poly(ethylene glycol)-cholane (PEG_{5kDa}-cholane) was synthesized according tothepreviously published protocol with modifications (Salmasoetal., 2012). Briefly, thionyl chloride (524 mL, 7.2 mmol) was added to 5b-cholanic acid (260 mg, 0.72 mmol) in 6 mL CH_2Cl_2. The mixture was refluxed under nitrogen atmosphere at 50 C for 3 h and then the unreacted thionyl chloride was removed by distillation. After solvent evaporation, an aliquot of activated cholane was reacted with CH_3OH and analyzed by ^{1}H NMR spectrometry using a Bruker Spectrospin 300 spectrometer (Bruker, Fallanden, Switzerland) to estimate the activation degree. Cholanyl chloride (218 mg, 0.576 mmol) in 1 mL CH_2Cl_2 was added of 53.5 mL TEA (0.384 mmol) and 4 mL CH_2Cl_2 of 242.7 mg/mL PEG_{5kDa}-NH_2 (970.8 mg, 0.192 mmol). The reaction solution was maintained overnight under stirring at room temperature and then dropwise added to 35 mL of diethyl ether. The precipitate was recovered by centrifugation at 4000 rpm for 15 min and re-dissolved in 5 mL CH_2Cl_2. The precipitation was repeated three times. The precipitate was desiccated under vacuum and finally lyophilized in a Hetossic equipment (HETO Lab, Birkerod, Denmark). The degree of PEG-NH_2 derivatization with cholanyl chloride was evaluated by the TNBS colorimetric assay, which allows for determination of unreacted amino groups (Snyder and Sobocinski, 1975) and by ^{1}H NMR spectrometry.

^{1}H NMR (300 MHz, $CDCl_3$): d 0.64 [s, 3H, CH_3 cholane], d 0.911—0.911–0.928 [s + d, 6H, CH_3 (C18) + CH_3 (C21) cholane], d 3.381 [s, 3H, CH_3O-MeO-PEG], d 3.645 [s, 4nH, (CH_2CH_2-O)$_n$ MeO–PEG].

2.2. Amphotericin B dissolution

Dissolution studies were carried out according to three methods: (1) direct dissolution; (2) co-solvent dissolution; (3) dissolution/pH change.

2.2.1. Direct dissolution

Samples of 4 mg AmB in 500 mL CH_3OH where desiccated using a speed-vac system. The dried samples were added of 500 mL of 0.5, 1, 1.5, 2, 3 and 6 mg/mL PEG_{5kDa}-cholane or PEG_{5kDa}-OH in water, pH 7.2, and maintained overnight under top–down mixing. The samples were centrifuged at 12,000 rpm for 10 min. The AmB concentration in the supernatant was determined by reverse-phase chromatography (RP-HPLC) using a Thermo Hypersil BDS® C18 column (200 4.6 mm, 5 mm) operated on a Jasco HPLC system equipped with a Jasco PU-1580 pump and UV–vis detector set at 406 nm (Jasco, Tokyo, Japan). The column was isocratically eluted at a flow rate of 1 mL/min with 52:4.3:43.7 v/v/v acetonitrile/acetic acid/water mobile phase (Espada et al., 2008a). The AmB concentration in the samples was determined

on the basis of the elution peak area, which was referred to a titration curve obtained by eluting AmB samples at concentrations in the range of 0.012–40 mg/mL [(AmB concentration) = 115.1(peak area)–1.665; R^2 = 1.00].

2.2.2. Co-solvent dissolution

Samples of 4 mg of AmB in 500 mL CH_3OH were added of 100 mL of 2.5, 5, 7.5, 10, 15 and 30 mg/mL PEG_{5kDa}-cholane or PEG_{5kDa}-OH in water, pH 7.2. The mixtures were dried in speed-vac and the residues were re-dispersed in 500 mL water at pH 7.2 and maintained overnight under top–down mixing. The samples were centrifuged at 12,000 rpm for 10 min and the AmB in the supernatant was analyzed by RP-HPLC as reported above.

2.2.3. Dissolution/pH change

The AmB dissolution was performed according to the method described by Higuchi and Connors (1965). Briefly, 20 mg of AmB were dissolved in 1 mL of 0.5, 1, 1.5, 2, 3 and 6 mg/mL PEG_{5kDa}-cholane or PEG_{5kDa}-OH in 0.05 N NaOH. The pH was then shifted to 7.2 with 0.1 M ortophosphoric acid and the suspensions were centrifuged at 12,000 rpm for 10 min. The AmB in the supernatant was analyzed by RP-HPLC as reported above.

2.3. Isothermal titration calorimetry

Isothermal titration calorimetry (ITC) analyses were carried out using an MSC-ITC instrument (Microcal Inc., Northampton, MA). AmB solutions were prepared by dissolution/pH change and concentration was determined by RP-HPLC analysis as reported above. AmB ($1.1\ 10^{-5}$ M) and PEG_{5kDa}-cholane ($0.6\ 10^{-3}$ M) solutions in water at pH 3.5, 5.5, 7.2, 8.5 and 11.0, were degassed and thermostated at 25 C before the analysis. At 5 min intervals, 5 mL volumes of PEG_{5kDa}-cholane solutions were injected in 10 s into the calorimeter cell containing 1.5 mL AmB solutions at the same pH. Each assay was performed in triplicate and the data analysis was performed with Microcal Origin 3.5 software.

2.4. Dynamic light scattering and zeta potential analyses

AmB/PEG_{5kDa}-cholane aqueous solutions (1 mg/mL AmB, 12:1 AmB/PEG_{5kDa}-cholane molar ratio) prepared by dissolution/ pH change were analyzed at different times (0, 7, 14, 21, 28, 35, 42, 49, 56 and 63 days) by dynamic light scattering (DLS) using a Malvern Zetasizer Nano-ZS (Malvern, Worcestershire, UK). The analyses were performed in triplicate at 25 C, 633 nm wavelength and 173 detection angle to assess the mean particle size, size distribution and zeta potential.

2.5. Freeze drying

AmB/PEG_{5kDa}-cholane samples (10 mL, 1 mg/mL AmB, 12:1 AmB/PEG_{5kDa}-cholane molar ratio) were prepared by dissolution/pH change, frozen with liquid N_2 and lyophilized using a Lio-labor[1] instrument (Telstar, Barcelona, Spain) for 48 h. The freezing and sublimation temperatures in the lyophilization chamber were 45 C and from 45 to 25 C, respectively. The sublimation pressure was $4.54\ 10^{-4}$ atm. The moisture content in the lyophilized product was determined as weight loss after heating at 105 C using a Mettler PM100 balance equipped with a Mettler LP16 infrared drying unit (Mettler Toledo, Greifensee, Switzerland). The end point was estimated after 120 s without weight variation. Reconstitution of the freeze dried samples was performed by the addition of 10 mL 10 mM phosphate buffer, 0.15 M NaCl (PBS), pH 7.2. Particle size and AmB concentration analyses of reconstituted solutions were carried out at times 0, 7, 14, 24 and 31 days by DLS and RP-HPLC, respectively, according to the analytical protocols reported above.

2.6. Physicochemical analyses

Samples of AmB, PEG_{5kDa}-OH, PEG_{5kDa}-cholane, lyophilized AmB/PEG_{5kDa}-cholane (12:1 AmB/PEG_{5kDa}-cholane molar ratio) prepared by dissolution/pH change and AmB/PEG_{5kDa}-cholane physical mixtures (12:1 AmB/PEG_{5kDa}-cholane molar ratio) obtained by mixing AmB and PEG_{5kDa}-cholane dry powders were analysed by differential scanning calorimetry, hot stage microsco-py, X-ray diffractometry and Fourier-transformed infrared spec-troscopy.

2.6.1. Differential scanning calorimetry (DSC)

DSC analyses were performed using a Mettler TA3000 differential scanning calorimeter DSC 20 (Mettler Toledo, Greifensee, Switzerland). Samples (10 mg) were placed on a pinhole aluminum lidded pan and heated in atmospheric air at a rate of 10 C/min from 30 to 250 C.

2.6.2. Hot stage microscopy (HSM)

HSM analyses were performed by placing the samples on a microscope covered slide and heated at a rate of 2 C/min from 25 to 250 C. Microscopy determinations were carried out using a Thermo Galen microscope fitted with the Kofler stage (Leica, Wien, Austria) (Ruiz-Caro and Veiga-Ochoa, 2009).

2.6.3. X-ray diffractometry (XRD)

XRD analyses were carried out with an X-ray diffractometer Philips[1] X'Pert-MPD (PANalytucal, Amelo, Netherlands). The samples were placed on a carrier, irradiated with monochromat-ized Cu$K\alpha$-radiation and analyzed between 2θ angles of 5 and 50 with 0.04 steps of 1 s. The assay was performed at 30 mV voltage and 30 mA intensity.

2.6.4. Fourier-transformed infrared spectroscopy (FT-IR)

FT-IR spectra were recorded over the range 4000–400 cm^{-1} using a FT-IR Nicolet Magna 750 spectrometer (0.5 cm^{-1} resolu-tion) equipped with an attenuated total reflectance (ATR) Spectra Tech Performer with diamond crystal (Thermo Fisher Scientific, Waltham, MA, USA). The data were analysed with Thermo software.

2.7. Transmission electron microscopy

Samples for negative-stain transmission electron microscopy (TEM) analysis were prepared by depositing one drop of AmB/ PEG_{5kDa}-cholane (12:1 molar ratio) micelles, prepared by dissolu-tion/pH change, stained with 1% phosphotungstic acid for 20 s into Formvar/carbon-coated TEM copper grids (size 3.05 mm) for 30 s. The grids were left drying at room temperature for 15 min before the analysis. The samples were examined and photographed in a Jeol JEM 1010 transmission electron microscope (Jeol Ltd., Tokyo, Japan) equipped with a Megaview II imaging camera and operating at 100 kV (resolution 0.35 nm).

2.8. Human serum albumin circular dichroism analyses

Human serum albumin (HSA) solutions ($1.5\ 10^{-7}$ M) in PBS, pH 7.2, in the absence or in the presence of $1.37\ 10^{-7}$ M AmB or equivalent AmB concentration of Fungizone[1], heated Fungizone[1] (obtained by 30 min heating Fungizone[1] at 70 C) or AmB/PEG_{5kDa}-cholane micelles (12:1 AmB/PEG_{5kDa}-cholane molar ratio) pre-pared by dissolution/pH change were analyzed by circular dichroism (CD) in the far UV (200–300 nm, 50 nm/s with 8 s

response and 2 nm band width) using a J-810 Jasco spectrodichro-graph (Jasco, Tokyo, Japan). The spectra were processed by Dicroprot software and the protein secondary structure was calculated by KD2 analysis. CD analyses were also performed after sample incubation at 37 C for 15 min (Hartsel et al., 2001).

2.9. Absorption and kinetics studies

AmB (5 10^{5} M) or AmB equivalent concentration of Fungizone®, heated Fungizone® and AmB/PEG_{5kDa}-cholane micelles (12:1 AmB/PEG_{5kDa}-cholane molar ratio) prepared by dissolution/pH change in PBS, pH 7.2, were 1:10 diluted with a 2.3 10^{4} M HSA in the same buffer and spectrophotometrically analyzed by UV absorption in the range of 300–450 nm at 25 and 37 C using an Evolution 201 UV–vis spectrophotometer equipped with a single cell peltier system (Thermo Fisher Scientific). Absorption spectra were recorded at 0, 1, 2, 5, 10, 20 and 45 min. Kinetic analysis were performed recording the absorption at 413 nm, at 15 s intervals for the first 5 min and then at 1 min intervals for further 40 min (Vakil and Kwon, 2007).

2.10. Dialysis studies

One millilter of 30 mg/mL AmB equivalent of AmB/PEG_{5kDa}-cholane micelles (12:1 AmB/PEG_{5kDa}-cholane molar ratio) in PBS, pH 7.4, were dialyzed against 500 mL PBS, pH 7.4 using a Float-A-Lyzer® G2 system, 3.5–5 kDa cut-off. The AmB concentration inside the dialysis bag was determined at fixed time points by RP-HPLC according to the method reported above.

2.11. Microbiological activity

In vitro antifungal activity of AmB and AmB/PEG_{5kDa}-cholane micelles (12:1 AmB/ PEG_{5kDa}-cholane molar ratio) in PBS, pH 7.2, prepared according by dissolution/pH change, was assessed against C. albicans CECT1394. Yeast cells were cultured in Petri dishes containing agar Sabouraud medium for 72 h at 30 C and then 3 mL of a 0.5 McFarland standard suspension (1–5 10^{6} CFU/ mL) were seeded in plates of Agar Mueller Hinton supplemented with glucose (Roling et al., 2002). Methylene blue was used as contrast agent. Paper disks, impregnated with the AmB dissolved in DMSO were used as reference (S_1 600 mg/mL; S_2 200 mg/mL; S_3 96 mg/mL; S_4 38.4 mg/mL; S_5 18.4 mg/mL). Twenty microliters of 96 mg/mL AmB or equivalent AmB concentration of AmB/ PEG_{5kDa}cholane in 0.2 M phosphate buffer, pH 10.5, were placed onto the paper disk that was then placed on the plates and incubated at 30 C. After 48 h of incubation, the inhibition zones were accurately measured using a caliper and referred to the reference (96 mg/mL AmB, S_3).

3. Results

3.1. AmB/PEG_{5kDa}-cholane solubility and association studies

Solubility studies were carried out at pH 3.5, 5.5, 7.2, 8.5 and 11.0 by combining fixed amounts of AmB with increasing amounts of PEG_{5kDa}-cholane according to three different experimental protocols: (1) direct dissolution; (2) co-solvent dissolution; (3) dissolution/pH change. For comparison, the solubility of AmB in the presence of increasing amounts of PEG_{5kDa}-OH was also examined.

Preliminary studies showed that in the absence of PEG_{5kDa}-cholane and PEG-OH, the direct AmB dissolution yielded lower drug concentrations than co-solvent dissolution and dissolution/ pH change. This behaviour was observed at all examined pHs (Supporting information, Fig. SI1) and was in fair agreement with studies reported in the literature (Mazerski et al., 1990). The UV spectra of dissolved AmB (Fig. SI2B) showed that the three dissolution methods yielded different physical forms of dissolved AmB, namely monomers and soluble aggregates such as dimers and tetramers. According to the literature, the absorption at 322 nm (Al_{322}) and 413 nm (Al_{413}) were elaborated to estimate the content of monomeric and nanoaggregated AmB in solution (Adams et al., 2003; Vakil and Kwon, 2007). The lower Al_{322}/Al_{413} ratio obtained by direct dissolution indicated that the monomeric form was the predominant AmB form in solution. On the contrary, the higher Al_{322}/Al_{413} ratio obtained by co-solvent dissolution and dissolution/pH change indicated that in such a case the main form in solution was nanoaggregated AmB. Therefore, AmB dissolved by direct dissolution tends to be in the monomeric form while AmB dissolved by dissolution/pH change and co-solubilization was mainly in aggregated form.

The solubility profiles reported in Fig. 1 show that PEG_{5kDa}-OH has not relevant effect on the AmB solubility, which increased from 6 mg/mL to 17 mg/mL as the polymer concentration increased from 0.5 to 6 mg/mL. Furthermore, similarly to AmB in the absence of polymers, the dissolution method did not affect remarkably the AmB solubility (data not shown). On the contrary, PEG_{5kDa}-cholane dramatically increased the drug solubility and the dissolution method was found to significantly affect the AmB solubility. The direct dissolution yielded less than 0.5:1 AmB/PEG_{5kDa}-cholane molar ratio while the co-solvent dissolution and the dissolution/ pH change protocols resulted in 12:1 AmB/PEG_{5kDa}-cholane molar ratio, with identical dissolution profiles.

The UV analysis of the AmB/PEG_{5kDa}-cholane obtained by direct dissolution (Fig. SI2B) showed that the dissolved AmB was mainly in the monomeric form while the high absorption at 322 nm of samples obtained by co-solvent dissolution and dissolution/pH change demonstrated that in these samples the nanoaggregated AmB form predominated.

The maximal solubility of AmB with PEG_{5kDa}-cholane could not be determined because high polymer concentrations produced viscous dispersions that prevented the accurate analysis of dissolved AmB.

Isothermal titration calorimetric (ITC) analyses were performed to investigate the AmB interaction with PEG_{5kDa}-cholane at different pHs: 3.5, 5.5, 7.2, 8.5 and 11.0. The ITC study was carried out by injecting volumes of polymer solutions into the cell containing the AmB solutions. The operative conditions were selected on the basis of the results obtained by the solubility studies. Blank runs were carried out by injecting polymer solutions

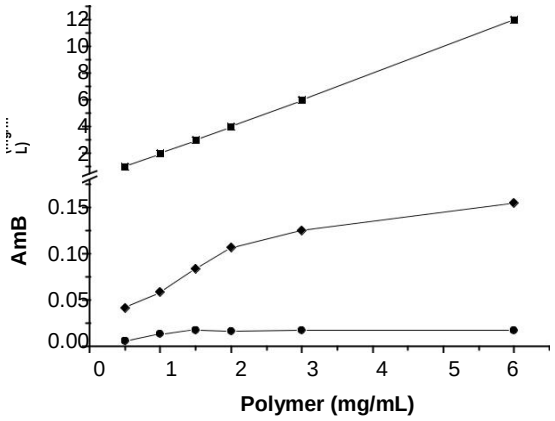

Fig. 1. Solubility profile of AmB with: PEG_{5kDa}-cholane by direct dissolution (-^-); PEG_{5kDa}-cholane by dissolution/pH change and by co-solubilization (-&-); PEG-OH by dissolution/pH change (-*-).

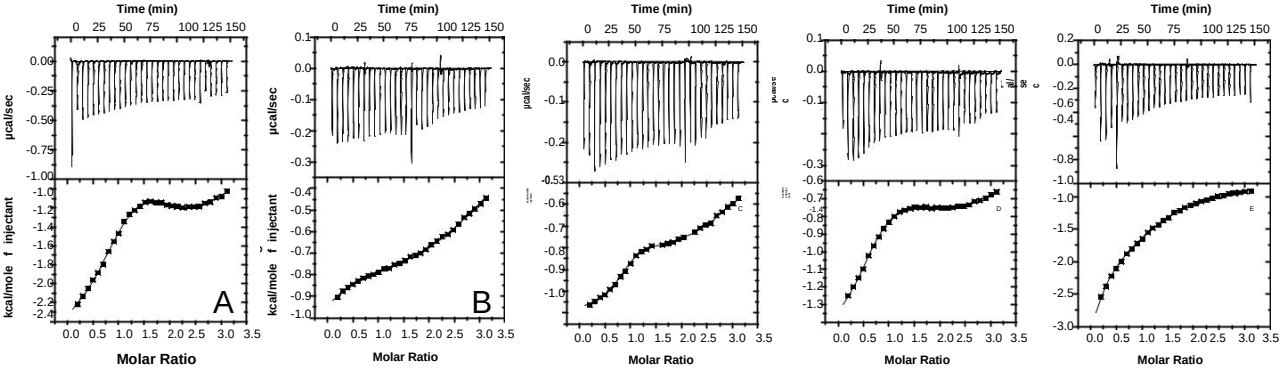

Fig. 2. Isothermal calorimetry profiles of AmB titrated with PEG_{5kDa}-cholane at pH 3.5 (A), 5.5 (B), 7.2 (C), 8.5 (D) and 11.0 (E).

into the cell containing AmB free buffer or by injecting buffer into the cell containing AmB solutions.

The buffer injection into AmB solutions did not elicit significant thermal effect. Instead, the injection of aliquots of polymer solutions into the cell containing buffer produced a pH indepen-dent bimodal exothermic ITC profile, which was due to the demicellisation and polymer dilution as reported elsewhere (Salmaso et al., 2014). The thermal profiles reported in Fig. 2 show that the polymer interaction with AmB occurs according to a multimodal pH-dependent behaviour. The calorimetric raw data subtracted of the values obtained with the corresponding blanks were found to fit a three sequential binding site fitting model, with good correlation (Chi^2). The association parameters derived from the analysis are summarized in Table 1.

In all cases, the binding affinity constants (K) were found to decrease from the first to the third binding site and the drug/ polymer interactions occurred according to strong exothermic contributions (DH). The first binding was found to occur with high enthalpic and entropic contribution (DH1 and DS1, respectively). The second binding occurred with the lowest enthalpic contribu-tion (DH2) even though it was strongly favoured by a positive entropic change (DS2). The third binding was characterized by the lowest affinity constant (K3) and entropic contribution (DS3) but the highest enthalpic contribution (DH3). To note that at pH 11.0, the third binding occurred with negative DS.

3.2. Dimensional, morphological and surface characterization of AmB/ PEG_{5kDa}-cholane formulations

Dynamic light scattering (DLS) and transmission electron microspcopy (TEM) analyses were performed to evaluate the dimensional, morphological and surface features of the AmB/ PEG_{5kDa}-cholane formulations obtained by dissolution/pH change. The DLS profile reported in Fig. 3A shows that the AmB association with PEG_{5kDa}-cholane forms monodisperse size distribution micelles with mean diameter of 33.2 1.2 nm (PDI 0.16), which was in good agreement with the dimensional values obtained with AmB free PEG_{5kDa}-cholane formulations (Salmaso et al., 2012). DLS analyses of AmB/PEG_{5kDa}-cholane formulations performed in the pH range of 3.5–11.0 yielded similar dimensional profiles of AmB/ PEG_{5kDa}-cholane formulations while AmB/PEG_{5kDa}-OH mixtures did not show micelle formation at all pHs. The TEM image reported in Fig. 3B confirms the dimensional features obtained by DLS. The AmB/PEG_{5kDa}-cholane micelles have circular shape and gray shadow around the micelles due to the negative-staining of the PEG chains by phosphotungstic acid.

Fig. 4 shows the zeta potential of the micelles at different pHs. At pH 5.5–7.2 the overall micelle surface was nearly neutral. At pH below 5.5 the zeta potential shifted to slightly positive values and above pH 7.2 to negative values. Similar zeta potential values were obtained with AmB free PEG_{5kDa}-cholane micelles.

3.3. AmB/MeO-PEG_{5kDa}-cholane formulation lyophilization and stability

The lyophilization of AmB/PEG_{5kDa}-cholane formulations obtained by dissolution/pH change produced yellowish, fluffy and slightly electrostatic powders (Fig. 5, insert A). The moisture content in the lyophilized product was 7%. The lyophilized powder rapidly re-dissolved in buffer at pH 7.2 (Fig. 5, insert B) to regenerate a clear yellow colloidal dispersion.

Table 1
Calorimetric parameters obtained by AmB titration with PEG_{5kDa}-cholane at pH 3.5, 5.5, 7.2, 8.5 and 11.0: affinity constant (K), differential enthalpy (DH) differential entropy (DS), Chi squared (Chi^2/DoF).

	pH				
	3.5	5.5	7.2	8.5	11.0
K1 10^5 M^{-1}	9.83 0.46	1.54 0.069	7.87 0.28	3.31 0.096	2.36 0.12
DH1	2349 14.3	1071 9.36	1101 3.64	1414 7.99	3206 47.0
DS1	19.5	20.1	23.3	20.5	13.8
K2 10^5 M^{-1}	1.22 0.088	0.554 0.023	0.356 0.027	0.435 0.016	1.52 0.12
DH2	485.4 24.5	769.1 21.4	964.5 29.3	104.9 19.3	125.5 56.4
DS2	21.6	19.1	17.6	20.9	23.3
K3 10^5 M^{-1}	0.149 0.009	0.531 0.022	0.234 0.012	0.246 0.008	0.062 0.004
DH3	5251 134	1061 23.8	2053 50.8	3127 27.2	6924 277
DS3	1.49	18.1	13.1	9.60	-5.87
Chi^2/DoF	114.7	17.87	18.29	19.19	142.5

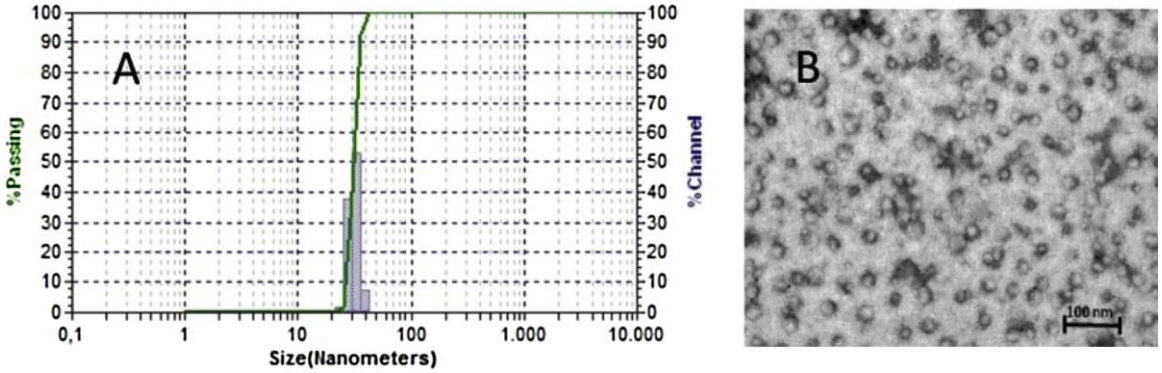

Fig. 3. Dynamic light scattering profile (A) and transmission electron microscopy image (B) of AmB/PEG$_{5kDa}$-cholane formulations.

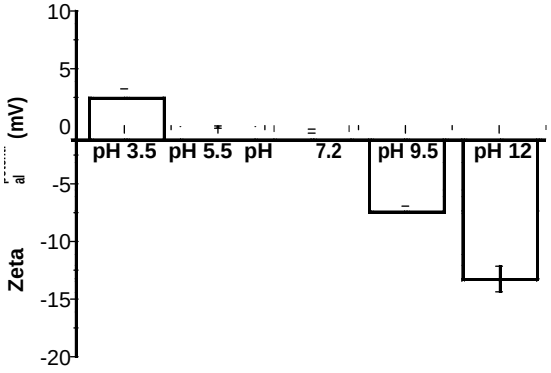

Fig. 4. Zeta potential profiles of AmB/PEG$_{5kDa}$-cholane micelles at different pHs.

After re-dispersion, at 25 C, the micelle size of the colloidal system was 32.2 3.4 nm and AmB was completely re-dissolved. Fig. 5 shows that both micelle size and AmB concentration remained stable over 1 month. After 2 months storage neither the micelle size nor the size distribution changed while the AmB concentration decreased by 8 0.3%. Similar results were obtained with freshly prepared micelles.

3.4. Structural characterizations

Comparative structural characterizations of AmB, PEG$_{5kDa}$-cholane, PEG$_{5kDa}$-OH, lyophilized AmB/PEG$_{5kDa}$-cholane micelles and physical AmB/PEG$_{5kDa}$-cholane mixture were performed by differential scanning calorimetry (DSC), X-ray diffractometry (XRD) and Fourier transformed infrared (FTIR).

The DSC profiles (Fig. SI3) showed the typical water loss, melting and decomposition behaviors of the various samples. Unformulated AmB exhibited the characteristic endothermic peak of this drug at 104.6 C corresponding to the water loss process (Zu et al., 2014) and the characteristic decomposition peak above 160 C, namely at 188.6 C (Rajagopalan et al., 1986). PEG$_{5kDa}$-cholane showed a sharp endothermic peak at 58.9 C, correspond-ing to the polymer melting as observed by hot stage microscopy (60 C), followed by an exothermic event at 171.3 C, which corresponds to the polymer decomposition. Similarly to PEG$_{5kDa}$-cholane, PEG$_{5kDa}$-OH melted at 64.1 C and decomposed at 155.0 C. The thermal profile of the physical AmB/PEG$_{5kDa}$-cholane mixture showed two endothermic peaks at 60.9 C and 92.9 C, and an exothermic peak at 178.5 C, which were in fair agreement with AmB melting and PEG$_{5kDa}$-cholane melting and decomposition. The DSC profiles of AmB/PEG$_{5kDa}$-cholane micelles showed only one endothermic peak at 172.5 C, corresponding to the PEG$_{5kDa}$-cholane decomposition.

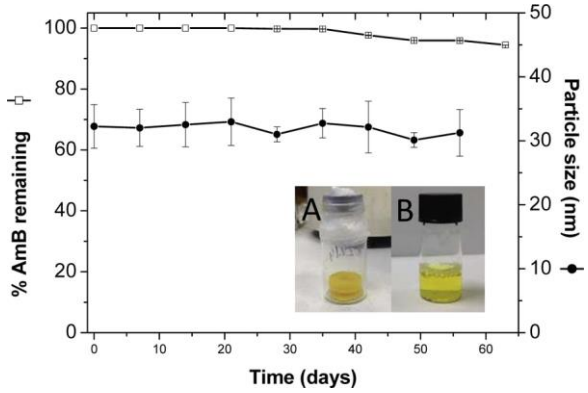

Fig. 5. Micelle size (-*-) and residual AmB content (-&-) time course profiles of lyophilized AmB/PEG$_{5kDa}$-cholane formulation re-dispersed in buffer at pH 7.2. Insert A lyophilized formulation; insert B re-dispersed formulation. (For interpretation of the references to colour in the text, the reader is referred to the web version of this article.)

The X-ray diffractometric (XRD) spectra (Fig. SI4) showed the characteristic peaks of the crystalline form of unformulated AmB at diffraction angles of 2u 14.82 , 17.22 , 18.38 , and 21.66 (Kim et al., 2010; Zu et al., 2014; Choi et al., 2008). PEG$_{5kDa}$-cholane displayed broad peaks at 19.02 and 23.38 while the AmB/PEG$_{5kDa}$-cholane physical mixture showed the peaks corresponding to both crystalline AmB and PEG$_{5kDa}$-cholane. The lyophilized AmB/ PEG$_{5kDa}$-cholane micelle formulation did not show the character-istic peaks of AmB and PEG$_{5kDa}$-cholane while exhibited two peaks at 22.11 and 26.14 .

The Fourier transformed infrared (FTIR) spectra (Fig. SI5) provided additional information about the physical AmB/PEG$_{5kDa}$-cholane interaction in the micelle lyophilized product. The unformulated AmB spectrum showed the typical signals reported in the literature (Gagos and Arczewska, 2010; Zu et al., 2014; Kim et al., 2010). The spectrum of the physical AmB/PEG$_{5kDa}$-cholane mixture showed the signals corresponding to both AmB, i.e. at 1039 cm ^{1}, [n(C O C)] pyranose, and PEG$_{5kDa}$ cholane, i.e. at

Table 2
Secondary structure (a-helix and b-helix content) of human serum albumin (HSA) and HSA incubated with AmB, Fungizone[1], Heated Fungizone[1] and AmB/MeO-PEG$_{5kDa}$-cholane.

	a-helix	b-helix
HSA	0.67	0.04
AmB	0.63	0.06
Fungizone[1]	0.63	0.06
Heated Fungizone[1]	0.64	0.05
AmB/MeO-PEG$_{5kDa}$cholane	0.69	0.04

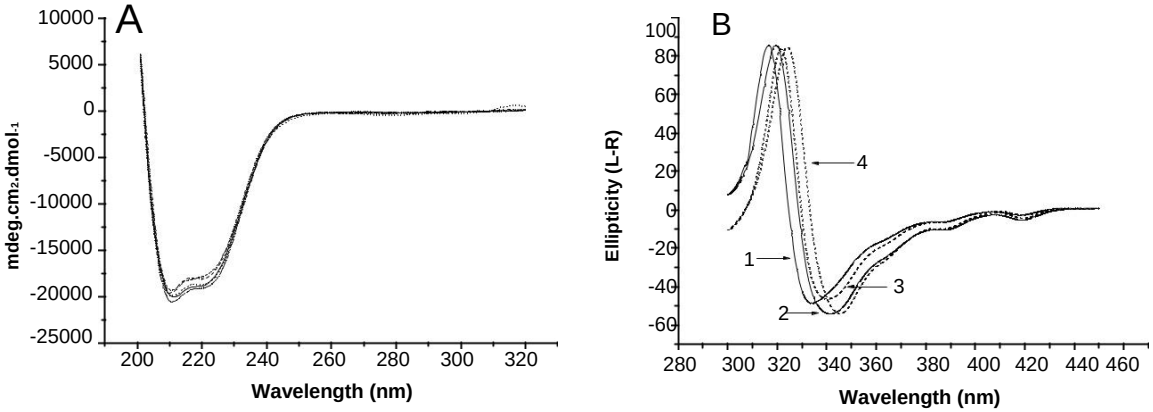

Fig. 6. Circular dichroism spectra. (A) Far UV spectra of HSA incubated with: AmB (—), Fungizone[1] ( ); heated Fungizone[1] (- -); AmB/PEG_{5kDa}-cholane micelles (-) (B) Near UV spectra of AmB/PEG_{5kDa}-cholane micelles in the absence of HSA (1); AmB/PEG_{5kDa}-cholane micelles in the presence of HSA (3); Fungizone[1] in the absence of HSA (2); Fungizone[1] in the presence of HSA (4).

1465 cm ^{1} [d(CH_2)], 1359 cm ^{1} [d(CH)], 840.43 cm ^{1} [d(C H)] cyclic. The lyophilized AmB/PEG_{5kDa}-cholane micelles displayed the same signals of the other samples. However, below 1700 cm ^{1} the main peaks characteristic of AmB [i.e. 1689.37 cm ^{1},n(C¼O); 1552.55 cm ^{1}, d(N H); 1006.68 cm ^{1}, d(¼C H)] (Nahar and Jain, 2009; Asher and Levin, 1977) and PEG_{5kDa}-cholane [i.e. at 1465 cm ^{1}, d(CH_2); 1342 cm ^{1}, d(C O); 1097 cm ^{1}, n(C N); 960 cm ^{1}, d(C H)] were missing.

3.5. Human serum albumin spectroscopic analyses

Circular dichroism studies were carried out to investigate the interaction of AmB with plasma proteins, which can either alter the protein structure or induce drug disaggregation (Vakil and Kwon, 2007; Hartsel et al., 2001). The study was comparatively performed using AmB, Fungizone[1], heated Fungizone[1] and AmB/PEG_{5kDa}-cholane.

Table 2 reports the secondary protein structure obtained by the KD2 elaboration of the far UV CD spectra shown in Fig. 6A. The results reported in the table show that the secondary protein structure was not significantly altered by AmB regardless the formulation.

Fig. 6B reports the near UV CD spectra of AmB/PEG_{5kDa}-cholane micelles and fungizone showing the typical doublet (intense biphasic dichroic signals) of AmB in the absence or in the presence of HSA. The wavelengths of maximum (l_{max}) and minimum (l_{min}) ellipticity and the maximum–minimum ellipticity amplitude intensity (Ai) represent the AmB aggregation: the lower l_{max} and l_{min}, the higher the AmB aggregation; the higher Ai, the higher AmB aggregation (Hartsel et al., 2001).

In the comparative study, AmB in solution (Fig. 6B) presented the highest l_{max} and l_{min} and the lowest Ai either in the absence or in the presence of HSA (l_{max} 327 nm, l_{min} 353 nm and Ai 83.8 u in the absence of HSA; l_{max} 326 nm, l_{min} 351 nm and Ai 44.4 u in the presence of HSA). In the absence of HSA the l_{max}, l_{min} and Ai of AmB/PEG_{5kDa}-cholane were 316.5 nm, 333.8 nm and 134.3 u, respectively, while in the presence of HSA l_{max}, l_{min} and Ai were 321.4 nm, 340.2 nm and 129.9 u, respectively. In the absence of HSA, Fungizone[1] showed 319.5 nm l_{max}, 341.3 nm l_{min} and 139.71 u Ai while in the presence of HSA l_{max}, l_{min} and Ai were 324 nm 345.3 nm 138.66 u. Heated Fungizone[1] (Fig. SI6) showed the lowest l_{max} and l_{min} and the highest Ai (l_{max} 313 nm, l_{min} 330 nm and Ai 175.7 u in the absence of HSA; l_{max} 314 nm, l_{min} 332 nm and Ai 184.59 u in the presence of HSA). Accordingly, the spectra obtained with Fungizone[1] and AmB/PEG_{5kDa}-cholane micelles showed a higher presence of aggregated AmB (Hartsel et al., 2001)

either in the absence or in the presence of HSA compared to unformulated AmB. In both cases, the l_{max} and l_{min} of the doublet of Fungizone[1] was 3–8 nm higher compared to the ones obtained with AmB/PEG_{5kDa}-cholane micelles indicating that AmB in Fungizone[1] was less aggregated than in the PEG_{5kDa}-cholane micelles. The addition of HSA was found to red-shift of 4–7 nm the doublet of AmB formulated with PEG_{5kDa}-cholane and Fungizone[1] indicating that in both cases HSA promotes the AmB disaggre-gation (Espuelas et al., 1997, 1998; Gaboriau et al., 1997).

UV–vis absorption spectroscopic studies were performed in the range 300–450 nm to determine the time course profile of AmB disaggregation in presence of HSA. The studies were comparatively performed with AmB, Fungizone[1], heated Fungizone[1] and AmB/ PEG_{5kDa}-cholane micelles at 25 C and 37 C and the AmB disaggregation was determined by Gaussian fit of peak IV. The increase of the absorption area of peak IV (l 413 nm), which represents the monomeric state of AmB, indicates the drug disaggregation.

The time course profiles reported in Fig. 7 show that at 37 C the unformulated AmB undergoes significant disaggregation. Fungizone[1] disaggregation was found to occur at less extent than free AmB while heated Fungizone[1] was pretty stable as its disaggregation was very low. The extent of AmB disaggregation from the AmB/PEG_{5kDa}-cholane micelles was found to be in

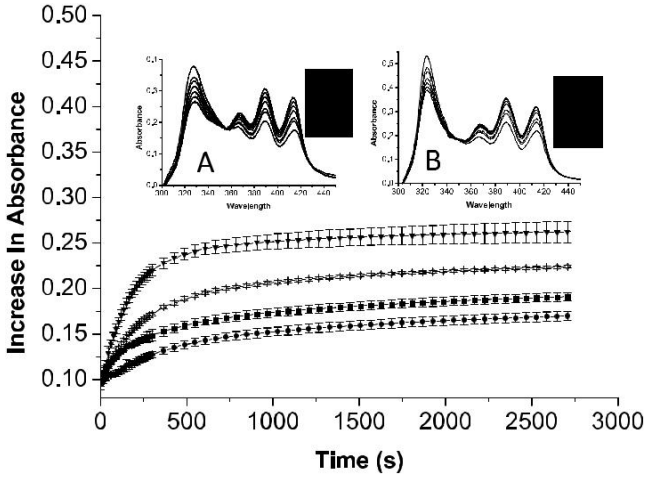

Fig. 7. Disaggregation profiles at 37 C of AmB (-!-), Fungizone[1] (-^-), heated Fungizone[1] (-*-) and AmB/PEG_{5kDa}-cholane micelles (-&-) incubated with HSA. Insert A and B: spectra profiles of Fungizone (A) and AmB/PEG_{5kDa}-cholane micelles
(B) registered at 0, 1, 2, 5, 10, 20, 45 min.

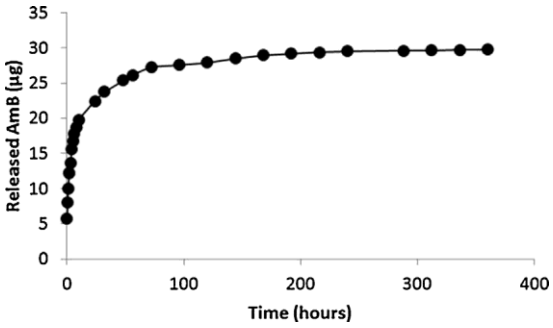

Fig. 8. AmB release profile from AmB/PEG_{5kDa}-cholane micelles by dialysis in PBS.

between Fungizone® and heated Fungizone®. After 45 min, the peak IV area was 2.1 and 1.7 for Fungizone® and AmB/PEG_{5kDa}-cholane, respectively.

The curves reported in Fig. 7 were found to fit a first order kinetic and were elaborated to get information on AmB dissocia-tion rate. At 37 C, the disaggregation half-life time ($t_{1/2}$) was 194, 335, 463 and 618 s for unformulated AmB, Fungizone®, heated Fungizone® and AmB/PEG_{5kDa}-cholane micelles, respectively. The $t_{1/2}$ values calculated from disaggregation profiles obtained at 25 C (Fig. SI7) were 397, 507, 573 and 997 s for AmB in solution, Fungizone®, heated Fungizone® and AmB/PEG_{5kDa}-cholane micelles, respectively.

3.6. AmB release and microbiological activity

The AmB release from the micelles was evaluated by dialysis under sink conditions. Fig. 8 shows a burst release after which 50% of the drug is released in 6 h and 80% in 48 h.

In vitro antifungal studies of AmB and AmB/PEG_{5kDa}-cholane micelles were performed against C. albicans (Klepser et al., 1997). The diameters of the inhibition halos were, for both formulations, higher than 15 mm (18.47 0.18 for AmB and 20.48 0.24 mm for AmB/PEG_{5kDa}-cholane micelles), indicating that they are active against C. albicans (Espinel-Ingroff et al., 2007a,b). The results reported in Fig. 9 show that AmB/PEG_{5kDa}-cholane micelles were 15% less active than the standard solution of AmB and 15% more active than AmB in buffer.

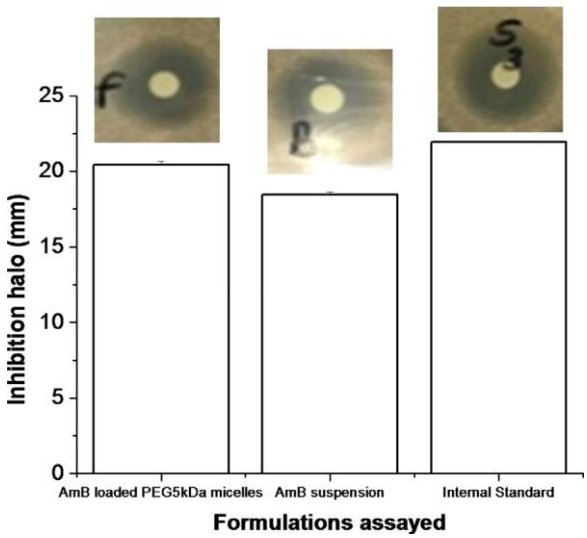

Fig. 9. C. albicans inhibition in the presence of AmB/PEG_{5kDa}-cholane, AmB in buffer (suspension) and AmB in DMSO ($p < 0.01$).

4. Discussion

The results reported in this paper show that PEG_{5kDa}-cholane can increase more than 10^3 times the AmB solubility according to a linear [dissolved drug]/[polymer concentration] correlation. Sol-utions up to 12 mg/mL AmB (6 mg/mL PEG_{5kDa}-cholane) were obtained without significant change of buffer viscosity. Higher drug/polymer concentrations increased the viscosity, which prevented the accurate determination of the maximal AmB solubility. However, neither AmB separation nor inhomogeneity were observed up to 60 mg/mL AmB (30 mg/mL PEG_{5kDa}-cholane). PEG_{5kDa}-OH was not found to significantly affect the AmB solubility indicating that the drug solubility was due to the supramolecular PEG_{5kDa}-cholane self-association into micelles as previously reported (Salmaso et al., 2012).

The remarkable effect of PEG_{5kDa}-cholane on AmB solubility is due to combined effects, which include the ability of PEG_{5kDa}-cholane to form stable micelles with a low CMC (Salmaso et al., 2012) and the affinity of AmB for sterol molecules. AmB displays in fact its antifungal activity and cytotoxicity by interaction with ergosterol and cholesterol located in membranes of fungi and mammalian cells, respectively (Gray et al., 2012; Wilcock et al., 2013). It should be noted that sterols in DSPE–PEG micelles were found to favour the formation of soluble AmB aggregates (Diezi and Kwon, 2012). This study showed that both AmB solubility and aggregation depend on the chemical structure and content of sterols in the DSPE–PEG vesicles.

High AmB solubility obtained using little amounts of excipients, namely solubilizing agents, is an important requisite for the development of safe products easily manageable in clinical practice. The use of high amounts of excipients may in fact be associated with toxic effect, in particular in parenteral admin-istrations, namely infusion. Little amounts of PEG_{5kDa}-cholane yielded very high AmB concentration solutions whilst commercial products, namely Fungizone® and Ambisome®, and other formulations described in the literature contain high amounts of solubilizing excipients (Vandermeulen et al., 2006). In Fungizone® and Ambisome®, for example, 50 mg AmB are formulated with 41 mg sodium deoxycholate and 350 mg phospholipids/cholester-ol/tochopherol, respectively (Fukui et al., 2003), which are re-constituted in 15 mL saline solution resulting in 3.33 mg/mL AmB. The same amount of AmB could be dissolved with 25 mg of PEG_{5kDa}-cholane in about 4 mL buffer to yield 12.5 mg/mL AmB. It is worth to note that previous cell culture studies showed that PEG_{5kDa}-cholane has negligible toxicity even at high doses. Furthermore, preliminary studies showed that, oppositely to sodium deoxycholate used in Fungizone®, PEG_{5kDa}-cholane does not display significant hemolytic effect (Salmaso et al., 2012).

The different capability of PEG_{5kDa}-cholane to solubilize AmB observed with different dissolution methods can be explained by the effect of the dissolution conditions in the formation of monomeric and multimeric soluble species, typically dimers and tetramers (Mazerski et al., 1990). According to the UV and CD spectrometric data, the direct AmB dissolution process produces low drug concentrations where AmB is mainly associated in the monomeric form with PEG_{5kDa}-cholane. On the contrary, the spectra obtained with AmB/PEG_{5kDa}-cholane prepared by co-solvent dissolution or by dissolution/pH change showed the typical profile of aggregated AmB. Therefore, the high drug concentration obtained by these methods can be ascribed to the formation of AmB nanoaggregates, which are promptly stabilized by the polymer interaction.

Dynamic light scattering (DLS) and transmission electron microscopy (TEM) confirmed that the AmB/PEG_{5kDa}-cholane association forms micelles with homogeneous size. The particles size was similar to other nanoformulations such as nanosomal

AmB (34.6 nm) (Sheikh et al., 2010) or Ambisome[1] (35–70 nm) (Lemke et al., 2005; Espada et al., 2008b; Fukui et al., 2003). The structure of the AmB/PEG_{5kDa}-cholane micelles was confirmed by the TEM analyses, which showed the polymeric chains exposed on the vesicle surface, while the hydrophobic cholane moieties were localized inside the micelles. The similar zeta-potential of AmB-free and AmB-loaded micelles indicates that the AmB ionization does not affect the overall surface charge of the micelle, confirming that the drug was localized in the micelle core.

The high affinity of AmB for PEG_{5kDa}-cholane observed by isothermal calorimetry (ITC) is in agreement with the high affinity of this drug for steroidal polycycles described in the literature, which is responsible for its antifungal activity and cytotoxicity (Gray et al., 2012; Wilcock et al., 2013). However, the isothermal calorimetry (ITC) results highlighted the complexity of the PEG_{5kDa}-cholane interaction with AmB, which takes place with different AmB soluble species, namely monomers, dimers, tetramers, and other multimeric nanoaggregates, which abun-dance depends on the pH. It has been reported that the presence of a net charge in the antibiotic molecule is the main factor that induces the solubility of AmB through the formation of the monomeric form. AmB pK_a values are 5.7 for the carboxyl group and 10.0 for the amino group. Therefore, at pH 11.0 AmB is mainly in the monomeric highly soluble anionic form (Mazerski et al., 1990). As the pH decreases to the isolectric point, the AmB anionic form and the drug solubility decrease with concurrent formation of less soluble nanoaggregates. At pH 3.5 the AmB solubility slightly increases with the increase of the cationic form, which was found to be less soluble than the anionic form. The similar thermal profile obtained at pH 5.5 and 7.2 and the similar ones obtained at 3.5 and 8.5 seem to indicate that the polymer interaction with the drug is strictly related to the solubility of AmB and hence to the relative abundance of the mono- or multi-meric species.

The three different binding sites calculated by ITC analyses reasonably result from the PEG_{5kDa}-cholane interaction with different AmB species through hydrophobic interactions between the cholane moiety and the heptaene side of the drug molecule to form different supramolecular structures. These results are in agreement with studies reported in the literature, which showed that the aggregation state of AmB depends on the sterol content physically incorporated in DSPE-PEG micelles. However, in all cases, the AmB/PEG_{5kDa}-cholane interaction is enthalpically favored, regardless the binding site and the pH, indicating that the cholane interaction with AmB is thermodynamically favored as expected by the interaction of hydrophobic moieties in aqueous solution.

The first and second bindings are also strongly entropically contributed suggesting that in these steps the polymer interaction with the drug provokes the disruption of ordered structures, namely AmB nanoaggregates, dimers and tetramers or by displacement of water molecules coordinated with the polymer and the drug. We hypothesize that these interactions occur by insertion of the cholanic moiety in between the heptaenic sides of coupled molecules in multimeric forms, dimers and tetramers.

The affinity constant for the third binding site (K3) was remarkably lower than that calculated for the other sites. Despite the strongest enthalpic contribution, the entropic contribution to this interaction was lower than the first two interactions, especially at high and low pHs. At pH 11.0, the DS was negative indicating that this interaction can occur with the formation of ordered structures. This seems to be in agreement with the XRD spectra, which showed that the AmB incorporation into the polymer micelles occurs with the destruction of the typical crystalline form of AmB while novel ordered structures are formed.

Importantly, the AmB/PEG_{5kDa}-cholane formulation was found to be pharmaceutically stable. The lyophilization process produced a fluffy powder with low moisture content without cake formation. The lyophilized product was stable for prolonged time as AmB/ PEG_{5kDa}-cholane solutions could be perfectly reconstituted by physiological buffer addition in few seconds, even without shaking, to yield a colloidal dispersion with the same physicochemical features of the freshly prepared formulation. It is worth to note that the reconstituted formulation was physically and chemically stable over 1 month at room temperature.

The spectrometric and thermal analyses performed on lyophi-lized AmB/PEG_{5kDa}-cholane provided information about the physical structure of the dried formulation. The Fourier transform infrared (FTIR) analysis showed new signals for the AmB/PEG_{5kDa}-cholane micelle formulations, while the AmB/PEG_{5kDa}-cholane physical mixture showed all the signals corresponding to the drug and the polymer. Similarly, the differential scanning calorimetry and X-ray diffraction (XRD) analyses evidenced the intimate AmB/ PEG_{5kDa}-cholane interaction with disappearance of the typical thermal and diffraction signals of crystalline AmB and PEG_{5kDa}-cholane. On the contrary, the AmB/PEG_{5kDa}-cholane physical mixture showed all signals of drug and polymer. However, it should be noted that as reported above the XRD spectrum of the lyophilized AmB/PEG_{5kDa}-cholane micelles showed new signals suggesting that novel non-amorphous species are formed.

The CD studies showed that, similarly to Fungizone[1] and heated Fungizone[1], AmB/PEG_{5kDa}-cholane micelles did not induce structural alterations of human serum albumin (HSA). This indicates that the formulation should not have detrimental effect on native proteins after administration. In the presence of HSA, the AmB nanoaggregates in the PEG_{5kDa}-cholane micelles are more stable and less rapidly disaggregated than in non-heated Fungizone[1], which can result in lower toxicity. The AmB displacement from the PEG_{5kDa}-cholane micelles is higher than from heated Fungizone[1]. Actually, heated Fungizone[1] was reported to contain higher amount of aggregated AmB compared to normal Fungizone[1], which results in a more stable and less toxic product (Gaboriau et al., 1997; Baas et al., 1999; Bartlett et al., 2004). Nevertheless, the therapeutic effect of heated Fungizone[1] is less reproducible than non-heated Fungizone[1] (Silva-Filho et al., 2012). Therefore, the aggregation results seem to indicate PEG_{5kDa}-cholane formulation can yield a product with higher AmB stability and lower toxicity compared to Fungizone[1] and enhanced reproducibility compared to heated Fungizone[1].

Finally, drug release and biological investigations were carried out to evaluate the pharmaceutical effectiveness of the novel delivery system. The dialysis study showed that AmB release occurs with an initial burst which is consistent with free drug non incorporated in the micelles. The remaining drug is freely released under the experimental conditions, which guarantee the drug availability.

The biological in vitro studies showed that the AmB formulated with PEG_{5kDa}-cholane maintains high antimicrobial activity, which is very close to AmB in solution. This confirms that the drug is released from the micelles to interact with the cell membrane. The slightly lower activity of AmB/PEG_{5kDa}-cholane compared to the standard may be ascribed to the drug release process from the micelles while the drug in solution is immediately available. Similarly, the higher activity of the micelle formulation compared to the AmB suspension may be attributed to the fastest drug release from the former than the dissolution from the solid dispersion. Moreover, considering that the mechanism for AmB activity seems to be related to the formation of multimeric drug associations, it could be possible that the drug released from the micelles is partially in the conformation for the interaction with the target. Furthermore, AmB in solution is obtained with DMSO, a solvent and absorption enhancer that also has irritant effects. The new formulation of AmB presented in this work shows a similar

antimicrobial activity without DMSO suggesting interesting practical application.

5. Conclusions

The results of this study show that, by virtue of its peculiar physicochemical features, PEG_{5kDa}-cholane can be properly exploited to yield efficient AmB delivery. Indeed, the AmB/ PEG_{5kDa}-cholane formulation possesses excellent biopharma-ceutical properties, namely high drug solubility and high physicochemical stability, which were in a few cases superior to the other formulations available in the market. Actually, PEG_{5kDa}-cholane can be exploited for the delivery of a variety of small hydrophobic molecules forming stable micelles. However, this study open a new concept to the design of micelle forming biomaterials. Amphiphilic biomaterials can be in fact properly designed by selecting the hydrophobic/hydrophilic components according to the specific physicochemical features of the molecule that must be loaded in the hydrophobic core. In the case of PEG_{5kDa}-cholane and AmB, the high loading efficiency is ascribable to the high affinity that the drug has for the polycyclic hydrophobic moiety of the polymer, which is structurally similar to the drug targets, namely ergosterol and cholesterol. This concept can be applied to other drug delivery systems resulting in efficient formulations.

Acknowledgements

This research was partially supported by a grant from the Ministerio de Educación, Cultura y Deporte of Spain (FPU program – AP2010/0748) and by University of Padova (fondi ex-60% and Assegno di ricerca Senior, Area Scientifica di Ateneo 04,Scienze del Farmaco, 2013 “pH responsive nanovesicles for improved site-selective delivery of anticancer drugs and proteins to the tumor”)

Appendix A. Supplementary data

Supplementary data associated with this article can be found, in the online version, at http://dx.doi.org/10.1016/j. ijpharm.2015.08.070.

References

Adams, M.L., Andes, D.R., Kwon, G.S., 2003. Amphotericin B encapsulated in micelles based on poly (ethylene oxide)-block-poly (L-amino acid) derivatives exerts reduced in vitro hemolysis but maintains potent in vivo antifungal activity. Biomacromolecules 4, 750–757.

Asher, I.M., Levin, I.W., 1977. Effects of temperature and molecular interactions on the vibrational infrared spectra of phospholipid vesicles. Biochim. Biophys. Acta (BBA)-Biomembr. 468, 63–72.

Baas, B., Scott, A., Scott, J., Mikulecky, P., Hartsel, S.C., 1999. Activity and kinetics of dissociation and transfer of amphotericin B from a novel delivery form. AAPS PharmSci 1, 21–31.

Bartlett, K., Yau, E., Hartsel, S.C., Hamer, A., Tsai, G., Bizzotto, D., Wasan, K.M., 2004. Effect of heat-treated amphotericin B on renal and fungal cytotoxicity. Antimicrob. Agents Chemother. 48, 333–336.

Brajtburg, J., Bolard, J., 1996. Carrier effects on biological activity of amphotericin B. Clin. Microbiol. Rev. 9, 512–531.

Chakraborty, K., Naik, S., 2003. Therapeutic and hemolytic evaluation of in situ liposomal preparation containing amphotericin-B complexed with different chemically modified b-cyclodextrins. J. Pharm. Pharm. Sci. 6, 231–237.

Choi, K., Bang, J., Kim, P., Kim, C., Song, C., 2008. Amphotericin B-incorporated polymeric micelles composed of poly (D-L-lactide-co-glycolide)/dextran graft copolymer. Int. J. Pharm. 355, 224–230.

Croy, S., Kwon, G., 2006. Polymeric micelles for drug delivery. Curr. Pharm. Des. 12, 4669–4684.

Das, S., Suresh, P.K., 2011. Nanosuspension: a new vehicle for the improvement of the delivery of drugs to the ocular surface. Application to amphotericin B. Nanomed. Nanotechnol. Biol. Med. 7, 242–247.

Diezi, T.A., Kwon, G., 2012. Amphotericin B/sterol co-loaded PEG-phospholipid micelles: effects of sterols on aggregation state and hemolytic activity of amphotericin B. Pharm. Res. 29, 1737–1744.

Elgart, A., Farber, S., Domb, A.J., Polacheck, I., Hoffman, A., 2010. Polysaccharide pharmacokinetics: amphotericin B arabinogalactan conjugate a drug delivery system or a new pharmaceutical entity? Biomacromolecules 11, 1972–1977.

Espada, R., Josa, J., Valdespina, S., Dea, M., Ballesteros, M., Alunda, J., Torrado, J., 2008a. HPLC assay for determination of amphotericin B in biological samples. Biomed. Chromatogr. 22, 402–407.

Espada, R., Valdespina, S., Alfonso, C., Rivas, G., Ballesteros, M.P., Torrado, J.J., 2008b. Effect of aggregation state on the toxicity of different amphotericin B preparations. Int. J. Pharm. 361, 64–69.

Espinel-Ingroff, A., Arthington-Skaggs, B., Iqbal, N., Ellis, D., Pfaller, M.A., Messer, S., Rinaldi, M., Fothergill, A., Gibbs, D.L., Wang, A., 2007a. Multicenter evaluation of a new disk agar diffusion method for susceptibility testing of filamentous fungi with voriconazole, posaconazole, itraconazole, amphotericin B, and caspofungin. J. Clin. Microbiol. 45, 1811–1820. doi:http://dx.doi.org/10.1128/ JCM.00134-07.

Espinel-Ingroff, A., Canton, E., Gibbs, D., Wang, A., 2007b. Correlation of neo-sensitabs tablet diffusion assay results on three different agar media with CLSI broth microdilution M27-A2 and disk diffusion M44-A results for testing susceptibilities of Candida spp. and Cryptococcus neoformans to amphotericin B, caspofungin, fluconazole, itraconazole, and voriconazole. J. Clin. Microbiol. 45, 858–864. doi:http://dx.doi.org/10.1128/JCM.01900-06.

Espuelas, M., Legrand, P., Cheron, M., Barratt, G., Puisieux, F., Devissaguet, J., Irache, J., 1998. Interaction of amphotericin B with polymeric colloids: a spectroscopic study. Colloids Surf. B: Biointerfaces 11, 141–151.

Espuelas, M., Legrand, P., Irache, J., Gamazo, C., Orecchioni, A., Devissaguet, J., Ygartua, P., 1997. Poly (e-caprolacton) nanospheres as an alternative way to reduce amphotericin B toxicity. Int. J. Pharm. 158, 19–27.

Fukui, H., Koike, T., Nakagawa, T., Saheki, A., Sonoke, S., Tomii, Y., Seki, J., 2003. Comparison of LNS-AmB, a novel low-dose formulation of amphotericin B with lipid nano-sphere (LNS), with commercial lipid-based formulations. Int. J. Pharm. 267, 101–112.

Gaboriau, F., Chéron, M., Leroy, L., Bolard, J.,1997. Physico-chemical properties of the heat-induced ‘superaggregates’ of amphotericin B. Biophys. Chem. 66, 1–12.

Gagos, M., Arczewska, M., 2010. Spectroscopic studies of molecular organization of antibiotic amphotericin B in monolayers and dipalmitoylphosphatidylcholine lipid multibilayers. Biochim. Biophys. Acta (BBA)-Biomembr. 1798, 2124–2130.

Gray, K.C., Palacios, D.S., Dailey, I., Endo, M.M., Uno, B.E., Wilcock, B.C., Burke, M.D., 2012. Amphotericin primarily kills yeast by simply binding ergosterol. Proc. Natl. Acad. Sci. U. S. A. 109, 2234–2239. doi:http://dx.doi.org/10.1073/ pnas.1117280109.

Hamill, R.J., 2013. Amphotericin B formulations: a comparative review of efficacy and toxicity. Drugs 73, 919–934.

Hartsel, S.C., Bauer, E., Kwong, E.H., Wasan, K.M., 2001. The effect of serum albumin on amphotericin B aggregate structure and activity. Pharm. Res. 18, 1305–1309.

He, Q., Wu, W., Xiu, K., Zhang, Q., Xu, F., Li, J., 2013. Controlled drug release system based on cyclodextrin-conjugated poly (lactic acid)-b-poly (ethylene glycol) micelles. Int. J. Pharm. 443, 110–119.

Higuchi, T., Connors, A., 1965. Phase solubility tecniques. Adv. Anal. Chem. Instrum. 4, 117–122.

Jung, S.H., Lim, D.H., Jung, S.H., Lee, J.E., Jeong, K., Seong, H., Shin, B.C., 2009. Amphotericin B-entrapping lipid nanoparticles and their in vitro and in vivo characteristics. Eur. J. Pharm. Sci. 37, 313–320.

Kim, Y., Shin, B., Garripelli, V.K., Kim, J., Davaa, E., Jo, S., Park, J., 2010. A thermosensitive vaginal gel formulation with HPgCD for the pH-dependent release and solubilization of amphotericin B. Eur. J. Pharm. Sci. 41, 399–406.

Klepser, M.E., Wolfe, E.J., Jones, R.N., Nightingale, C.H., Pfaller, M.A., 1997. Antifungal pharmacodynamic characteristics of fluconazole and amphotericin B tested against Candida albicans. Antimicrob. Agents Chemother. 41, 1392–1395.

Larabi, M., Yardley, V., Loiseau, P.M., Appel, M., Legrand, P., Gulik, A., Bories, C., Croft, S.L., Barratt, G., 2003. Toxicity and antileishmanial activity of a new stable lipid suspension of amphotericin B. Antimicrob. Agents Chemother. 47, 3774–3779.

Lemke, A., Kiderlen, A., Kayser, O., 2005. Amphotericin B. Appl. Microbiol. Biotechnol. 68, 151–162.

Li, F., Danquah, M., Mahato, R.I., 2010. Synthesis and characterization of amphiphilic lipopolymers for micellar drug delivery. Biomacromolecules 11, 2610–2620.

Lukyanov, A.N., Torchilin, V.P., 2004. Micelles from lipid derivatives of water-soluble polymers as delivery systems for poorly soluble drugs. Adv. Drug Deliv. Rev. 56, 1273–1289.

Mazerski, J., Grzybowska, J., Borowski, E., 1990. Influence of net charge on the aggregation and solubility behaviour of amphotericin B and its derivatives in aqueous media. Eur. Biophys. J. 18, 159–164.

Nahar, M., Jain, N.K., 2009. Preparation, characterization and evaluation of targeting potential of amphotericin B-loaded engineered PLGA nanoparticles. Pharm. Res. 26, 2588–2598.

Oka, M., Kamimori, H., 2013. Lipid membrane-binding properties of amphotericin B deoxycholate (fungizone) using surface plasmon resonance. Anal. Sci. 29, 697– 702.

Rajagopalan, N., Chen, S.C., Chow, W., 1986. A study of the inclusion complex of amphotericin-B with g-cyclodextrin. Int. J. Pharm. 29, 161–168.

Roling, E.E., Klepser, M.E., Wasson, A., Lewis, R.E., Ernst, E.J., Pfaller, M.A., 2002. Antifungal activities of fluconazole, caspofungin (MK0991), and anidulafungin (LY 303366) alone and in combination against Candida spp. and Crytococcus neoformans via time-kill methods. Diagn. Microbiol. Infect. Dis. 43, 13–17.

-Caro, R., Veiga-Ochoa, M.D., 2009. Characterization and dissolution study of chitosan freeze-dried systems for drug controlled release. Molecules 14, 4370–4386.

ıaso, S., Bersani, S., Mastrotto, F., Tonon, G., Schrepfer, R., Genovese, S., Caliceti, P., 2012. Self-assembling nanocomposites for protein delivery: Supramolecular interactions between PEG-cholane and rh-G-CSF. J. Control. Release 162, 176–184.

ıaso, S., Bersani, S., Scomparin, A., Balasso, A., Brazzale, C., Barattin, M., Caliceti, P., 2014. A novel soluble supramolecular system for sustained rh-GH delivery. J. Control. Release 194, 168–177.
ıaso, S., Semenzato, A., Bersani, S., Matricardi, P., Rossi, F., Caliceti, P., 2007. Cyclodextrin/PEG based hydrogels for multi-drug delivery. Int. J. Pharm. 345, 42–50.

eier, S., Malheiros, S.V., de Paula, E., 2000. Surface active drugs: self-association and interaction with membranes and surfactants. Physicochemical and biological aspects. Biochim. Biophys. Acta (BBA)-Biomembr. 1508, 210–234.
kh, S., Ali, S.M., Ahmad, M.U., Ahmad, A., Mushtaq, M., Paithankar, M., Mandal, J., Saptarishi, D., Sehgal, A., Maheshwari, K., 2010. Nanosomal amphotericin B is an efficacious alternative to Ambisome[1] for fungal therapy. Int. J. Pharm. 397, 103–108.

ı-Filho, M.A., Siqueira, S.D., Freire, L.B., Araujo, I.B., Holanda e Silva, K.G., Medeiros Ada, C., Araujo-Filho, I., Oliveira, A.G., Egito, E.S., 2012. How can micelle systems be rebuilt by a heating process? Int. J. Nanomed. 7, 141–150. doi: http://dx.doi.org/10.2147/IJN.S25761.

Snyder, S.L., Sobocinski, P.Z., 1975. An improved 2, 4, 6-trinitrobenzenesulfonic acid method for the determination of amines. Anal. Biochem. 64, 284–288.
Vakil, R., Kwon, G.S., 2007. Effect of cholesterol on the release of amphotericin B from PEG-phospholipid micelles. Mol. Pharm. 5, 98–104.
Vandermeulen, G., Rouxhet, L., Arien, A., Brewster, M., Préat, V., 2006. Encapsulation of amphotericin B in poly (ethylene glycol)-block-poly (ɛ-caprolactone-co-trimethylenecarbonate) polymeric micelles. Int. J. Pharm. 309, 234–240.
Volmer, A.A., Szpilman, A.M., Carreira, E.M., 2010. Synthesis and biological evaluation of amphotericin B derivatives. Nat. Prod. Rep. 27, 1329–1349.
Wilcock, B.C., Endo, M.M., Uno, B.E., Burke, M.D., 2013. $C2^{0}$-OH of amphotericin B plays an important role in binding the primary sterol of human cells but not yeast cells. J. Am. Chem. Soc. 135, 8488–8491.
Yu, B., Okano, T., Kataoka, K., Sardari, S., Kwon, G., 1998a. In vitro dissociation of antifungal efficacy and toxicity for amphotericin B-loaded poly (ethylene oxide)-block-poly (ɒ-benzyl-ʟ-aspartate) micelles. J. Control. Release 56, 285–291.

Yu, B., Okano, T., Kataoka, K., Kwon, G., 1998b. Polymeric micelles for drug delivery: solubilization and haemolytic activity of amphotericin B. J. Control. Release 53, 131–136.

Zu, Y., Sun, W., Zhao, X., Wang, W., Li, Y., Ge, Y., Liu, Y., Wang, K., 2014. Preparation and characterization of amorphous amphotericin B nanoparticles for oral administration through liquid antisolvent precipitation. Eur. J. Pharm. Sci. 53, 109–117.

DRUG UNIPD AMPHOTERICIN B PEG_{5KDA}-CHOLANE FTIR HSM HEMOLYSIS ORAL UCM MONOMER POLYAGGREGATES ITC *IN VITRO* INTRAVENOUS Ke SYNTHESIS mV TNBS RESISTANCE $T_{1/2}$ NMR XRD FORMULATION ACTIVATION IR CANDIDA HPLC 1959 EFFICACY SYNCHROTRON CHOLESTEROL pH CMAX DIMER ORAL NAIL CHARACTERIZATION ΔH 924Da CRITICAL AGGREGATION CONCENTRATION MIC CMC

5. CONCLUSIONS

CIRCULAR DICHROISM ONYCHOMYCOSIS STABILITY RELEASE UV TOXICITY TEA HSA C24 TOPICAL ADMINISTRATION AMORPHOUS CONJUGATION AUC MIXED INFECTIONS MEMBRANE ΔS PENETRATION EXCIPIENTS BETA-SHEET $C_{47}H_{73}NO_{17}$ KD2 CM^{-1} ALPHA-HELIX EF ERGOSTEROL FILM-FORMING DERMATHOPHYTE MOLDS AMPHOTERIC PKA DISSOCIATION CRYSTALLINE INTERACTION BALB/C

5. CONCLUSIONS

Note:

This thesis includes the development of two different types of amphotericin B formulations: one topical formulation for the treatment of nail infections (AmB water-impermeable nail lacquer), which is addressed in the Experimental part 1 (conclusions 1-3) and another one for the treatment of sytemic fungal infections. The latest, tackled in Experimental part 2, consists of an AmB-pegylated nanoformulation (conclusions 4-12).

Conclusions:

1.- A new water-impermeable stable nail lacquer formulation containing amphotericin B has been designed for the treatment of onychomycosis. The polymer (Eudragit L100®) and the amphotericin B solvent used (N-methyl-2-pyrrolidone) showed no incompatibility problems. Once applied over a surface, the nail lacquer formed a continuous, homogenous and smooth film resistant to water.

2.- *In vitro* nail penetration studies showed that the lacquer was able to penetrate the nail (enhancement factor almost twice than the control). *In vitro* activity studies demonstrated the efficacy of the nail lacquer against dermatophyte and non-dermatophyte molds as well as yeasts (gender Candida).

3.- *In vivo* efficacy studies on keratinized structures of animal origin supported the efficacy of amphotericin B. After 30 days treatment on alternate days, the nail lacquer was able to clear up the infections caused by *Trichophyton mentagrophytes*, *Trichophyton rubrum*, *Aspergillus niger*, *Fusarium. oxysporum* and *Fusarium solani*.

4.- A novel formulation for amphotericin B delivery has been developed by using a micelle forming 5 kDa monomethoxy-polyethylene glycol end functionalized with cholanic acid (PEG_{5kDa}-cholane). This polymer was found to increase 10^5 times the amphotericin B solubility with a 12:1 AmB/PEG_{5kDa}-cholane molar ratio (2:1 w/w ratio).

5.- The system AmB/PEG_{5kDa}-cholane forms 30 nm micelles with the hydrophobic cholane moieties localized inside the micelles. Zeta potential analysis showed that at neutral pHs (5.5-7.2) the overall micelle surface is nearly neutral. The PEG_{5kDa}-cholane interacts with amphotericin B according to three binding sites depending on the pH, suggesting that the polymer interaction depends on the amphotericin B ionization and aggregation.

6.- Once lyophilized, the freeze-dried product could be promptly redispersed to form an homogeneous colloidal dispersion. The dispersion was physicochemically stable. Fourier Transform infrared spectrometry, differential scanning calorimetry and X-ray diffractometry showed that in the lyophilized product, amphotericin B and PEG_{5kDa}-cholane interacts intimately.

7.- The amphotericin B release from the PEG_{5kDa}-cholane micelles showed a biphasic profile. The best fittings were obtained with the Higuchi and Korsmeyer-Peppas models.

8.- The toxicity of the new formulation was tested as hemolysis. The new AmB/PEG_{5kDa}-cholane nanoformulation was always less hemolytic than the reference marketed formulation Fungizone®.

9.- The amphotericin B antifungal activity assayed against *Candida albicans* showed that AmB/PEG_{5kDa}-cholane was 15% more active than the free amphotericin B in buffer.

10.- The IV pharmacokinetics profiles of the different formulations studied (Ambisome®, Fungizone® and AmB/PEG_{5kDa}-cholane) were significantly different. The apparent elimination constant (Ke) of the new formulation is significantly ($P<0.01$) lower than both Ambisome® and Fungizone®. Accordingly, the half-life value of this new formulation was found to be higher. The IV administration of 1 mg/kg AmB/PEG_{5kDa}-cholane caused less pain effect in the mice than the administration of the same dose of Fungizone® or Ambisome®.

11.- Oral pharmacokinetic studies confirmed that this new formulation has a higher half-life than Ambisome® and Fungizone® marketed formulations. The AUC_{0-24} values were similar for all tested formulations.

12.- It can be concluded that the new AmB/PEG_{5kDa}-cholane formulation is a promising soluble controlled delivery system for amphotericin B with lower toxicity than the reference marketed formulation Fungizone®.

DRUG UNIPD AMPHOTERICIN B PEG_{5KDA}-CHOLANE FTIR HSM HEMOLYSIS ORAL UCM MONOMER POLYAGGREGATES ITC *IN VITRO* INTRAVENOUS Ke SYNTHESIS mV TNBS RESISTANCE $T_{1/2}$ NMR XRD FORMULATION ACTIVATION IR CANDIDA HPLC 1959 EFFICACY SYNCHROTRON CHOLESTEROL pH CMAX DIMER ORAL NAIL CHARACTERIZATION ΔH 924Da CRITICAL AGGREGATION CONCENTRATION MIC CMC

6. REFERENCES

CIRCULAR DICHROISM ONYCHOMYCOSIS STABILITY RELEASE UV TOXICITY TEA HSA C24 TOPICAL ADMINISTRATION AMORPHOUS CONJUGATION AUC MIXED INFECTIONS MEMBRANE ΔS PENETRATION EXCIPIENTS BETA-SHEET $C_{47}H_{73}NO_{17}$ KD2 CM^{-1} ALPHA-HELIX EF ERGOSTEROL FILM-FORMING DERMATHOPHYTE MOLDS AMPHOTERIC PKA DISSOCIATION CRYSTALLINE INTERACTION BALB/C

6. REFERENCES

(1) Hamilton-Miller JM. Chemistry and biology of the polyene macrolide antibiotics. Bacteriol Rev 1973 Jun;37(2):166-196.

(2) Hammond S. Biological activity of polyene antibiotics. Prog Med Chem 1977;14:105-179.

(3) Kotler-Brajtburg J, Medoff G, Kobayashi GS, Boggs S, Schlessinger D, Pandey RC, et al. Classification of polyene antibiotics according to chemical structure and biological effects. Antimicrob Agents Chemother 1979 May;15(5):716-722.

(4) Armstrong J, Grove J, Turner W, Ward G. An Antifungal Triene from a Streptomyces sp. Nature 1965;206:399-400.

(5) Coronelli C, Pasqualucci RC, Thiemann JE, Tamoni G. Mycotrienin, a new polyene antibiotic isolated from Streptomyces. J Antibiot (Tokyo) 1967 Nov;20(6):329-333.

(6) Nesemann G, Praeve P, Sukatsch D, Vertesy L. Ein Polyen-Antibiotikum aus Bakterien. Naturwissenschaften 1972;59(2):81-82.

(7) Vertesy L. Proticin, a new phosphorus-containing antibiotic. II. J Antibiot 1972;25(1):4-10.

(8) Aizawa S, SHIBUYA M, SHIRATO S. Resistaphylin, a new antibiotic. I. J Antibiot 1971;24(6):393-396.

(9) Aszalos A, Robison RS, Lemanski P, Berk B. Trienine, an antitumor triene antibiotic. J Antibiot 1968;21(10):611-615.

(10) STILLER ET, VANDEPUTTE J, WACHTEL JL. Amphotericins A and B, antifungal antibiotics produced by a streptomycete. II. The isolation and properties of the crystalline amphotericins. Antibiot Annu 1955 -1956;3:587-591.

(11) DONOVICK R, GOLD W, PAGANO JF, STOUT HA. Amphotericins A and B, antifungal antibiotics produced by a streptomycete. I. In vitro studies. Antibiot Annu 1955 -1956;3:579-586.

(12) ARCAMONE F, BERTAZZOLI C, CANEVAZZI G, Di MARCO A, GHIONE M, GREIN A. Etruscomycin, A New Antifungal Antibiotic from Streptomyces lucensis. Giornale di Microbiologia 1957;4(2):119-128.

(13) Gaudiano S, Bravo P, Quilico A. The structure of lucensomycin. Part I. Tetrahedron Lett 1966;7(30):3559-3565.

(14) Gaudiano S, Bravo P, Quilico A, Golding B, Rickards R. The structure of lucensomycin. Part II. Tetrahedron Lett 1966;7(30):3567-3571.

(15) Gaudiano G, Bravo P, Quilico A, Golding B, Rickards R. Struttura della lucensomicina. Nota III. Gazz.Chim.Ital 1966;96:1470-1491.

(16) HAZEN EL, BROWN R. Two antifungal agents produced by a soil actinomycete. Science 1950 Oct 13;112(2911):423.

(17) Chong C, Rickards R. Macrolide antibiotic studies. XVI. The structure of nystatin. Tetrahedron Lett 1970;11(59):5145-5148.

(18) KOE BK, TANNER FW,Jr, RAO KV, SOBIN BA, CELMER WD. Pa 150, PA 153, and PA 166: new polyene antifungal antibiotics. Antibiot Annu 1957 -1958;5:897-905.

(19) Rinehart Jr KL, Pandey RC, German VF, Nishikawa Y. Polyene antibiotics. II. Structure of tetrin A. J Am Chem Soc 1971;93(15):3738-3747.

(20) Struyk A, Drost G, Haisvisz J, van Eek T, Hoogerheide J. Pimaricin, a new antifungal antibiotic. Antibiot.Ann.1957-1958 1958:878-885.

(21) Golding B, Richards R, Meyer W, Patrick J, Barber M. The structure of the macrolide antibiotic pimaricin. Tetrahedron Lett 1966;7(30):3551-3557.

(22) DAVISSON JW, TANNER FW,Jr, FINLAY AC, SOLOMONS IA. Rimocidin, a new antibiotic. Antibiot Chemother (Northfield) 1951 Aug;1(5):289-290.

(23) Cope AC, Axen U, Burrows EP. Rimocidin. II. Oxygenation Pattern of the Aglycone1. J Am Chem Soc 1966;88(18):4221-4227.

(24) Dornberger K, FÜGNER R, BRADLER G, THRUM H. Tetramycin, a new polyene antibiotic. J Antibiot 1971;24(3):172-177.

(25) Gottlieb D, Pote H. Tetrin, an antifungal antibiotic. Phytopathology 1960;50(11):817-822.

(26) Rinehart Jr KL, Tucker WP, Pandey RC. 1 Polyene antibiotics. III. Structure of tetrin B. J Am Chem Soc 1971;93(15):3747-3751.

(27) Matsuoka M, Umezawa H. Unamycin, an antifungal substance produced by Streptomyces fungicidicus. J Antibiot 1960;13(2):114-120.

(28) Soeda M, FUJITO H. Akitamycin, an antifungal antibiotic. I. J Antibiot 1959;12(4):293-294.

(29) Fujita H. Chemical study of Akitamycin, an antifungal antibiotic. J.Antibiotics (Tokyo) 1959;12.

(30) Raubitscheck F, Acker RF, Waksman SA. Production of an antifungal agent of the fungicidin type by Streptomyces aureus. Antibiotics & chemotherapy 1952;2(4):179-183.

(31) Wakaki S, Akanabe S, Hamada K, Asahina T. Antifungal substances produced by actinomyces. Antibiotics from strain C-6. J.Antibiotics 1952;5(12):677-681.

(32) Wakaki S, Hamada K, Akanabe S, Asahina T. Studies of the antifungal antibiotic from streptomyces. IV. On the physicochemical properties of chromin. J.Antibiotics, Ser.A 1953;6(3):145-146.

(33) Gottlieb D, Bhattacharyya P, Carter H, Anderson H. Endomycin, a new antibiotic. Phytopathology 1951;41(5):393-400.

(34) Vining L, Taber W. Separation of endomycins A and B, and their identification as members of the polyene groups of antifungal antibiotics. Canadian Journal of Chemistry 1957;35(12):1461-1466.

(35) Kotiuszko D, Wituch K, Morawska H, Siejko D. Polifungin, a new antifungal antibiotic. I. Morphological, cultural, and physiological properties of Streptomyces sp. strain producing a new complex of tetraene antibiotics. Acta Microbiol Pol A 1971;4(1):135-143.

(36) Porowska N, Halski L, Płóciennik Z, Kotiuszko D, Morawska H, Kowszyk- Gindifer Z, et al. Composition of polifungin, a new antifungal agent. Recueil des Travaux Chimiques des Pays-Bas 1972;91(7):780-784.

(37) SAKAMOTO J. Etude sur antibiotique antifongique. I. La protocidine, un nouvel antibiotique produit par les Streptomycete. J Antibiot 1957;10(3):128-131.

(38) Sakamoto JMJ. Etude sur antibiotique antifongique. III. La moldcidine A, un nouvel antibiotique produit par les Streptomycete. J.Antibiotics, Ser.A 1959;12(4):169-172.

(39) Arima N, Sakamoto J, Okamoto E. Protocidin, an antibiotic substance. Japanese Patent 1960;8648:60.

(40) Despois R, Pinnert-Sindico S, Ninet L, Preudhomme J. Trois antibiotiques de groupes différents produits par une meme souche de Streptomyces. Giorn.Microbiol 1956;2:76-90.

(41) Oroshnik W, Mebane A. The polyene antifungal antibiotics. Progress in the Chemistry of Organic Natural Products/Progrès Dans La Chimie Des Substances Organiques Naturelles: Springer; 1963. p. 17-79.

(42) The structure of'aurenin. Proc. 7th Int. Symp. Chem. Nat. Prod; 1970.

(43) Ogata K, Igarashi S, Nakao Y. Culture medium for separation of bacteria from mixture of bacteria, yeasts and moulds. Japanese Patent 1958;9245:58.

(44) Gopalkrishnan K, Narasimhachari N, Joshi V, Thirumalachar M. Chainin: a new methylpentaene antibiotic from a species of Chainia. 1968.

(45) Pandey RC, Narasimhachari N, Rinehart Jr KL, Millington DS. Polyene antibiotics. IV. Structure of chainin. J Am Chem Soc 1972;94(12):4306-4310.

(46) Gordon MA, Lapa EW. Durhamycin, a Pentaene Antifungal Antibiotic from Streptomyces durhamensis sp. n. Appl Microbiol 1966 Sep;14(5):754-760.

(47) WHITEFIELD IC. Two-tone' inhibition at the trapezoid body level. J Physiol 1955 Jul 28;129(1):15-6P.

(48) Tytell A, McCarthy F, Fisher W, Bolhofer W, Charney J. Fungichromin and fungichromatin: New polyene antifungal agents. Antibiotics Annual 1955:716-718.

(49) Bhate D, Acharya S. Aureofungin. A new antifungal antibiotic. II. Isolation and physico-chemical properties. Hindustan Antibiot Bull 1964;6(4):170-172.

(50) Rakhit S. Fungicides, antibiotics 1982.

(51) UMEZAWA S, Tanaka Y. A new antifungal antibiotic, pentamycin. Antibiot. 1958;11(1):26-29.

(52) Umezawa S, Ooka M, Shiotsu S. Pentamycin, a new antibiotic. Japanese Pat-ent 1959;6000:59.

(53) Ogawa H. Chemical study on moldcidin B and its identification with pentamycin. Journal of Antibiotics Ser.A 1960;13(5):????.

(54) Arishima M, Sakamoto J. Moldcidin A, an antibiotic substance. Japanese Patent 1961;1148:61.

(55) Schlegel R, Thrum H. Flavomycoin, ein neues antifungales Polyenantibiotikum. Experientia 1968;24(1):11-12.

(56) Schlegel R, Thrum H. A NEW POLYENE ANTIBIOTIC, FLAVOMYCOIN STRUCTURAL INVESTIGATIONS. I. J Antibiot 1971;24(6):360-367.

(57) Burke RC, Swartz JH, Chapman S, Huang W. Mycoticin, a new antifungal antibiotic. J Invest Dermatol 1954;23(3):163-168.

(58) Wasserman H, Van Verth J, McCaustland D, Borowitz I, Kamber B. The mycoticins, polyene macrolides from Streptomyces ruber. J Am Chem Soc 1967;89(6):1535-1536.

(59) NAKAZAWA K. Studies on streptomycetes. Eurocidin, an antibiotic produced by Streptomyces albireticuli (III). J.Agric.Chem.Soc.Jpn 1955;29:650-652.

(60) Horii S, SHIMA T, OUCHIDA A. Partial structure of the eurocidin complex. J Antibiot 1970;23(2):102-104.

(61) IGARASI S, OGATA K, Miyake A. Studies on Streptomyces. Pantaene group substance. I. An antifungal antibiotic produced by Streptomyces acidomyceticus. J.Antibiotics, Ser.B 1956;9(3):101-103.

(62) Brown R, HAZEN EL. Capacidin, a New Member of the Polyene Antibiotic Group. Antibiotics & Chemotherapy 1960;10(11):702-708.

(63) Thirumalachar M, Rahalkar P. PENTAENE ANTIBIOTICS FROM SOME STREPTOVERTICILLIUM SPECIES IN INDIA. Progress in antimicrobial and anticancer chemotherapy: proceedings 1970;1:70.

(64) Thirumalachar M, Menon S. Dermostatin, a new antifungal antibiotic. I. Microbiological studies. Hindustan Antibiot Bull 1962;4:106-108.

(65) Narasimhachari N, Swami M. Dermostatin: a revised hexaene structure. J Antibiot 1970;23(11):566-566.

(66) Ragni G, Szybalski W, Borowski E, Schaffner C. N-Acetylcandidin, a water-soluble polyene antibiotic for fungal prophylaxis and decontamination of tissue cultures. Antibiotics & Chemotherapy 1961;11(12):797-799.

(67) Vining L, Taber W. Separation of endomycins A and B, and their identification as members of the polyene groups of antifungal antibiotics. Canadian Journal of Chemistry 1957;35(12):1461-1466.

(68) TAkAHasHI I. A new antifungal substance'flavacid'. Studies on the antibiotic substances from Actinomyces, XXVIII. J Antibiot 1953;6(3):117-121.

(69) Swart EA, Romano AH, Waksman SA. Fradicin, an Antifungal Agent Produced by Streptomyces fradiae. Exp Biol Med 1950;73(3):376-378.

(70) Okami Y, Utahara R, Nakamura S, Umezawa H. On streptomyces producing a new antifungal substance mediocidin and antifungal substances of fungicidin-rimocidin-chromin group, eurocidin group and trichomycin-ascosin-candicidin group. J.Antibiotics, Ser.A 1954;7:98-103.

(71) Aiso K, Arai T, Washida K, Tanaami T. Mycelin, a new antifungal substance extracted from the mycelium of a Streptomyces. J.Antibiot 1952;5:218-219.

(72) Ogata K, IGARASHI S, YAMAMOTO H. Mycelin IMO, a new antibiotic. Japan Patent 1957:57-5,898.

(73) Craveri R, Coronelli C, Beretta G, Tamoni G, Sensi P. Isolation and study of the antibiotic tetraesin. Ann.Microbiol.Enzimol 1962;12:155-164.

(74) Craveri R, Cornelli C, Sensi P. Tetrahexin and process for preparing same 1974.

(75) DONOVICK R, GOLD W, PAGANO JF, STOUT HA. Amphotericins A and B, antifungal antibiotics produced by a streptomycete. I. In vitro studies. Antibiot Annu 1955 -1956;3:579-586.

(76) Mechlinski W, Schaffner CP, Ganis P, Avitabile G. Structure and absolute configuration of the polyene macrolide antibiotic amphotericin B. Tetrahedron Lett 1970;11(44):3873-3876.

(77) Taber WA, Vining L, Waksman S. Candidin, a New Antifungal Antibiotic producedby Streptomyces viridoflauus. Antibiotics & chemotherapy 1954;4(4):455-461.

(78) Borowski E, Falkowski L, Golik J, Zieliński J, Zimiński T, Mechliński W, et al. The structure of candidin, a polyene macrolide antifungal antibiotic. Tetrahedron Lett 1971;12(22):1987-1992.

(79) Borowski E, Malyshkina M, Kotienko T, Soloviev S. Mycoheptin, a new member of non-aromatic group of heptaene macrolide antifungal antibiotics. Chemotherapy 1964;9(6):359-369.

(80) Kannan L. A new heptaene antibiotic (X-63) from a streptomyces species.(Notes). Journal of Antibiotics Ser.A 1967;20(5):293-294.

(81) Shibata M, Honjo M, Tokui Y, Nakazawa K. On a new antifungal and antiyeast substance, candimycin, produced by a streptomyces. J.Antibiotics 1954;7.

(82) Horii S, SHIMA T, OUCHIDA A. Partial structure of the eurocidin complex. J Antibiot 1970;23(2):102-104.

(83) Bohlmann F, Dehmlow E, Neuhahn H, Brandt R, Reinicke B. Neue heptaen-makrolide—I: Charakterisierung und abbau. Tetrahedron 1970;26(9):2191-2198.

(84) Bohlmann F, Dehmlow E, Neuhahn H, Brandt R, Bethke H. Neue heptaen-makrolide—II: Grundskelett, stellung der funktionellen gruppen und struktur der aglykone. Tetrahedron 1970;26(9):2199-2207.

(85) OSWALD EJ, RANDALL WA, REEDY RJ. An antifungal agent, 1968, produced by a new Streptomyces species. Antibiot Annu 1955 -1956;3:236-239.

(86) Lee C, Schaffner C. Perimycin: the structure of some degradation products. Tetrahedron 1969;25(10):2229-2232.

(87) Hagemann G, Nomine G, Penasse L. Antifungin 4915. German Patent 1959;1053738.

(88) HOSOYA S, SOEDA M, OKADA K, FUJITA H. Eurotin, an anti-fungal antibiotic. I. Toho Igakkai Zasshi 1959;6:285-292.

(89) Craveri R, Giolitti G. Isolation and study of an antifungal antibiotic. Ann.Micro-biol 1956;7:81-92.

(90) Gupta K. Monicamycin, a new; polyene antifungal antibiotic. Antimicrob Agents Chemother 1965:65-67.

(91) Thirumalachar M, Ramachandran S, Rahalkar P, Padhye A. Neoheptaene, a new antifungal antibiotic. Neoheptaene, a new antifungal antibiotic. 1966.

(92) KOE BK, TANNER FW,Jr, RAO KV, SOBIN BA, CELMER WD. Pa 150, PA 153, and PA 166: new polyene antifungal antibiotics. Antibiot Annu 1957 -1958;5:897-905.

(93) Hickey R, Corum C, Hidy P, Cohen I, Nager U, Kropp E. Ascosin, an Antifungal Antibiotic produced by a Streptomycete. Antibiotics & chemotherapy 1952;2(9):472-483.

(94) Thirumalachar M, Rahalkar P, Sukapure R, GOPALAKRISHNAN K. Aureofungin, a new heptaene antibiotic. Hindustan Antibiot Bull 1964;6(3):108-111.

(95) Kaplan M, Heinemann B, MYDLINSKI I, Buckwalter F, LLIN J, Hooper I. An antifungal antibiotic (AYF) produced by a strain of Streptomyces aureofaciens. Antibiotics & chemotherapy 1958;8(10):491-495.

(96) Pridham T, Shotwell O, Stodola F, Lindenfelser L, Benedict R, Jackson R. ANTIBIOTICS AGAINST PLANT DISEASE. 2. EFFECTIVE AGENTS PRODUCED BY STREPTOMYCES-CINNAMOMEUS FORMA AZACOLUTA F NOV. Phytopathology 1956;46(10):575-581.

(97) CRAVERI R, SHOTWELL OL, DWORSCHACK RG, PRIDHAM TG, JACKSON RW. Antibiotics against plant disease. VII. The antifungal hepataene component (F-17-C) produced by Streptomyces cinnamomeus f. azacoluta. Antibiot Chemother (Northfield) 1960 Jul;10:430-439.

(98) Lechevalier H, Acker RF, Corke CT, Haenseler CM, Waksman SA. Candicidin, a new antifungal antibiotic. Mycologia 1953:155-171.

(99) Waksman SA, Lechevalier HA, Schaffner CP. Candicidin and other polyenic antifungal antibiotics. Bull World Health Organ 1965;33(2):219-226.

(100) Thirumalachar M, Menon S, Bhatt V. Hamycin, a New Antifangal Antibiotic. I. Discovery and Biological Studies. Hindustan Antibiot Bull 1961;3(4):136-138.

(101) Deshpande GR, Kerur DR, Narasimhachari N. Chemical studies on hamycin. I. Purification, counter-current distribution and chemical degradation. Hindustan Antibiot Bull 1966 May;8(4):185-193.

(102) Henis Y, Grossowicz N, Aschner M. Heptamycin, an antifungal and antiprotozoal antibiotic. Bull.Res.Council Israel E ;6.

(103) Borowski E, Malyshkina M, Soloviev S, Zimiński T. Isolation and Characterization of Levorin A and B, the Heptaene Macrolide Antifungal Antibiotics of 'Aromatic'Subgroup. Chemotherapy 1965;10(3):176-194.

(104) Hosoya S, Komatsu N, Soeda M, Yuwaguchi T, Sonoda Y. Trichomycin, a new antibiotic with trichomonadicidal and antifungal activities. J.Antibiotics 1952;5(10):564-566.

(105) HATTORI K. Studies on trichomycin. 8. On the chemical structure of trichomycin A. J Antibiot B 1962 Apr;15:39-43.

(106) Lemke A, Kiderlen A, Kayser O. Amphotericin B. Appl Microbiol Biotechnol 2005;68(2):151-162.

(107) Norman AW, Spielvogel AM, Wong RG. Polyene antibiotic-sterol interaction. Adv Lipid Res 1976;14:127-170.

(108) Cass A, Finkelstein A, Krespi V. The ion permeability induced in thin lipid membranes by the polyene antibiotics nystatin and amphotericin B. J Gen Physiol 1970 Jul;56(1):100-124.

(109) Kasumov K, Liberman EA. Ionic permeability of bimolecular membranes in the presence of polyene antibiotics. I. Nystatin and amphotericin B. Biofizika 1972 Nov-Dec;17(6):1024-1031.

(110) Gale E. The release of potassium ions from Candida albicans in the presence of polyene antibiotics. Microbiology 1974;80(2):451-465.

(111) Kitajima Y, Sekiya T, Nozawa Y. Freeze-fracture ultrastructural alterations induced by filipin, pimaricin, nystatin and amphotericin B in the plasma membranes of Epidermophyton, Saccharomyces and red blood cells. A proposal of models for polyene· ergosterol complex-induced membrane lesions. Biochimica et Biophysica Acta (BBA)-Biomembranes 1976;455(2):452-465.

(112) Kleinschmidt MG, Chough KS. Effect of filipin on liposomes prepared with different types of steroids. Plant Physiol 1972 May;49(5):852-856.

(113) Kotler-Brajtburg J, Price HD, Medoff G, Schlessinger D, Kobayashi GS. Molecular basis for the selective toxicity of amphotericin B for yeast and filipin for animal cells. Antimicrob Agents Chemother 1974 Apr;5(4):377-382.

(114) Cirillo VP, Harsch M, Lampen J. Action of the polyene antibiotics filipin, nystatin and N-acetylcandidin on the yeast cell membrane. Microbiology 1964;35(2):249-259.

(115) Gent MP, Prestegard JM. Interaction of the polyene antibiotics with lipid bilayer vesicles containing cholesterol. Biochimica et Biophysica Acta (BBA)-Biomembranes 1976;426(1):17-30.

(116) Kotler-Brajtburg J, Medoff G, Schlessinger D, Kobayashi GS. Amphotericin B and filipin effects on L and HeLa cells: dose response. Antimicrob Agents Chemother 1977 May;11(5):803-808.

(117) Liras P, Lampen JO. Sequence of candicidin action on yeast cells. Biochimica et Biophysica Acta (BBA)-General Subjects 1974;372(1):141-153.

(118) Medoff G, Kobayashi GS. Amphotericin B: Old drug, new therapy. JAMA 1975;232(6):619-620.

(119) Valeriote F, Lynch R, Medoff G, Kumar BV. Protective effects of amphotericin B against spontaneous and transplantable murine tumors. J Natl Cancer Inst 1976 Mar;56(3):557-560.

(120) Little JR, Plut EJ, Kotler-Brajtburg J, Medoff G, Kobayashi GS. Relationship between the antibiotic and immunoadjuvant effects of amphotericin B methyl ester. Immunochemistry 1978;15(4):219-224.

(121) Hammarström L, Smith C. In vitro activating properties of polyene antibiotics for murine lymphocytes. Acta Pathologica Microbiologica Scandinavica Section C Immunology 1977;85(4):277-283.

(122) Dutcher JD, William G, Pagano JF, John V. Amphotericin B, its production, and its salts 1959.

(123) Gallis HA, Drew RH, Pickard WW. Amphotericin B: 30 years of clinical experience. Review of Infectious Diseases 1990;12(2):308-329.

(124) TREJO WH, BENNETT RE. Streptomyces nodosus sp. n., the amphotericin-producing organism. J Bacteriol 1963 Feb;85:436-439.

(125) Lemke A, Kiderlen A, Kayser O. Amphotericin B. Appl Microbiol Biotechnol 2005;68(2):151-162.

(126) Nicolaou K, Daines R, Chakraborty T, Ogawa Y. Total synthesis of amphotericin B. J Am Chem Soc 1987;109(9):2821-2822.

(127) Gallo G, Radaelli P. Analytical profiles of drug substances and excipients, K. Florey's/HG Brittain: Oxford University Press 1977;5:467-513.

(128) Moffat A. Clarke's isolation and identification of drugs. 1986.

(129) Tevyashova AN, Olsufyeva EN, Solovieva SE, Printsevskaya SS, Reznikova MI, Trenin AS, et al. Structure-antifungal activity relationships of polyene antibiotics of the amphotericin B group. Antimicrob Agents Chemother 2013 Aug;57(8):3815-3822.

(130) Brautaset T, Sletta H, Degnes KF, Sekurova ON, Bakke I, Volokhan O, et al. New nystatin-related antifungal polyene macrolides with altered polyol region generated via biosynthetic engineering of Streptomyces noursei. Appl Environ Microbiol 2011 Sep;77(18):6636-6643.

(131) Soler L, Caffrey P, McMahon HE. Effects of new amphotericin analogues on the scrapie isoform of the prion protein. Biochimica et Biophysica Acta (BBA)-General Subjects 2008;1780(10):1162-1167.

(132) Dolores R. Serrano. Nuevas formulaciones orales, tópicas y parenterales de anfotericina B con acción antifúngica y antiparasitaria; 2013.

(133) Bennett J, Mandell G, Dolin R. Antifungal agents. Mandell, Douglas and Bennett's principles and practice of infectious diseases.Volume 1. 1995(Ed. 4):401-410.

(134) Yu B, Okano T, Kataoka K, Kwon G. Polymeric micelles for drug delivery: solubilization and haemolytic activity of amphotericin B. J Controlled Release 1998;53(1):131-136.

(135) Bushra R, Shahadat M, Ahmad A, Nabi S, Umar K, Oves M, et al. Synthesis, characterization, antimicrobial activity and applications of polyanilineTi (IV) arsenophosphate adsorbent for the analysis of organic and inorganic pollutants. J Hazard Mater 2014;264:481-489.

(136) Legrand P, Romero EA, Cohen BE, Bolard J. Effects of aggregation and solvent on the toxicity of amphotericin B to human erythrocytes. Antimicrob Agents Chemother 1992 Nov;36(11):2518-2522.

(137) Mazerski J, Bolard J, Borowski E. Self-association of some polyene macrolide antibiotics in aqueous media. Biochimica et Biophysica Acta (BBA)-General Subjects 1982;719(1):11-17.

(138) Strauss G, Kral F. Borate complexes of amphotericin B: Polymeric species and aggregates in aqueous solutions. Biopolymers 1982;21(2):459-470.

(139) Mazerski J, Grzybowska J, Borowski E. Influence of net charge on the aggregation and solubility behaviour of amphotericin B and its derivatives in aqueous media. European Biophysics Journal 1990;18(3):159-164.

(140) Aramwit P, Yu BG, Lavasanifar A, Samuel J, Kwon GS. The effect of serum albumin on the aggregation state and toxicity of amphotericin B. J Pharm Sci 2000;89(12):1589-1593.

(141) Mazerski J, Grzybowska J, Borowski E. Influence of net charge on the aggregation and solubility behaviour of amphotericin B and its derivatives in aqueous media. European Biophysics Journal 1990;18(3):159-164.

(142) Mazerski J, Borowski E. Molecular dynamics of amphotericin B. II. Dimer in water. Biophys Chem 1996;57(2):205-217.

(143) Wasko P, Luchowski R, Tutaj K, Grudzinski W, Adamkiewicz P, Gruszecki WI. Toward understanding of toxic side effects of a polyene antibiotic amphotericin B: fluorescence spectroscopy reveals widespread formation of the specific supramolecular structures of the drug. Molecular pharmaceutics 2012;9(5):1511-1520.

(144) Ernst C, Grange J, Rinnert H, Dupont G, Lematre J. Structure of amphotericin B aggregates as revealed by UV and CD spectroscopies. Biopolymers 1981;20(8):1575-1588.

(145) Mazerski J, Grzybowska J, Borowski E. Influence of net charge on the aggregation and solubility behaviour of amphotericin B and its derivatives in aqueous media. European Biophysics Journal 1990;18(3):159-164.

(146) Bolard J, Legrand P, Heitz F, Cybulska B. One-sided action of amphotericin B on cholesterol-containing membranes is determined by its self-association in the medium. Biochemistry 1991;30(23):5707-5715.

(147) Gruda I, Dussault N. Effect of the aggregation state of amphotericin B on its interaction with ergosterol. Biochemistry and Cell Biology 1988;66(3):177-183.

(148) Brajtburg J, Bolard J. Carrier effects on biological activity of amphotericin B. Clin Microbiol Rev 1996 Oct;9(4):512-531.

(149) Lamy- Freund MT, Schreier S, Peitzsch RM, Reed WF. Characterization and time dependence of amphotericin B: deoxycholate aggregation by quasielastic light scattering. J Pharm Sci 1991;80(3):262-266.

(150) Barwicz J, Christian S, Gruda I. Effects of the aggregation state of amphotericin B on its toxicity to mice. Antimicrob Agents Chemother 1992 Oct;36(10):2310-2315.

(151) Hartsel SC, Bauer E, Kwong EH, Wasan KM. The effect of serum albumin on amphotericin B aggregate structure and activity. Pharm Res 2001;18(9):1305-1309.

(152) Yu B, Okano T, Kataoka K, Sardari S, Kwon G. In vitro dissociation of antifungal efficacy and toxicity for amphotericin B-loaded poly (ethylene oxide)-block-poly (β-benzyl-L-aspartate) micelles. J Controlled Release 1998;56(1):285-291.

(153) Torrado J, Espada R, Ballesteros M, Torrado- Santiago S. Amphotericin B formulations and drug targeting. J Pharm Sci 2008;97(7):2405-2425.

(154) Darole PS, Hegde DD, Nair HA. Formulation and evaluation of microemulsion based delivery system for amphotericin B. Aaps Pharmscitech 2008;9(1):122-128.

(155) Vandermeulen G, Rouxhet L, Arien A, Brewster M, Préat V. Encapsulation of amphotericin B in poly (ethylene glycol)-block-poly (ε-caprolactone-co-trimethylenecarbonate) polymeric micelles. Int J Pharm 2006;309(1):234-240.

(156) Espada R, Valdespina S, Alfonso C, Rivas G, Ballesteros MP, Torrado JJ. Effect of aggregation state on the toxicity of different amphotericin B preparations. Int J Pharm 2008;361(1):64-69.

(157) Barwicz J, Gruszecki WI, Gruda I. Spontaneous organization of amphotericin B in aqueous medium. J Colloid Interface Sci 1993;158(1):71-76.

(158) Rinnert H, Thirion C, Dupont G, Lematre J. Structural studies on aqueous and hydroalcoholic solutions of a polyene antibiotic: Amphotericin B. Biopolymers 1977;16(11):2419-2427.

(159) Schwartzman G, Asher I, Folen V, Brannon W, Taylor J. Ambiguities in IR and X- ray characterization of amphotericin B. J Pharm Sci 1978;67(3):398-400.

(160) Mesa-Arango AC, Scorzoni L, Zaragoza O. It only takes one to do many jobs: Amphotericin B as antifungal and immunomodulatory drug. Frontiers in microbiology 2012.

(161) Brajtburg J, Powderly WG, Kobayashi GS, Medoff G. Amphotericin B: current understanding of mechanisms of action. Antimicrob Agents Chemother 1990 Feb;34(2):183-188.

(162) Herve M, Debouzy J, Borowski E, Cybulska B, Gary-Bobo C. The role of the carboxyl and amino groups of polyene macrolides in their interactions with sterols and their selective toxicity. A 31 P-NMR study. Biochimica et Biophysica Acta (BBA)-Biomembranes 1989;980(3):261-272.

(163) Fournier I, Barwicz J, Auger M, Tancrède P. The chain conformational order of ergosterol-or cholesterol-containing DPPC bilayers as modulated by Amphotericin B: a FTIR study. Chem Phys Lipids 2008;151(1):41-50.

(164) Bagiński M, Tempczyk A, Borowski E. Comparative conformational analysis of cholesterol and ergosterol by molecular mechanics. European Biophysics Journal 1989;17(3):159-166.

(165) Palacios DS, Dailey I, Siebert DM, Wilcock BC, Burke MD. Synthesis-enabled functional group deletions reveal key underpinnings of amphotericin B ion channel and antifungal activities. Proc Natl Acad Sci U S A 2011 Apr 26;108(17):6733-6738.

(166) Chattopadhyay A, Jafurulla M. A novel mechanism for an old drug: amphotericin B in the treatment of visceral leishmaniasis. Biochem Biophys Res Commun 2011;416(1):7-12.

(167) Zhang Y, Gamarra S, Garcia-Effron G, Park S, Perlin DS, Rao R. Requirement for ergosterol in V-ATPase function underlies antifungal activity of azole drugs. PLoS Pathog 2010;6(6):e1000939.

(168) Gray KC, Palacios DS, Dailey I, Endo MM, Uno BE, Wilcock BC, et al. Amphotericin primarily kills yeast by simply binding ergosterol. Proc Natl Acad Sci U S A 2012 Feb 14;109(7):2234-2239.

(169) Baginski M, Sternal K, Czub J, Borowski E. Molecular modelling of membrane activity of amphotericin B, a polyene macrolide antifungal antibiotic. ACTA BIOCHIMICA POLONICA-ENGLISH EDITION- 2005;52(3):655.

(170) Hartsel SC, Benz SK, Ayenew W, Bolard J. Na , K and Cl− selectivity of the permeability pathways induced through sterol-containing membrane vesicles by amphotericin B and other polyene antibiotics. European biophysics journal 1994;23(2):125-132.

(171) Romero EA, Valdivieso E, Cohen BE. Formation of two different types of ion channels by amphotericin B in human erythrocyte membranes. J Membr Biol 2009;230(2):69-81.

(172) Mouri R, Konoki K, Matsumori N, Oishi T, Murata M. Complex Formation of Amphotericin B in Sterol-Containing Membranes As Evidenced by Surface Plasmon Resonance†. Biochemistry 2008;47(30):7807-7815.

(173) Baginski M, Resat H, Borowski E. Comparative molecular dynamics simulations of amphotericin B–cholesterol/ergosterol membrane channels. Biochimica et Biophysica Acta (BBA)-Biomembranes 2002;1567:63-78.

(174) Baginski M, Resat H, McCammon JA. Molecular properties of amphotericin B membrane channel: a molecular dynamics simulation. Mol Pharmacol 1997 Oct;52(4):560-570.

(175) Silberstein A. Conformational analysis of amphotericin B—cholesterol channel complex. J Membr Biol 1998;162(2):117-126.

(176) Vertut-Croquin A, Bolard J, Chabbert M, Gary-Bobo C. Differences in the interaction of the polyene antibiotic amphotericin B with cholesterol-or ergosterol-containing phospholipid vesicles. A circular dichroism and permeability study. Biochemistry 1983;22(12):2939-2944.

(177) Cotero BV, Rebolledo-Antúnez S, Ortega-Blake I. On the role of sterol in the formation of the amphotericin B channel. Biochimica et Biophysica Acta (BBA)-Biomembranes 1998;1375(1):43-51.

(178) Marty A, Finkelstein A. Pores formed in lipid bilayer membranes by nystatin, Differences in its one-sided and two-sided action. J Gen Physiol 1975 Apr;65(4):515-526.

(179) Palacios DS, Anderson TM, Burke MD. A post-PKS oxidation of the amphotericin B skeleton predicted to be critical for channel formation is not required for potent antifungal activity. J Am Chem Soc 2007;129(45):13804-13805.

(180) Mowat E, Lang S, Williams C, McCulloch E, Jones B, Ramage G. Phase-dependent antifungal activity against Aspergillus fumigatus developing multicellular filamentous biofilms. J Antimicrob Chemother 2008 Dec;62(6):1281-1284.

(181) Sokol-Anderson ML, Brajtburg J, Medoff G. Amphotericin B-induced oxidative damage and killing of Candida albicans. J Infect Dis 1986 Jul;154(1):76-83.

(182) Liu TT, Lee RE, Barker KS, Lee RE, Wei L, Homayouni R, et al. Genome-wide expression profiling of the response to azole, polyene, echinocandin, and pyrimidine antifungal agents in Candida albicans. Antimicrob Agents Chemother 2005 Jun;49(6):2226-2236.

(183) Brajtburg J, Bolard J. Carrier effects on biological activity of amphotericin B. Clin Microbiol Rev 1996 Oct;9(4):512-531.

(184) Suschek CV, Bonmann E, Kapsokefalou A, Hemmrich K, Kleinert H, Forstermann U, et al. Revisiting an old antimicrobial drug: amphotericin B induces interleukin-1-converting enzyme as the main factor for inducible nitric-oxide synthase expression in activated endothelia. Mol Pharmacol 2002 Oct;62(4):936-946.

(185) Shadkchan Y, Keisari Y, Segal E. Cytokines in mice treated with amphotericin B-intralipid. Med Mycol 2004 Apr;42(2):123-128.

(186) Yano T, Itoh Y, Kawamura E, Maeda A, Egashira N, Nishida M, et al. Amphotericin B-induced renal tubular cell injury is mediated by Na+ Influx through ion-permeable pores and subsequent activation of mitogen-activated protein kinases and elevation of intracellular Ca2+ concentration. Antimicrob Agents Chemother 2009 Apr;53(4):1420-1426.

(187) Bellocchio S, Gaziano R, Bozza S, Rossi G, Montagnoli C, Perruccio K, et al. Liposomal amphotericin B activates antifungal resistance with reduced toxicity by diverting Toll-like receptor signalling from TLR-2 to TLR-4. J Antimicrob Chemother 2005 Feb;55(2):214-222.

(188) Sau K, Mambula SS, Latz E, Henneke P, Golenbock DT, Levitz SM. The antifungal drug amphotericin B promotes inflammatory cytokine release by a Toll-like receptor- and CD14-dependent mechanism. J Biol Chem 2003 Sep 26;278(39):37561-37568.

(189) Louria DB. Some aspects of the absorption, distribution, and excretion of amphotericin B in man. Antibiotic Med. 1958;5(5):295-301.

(190) Hofstra W, de Vries-Hospers HG, Van der Waaij D. Concentrations of amphotericin B in faeces and blood of healthy volunteers after the oral administration of various doses. Infection 1982;10(4):223-227.

(191) HPLC measurement of amphotericin B serum levels in cancer patients. 27th Interscience Conference on Antimicrobial Agents and Chemotherapy, abstract; 1987.

(192) Fields BT,Jr, Bates JH, Abernathy RS. Effect of rapid intravenous infusion on serum concentrations of amphotericin B. Appl Microbiol 1971 Oct;22(4):615-617.

(193) Atkinson AJ,Jr, Bennett JE. Amphotericin B pharmacokinetics in humans. Antimicrob Agents Chemother 1978 Feb;13(2):271-276.

(194) Wiederhold NP, Tam VH, Chi J, Prince RA, Kontoyiannis DP, Lewis RE. Pharmacodynamic activity of amphotericin B deoxycholate is associated with peak plasma concentrations in a neutropenic murine model of invasive pulmonary aspergillosis. Antimicrob Agents Chemother 2006 Feb;50(2):469-473.

(195) Kan VL, Bennett JE, Amantea MA, Smolskis MC, McManus E, Grasela DM, et al. Comparative safety, tolerance, and pharmacokinetics of amphotericin B lipid complex and amphotericin B desoxycholate in healthy male volunteers. J Infect Dis 1991 Aug;164(2):418-421.

(196) Sanders SW, Buchi KN, Goddard MS, Lang JK, Tolman KG. Single-dose pharmacokinetics and tolerance of a cholesteryl sulfate complex of amphotericin B administered to healthy volunteers. Antimicrob Agents Chemother 1991 Jun;35(6):1029-1034.

(197) Heinemann V, Bosse D, Jehn U, Kahny B, Wachholz K, Debus A, et al. Pharmacokinetics of liposomal amphotericin B (Ambisome) in critically ill patients. Antimicrob Agents Chemother 1997 Jun;41(6):1275-1280.

(198) Patel R. Amphotericin B colloidal dispersion. Expert Opin Pharmacother 2000;1(3):475-488.

(199) Dupont B. Overview of the lipid formulations of amphotericin B. J Antimicrob Chemother 2002 Feb;49 Suppl 1:31-36.

(200) BLOCK ER, BENNETT JE, LIVOTI LG, KLEIN WJ, MacGREGOR RR, HENDERSON L. Flucytosine and amphotericin B: hemodialysis effects on the plasma concentration and clearance: studies in man. Ann Intern Med 1974;80(5):613-617.

(201) Bury RW, Mashford L, Kong B, Sabto J, Gurr W, Somogyi AA. Elimination of amphotericin B in impaired renal function. 1983.

(202) Veerareddy PR, Vobalaboina V. Lipid-based formulations of amphotericin B. Drugs of Today 2004;40(2):133-146.

(203) Brajtburg J, Elberg S, Bolard J, Kobayashi GS, Levy RA, Ostlund RE,Jr, et al. Interaction of plasma proteins and lipoproteins with amphotericin B. J Infect Dis 1984 Jun;149(6):986-997.

(204) Koldin MH, Kobayashi GS, Brajtburg J, Medoff G. Effects of elevation of serum cholesterol and administration of amphotericin B complexed to lipoproteins on amphotericin B-induced toxicity in rabbits. Antimicrob Agents Chemother 1985 Jul;28(1):144-145.

(205) Wasan KM, Kennedy AL, Cassidy SM, Ramaswamy M, Holtorf L, Chou JW, et al. Pharmacokinetics, distribution in serum lipoproteins and tissues, and renal toxicities of amphotericin B and amphotericin B lipid complex in a hypercholesterolemic rabbit model: single-dose studies. Antimicrob Agents Chemother 1998 Dec;42(12):3146-3152.

(206) Bennett J. Amphotericin B binding to serum betalipoprotein. Recent advances in medical and veterinary mycology.University Park Press, Baltimore 1977:107.

(207) Bekersky I, Fielding RM, Dressler DE, Lee JW, Buell DN, Walsh TJ. Plasma protein binding of amphotericin B and pharmacokinetics of bound versus unbound amphotericin B after administration of intravenous liposomal amphotericin B (AmBisome) and amphotericin B deoxycholate. Antimicrob Agents Chemother 2002 Mar;46(3):834-840.

(208) Torrado J, Espada R, Ballesteros M, Torrado- Santiago S. Amphotericin B formulations and drug targeting. J Pharm Sci 2008;97(7):2405-2425.

(209) Ayestaran A, Lopez RM, Montoro JB, Estibalez A, Pou L, Julia A, et al. Pharmacokinetics of conventional formulation versus fat emulsion formulation of amphotericin B in a group of patients with neutropenia. Antimicrob Agents Chemother 1996 Mar;40(3):609-612.

(210) Agencia Española de Medicamentos y Productos Sanitarios. Ficha Técnica: Abelcet 5mg/mL concentrado para suspensión por perfusión. Abril 2012; Available at: https://www.aemps.gob.es/cima/pdfs/es/ft/60945/60945_ft.pdf. Accessed 02/20, 2016.

(211) Adedoyin A, Swenson CE, Bolcsak LE, Hellmann A, Radowska D, Horwith G, et al. A pharmacokinetic study of amphotericin B lipid complex injection (Abelcet) in patients with definite or probable systemic fungal infections. Antimicrob Agents Chemother 2000 Oct;44(10):2900-2902.

(212) Walsh TJ, Whitcomb P, Piscitelli S, Figg WD, Hill S, Chanock SJ, et al. Safety, tolerance, and pharmacokinetics of amphotericin B lipid complex in children with hepatosplenic candidiasis. Antimicrob Agents Chemother 1997 Sep;41(9):1944-1948.

(213) Walsh TJ, Yeldandi V, McEvoy M, Gonzalez C, Chanock S, Freifeld A, et al. Safety, tolerance, and pharmacokinetics of a small unilamellar liposomal formulation of amphotericin B (AmBisome) in neutropenic patients. Antimicrob Agents Chemother 1998 Sep;42(9):2391-2398.

(214) Romero EL, Morilla MJ. Drug delivery systems against leishmaniasis? Still an open question. Expert opinion on drug delivery 2008;5(7):805-823.

(215) Bekersky I, Fielding RM, Dressler DE, Lee JW, Buell DN, Walsh TJ. Pharmacokinetics, excretion, and mass balance of liposomal amphotericin B (AmBisome) and amphotericin B deoxycholate in humans. Antimicrob Agents Chemother 2002 Mar;46(3):828-833.

(216) Bellmann R. Clinical pharmacokinetics of systemically administered antimycotics. Current clinical pharmacology 2007;2(1):37-58.

(217) Daneshmend T, Warnock D. Clinical pharmacokinetics of systemic antifungal drugs. Clin Pharmacokinet 1983;8(1):17-42.

(218) Lawrence RM, Hoeprich PD, Jagdis FA, Monji N, Huston AC, Schaffner CP. Distribution of doubly radiolabelled amphotericin B methyl ester and amphotericin B in the non-human primate, Macaca mulatta. J Antimicrob Chemother 1980 Mar;6(2):241-249.

(219) Tissue storage of amphotericin B and amphotericin B methyl ester aspartate. 19th Interscience Conference on Antimicrobial Agents and Chemotherapy, abstract; 1979.

(220) Ellis D. Amphotericin B: spectrum and resistance. J Antimicrob Chemother 2002 Feb;49 Suppl 1:7-10.

(221) Manavathu EK, Cutright JL, Chandrasekar PH. Organism-dependent fungicidal activities of azoles. Antimicrob Agents Chemother 1998 Nov;42(11):3018-3021.

(222) Agencia Española de Medicamentos y Productos Sanitarios. Ficha Técnica: Fungizona 50 mg polvo para solución para perfusión Anfotericina B
. 2002; Available at: https://www.aemps.gob.es/cima/pdfs/es/ft/46773/FT_46773.pdf. Accessed 02/24, 2016.

(223) Arthington-Skaggs BA, Motley M, Warnock DW, Morrison CJ. Comparative evaluation of PASCO and national committee for clinical laboratory standards M27-A broth microdilution methods for antifungal drug susceptibility testing of yeasts. J Clin Microbiol 2000 Jun;38(6):2254-2260.

(224) Pfaller MA, Arikan S, Lozano-Chiu M, Chen Y, Coffman S, Messer SA, et al. Clinical evaluation of the ASTY colorimetric microdilution panel for antifungal susceptibility testing. J Clin Microbiol 1998 Sep;36(9):2609-2612.

(225) Pfaller MA, Bale M, Buschelman B, Lancaster M, Espinel-Ingroff A, Rex JH, et al. Quality control guidelines for National Committee for Clinical Laboratory Standards recommended broth macrodilution testing of amphotericin B, fluconazole, and flucytosine. J Clin Microbiol 1995 May;33(5):1104-1107.

(226) Davey KG, Holmes AD, Johnson EM, Szekely A, Warnock DW. Comparative evaluation of FUNGITEST and broth microdilution methods for antifungal drug susceptibility testing of Candida species and Cryptococcus neoformans. J Clin Microbiol 1998 Apr;36(4):926-930.

(227) Espinel-Ingroff A. In vitro activity of the new triazole voriconazole (UK-109,496) against opportunistic filamentous and dimorphic fungi and common and emerging yeast pathogens. J Clin Microbiol 1998 Jan;36(1):198-202.

(228) Chang HC, Chang JJ, Huang AH, Chang TC. Evaluation of a capacitance method for direct antifungal susceptibility testing of yeasts in positive blood cultures. J Clin Microbiol 2000 Mar;38(3):971-976.

(229) Haido RMT, Barreto-Bergter E. Amphotericin B-induced damage of Trypanosoma cruzi epimastigotes. Chem Biol Interact 1989;71(1):91-103.

(230) Duma RJ, Finley R. In vitro susceptibility of pathogenic Naegleria and Acanthamoeba speicies to a variety of therapeutic agents. Antimicrob Agents Chemother 1976 Aug;10(2):370-376.

(231) Hatabu T, Takada T, Taguchi N, Suzuki M, Sato K, Kano S. Potent plasmodicidal activity of a heat-induced reformulation of deoxycholate-amphotericin B (Fungizone) against Plasmodium falciparum. Antimicrob Agents Chemother 2005 Feb;49(2):493-496.

(232) Rain AN, Radzan T, Sajiri S, Mak J. In vitro drug susceptibility of Acanthamoeba castellani to chloroquine, ivermectin and fungizon. Southeast Asian J Trop Med Public Health 1996;27:319-324.

(233) Li RK, Ciblak MA, Nordoff N, Pasarell L, Warnock DW, McGinnis MR. In vitro activities of voriconazole, itraconazole, and amphotericin B against Blastomyces dermatitidis, Coccidioides immitis, and Histoplasma capsulatum. Antimicrob Agents Chemother 2000 Jun;44(6):1734-1736.

(234) Sugar AM, Liu XP. In vitro and in vivo activities of SCH 56592 against Blastomyces dermatitidis. Antimicrob Agents Chemother 1996 May;40(5):1314-1316.

(235) McGinnis M, Pasarell L, Sutton D, Fothergill A, Cooper C, Rinaldi M. In vitro activity of voriconazole against selected fungi. Medical mycology 1998;36(4):239-242.

(236) Arikan S, Lozano-Chiu M, Paetznick V, Nangia S, Rex JH. Microdilution susceptibility testing of amphotericin B, itraconazole, and voriconazole against clinical isolates of Aspergillus and Fusarium species. J Clin Microbiol 1999 Dec;37(12):3946-3951.

(237) Espinel-Ingroff A, Bartlett M, Bowden R, Chin NX, Cooper C,Jr, Fothergill A, et al. Multicenter evaluation of proposed standardized procedure for antifungal susceptibility testing of filamentous fungi. J Clin Microbiol 1997 Jan;35(1):139-143.

(238) Rex JH, Walsh TJ, Sobel JD, Filler SG, Pappas PG, Dismukes WE, et al. Practice guidelines for the treatment of candidiasis. Infectious Diseases Society of America. Clin Infect Dis 2000 Apr;30(4):662-678.

(239) Cuenca-Estrella M, Ruiz-Diez B, Martinez-Suarez JV, Monzon A, Rodriguez-Tudela JL. Comparative in-vitro activity of voriconazole (UK-109,496) and six other antifungal agents against clinical isolates of Scedosporium prolificans and Scedosporium apiospermum. J Antimicrob Chemother 1999 Jan;43(1):149-151.

(240) Johnson EM, Szekely A, Warnock DW. In vitro activity of Syn-2869, a novel triazole agent, against emerging and less common mold pathogens. Antimicrob Agents Chemother 1999 May;43(5):1260-1263.

(241) Guarro J, Llop C, Aguilar C, Pujol I. Comparison of in vitro antifungal susceptibilities of conidia and hyphae of filamentous fungi. Antimicrob Agents Chemother 1997 Dec;41(12):2760-2762.

(242) Aguilar C, Pujol I, Sala J, Guarro J. Antifungal susceptibilities of Paecilomyces species. Antimicrob Agents Chemother 1998 Jul;42(7):1601-1604.

(243) Espinel-Ingroff A, Dawson K, Pfaller M, Anaissie E, Breslin B, Dixon D, et al. Comparative and collaborative evaluation of standardization of antifungal susceptibility testing for filamentous fungi. Antimicrob Agents Chemother 1995 Feb;39(2):314-319.

(244) Wildfeuer A, Seidl HP, Paule I, Haberreiter A. In vitro activity of voriconazole against yeasts, moulds and dermatophytes in comparison with fluconazole, amphotericin B and griseofulvin. Arzneimittelforschung 1997 Nov;47(11):1257-1263.

(245) Ostrosky-Zeichner L, Marr KA, Rex JH, Cohen SH. Amphotericin B: time for a new "gold standard". Clin Infect Dis 2003 Aug 1;37(3):415-425.

(246) Ouellette M, Drummelsmith J, Papadopoulou B. Leishmaniasis: drugs in the clinic, resistance and new developments. Drug Resistance Updates 2004;7(4):257-266.

(247) Khot PD, Suci PA, Miller RL, Nelson RD, Tyler BJ. A small subpopulation of blastospores in candida albicans biofilms exhibit resistance to amphotericin B associated with differential regulation of ergosterol and beta-1,6-glucan pathway genes. Antimicrob Agents Chemother 2006 Nov;50(11):3708-3716.

(248) Kelly S, Lamb D, Kelly D, Manning N, Loeffler J, Hebart H, et al. Resistance to fluconazole and cross- resistance to amphotericin B in Candida albicans from AIDS patients caused by defective sterol Δ5, 6- desaturation. FEBS Lett 1997;400(1):80-82.

(249) Geraghty P, Kavanagh K. Disruption of mitochondrial function in Candida albicans leads to reduced cellular ergosterol levels and elevated growth in the presence of amphotericin B. Arch Microbiol 2003;179(4):295-300.

(250) Vazquez JA, Arganoza MT, Boikov D, Yoon S, Sobel JD, Akins RA. Stable phenotypic resistance of Candida species to amphotericin B conferred by preexposure to subinhibitory levels of azoles. J Clin Microbiol 1998 Sep;36(9):2690-2695.

(251) Arana DM, Nombela C, Pla J. Fluconazole at subinhibitory concentrations induces the oxidative- and nitrosative-responsive genes TRR1, GRE2 and YHB1, and enhances the resistance of Candida albicans to phagocytes. J Antimicrob Chemother 2010 Jan;65(1):54-62.

(252) Hillery AM. Supramolecular lipidic drug delivery systems: From laboratory to clinic A review of the recently introduced commercial liposomal and lipid-based formulations of amphotericin B. Adv Drug Deliv Rev 1997;24(2):345-363.

(253) Schreier S, Malheiros SV, de Paula E. Surface active drugs: self-association and interaction with membranes and surfactants. Physicochemical and biological aspects. Biochimica et Biophysica Acta (BBA)-Biomembranes 2000;1508(1):210-234.

(254) Clements JS,Jr, Peacock JE,Jr. Amphotericin B revisited: reassessment of toxicity. Am J Med 1990 May;88(5N):22N-27N.

(255) Hartsel S, Bolard J. Amphotericin B: new life for an old drug. Trends Pharmacol Sci 1996;17(12):445-449.

(256) Hiemenz JW, Walsh TJ. Lipid formulations of amphotericin B: recent progress and future directions. Clin Infect Dis 1996 May;22 Suppl 2:S133-44.

(257) Hughes CE, Bennett RL, Beggs WH. Broth dilution testing of Candida albicans susceptibility to ketoconazole. Antimicrob Agents Chemother 1987 Apr;31(4):643-646.

(258) Silva-Filho MA, Siqueira SD, Freire LB, Araujo IB, Holanda e Silva KG, Medeiros Ada C, et al. How can micelle systems be rebuilt by a heating process? Int J Nanomedicine 2012;7:141-150.

(259) Oka M, Kamimori H. Lipid membrane-binding properties of amphotericin B deoxycholate (fungizone) using surface plasmon resonance. Analytical Sciences 2013;29(7):697-702.

(260) Espada R, Valdespina S, Dea MA, Molero G, Ballesteros MP, Bolas F, et al. In vivo distribution and therapeutic efficacy of a novel amphotericin B poly-aggregated formulation. J Antimicrob Chemother 2008 May;61(5):1125-1131.

(261) Panosian CB, Barza M, Szoka F, Wyler DJ. Treatment of experimental cutaneous leishmaniasis with liposome-intercalated amphotericin B. Antimicrob Agents Chemother 1984 May;25(5):655-656.

(262) Oliva G, Gradoni L, Ciaramella P, De Luna R, Cortese L, Orsini S, et al. Activity of liposomal amphotericin B (AmBisome) in dogs naturally infected with Leishmania infantum. J Antimicrob Chemother 1995 Dec;36(6):1013-1019.

(263) Davidson RN, di Martino L, Gradoni L, Giacchino R, Gaeta GB, Pempinello R, et al. Short-course treatment of visceral leishmaniasis with liposomal amphotericin B (AmBisome). Clin Infect Dis 1996 Jun;22(6):938-943.

(264) Ramos H, Valdivieso E, Gamargo M, Dagger F, Cohen B. Amphotericin B kills unicellular leishmanias by forming aqueous pores permeable to small cations and anions. J Membr Biol 1996;152(1):65-75.

(265) Yardley V, Croft SL. A comparison of the activities of three amphotericin B lipid formulations against experimental visceral and cutaneous leishmaniasis. Int J Antimicrob Agents 2000;13(4):243-248.

(266) Sundar S, Agrawal G, Rai M, Makharia MK, Murray HW. Treatment of Indian visceral leishmaniasis with single or daily infusions of low dose liposomal amphotericin B: randomised trial. BMJ 2001 Aug 25;323(7310):419-422.

(267) Carrillo-Munoz AJ, Quindos G, Tur C, Ruesga MT, Miranda Y, del Valle O, et al. In-vitro antifungal activity of liposomal nystatin in comparison with nystatin, amphotericin B cholesteryl sulphate, liposomal amphotericin B, amphotericin B lipid complex, amphotericin B desoxycholate, fluconazole and itraconazole. J Antimicrob Chemother 1999 Sep;44(3):397-401.

(268) Garcia A, Adler-Moore JP, Proffitt RT. Single-dose AmBisome (Liposomal amphotericin B) as prophylaxis for murine systemic candidiasis and histoplasmosis. Antimicrob Agents Chemother 2000 Sep;44(9):2327-2332.

(269) Sheikh S, Ali SM, Ahmad MU, Ahmad A, Mushtaq M, Paithankar M, et al. Nanosomal Amphotericin B is an efficacious alternative to Ambisome® for fungal therapy. Int J Pharm 2010;397(1):103-108.

(270) Berman JD, Ksionski G, Chapman WL, Waits VB, Hanson WL. Activity of amphotericin B cholesterol dispersion (Amphocil) in experimental visceral leishmaniasis. Antimicrob Agents Chemother 1992 Sep;36(9):1978-1980.

(271) Mullen AB, Carter KC, Baillie AJ. Comparison of the efficacies of various formulations of amphotericin B against murine visceral leishmaniasis. Antimicrob Agents Chemother 1997 Oct;41(10):2089-2092.

(272) Dupont B. Clinical efficacy of amphotericin B colloidal dispersion against infections caused by Candida spp. Chemotherapy 1999 Jun;45 Suppl 1:27-33.

(273) Herbrecht R, Letscher-Bru V, Bowden R, Kusne S, Anaissie E, Graybill J, et al. Treatment of 21 cases of invasive mucormycosis with amphotericin B colloidal dispersion. European Journal of Clinical Microbiology and Infectious Diseases 2001;20(7):460-466.

(274) Cetin H, Yalaz M, Akisu M, Hilmioglu S, Metin D, Kultursay N. The efficacy of two different lipid- based amphotericin B in neonatal Candida septicemia. Pediatrics international 2005;47(6):676-680.

(275) Wiley JM, Seibel NL, Walsh TJ. Efficacy and safety of amphotericin B lipid complex in 548 children and adolescents with invasive fungal infections. Pediatr Infect Dis J 2005;24(2):167-174.

(276) Jain V, Gupta A, Pawar VK, Asthana S, Jaiswal AK, Dube A, et al. Chitosan-Assisted Immunotherapy for Intervention of Experimental Leishmaniasis via Amphotericin B-Loaded Solid Lipid Nanoparticles. Appl Biochem Biotechnol 2014;174(4):1309-1330.

(277) Kayser O, Olbrich C, Yardley V, Kiderlen A, Croft S. Formulation of amphotericin B as nanosuspension for oral administration. Int J Pharm 2003;254(1):73-75.

(278) Lemke A, Kiderlen AF, Petri B, Kayser O. Delivery of amphotericin B nanosuspensions to the brain and determination of activity against Balamuthia mandrillaris amebas. Nanomedicine: Nanotechnology, Biology and Medicine 2010;6(4):597-603.

(279) Das S, Suresh PK. Nanosuspension: a new vehicle for the improvement of the delivery of drugs to the ocular surface. Application to amphotericin B. Nanomedicine: Nanotechnology, Biology and Medicine 2011;7(2):242-247.

(280) Dea- Ayuela M, Rama- Íñiguez S, Sánchez- Brunete J, Torrado J, Alunda J, Bolás- Fernández F. Anti- leishmanial activity of a new formulation of amphotericin B. Tropical Medicine & International Health 2004;9(9):981-990.

(281) Kretschmar M, Amselem S, Zawoznik E, Mosbach K, Dietz A, Hof H, et al. Efficient treatment of murine systemic infection with Candida albicans using amphotericin B incorporated in nanosize range particles (emulsomes). Mycoses 2001;44(7- 8):281-286.

(282) Pahissa A. Amphotericin B. Lipid complex versus liposomes. Which, why, when? Enferm Infecc Microbiol Clin 1997 Jan;15(1):1-3.

(283) Lamothe J. Activity of amphotericin B in lipid emulsion in the initial treatment of canine leishmaniasis. J Small Anim Pract 2001;42(4):170-175.

(284) Caillot D, Casasnovas O, Solary E, Chavanet P, Bonnotte B, Reny G, et al. Efficacy and tolerance of an amphotericin B lipid (Intralipid) emulsion in the treatment of candidaemia in neutropenic patients. J Antimicrob Chemother 1993 Jan;31(1):161-169.

(285) Sievers TM, Kubak BM, Wong-Beringer A. Safety and efficacy of Intralipid emulsions of amphotericin B. J Antimicrob Chemother 1996 Sep;38(3):333-347.

(286) Petit C, Yardley V, Gaboriau F, Bolard J, Croft SL. Activity of a heat-induced reformulation of amphotericin B deoxycholate (fungizone) against Leishmania donovani. Antimicrob Agents Chemother 1999 Feb;43(2):390-392.

(287) Ranchere JY, Latour JF, Fuhrmann C, Lagallarde C, Loreuil F. Amphotericin B intralipid formulation: stability and particle size. J Antimicrob Chemother 1996 Jun;37(6):1165-1169.

(288) Adams ML, Andes DR, Kwon GS. Amphotericin B Encapsulated in Micelles Based on Poly (ethylene oxide)-b lock-poly (l-amino acid) Derivatives Exerts Reduced in Vitro Hemolysis but Maintains Potent in Vivo Antifungal Activity. Biomacromolecules 2003;4(3):750-757.

(289) Kumar V, Gupta PK, Pawar VK, Verma A, Khatik R, Tripathi P, et al. In-Vitro and In-Vivo Studies on Novel Chitosan-g-Pluronic F-127 Copolymer Based Nanocarrier of Amphotericin B for Improved Antifungal Activity. Journal of Biomaterials and Tissue Engineering 2014;4(3):210-216.

(290) Ruiz HK, Serrano DR, Dea-Ayuela MA, Bilbao-Ramos PE, Bolás-Fernández F, Torrado JJ, et al. New amphotericin B-gamma cyclodextrin formulation for topical use with synergistic activity against diverse fungal species and Leishmania spp. Int J Pharm 2014;473(1):148-157.

(291) Serrano D, Ruiz-Saldana H, Molero G, Ballesteros M, Torrado J. A novel formulation of solubilised amphotericin B designed for ophthalmic use. Int J Pharm 2012;437(1):80-82.

(292) Kim Y, Shin B, Garripelli VK, Kim J, Davaa E, Jo S, et al. A thermosensitive vaginal gel formulation with HPγCD for the pH-dependent release and solubilization of amphotericin B. European Journal of Pharmaceutical Sciences 2010;41(2):399-406.

(293) Santangelo R, Paderu P, Delmas G, Chen ZW, Mannino R, Zarif L, et al. Efficacy of oral cochleate-amphotericin B in a mouse model of systemic candidiasis. Antimicrob Agents Chemother 2000 Sep;44(9):2356-2360.

(294) Sesana AM, Monti-Rocha R, Vinhas SA, Morais CG, Dietze R, Lemos EM. In vitro activity of amphotericin B cochleates against Leishmania chagasi. Memórias do Instituto Oswaldo Cruz 2011;106(2):251-253.

(295) Zarif L, Graybill JR, Perlin D, Najvar L, Bocanegra R, Mannino RJ. Antifungal activity of amphotericin B cochleates against Candida albicans infection in a mouse model. Antimicrob Agents Chemother 2000 Jun;44(6):1463-1469.

(296) Delmas G, Park S, Chen ZW, Tan F, Kashiwazaki R, Zarif L, et al. Efficacy of orally delivered cochleates containing amphotericin B in a murine model of aspergillosis. Antimicrob Agents Chemother 2002 Aug;46(8):2704-2707.

(297) Venier-Julienne M, Vouldoukis I, Monjour L, Benoit J. In vitro study of the anti-leishmanial activity of biodegradable nanoparticles. J Drug Target 1995;3(1):23-29.

(298) Ordónez-Gutiérrez L, Espada-Fernández R, Dea-Ayuela MA, Torrado JJ, Bolás-Fernandez F, Alunda JM. In vitro effect of new formulations of amphotericin B on amastigote and promastigote forms of Leishmania infantum. Int J Antimicrob Agents 2007;30(4):325-329.

(299) Italia JL, Sharp A, Carter KC, Warn P, Kumar MR. Peroral amphotericin B polymer nanoparticles lead to comparable or superior in vivo antifungal activity to that of intravenous Ambisome® or Fungizone™. PLoS One 2011;6(10):e25744.

(300) Amaral AC, Bocca AL, Ribeiro AM, Nunes J, Peixoto DL, Simioni AR, et al. Amphotericin B in poly(lactic-co-glycolic acid) (PLGA) and dimercaptosuccinic acid (DMSA) nanoparticles against paracoccidioidomycosis. J Antimicrob Chemother 2009 Mar;63(3):526-533.

(301) Mohamed-Ahmed AH, Les KA, Seifert K, Croft SL, Brocchini S. Noncovalent complexation of amphotericin-B with Poly (α-glutamic acid). Molecular pharmaceutics 2013;10(3):940-950.

(302) Sen N, Samanta A, Baidya S, Gupta BK, Ghosh LK. Development of amphotericin B loaded nanoparticles. Boll Chim Farm 1998 Sep;137(8):295-297.

(303) Xu N, Gu J, Zhu Y, Wen H, Ren Q, Chen J. Efficacy of intravenous amphotericin B-polybutylcyanoacrylate nanoparticles against cryptococcal meningitis in mice. Int J Nanomedicine 2011;6:905-913.

(304) Sangeetha S, Venkatesh DN, Adhiyaman R, Santhi K, Suresh B. Formulation of sodium alginate nanospheres containing amphotericin B for the treatment of systemic candidiasis. Tropical Journal of Pharmaceutical Research 2007;6(1):653-659.

(305) Gupta PK, Jaiswal AK, Asthana S, Verma A, Kumar V, Shukla P, et al. Self assembled ionically sodium alginate cross-linked amphotericin B encapsulated glycol chitosan stearate nanoparticles: applicability in better chemotherapy and non-toxic delivery in visceral leishmaniasis. Pharm Res 2015;32(5):1727-1740.

(306) Tiyaboonchai W, Limpeanchob N. Formulation and characterization of amphotericin B–chitosan–dextran sulfate nanoparticles. Int J Pharm 2007;329(1):142-149.

(307) Tiyaboonchai W, Woiszwillo J, Middaugh CR. Formulation and characterization of amphotericin B–polyethylenimine–dextran sulfate nanoparticles. J Pharm Sci 2001;90(7):902-914.

(308) Nahar M, Mishra D, Dubey V, Jain NK. Development, characterization, and toxicity evaluation of amphotericin B–loaded gelatin nanoparticles. Nanomedicine: Nanotechnology, Biology and Medicine 2008;4(3):252-261.

(309) Serrano DR, Lalatsa A, Dea-Ayuela MA, Bilbao-Ramos PE, Garrett NL, Moger J, et al. Oral particle uptake and organ targeting drives the activity of amphotericin B nanoparticles. Molecular pharmaceutics 2015;12(2):420-431.

(310) Jung SH, Lim DH, Jung SH, Lee JE, Jeong K, Seong H, et al. Amphotericin B-entrapping lipid nanoparticles and their in vitro and in vivo characteristics. European Journal of Pharmaceutical Sciences 2009;37(3):313-320.

(311) Chakraborty K, Naik S. Therapeutic and hemolytic evaluation of in–situ liposomal preparation containing amphotericin B complexed with different chemically modified Beta cyclodextrins. J Pharm Pharm Sci 2003;6:231-237.

(312) Cordonnier C, Mohty M, Faucher C, Pautas C, Robin M, Vey N, et al. Safety of a weekly high dose of liposomal amphotericin B for prophylaxis of invasive fungal infection in immunocompromised patients: PROPHYSOME Study. Int J Antimicrob Agents 2008;31(2):135-141.

(313) Efficiency and safety of inhaled amphotericin B lipid complex (Abelcet) in the prophylaxis of invasive fungal infections following lung transplantation. Transplantation proceedings: Elsevier; 2008.

(314) Fukui H, Koike T, Saheki A, Sonoke S, Seki J. A novel delivery system for amphotericin B with lipid nano-sphere (LNS®). Int J Pharm 2003;265(1):37-45.

(315) Richardson M, De Pauw B. A perspective on liposomal amphotericin B (AmBisome®). Clinical Microbiology and Infection 2008;14(s4):1-4.

(316) Vyas SP, Gupta S. Optimizing efficacy of amphotericin B through nanomodification. International journal of nanomedicine 2006;1(4):417.

(317) Maesaki S. Drug delivery system of anti-fungal and parasitic agents. Curr Pharm Des 2002;8(6):433-440.

(318) Jain JP, Kumar N. Development of amphotericin B loaded polymersomes based on (PEG)< sub> 3</sub>-PLA co-polymers: Factors affecting size and< i> in vitro</i> evaluation. European Journal of Pharmaceutical Sciences 2010;40(5):456-465.

(319) Lemke A, Kiderlen A, Kayser O. Amphotericin B. Appl Microbiol Biotechnol 2005;68(2):151-162.

(320) Adler-Moore JP, Proffitt RT. Development, characterization, efficacy and mode of action of AmBisome, a unilamellar liposomal formulation of amphotericin B. J Liposome Res 1993;3(3):429-450.

(321) Bangham AD. Liposomes: realizing their promise. Hosp Pract (Off Ed) 1992 Dec 15;27(12):51-6, 61-2.

(322) Davidson RN, Di Martino L, Gradoni L, Giacchino R, Russo R, Gaeta GB, et al. Liposomal amphotericin B (AmBisome) in Mediterranean visceral leishmaniasis: a multi-centre trial. Q J Med 1994 Feb;87(2):75-81.

(323) Ringden O, Andstrom E, Remberger M, Svahn BM, Tollemar J. Safety of liposomal amphotericin B (AmBisome) in 187 transplant recipients treated with cyclosporin. Bone Marrow Transplant 1994;14 Suppl 5:S10-4.

(324) Emminger W, Graninger W, Emminger-Schmidmeier W, Zoubek A, Pillwein K, Susani M, et al. Tolerance of high doses of amphotericin B by infusion of a liposomal formulation in children with cancer. Ann Hematol 1994;68(1):27-31.

(325) Fukui H, Koike T, Nakagawa T, Saheki A, Sonoke S, Tomii Y, et al. Comparison of LNS-AmB, a novel low-dose formulation of amphotericin B with lipid nano-sphere (LNS< sup>®</sup>), with commercial lipid-based formulations. Int J Pharm 2003;267(1):101-112.

(326) Storm G, Crommelin DJ. Liposomes: quo vadis? Pharm Sci Technol Today 1998;1(1):19-31.

(327) Stevens DA. Overview of amphotericin B colloidal dispersion (Amphocil). J Infect 1994;28:45-49.

(328) Hamill RJ. Amphotericin B formulations: a comparative review of efficacy and toxicity. Drugs 2013;73(9):919-934.

(329) Croy S, Kwon G. Polymeric micelles for drug delivery. Curr Pharm Des 2006;12(36):4669-4684.

(330) Yu B, Okano T, Kataoka K, Sardari S, Kwon G. In vitro dissociation of antifungal efficacy and toxicity for amphotericin B-loaded poly (ethylene oxide)-block-poly (β-benzyl-l-aspartate) micelles. J Controlled Release 1998;56(1):285-291.

(331) Lukyanov AN, Torchilin VP. Micelles from lipid derivatives of water-soluble polymers as delivery systems for poorly soluble drugs. Adv Drug Deliv Rev 2004;56(9):1273-1289.

(332) Lavasanifar A, Samuel J, Kwon GS. The effect of fatty acid substitution on the in vitro release of amphotericin B from micelles composed of poly (ethylene oxide)-< i> block</i>-poly (< i> N</i>-hexyl stearate-l-aspartamide). J Controlled Release 2002;79(1):165-172.

(333) Li S, He Q, Chen T, Wu W, Lang K, Li Z, et al. Controlled co-delivery nanocarriers based on mixed micelles formed from cyclodextrin-conjugated and cross-linked copolymers. Colloids and Surfaces B: Biointerfaces 2014;123:486-492.

(334) Li F, Danquah M, Mahato RI. Synthesis and characterization of amphiphilic lipopolymers for micellar drug delivery. Biomacromolecules 2010;11(10):2610-2620.

(335) Salmaso S, Bersani S, Mastrotto F, Tonon G, Schrepfer R, Genovese S, et al. Self- assembling nanocomposites for protein delivery: Supramolecular interactions between PEG- cholane and rh- G- CSF. J Controlled Release 2012;162(1):176-184.

(336) Salmaso S, Bersani S, Scomparin A, Balasso A, Brazzale C, Barattin M, et al. A novel soluble supramolecular system for sustained rh-GH delivery. J Controlled Release 2014;194:168-177.

(337) Roling EE, Klepser ME, Wasson A, Lewis RE, Ernst EJ, Pfaller MA. Antifungal activities of fluconazole, caspofungin (MK0991), and anidulafungin (LY 303366) alone and in combination against Candida spp. and Crytococcus neoformans via time-kill methods. Diagn Microbiol Infect Dis 2002;43(1):13-17.

(338) Naumann S, Meyer J, Kiesow A, Mrestani Y, Wohlrab J, Neubert RH. Controlled nail delivery of a novel lipophilic antifungal agent using various modern drug carrier systems as well as in vitro and ex vivo model systems. J Controlled Release 2014;180:60-70.

(339) Yu L, Zhang W, Wang L, Yang J, Liu T, Peng J, et al. Transcriptional profiles of the response to ketoconazole and amphotericin B in Trichophyton rubrum. Antimicrob Agents Chemother 2007 Jan;51(1):144-153.

(340) Yenişehirli G, Tunçoğlu E, Yenişehirli A, Bulut Y. In vitro activities of antifungal drugs against dermatophytes isolated in Tokat, Turkey. Int J Dermatol 2013;52(12):1557-1560.

(341) Lalitha P, Shapiro BL, Srinivasan M, Prajna NV, Acharya NR, Fothergill AW, et al. Antimicrobial susceptibility of Fusarium, Aspergillus, and other filamentous fungi isolated from keratitis. Arch Ophthalmol 2007;125(6):789-793.

(342) Pujol I, Guarro J, Gene J, Sala J. In-vitro antifungal susceptibility of clinical and environmental Fusarium spp. strains. J Antimicrob Chemother 1997 Feb;39(2):163-167.

(343) Azor M, Gene J, Cano J, Guarro J. Universal in vitro antifungal resistance of genetic clades of the Fusarium solani species complex. Antimicrob Agents Chemother 2007 Apr;51(4):1500-1503.

(344) O'Donnell K, Sutton DA, Fothergill A, McCarthy D, Rinaldi MG, Brandt ME, et al. Molecular phylogenetic diversity, multilocus haplotype nomenclature, and in vitro antifungal resistance within the Fusarium solani species complex. J Clin Microbiol 2008 Aug;46(8):2477-2490.

(345) Alastruey-Izquierdo A, Cuenca-Estrella M, Monzon A, Mellado E, Rodriguez-Tudela JL. Antifungal susceptibility profile of clinical Fusarium spp. isolates identified by molecular methods. J Antimicrob Chemother 2008 Apr;61(4):805-809.

(346) Garcia-Martos P, Garcia-Agudo L, Gutierrez-Calzada J, Ruiz-Aragon J, Saldarreaga A, Marin P. In vitro activity of amphotericin B, itraconazole and voriconazole against 20 species of Aspergillus using the Sensititre microdilution method. Enferm Infecc Microbiol Clin 2005 Jan;23(1):15-18.

(347) Pfaller MA, Messer SA, Hollis RJ, Jones RN, SENTRY Participants Group. Antifungal activities of posaconazole, ravuconazole, and voriconazole compared to those of itraconazole and amphotericin B against 239 clinical isolates of Aspergillus spp. and other filamentous fungi: report from SENTRY Antimicrobial Surveillance Program, 2000. Antimicrob Agents Chemother 2002 Apr;46(4):1032-1037.

(348) Wildfeuer A, Seidl H, Paule I, Haberreiter A. In vitro evaluation of voriconazole against clinical isolates of yeasts, moulds and dermatophytes in comparison with itraconazole, ketoconazole, amphotericin B and griseofulvin. Mycoses 1998;41(7- 8):309-319.

(349) Snyder SL, Sobocinski PZ. An improved 2, 4, 6-trinitrobenzenesulfonic acid method for the determination of amines. Anal Biochem 1975;64(1):284-288.

(350) Satake K, Okuyama T, OHASHI M, SHINODA T. The spectrophotometric determination of amine, amino acid and peptide with 2, 4, 6-trinitrobenzene 1-sulfonic acid. The Journal of Biochemistry 1960;47(5):654-660.

(351) Higuchi T, Connors A. Phase-solubility techniques. 1965.

(352) Espada R, Josa J, Valdespina S, Dea M, Ballesteros M, Alunda J, et al. HPLC assay for determination of amphotericin B in biological samples. Biomedical Chromatography 2008;22(4):402-407.

(353) Freire E, Mayorga OL, Straume M. Isothermal titration calorimetry. Anal Chem 1990;62(18):950A-959A.

(354) Jelesarov I, Bosshard HR. Isothermal titration calorimetry and differential scanning calorimetry as complementary tools to investigate the energetics of biomolecular recognition. Journal of molecular recognition 1999;12(1):3-18.

(355) Ruiz-Caro R, Veiga-Ochoa MD. Characterization and dissolution study of chitosan freeze-dried systems for drug controlled release. Molecules 2009;14(11):4370-4386.

(356) Kelly SM, Jess TJ, Price NC. How to study proteins by circular dichroism. Biochimica et Biophysica Acta (BBA)-Proteins and Proteomics 2005;1751(2):119-139.

(357) Kelly SM, Price NC. The use of circular dichroism in the investigation of protein structure and function. Current protein and peptide science 2000;1(4):349-384.

(358) Vakil R, S. Kwon G. Effect of cholesterol on the release of amphotericin B from PEG-phospholipid micelles. Molecular pharmaceutics 2007;5(1):98-104.

(359) Guideline IHT. Stability testing of new drug substances and products. Q1A (R2), Current Step 2003;4.

(360) European Pharmacopoeia 8.0. 5.17.1. Recommendations on dissolution Testing. Simulated gastric fluid. In: European Council, editor. ; 2013. p. 727-728.

(361) Pidgeon C. Advanced Tutorials for Biomedical Sciences: Animations, Simulations, and Calculations Using Mathematica

. ; 1996.

(362) Fukui H, Koike T, Nakagawa T, Saheki A, Sonoke S, Tomii Y, et al. Comparison of LNS-AmB, a novel low-dose formulation of amphotericin B with lipid nano-sphere (LNS®), with commercial lipid-based formulations. Int J Pharm 2003;267(1):101-112.

(363) van Etten EW, van Vianen W, Roovers P, Frederik P. Mild heating of amphotericin B-desoxycholate: effects on ultrastructure, in vitro activity and toxicity, and therapeutic efficacy in severe candidiasis in leukopenic mice. Antimicrob Agents Chemother 2000 Jun;44(6):1598-1603.

(364) Zu Y, Sun W, Zhao X, Wang W, Li Y, Ge Y, et al. Preparation and characterization of amorphous amphotericin B nanoparticles for oral administration through liquid antisolvent precipitation. European Journal of Pharmaceutical Sciences 2014;53:109-117.

(365) Fukui H, Koike T, Saheki A, Sonoke S, Tomii Y, Seki J. Evaluation of the efficacy and toxicity of amphotericin B incorporated in lipid nano-sphere (LNS®). Int J Pharm 2003;263(1):51-60.

(366) Nimtrakul P, Tiyaboonchai W, Lamlertthon S. Effect of types of solid lipids on the physicochemical properties and self-aggregation of amphotericin B loaded nanostructured lipid carriers (NLCs). Asian Journal of Pharmaceutical Sciences 2015.

(367) Siqueira SD, Silva-Filho MA, Silva CA, Araújo IB, Silva AE, Fernandes-Pedrosa MF, et al. Influence of the Freeze-Drying Process on the Physicochemical and Biological Properties of Pre-heated Amphotericin B Micellar Systems. AAPS PharmSciTech 2014;15(3):612-619.

(368) Adams ML, Kwon GS. Relative aggregation state and hemolytic activity of amphotericin B encapsulated by poly (ethylene oxide)-block–poly (N-hexyl-l-aspartamide)-acyl conjugate micelles: effects of acyl chain length. J Controlled Release 2003;87(1):23-32.

(369) Salmaso S, Bersani S, Mastrotto F, Tonon G, Schrepfer R, Genovese S, et al. Self- assembling nanocomposites for protein delivery: Supramolecular interactions between PEG- cholane and rh- G- CSF. J Controlled Release 2012;162(1):176-184.

(370) Rajagopalan N, Chen SC, Chow W. A study of the inclusion complex of amphotericin-B with γ-cyclodextrin. Int J Pharm 1986;29(2):161-168.

(371) Choi K, Bang J, Kim P, Kim C, Song C. Amphotericin B-incorporated polymeric micelles composed of poly (d, l-lactide-co-glycolide)/dextran graft copolymer. Int J Pharm 2008;355(1):224-230.

(372) Gagoś M, Arczewska M. Spectroscopic studies of molecular organization of antibiotic amphotericin B in monolayers and dipalmitoylphosphatidylcholine lipid multibilayers. Biochimica et Biophysica Acta (BBA)-Biomembranes 2010;1798(11):2124-2130.

(373) Nahar M, Jain NK. Preparation, characterization and evaluation of targeting potential of amphotericin B-loaded engineered PLGA nanoparticles. Pharm Res 2009;26(12):2588-2598.

(374) Asher IM, Levin IW. Effects of temperature and molecular interactions on the vibrational infrared spectra of phospholipid vesicles. Biochimica et Biophysica Acta (BBA)-Biomembranes 1977;468(1):63-72.

(375) Espuelas M, Legrand P, Cheron M, Barratt G, Puisieux F, Devissaguet J, et al. Interaction of amphotericin B with polymeric colloids: A spectroscopic study. Colloids and Surfaces B: Biointerfaces 1998;11(3):141-151.

(376) Espuelas M, Legrand P, Irache J, Gamazo C, Orecchioni A, Devissaguet J, et al. Poly (ε-caprolacton) nanospheres as an alternative way to reduce amphotericin B toxicity. Int J Pharm 1997;158(1):19-27.

(377) Gaboriau F, Chéron M, Leroy L, Bolard J. Physico-chemical properties of the heat-induced 'superaggregates' of amphotericin B. Biophys Chem 1997;66(1):1-12.

(378) Klepser ME, Wolfe EJ, Jones RN, Nightingale CH, Pfaller MA. Antifungal pharmacodynamic characteristics of fluconazole and amphotericin B tested against Candida albicans. Antimicrob Agents Chemother 1997 Jun;41(6):1392-1395.

(379) Espinel-Ingroff A, Arthington-Skaggs B, Iqbal N, Ellis D, Pfaller MA, Messer S, et al. Multicenter evaluation of a new disk agar diffusion method for susceptibility testing of filamentous fungi with voriconazole, posaconazole, itraconazole, amphotericin B, and caspofungin. J Clin Microbiol 2007 Jun;45(6):1811-1820.

(380) Espinel-Ingroff A, Canton E, Gibbs D, Wang A. Correlation of Neo-Sensitabs tablet diffusion assay results on three different agar media with CLSI broth microdilution M27-A2 and disk diffusion M44-A results for testing susceptibilities of Candida spp. and Cryptococcus neoformans to amphotericin B, caspofungin, fluconazole, itraconazole, and voriconazole. J Clin Microbiol 2007 Mar;45(3):858-864.

(381) Wilcock BC, Endo MM, Uno BE, Burke MD. C2′-OH of amphotericin B plays an important role in binding the primary sterol of human cells but not yeast cells. J Am Chem Soc 2013;135(23):8488-8491.

(382) Diezi TA, Kwon G. Amphotericin B/sterol co-loaded PEG-phospholipid micelles: effects of sterols on aggregation state and hemolytic activity of amphotericin B. Pharm Res 2012;29(7):1737-1744.

(383) Gaboriau F, Cheron M, Petit C, Bolard J. Heat-induced superaggregation of amphotericin B reduces its in vitro toxicity: a new way to improve its therapeutic index. Antimicrob Agents Chemother 1997 Nov;41(11):2345-2351.

(384) Baas B, Scott A, Scott J, Mikulecky P, Hartsel SC. Activity and kinetics of dissociation and transfer of amphotericin B from a novel delivery form. Aaps Pharmsci 1999;1(3):21-31.

(385) Bartlett K, Yau E, Hartsel SC, Hamer A, Tsai G, Bizzotto D, et al. Effect of heat-treated amphotericin B on renal and fungal cytotoxicity. Antimicrob Agents Chemother 2004 Jan;48(1):333-336.

(386) Silva-Filho MA, Siqueira SD, Freire LB, Araujo IB, Holanda e Silva KG, Medeiros Ada C, et al. How can micelle systems be rebuilt by a heating process? Int J Nanomedicine 2012;7:141-150.

(387) Segarra I, Movshin DA, Zarif L. Pharmacokinetics and tissue distribution after intravenous administration of a single dose of amphotericin B cochleates, a new lipid- based delivery system. J Pharm Sci 2002;91(8):1827-1837.

(388) Yang ZL, Li XR, Yang KW, Liu Y. Amphotericin B- loaded poly (ethylene glycol)–poly (lactide) micelles: Preparation, freeze- drying, and in vitro release. Journal of Biomedical Materials Research Part A 2008;85(2):539-546.

(389) Sahoo SK, Panyam J, Prabha S, Labhasetwar V. Residual polyvinyl alcohol associated with poly (D, L-lactide-co-glycolide) nanoparticles affects their physical properties and cellular uptake. J Controlled Release 2002;82(1):105-114.

(390) Sant VP, Nagarsenker MS. Synthesis of Monomethoxypolyethyleneglycol—Cholesteryl Ester and Effect of its Incorporation in Liposomes. AAPS PharmSciTech 2011;12(4):1056-1063.

(391) Piraccini BM, Alessandrini A. Onychomycosis: A Review. Journal of Fungi 2015;1(1):30-43.

(392) Gupta AK, Daigle D. Tavaborole (AN-2690) for the treatment of onychomycosis of the toenail in adults. Expert review of anti-infective therapy 2014;12(7):735-742.

(393) Elewski B, Pollak R, Ashton S, Rich P, Schlessinger J, Tavakkol A. A randomized, placebo- and active- controlled, parallel- group, multicentre, investigator- blinded study of four treatment regimens of posaconazole in adults with toenail onychomycosis. Br J Dermatol 2012;166(2):389-398.

(394) Ngwogu A, Mba I, Ngwogu K. Onychomycosis: Etiology, diagnosis, and treatment. Journal of Medical Investigations and Practice 2014;9(1):43.

(395) Ameen M, Lear J, Madan V, Mohd Mustapa M, Richardson M. British Association of Dermatologists' guidelines for the management of onychomycosis 2014. Br J Dermatol 2014;171(5):937-958.

(396) Shemer A. Update: medical treatment of onychomycosis. Dermatologic therapy 2012;25(6):582-593.

(397) Ledon JA, Savas J, Franca K, Chacon A, Nouri K. Laser and light therapy for onychomycosis: a systematic review. Lasers in medical science 2014;29(2):823-829.

(398) Grover C, Khurana A. An update on treatment of onychomycosis. Mycoses 2012;55(6):541-551.

(399) Welsh O, Vera-Cabrera L, Welsh E. Onychomycosis. Clin Dermatol 2010;28(2):151-159.

(400) Kaur R, Kashyap B, Bhalla P. Onychomycosis--epidemiology, diagnosis and management. Indian J Med Microbiol 2008 Apr-Jun;26(2):108-116.

(401) Clayton Y. Clinical and mycological diagnostic aspects of onychomycoses and dermatomycoses. Clin Exp Dermatol 1992;17(s1):37-40.

(402) Morales- Cardona CA, Valbuena- Mesa MC, Alvarado Z, Solorzano- Amador A. Non- dermatophyte mould onychomycosis: a clinical and epidemiological study at a dermatology referral centre in Bogota, Colombia. Mycoses 2014;57(5):284-293.

(403) Gupta AK, Drummond-Main C, Cooper EA, Brintnell W, Piraccini BM, Tosti A. Systematic review of nondermatophyte mold onychomycosis: diagnosis, clinical types, epidemiology, and treatment. J Am Acad Dermatol 2012;66(3):494-502.

(404) Moreno G, Arenas R. Other fungi causing onychomycosis. Clin Dermatol 2010;28(2):160-163.

(405) Tosti A, Piraccini BM, Lorenzi S. Onychomycosis caused by nondermatophytic molds: clinical features and response to treatment of 59 cases. J Am Acad Dermatol 2000;42(2):217-224.

(406) Jayatilake J, Tilakaratne W, Panagoda G. Candidal onychomycosis: a mini-review. Mycopathologia 2009;168(4):165-173.

(407) Arenas R. Onicomicosis por Candida en las uñas de las manos. Dermatología Revista mexicana 2014;58(4):323-330.

(408) Soraya E. Cuenca . Utilidad del examen directo y estudio histopatológico de lámina ungueal en relación al culti micológico en el diagnóstico de onicomicosis. Área de consulta externa del hospital Luis Vernaza en el período Octubre 2009-Septiembre 2010; 2012.

(409) Dias, Maria Fernanda Reis Gavazzoni, Quaresma-Santos MVP, Bernardes-Filho F, Amorim, Adriana Gutstein da Fonseca, Schechtman RC, Azulay DR. Update on therapy for superficial mycoses: review article part I. An Bras Dermatol 2013;88(5):764-774.

(410) Lizardo-Castro G, Lizardo AE. Presentación inusual de onicomicosis por candida albicans. CONSEJO EDITORIAL 2011-2012 2012;80(2):61.

(411) Evans E. Causative pathogens in onychomycosis and the possibility of treatment resistance: a review. J Am Acad Dermatol 1998;38(5):S32-S36.

(412) Scher R, Baran R. Onychomycosis in clinical practice: factors contributing to recurrence. Br J Dermatol 2003;149(s65):5-9.

(413) Scher RK. Onychomycosis: a significant medical disorder. J Am Acad Dermatol 1996;35(3):S2-S5.

(414) Rodney PD. Chapter 1. Science of the Nail Apparatus. In: Taylor & Francis Group, LLC, editor. A text Atlas of Nail Disorders: Techniques in Investigation and Diagnosis. Tercera ed. Boca Ranton, Florida: CR Press; 2005. p. 1.

(415) Elewski BE. Onychomycosis: pathogenesis, diagnosis, and management. Clin Microbiol Rev 1998 Jul;11(3):415-429.

(416) Thatai P, Sapra B. Transungual delivery: deliberations and creeds. Int J Cosmetic Sci 2014;36(5):398-411.

(417) Walters KA, Abdalghafor HM, Lane ME. The human nail–barrier characterisation and permeation enhancement. Int J Pharm 2012;435(1):10-21.

(418) LEWIN K. The normal finger nail. Br J Dermatol 1965;77(8- 9):421-430.

(419) Zaias N. The Nail in Health and Disease. Florida: Springer; 2012.

(420) Levit, E. & Scher, R. Chapter 6. Basic Science of the nail. In: Freinkel, Ruth & Woodley, D., editor. The Biology of the Skin. Third Edition ed. UK: Parthenon Publishing Group, Inc.; 2001. p. 101.

(421) Perea S, Ramos MJ, Garau M, Gonzalez A, Noriega AR, del Palacio A. Prevalence and risk factors of tinea unguium and tinea pedis in the general population in Spain. J Clin Microbiol 2000 Sep;38(9):3226-3230.

(422) Schein JR, Gause D, Stier DM, Lubeck DP, Bates MM, Fisk R. Onychomycosis. Baseline results of an observational study. J Am Podiatr Med Assoc 1997 Nov;87(11):512-519.

(423) Zaias N, Glick B, Rebell G. Diagnosing and treating onychomycosis. J Fam Pract 1996;42(5):513-519.

(424) Levy LA. Epidemiology of onychomycosis in special-risk populations. J Am Podiatr Med Assoc 1997 Dec;87(12):546-550.

(425) Kolodchenko YV, Baetul VI. A Novel Method for the Treatment of Fungal Nail Disease with 1064 nm Nd: YAG. J Laser Health Acad 2013;1:42-47.

(426) Dompmartin D, Dompmartin A, Deluol A, Grosshans E, Coulaud J. Onychomycosis and AIDS. Int J Dermatol 1990;29(5):337-339.

(427) Faergemann J, Baran R. Epidemiology, clinical presentation and diagnosis of onychomycosis. Br J Dermatol 2003;149(s65):1-4.

(428) Baran R, Tosti A. Chemical avulsion with urea nail lacquer. J Dermatol Treat 2002;13(4):161-164.

(429) Murdan S. Drug delivery to the nail following topical application. Int J Pharm 2002;236(1):1-26.

(430) Vejnovic I, Huonder C, Betz G. Permeation studies of novel terbinafine formulations containing hydrophobins through human nails in vitro. Int J Pharm 2010;397(1):67-76.

(431) Vejnovic I, Simmler L, Betz G. Investigation of different formulations for drug delivery through the nail plate. Int J Pharm 2010;386(1):185-194.

(432) Rajendra VB, Baro A, Kumari A, Dhamecha DL, Lahoti SR, Shelke SD. Transungual drug delivery: an overview. J Appl Pharm Sci 2012;2(1):203-209.

(433) Elkeeb R, AliKhan A, Elkeeb L, Hui X, Maibach HI. Transungual drug delivery: current status. Int J Pharm 2010;384(1):1-8.

(434) Quintanar-Guerrero D, Ganem-Quintanar A, Tapia-Olguin P, Kalia YN, Buri P. The effect of keratolytic agents on the permeability of three imidazole antimycotic drugs through the human nail. Drug Dev Ind Pharm 1998;24(7):685-690.

(435) Brown M, Khengar RH, Turner RB, Forbes B, Traynor M, Evans C, et al. Overcoming the nail barrier: a systematic investigation of ungual chemical penetration enhancement. Int J Pharm 2009;370(1):61-67.

(436) Murdan S. 1st Meeting on Topical Drug Delivery to the Nail: 2 April, 2007, London, UK. Expert opinion on drug delivery 2007;4(4):453-455.

(437) Mohorčič M, Torkar A, Friedrich J, Kristl J, Murdan S. An investigation into keratinolytic enzymes to enhance ungual drug delivery. Int J Pharm 2007;332(1):196-201.

(438) Hao J, Li SK. Transungual iontophoretic transport of polar neutral and positively charged model permeants: effects of electrophoresis and electroosmosis. J Pharm Sci 2008;97(2):893-905.

(439) Narasimha Murthy S, Wiskirchen DE, Paul Bowers C. Iontophoretic drug delivery across human nail. J Pharm Sci 2007;96(2):305-311.

(440) Kassan DG, Lynch AM, Stiller MJ. Physical enhancement of dermatologic drug delivery: iontophoresis and phonophoresis. J Am Acad Dermatol 1996;34(4):657-666.

(441) Repka MA, Mididoddi PK, Stodghill SP. Influence of human nail etching for the assessment of topical onychomycosis therapies. Int J Pharm 2004;282(1):95-106.

(442) Rothermel E, Apfelberg DB. Carbon dioxide laser use for certain diseases of the toenails. Clin Podiatr Med Surg 1987 Oct;4(4):809-821.

(443) Nogueiras-Nieto L, Gómez-Amoza J, Delgado-Charro MB, Otero-Espinar F. Hydration and N-acetyl-l-cysteine alter the microstructure of human nail and bovine hoof: Implications for drug delivery. J Controlled Release 2011;156(3):337-344.

(444) Elewski BE. Onychomycosis. Treatment, quality of life, and economic issues. Am J Clin Dermatol 2000 Jan-Feb;1(1):19-26.

(445) Gupta AK, Paquet M, Simpson FC. Therapies for the treatment of onychomycosis. Clin Dermatol 2013;31(5):544-554.

(446) Iorizzo M, Piraccini BM, Tosti A. Today's treatments options for onychomycosis. JDDG: Journal der Deutschen Dermatologischen Gesellschaft 2010;8(11):875-879.

(447) Gupta AK, Skinner AR. Ciclopirox for the treatment of superficial fungal infections: a review. Int J Dermatol 2003;42(S1):3-9.

(448) Bohn M, Kraemer KT. Dermatopharmacology of ciclopirox nail lacquer topical solution 8% in the treatment of onychomycosis. J Am Acad Dermatol 2000;43(4):S57-S69.

(449) Cryer J, Robinson C. In vitro study to establish the efficacy of 28% Tioconazole solution (Trosyl) against Trichophyton rubrum and Candida albicans. The Foot 1997;7(1):27-29.

(450) Pollak RA. Efinaconazole Topical Solution, 10% The Development of a New Topical Treatment for Toenail Onychomycosis. J Am Podiatr Med Assoc 2014;104(6):568-573.

(451) Elewski BE, Rich P, Pollak R, Pariser DM, Watanabe S, Senda H, et al. Efinaconazole 10% solution in the treatment of toenail onychomycosis: two phase III multicenter, randomized, double-blind studies. J Am Acad Dermatol 2013;68(4):600-608.

(452) Joseph WS, Vlahovic TC, Pillai R, Olin JT. Efinaconazole 10% Solution in the Treatment of Onychomycosis of the Toenails. J Am Podiatr Med Assoc 2014;104(5):479-485.

(453) Elewski BE, Aly R, Baldwin SL, Soto RFG, Rich P, Weisfeld M, et al. Efficacy and safety of tavaborole topical solution, 5%, a novel boron-based antifungal agent, for the treatment of toenail onychomycosis: Results from 2 randomized phase-III studies. J Am Acad Dermatol 2015;73(1):62-69.

(454) Food and Drug Administration. Full Prescribing information: Kerydin (Tavaborole) topical solution 5%. 2014; Available at: http://www.accessdata.fda.gov/drugsatfda_docs/label/2014/204427s000lbl.pdf. Accessed 01/30, 2016.

(455) Scher RK, Nakamura N, Tavakkol A. Luliconazole: a review of a new antifungal agent for the topical treatment of onychomycosis. Mycoses 2014;57(7):389-393.

(456) Gianni C, Cerri A, Crosti C. Non-dermatophytic onychomycosis. An understimated entity? A study of 51 cases Nicht-Dermatophyten-Onychomykose: Eine unterschätzte Krankheit? Eine Studie von 51 Fällen. Mycoses 2000;43:29-33.

(457) Gupta AK, Drummond-Main C, Paquet M. Evidence-based optimal fluconazole dosing regimen for onychomycosis treatment. J Dermatol Treat 2013;24(1):75-80.

(458) Spriet I, Lambrecht C, Lagrou K, Verhamme B. Successful eradication of Scytalidium dimidiatum-induced ungual and cutaneous infection with voriconazole. European Journal of Dermatology 2012;22(2):197-199.

(459) Bueno J, Martinez C, Zapata B, Sanclemente G, Gallego M, Mesa A. In vitro activity of fluconazole, itraconazole, voriconazole and terbinafine against fungi causing onychomycosis. Clin Exp Dermatol 2010;35(6):658-663.

(460) Scheinfeld N. A review of the new antifungals: posaconazole, micafungin, and anidulafungin. J Drugs Dermatol 2007 Dec;6(12):1249-1251.

(461) Gupta A, Leonardi C, Stoltz R, Pierce P, Conetta B. A phase I/II randomized, double- blind, placebo- controlled, dose- ranging study evaluating the efficacy, safety and pharmacokinetics of ravuconazole in the treatment of onychomycosis. Journal of the European Academy of Dermatology and Venereology 2005;19(4):437-443.

(462) Bornstein E, Hermans W, Gridley S, Manni J. Near- infrared Photoinactivation of Bacteria and Fungi at Physiologic Temperatures. Photochem Photobiol 2009;85(6):1364-1374.

(463) Hees H, Raulin C, Bäumler W. Laser treatment of onychomycosis: an in vitro pilot study. JDDG: Journal der Deutschen Dermatologischen Gesellschaft 2012;10(12):913-917.

(464) Potter LP, Mathias SD, Raut M, Kianifard F, Landsman A, Tavakkol A. The impact of aggressive debridement used as an adjunct therapy with terbinafine on perceptions of patients undergoing treatment for toenail onychomycosis. J Dermatol Treat 2007;18(1):46-52.

(465) Munro I, Newberne P, Young V, Bär A. Safety assessment of γ-cyclodextrin. Regulatory Toxicology and Pharmacology 2004;39:3-13.

(466) VIKMON M, STADLER-SZÖKE Á, SZEJTLI J. Solubilization of amphotericin B with. GAMMA.-cyclodextrin. J Antibiot 1985;38(12):1822-1824.

(467) Scientific Committee on Consumer Safety. Opinion on N-Methyl-2-pyrrolidone (NMP). 2011; Available at: http://ec.europa.eu/health/scientific_committees/consumer_safety/docs/sccs_o_050.pdf. Accessed 11/01, 2015.

(468) Akesson B. N-methyl-2-pyrrolidone. 2001.

(469) Junyaprasert VB, Singhsa P, Jintapattanakit A. Influence of chemical penetration enhancers on skin permeability of ellagic acid-loaded niosomes. asian journal of pharmaceutical sciences 2013;8(2):110-117.

(470) Chaudhuri B, Chim MF, Bucks D. Topical formulations for the treatment of nail fungal diseases 2000.

(471) Frömming K, Szejtli J. Cyclodextrins in pharmacy. : Springer Science & Business Media; 1993.

(472) Fluhr JW, Cavallotti C, Berardesca E. Emollients, moisturizers, and keratolytic agents in psoriasis. Clin Dermatol 2008;26(4):380-386.

(473) Nogueiras-Nieto L, Delgado-Charro MB, Otero-Espinar FJ. Thermogelling hydrogels of cyclodextrin/poloxamer polypseudorotaxanes as aqueous-based nail lacquers: application to the delivery of triamcinolone acetonide and ciclopirox olamine. European Journal of Pharmaceutics and Biopharmaceutics 2013;83(3):370-377.

(474) Chesnoy S, Delaunois M, Coubetergues H, Lefrancois P. Urea-based film-forming solution for treating nail psoriasis 2009.